

Click Chemistry: Developing New Tools & Reactions for Practical Applications

Andrew Steven Barrow, MChem.

Thesis submitted to the University of Nottingham for the degree of Doctor of Philosophy

September 2016

ABSTRACT

This thesis primarily concerns the development of new tools and reactions through the activation of chemical moieties to generate either function, as protein labels or the synthetically valuable sulfonyl azides, or unusual chemical reactivity. Chapter 1 contains a brief introduction to the concept of Click Chemistry, with an overview of the nature of Click Chemistry reactions and their corresponding applications.

Chapter 2 focusses on the use of diazirines, high energy but remarkably stable functionality as tools to probe protein structure. A protein footprinting technique has been developed employing aromatic based diazirine photoactive labels to decorate the protein surface. Following analysis by mass spectrometry, information could be inferred regarding the binding site of an Ub-IsoT ZnF protein complex. In addition, a range of diazirine probes of varying steric and electronic demands have been synthesised and their labelling properties characterised.

The recently developed SuFEx activation has been applied in Chapter 3, with the development of a protocol for formation of sulfonyl azides from the robust sulfonyl fluorides. The methodology was extended to an *in situ* diazo transfer reaction, which circumvents the requirement to handle the potentially unstable diazo transfer reagent.

Additionally, it was the pursuit of a novel mode of activation for the azide-alkyne cycloaddition, which generated a serendipitous result that led to the results in Chapter 4. Radical cation activation led to a selection of reactive intermediates that engaged in unusual chemistry.

ACKNOWLEDGEMENTS

Firstly, I would like to thank my supervisor, Dr. John Moses, for giving me the opportunity to work in his group for the last four years. His guidance, support and constant source of ideas have been invaluable to me over the course of my PhD studies. I would also like to thank all of the past and present members of the Moses group, for helping to create a positive and productive work environment.

In addition I would like to acknowledge Professor Neil Oldham and his group, particular Lucio Manzi, for their expert guidance on the mass spectrometry section of the work undertaken.

I would also like to express my gratitude to the departmental technical, analytical and support staff for their assistance over the past few years, in particular Sue, without whom the department would simply not function.

Finally, I must thank all of the friends and family who have provided endless help and support over the past four years.

ABBREVIATIONS

ABPP	activity based protein profiling
amu	atomic mass unit
aq.	aqueous
^{o}C	degrees Celsius
CID	collision induced dissociation
CuAAC	copper(I) catalysed alkyne-azide cycloaddition
DMAP	4-dimethylaminopyridine
DMP	Dess-Martin periodinane
ECD	electron capture dissociation
ESI	electrospray ionisation
G	gram(s)
H	hour(s)
HRMS	high resolution mass spectrometry
hv	irradiation with light
IR	infra-red
IsoT	isopeptidase T
LC-MS	liquid chromatography/mass spectrometry
LC-MS/MS	liquid chromatography/mass spectrometry/mass spectrometry
M	molar
mg	milligram(s)
MHz	megahertz
min	minute(s)
mL	millilitre(s)
mmol	millimole(s)
m/z	mass to charge ratio
NMR	nuclear magnetic resonance
ppm	parts per million
r.t.	room temperature
SuFEx	sulfur(VI) fluoride exchange
TBPA	tris-(*p*-bromophenyl)aminium hexachloroantimonate
TLC	thin layer chromatography
THF	tetrahydrofuran
$TMSN_3$	trimethylsilyl azide
Ub	ubiquitin
UBD	ubiquitin binding domain
UV	ultraviolet
ZnF	zinc finger

CONTENTS

Abstract i
Acknowledgements ii
Abbreviations iii
Chapter 1 : Click Chemistry 1
Click Chemistry 2
The Copper(I)-Catalysed Azide Alkyne 1,3 –dipolar Cycloaddition 4
SuFEx: Sulfur-Fluoride Exchange 7
Chapter 2 : Synthesis and Development of Aromatic Diazirines for the Study of Protein-Protein Interactions 9
Introduction 10
X-Ray Crystallography 12
Nuclear Magnetic Resonance Spectroscopy 13
Mass Spectrometry 14
Protein Footprinting 20
Photoactivable labels 24
Development of diazirines for use in photo-labelling 31
Diazirines in protein footprinting 35
Project Hypothesis and Aims 40
Results and Discussion 42
Synthesis of Aromatic Diazirine Label 43
Protein Labelling Work Flow 45
Ubiquitin Labelling 47
Differential Labelling of a Ubiquitin Complex 53
Optimisation of Labelling Conditions 57
Synthesis of a Cationic Diazirine Label 64
Synthesis of a Pyridinium Diazirine Label 71
Labelling Behaviour of the Cationic Diazirine Probe 76
Synthesis of a Selection of Isomeric Diazirine Probes 79
Labelling Studies of Additional Diazirines 89
Conclusions and Future Work 94
Experimental Section 96
Chapter 3 : Synthesis of Sulfonyl Azides Through SuFEx 143
Aims and Objectives 144
Introduction 146
Activation and Reactions of Sulfonyl Fluorides 146
Synthesis of Sulfonyl Azides 150
Applications of Sulfonyl Azides in Synthesis 154
i) Diazo-transfer 155

ii) Sulfonyl Azides in Click Chemistry 158
iii) Azide Transfer 161
Results and Discussion 163
Development of Methodology to Form Sulfonyl Azides 163
Optimisation of Conditions for Base-Sensitive Substrates 171
Development of a more complex substrate 174
Development of an *in situ* diazo-transfer reaction 176
Mechanistic Studies 180
Conclusions and Future Work 185
Experimental Section 187
Chapter 4 : Radical Cation Initiated Enyne Hydration 209
Background 210
Introduction 213
Radical Cations 213
Electrochemical oxidation 215
Photoinduced Electron Transfer 217
Chemical Oxidation 220
Applications of Triarylamine Radical Cations 222
Alkyne Hydration 225
Hydration of Enynes 230
Results and Discussion 232
Mechanistic Studies 237
Investigation of Intramolecular Cyclisation Reactions 243
Mechanistic Studies of the Cyclisation Reaction 249
Reaction Scope 255
Conclusions And Future Work 259
Experimental Section 261
Chapter 5 : References 296

Chapter 1 : Click Chemistry

CLICK CHEMISTRY

The Click Chemistry philosophy, pioneered by Sharpless *et al*., describes a strategy for organic chemistry that prioritises the role of function over structure. This principle, inspired by Nature, was designed to fulfil the demands of modern day science, particularly in the field of drug discovery.[1]

In 1996, Guida *et al*. estimated that between 10^{62} and 10^{63} discrete molecules exist in the pool of drug-like candidates (≤500 daltons, ≤ 30 non-hydrogen atoms and likely to be stable in the presence of water and oxygen).[2] Following this, Sharpless *et al*. stated that due to the vast amount of structural space available, targets for drug discovery should all follow the rule *"all searches must be restricted to molecules that are easy to make"*.[1]

Polypeptides, polysaccharides and polynucleotides are macromolecules central to life processes, and are assembled by Nature through carbon-heteroatom linkages. In contrast, many of the targets for natural product chemists contain complex carbon frameworks, which has resulted in the extensive development of methodologies to install carbon-carbon bonds.

It was Sharpless' view that the chemical community should follow Nature's lead and employ thermodynamically favourable carbon-heteroatom connections to generate function through the reliable and rapid combination of modular building blocks. The defined criteria of Click Chemistry states that reactions should be:[1]

- Modular
- Wide in scope
- High yielding
- Operationally simple
- Only utilise benign or easily removed solvent
- Easy to purify
- Generate only inoffensive byproducts

Only a handful of reactions fit these stringent criteria and these are limited to those with a strong thermodynamic driving force. Key examples include electrophilic addition to alkenes and alkynes, non-aldol carbonyl condensation chemistry, nucleophilic ring openings of aziridines and epoxides and, perhaps most commonly, cycloaddition reactions (Figure 1.1).

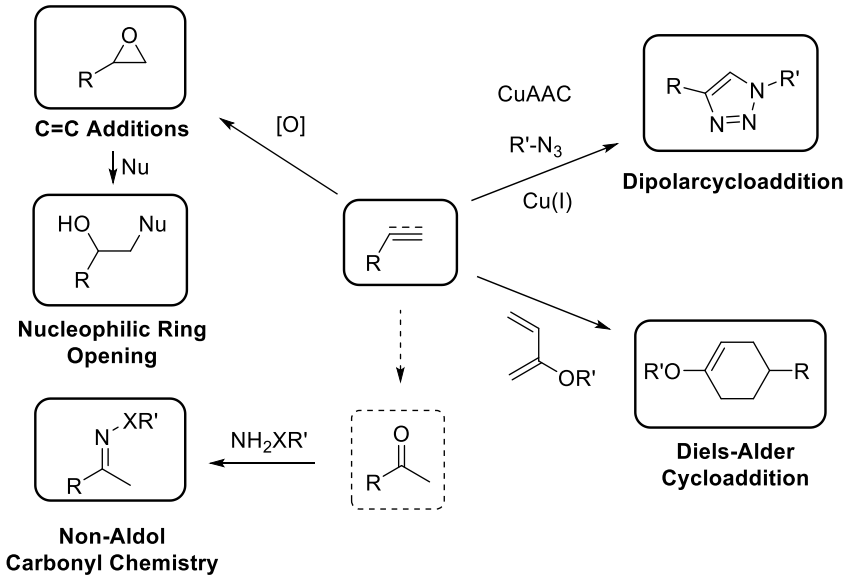


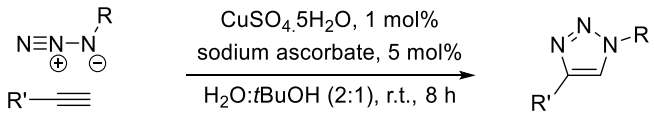
Figure 1.1: *Common classes of Click Reactions.*[3]

Since the seminal publication introducing Click Chemistry, there has been an explosive growth in the application of this practical approach in a diverse range of disciplines, notably: materials science; drug discovery and bioconjugation.[3]

Due to the dramatic impact that Click Chemistry has had in recent years, it is perhaps unsurprising that the applications of this philosophy have been extensively discussed. It is impossible to fully describe the uses of Click Chemistry in this brief introduction and readers are therefore directed towards more detailed and subject specific reviews.[3–5]

THE COPPER(I)-CATALYSED AZIDE ALKYNE 1,3 –DIPOLAR CYCLOADDITION

Described as "*the cream of the crop*" of Click Chemistry, the Huisgen 1,3-dipolar cycloaddition of alkynes and azides to yield 1,2,3-triazoles has often been referred to as "*The Click Reaction*".[1,3] In 2002, a dramatic rate acceleration of this transformation under copper(I) catalysis was reported almost simultaneously by the groups of Sharpless and Meldal (Scheme 1.1).[6,7] The catalysed reaction also resulted in the exclusive formation of the 1,4-disubstituted triazole.



Scheme 1.1: *Copper-catalysed 1,3-dipolar cycloaddition of azides and alkynes.*[6]

The observed regioselective rate enhancement, coupled with the kinetic stability, functional group tolerance and facile synthesis of azides and alkynes, resulted in the copper-catalysed azide alkyne cycloaddition (CuAAc) reaction becoming synonymous with the philosophy of Click Chemistry.

Click Chemistry has been used to rapidly generate large lead discovery libraries, with diversity generated from just one or two "spring-loaded" reactions.[4] Aside from the formation of compound libraries, the generated triazoles are considered attractive scaffolds, and have been used as stable amide mimetics, due to their similar electronic and topological properties.

Past work by the Moses group has employed click chemistry in drug discovery projects, with one example involving a fragment based approach to the production of bifunctional inhibitors of hLDH-5, a target for anti-glycolytic cancer treatment.[8] Inspired by the NADH co-factor structure, a number of ligands were designed to incorporate both adenosine and oxamate mimetics. The complementary azide and alkyne functionality present in the synthesised fragments allowed the two molecules to be tethered through a triazole linker. This strategy proved successful, with the identification of promising lead structures with impressive selectivity and activity, an example of which is displayed in Figure 1.2.

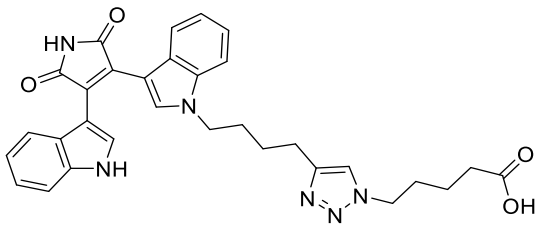


***Figure 1.2**: Example of a triazole containing hLDH-5 ligand.*

A similar approach was employed for the development of ligands for G-quadruplex formation, which are tertiary structures of DNA shown to inhibit the telomerase enzyme responsible for cancer cell immortality.[9] As Figure 1.3 depicts, two distinct motifs were chosen in the ligand design, with the central core containing either symmetrical di-triazoles or asymmetric triazoles.

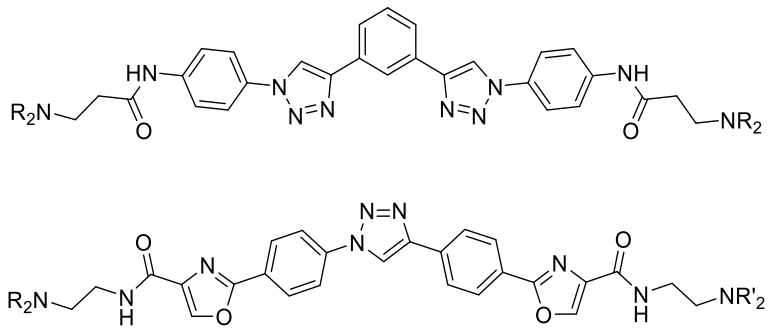


Figure 1.3: *Design motifs of triazole based G-quadruplex ligands.*[9]

The CuAAC reaction has also been extensively used in bioconjugation; a chemical strategy used to ligate biomolecules. Alkynes and azides are biorthogonal and tolerant to aqueous conditions, making them ideal partners for the fusion of synthetic labels to biomolecules.

The small, non-polar nature of azides coupled with their essential absence from biological systems makes them ideal bio-orthogonal participants, without significant perturbation of the parent biomolecule.[10]

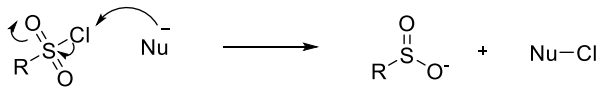
The CuAAC reaction has been used to introduce a range of functionality onto biomolecules such as DNA, proteins and oligosaccharides in a reliable manner.[3] A pertinent example of this is the functionalisation of alkyne-modified DNA by Carell *et al*.[11] Modified DNA was synthesised through phosphoramidate chemistry with the use of alkyne-containing nucleosides. Various azides were then used to decorate the DNA post-synthetically, highlighting the robustness of the CuAAC reaction, not just as a purely synthetic reaction, but as a valuable tool for bioconjugation and chemical biology.

SuFEx: Sulfur-Fluoride Exchange

In 2014, Sharpless *et al*. unveiled the next major development of Click Chemistry: Sulfur(VI) fluoride exchange (SuFEx).[12] SuFEx exploits the activation of usually robust sulfonyl fluorides and fluorosulfates, utilising protons or silicon centres to allow reliable substitution of the fluoride ion.[12] This has resulted in S^{VI}-F bond becoming a key precursor to stable sulfuryl/sulfonyl connections Z-SO^2-Z' (Z, Z' = C, O, N).

The development of SuFEx is based on the robustness of the S^{VI}-F bond and in order to best demonstrate the enhanced stability of the sulfonyl fluoride over the corresponding chloride, a discussion of their varying reactivity is required.

Sulfonyl chlorides are often used as precursors to both sulfates and sulfonamides. However, the use of these moieties is not always reliable, due to the S^{VI}-Cl bond being prone to reductive collapse. The reductive failure this bond can occur with a range of nucleophiles, with attack at the chlorine, as opposed to at sulfur resulting in the formal reduction of sulfur from a +6 oxidation state to +4 (Figure 1.4).

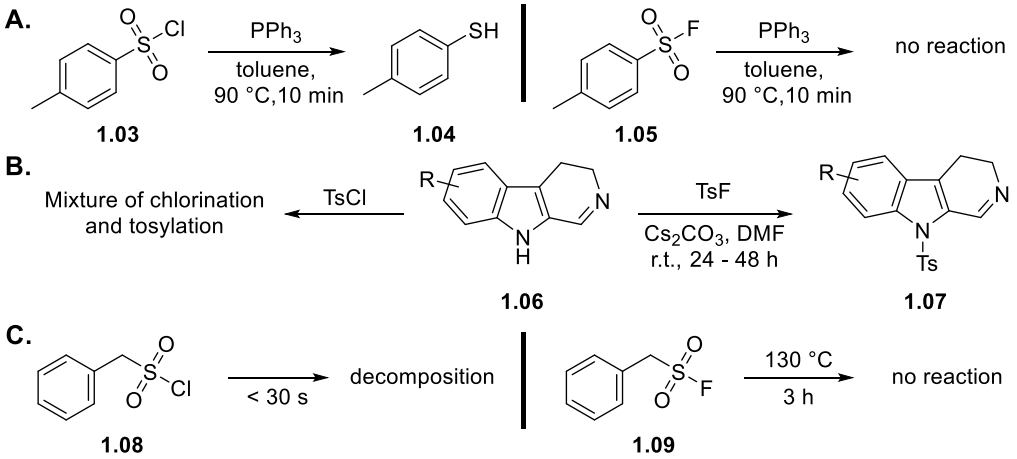


1.01 **1.02**

Figure 1.4: *Reductive collapse of sulfonyl chlorides with nucleophiles.[12]*

The instability of sulfonyl chlorides results in unpredictable reactivity, often resulting in the formation of undesired reaction byproducts. Conversely, the robust nature of the analogous sulfonyl fluoride allows it to undergo clean reactions.

For example, triphenylphosphine reduces sulfonyl chlorides to the corresponding thiol, whereas the sulfonyl fluorides are inert under these coniditions (Scheme 1.2.A).[13] During the attempted sulfonylation of 3,4-dihydro-β-carboline derivatives, Jacobsen found that the use of the sulfonyl chloride resulted in a mixture of both tosylated and chlorinated products, whereas tosyl fluoride gave only the tosylate **1.07** (Scheme 1.2.B).[14]



***Scheme 1.2**: Comparison of the reactions of RSO_2Cl and RSO_2F.*

Sulfonyl fluorides also have increased thermostability compared to their chloride counterparts. An example of this was demonstrating by heating the phenylmethylsulfonyl halides. Whereas the sulfonyl fluoride substrate **1.09** did not react even after prolonged heat exposure; degradation of the chloride **1.08** was noted after less than 30 seconds (Scheme 1.2.C).[12]

These select examples demonstrate the robust nature of the S^{VI}-F bond, which when combined with the activation of the functionality makes the development of SuFEx chemistry a powerful tool for a range of applications. A more detailed discussion detailing the activation and reactions of sulfonyl fluorides can be found in Chapter 3 of this thesis.

Chapter 2 : Synthesis and Development of Aromatic Diazirines for the Study of Protein-Protein Interactions

The work is this chapter is partially described in the following publication:

Manzi, L.; Barrow, A. S.; Scott, D.; Layfield, R.; Wright, T. G.; Moses, J. E.; Oldham, N. J. *Nat. Commun.* **2016**, 13288

INTRODUCTION

Proteins are vital to all living processes and undertake a wide range of functions essential to sustain life. These complex biomolecules are assembled from one or more peptide chains, each consisting of up to hundreds or thousands of amino acid units.[15]

Protein structure is divided into four levels: primary, second, tertiary and quaternary.[15] The primary structure of a protein refers to the amino acid sequence, with the terms C-terminus (carboxyl terminus) and N-terminus (amino terminus) used to refer to the respective ends of the polypeptide chain. Protein secondary structure is determined by hydrogen bonding interactions and corresponds to repeating local sub-structures, most commonly α-helices and β-sheets.

Tertiary structure determines the overall shape of a single protein molecule, by defining the spatial orientation of the secondary structures. This level of structure is stabilised by a range of interactions, commonly through salt bridges and the formation of disulfide bonds and hydrophobic cores. The quaternary structure refers to the arrangement of multiple protein subunits and this can include simple homodimers to more complex oligomers.[15]

The combination of these four levels of organisation gives a protein a unique 3-dimensional structure and specific function. The functions of proteins can vary widely, acting as enzymes and messengers as well as being as structural and storage components in cells.[15]

Given the central role of proteins in biology, the study of these biomolecules is of central importance in helping to understand the nature of these life processes. As with all molecules, structure and function are intertwined, and therefore to understand one, we must know the other. The wide range of

functions undertaken by proteins are generally governed by protein-protein interactions, and so the study of these interactions are of particular importance.[16]

Due to the complex nature of proteins, a number of techniques are required to understand and elucidate their physical properties, structure and topology. Over the years, several methods have been developed for this purpose including X-ray crystallography,[17] nuclear magnetic resonance (NMR),[18] computer modelling[19] and mass spectrometry.[20]

Of all the available techniques, it is reasonable to say that X-ray crystallography and NMR are the most established and widely used techniques for probing the structural characteristics of protein-protein interactions.

X-RAY CRYSTALLOGRAPHY

X-ray crystallography is the study of the atomic and molecular structure of crystalline samples through X-ray diffraction. Through analysis of the diffraction beams an image of the electron density within the crystal can be generated, allowing structural assignment.

The first application of X-ray crystallography into protein structure was described in the seminal work of Kendrew *et al*., with the determination of the three dimensional structure of the globular protein myoglobin.[21]

Since its establishment in 1971, the Protein Data Bank (PDB) has expanded from an initial 7 entries to 121654 entries as of August 2016.[22] To highlight the importance of X-ray crystallography it is noteworthy that this technique has been used to elucidate 89.4% of the PDB's protein structures.

Protein X-ray crystallography has an advantage over alternative techniques; the size of the protein is not limited, with high degrees of resolution achieved irrespective of size.[17] Additionally, with the development and availability of synchrotron sources and the ability to rapidly collect data, the time required to collect and analyse crystal data has been significantly shortened.[17]

The technique of X-ray crystallography for the determination of protein structure is not without drawbacks. Various ligands and solvents are often required to induce protein crystallisation, which can result in perturbations of the protein structure. Additionally, due to the ordered structure in the crystalline form, the technique provides a "snapshot" of how the protein is orientated, which may not be a true representation in real time.

NUCLEAR MAGNETIC RESONANCE SPECTROSCOPY

Nuclear magnetic resonance (NMR) is a technique that allows the study of conformational changes in the solution phase.[23] The field of protein NMR was pioneered by the work of Wüthrich who developed 2D NMR techniques for biomolecules.[24] The technique was exemplified through the first *de novo* structure determination through NMR of a globular protein, the bull seminal protease inhibitor (BUSI) in 1985.[25]

Heteronuclear 2D NMR experiments are commonly employed with ^{13}C and ^{15}N nuclei labelling to elucidate protein structure, with biomolecules of up to 30-50 kDa in size.[23,26,27] Advances in techniques to overcome resolution and sensitivity issues has allowed structural information to be inferred on significantly larger proteins.[28]

Although the resolution achieved by NMR has improved significantly, the technique is bound by the solubility and concentration of the samples. The amount of protein required, and the economic cost of the equipment can render protein NMR an extremely expensive technique.

Both of the described methods of X-ray crystallography and NMR have advantages and limitations which has led to their complementary use in investigating proteins. Given the wide application and impact of these techniques, it is clear that both are incredibly important.

However, considering the above discussion, there has been a growing demand for approaches to complement NMR and X-ray, particularly in the arena of protein-protein interactions.

MASS SPECTROMETRY

Mass spectrometry has developed immensely to become powerful method for probing protein structure and function.[29] It is a quantitative analytical technique that measures the mass to charge ratio (m/z) of gaseous ions, which can be used to identify molecules in a range of mixtures.

A general schematic of a mass spectrometer is illustrated in Figure 2.1.[30] The sample is introduced into the system through the inlet, such as a gas or liquid chromatograph. An ionization source is then required to produce gaseous ions from the sample. One or more mass analysers are employed in tandem to separate and fragment the ions, with a detector positioned after the last analyser to "count" the emerging ions. A system for data processing then collates the data into a mass spectrum.

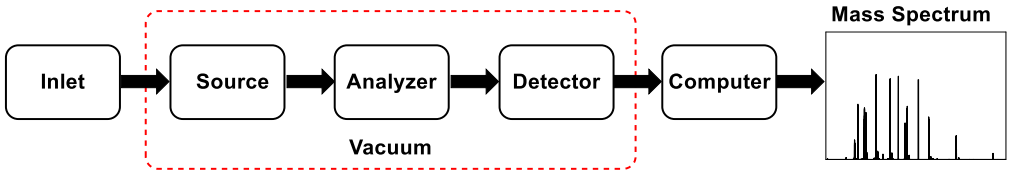


***Figure 2.1**: Schematic of the basic mass spectrometer components.*

The study of proteins by mass spectrometry was enabled by the advent of techniques such as electrospray ionisation (ESI) and matrix-assisted laser desorption/ionisation (MALDI).

Fenn *et al*. demonstrated that ESI could be used to produce multiply charged ions from proteins, which allowed their molecular weights to be determined on spectrometers with a limited mass range.[31] ESI is a "soft ionisation" technique that applies a high voltage to a liquid sample, resulting in the

formation of an aerosol which subsequently enters the mass spectrometer. Minimal fragmentation is observed through the use of ESI, ensuring the visibility of the molecular ion, however, relatively little structural information can be inferred through this technique. This limitation can be overcome by coupling ESI to tandem mass spectroscopy (ESI-MS/MS), resulting in the ability to study proteins from the peptide or even amino-acid residue level.[32]

Tandem mass spectroscopy, commonly referred to as MS/MS, is a technique that fragments precursor ions into product ions, which can be used to reveal structural information about the precursor ion. After ionisation, ions of a specified mass to charge ratio are separated and fragmented, resulting in the formation of product ions, which are then detected.

A range of methods are employed for the fragmentation of precursor ions, with perhaps the two most common being collision induced dissociation (CID) and electron capture dissociation (ECD). These techniques produce different product ions, with CID generating b- and y-ions and ECD forming c- and z- ions respectively (Figure 2.2).

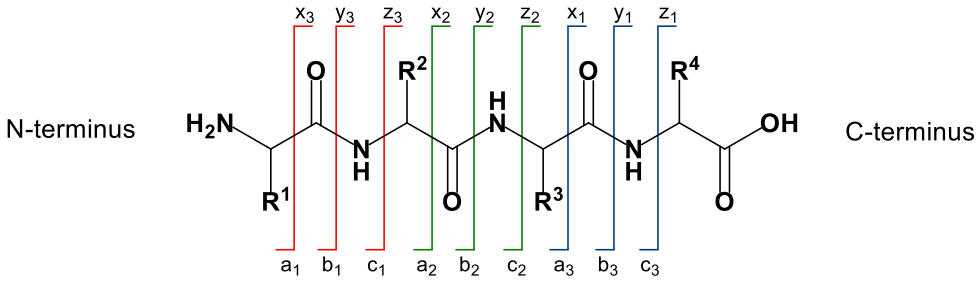


***Figure 2.2**: Ions generated from tandem mass spectrometry.*

Collision induced dissociation (CID) involves the fragmentation of the precursor ions through collision with inert gas molecules.[33,34] As a result of this collision, kinetic energy is converted into internal energy which

subsequently induces bond breakage and fragmentation of the precursor ion.

Electron capture dissociation (ECD) employs a different approach. The separated precursor ions capture low-energy electrons, increasing the internal energy of the ions which results in fragmentation.[34] This activation process is extremely short, which results in direct bond cleavage. Generally the weakest bonds are not preferentially cleaved, resulting in ECD being described as a "non-erdogic" process. The development of both of these tandem mass spectrometric methods has coincided with the use of ESI to study proteins and their interactions.

A key feature of ESI is that information from the solution-phase is retained in the gas phase, allowing the study of non-covalent interactions. Another advantage is that the formation of multiply charged species from larger biomolecules improves the sensitivity of the mass spectrometer's detector. An example of an ESI spectrum is displayed in Figure 2.3, highlighting the multiple charge states of ubiquitin.

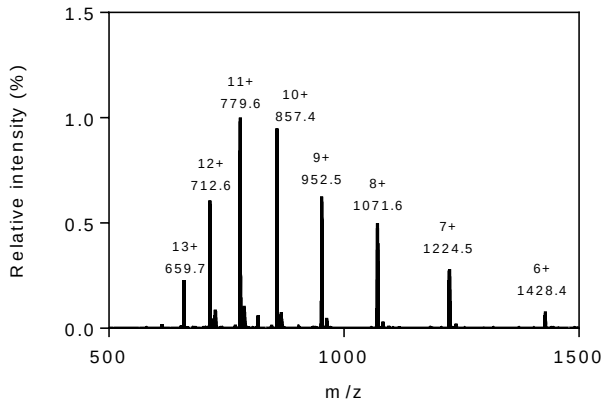


Figure 2.3: *ESI spectrum of ubiquitin with the charge state indicated on each peak.*

The ability to couple ESI-MS with liquid chromatography (LC) is well suited for the quantitative analysis of proteins and peptides and has found multiple applications in the discipline of protein labelling.[32] This technique involves the structural modification of biomolecules to infer information about the structure, topology or activity of the species of interest.

Protein Labelling

In general there are three commonly used forms of protein labelling: Activity based protein profiling (ABPP), affinity labelling and protein footprinting (Figure 2.4).

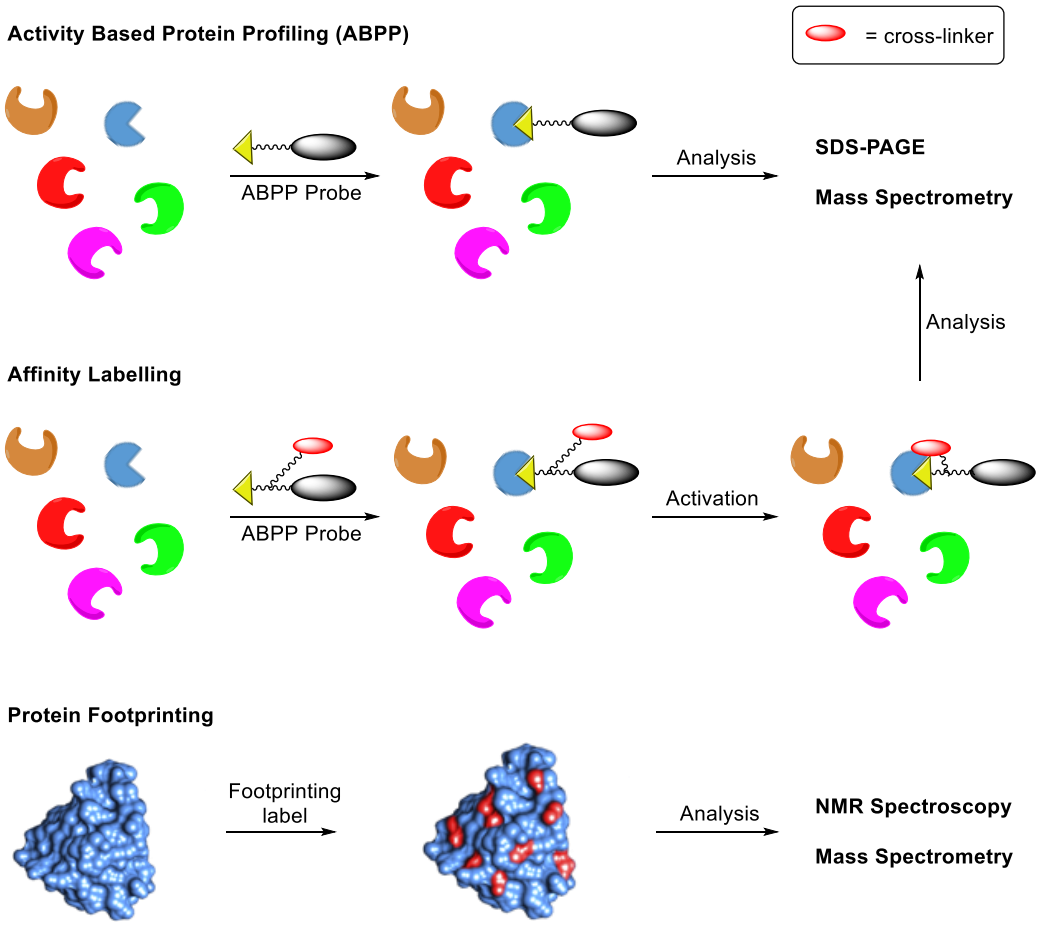


***Figure 2.4**: Visual schematics of ABPP and protein footprinting.*

Activity Based Protein Profiling and Affinity Labelling

As depicted in Figure 2.4, ABPP involves the use of synthetic probes, often analogues of substrates with proven activity, to study specific subsets of enzymes in proteomes and their associated modes of action.[35] ABBP typically targets a fraction of the proteome, which is often mechanistically related.[35]

ABPP probes generally consist of three structural elements: a reactive group, commonly referred to as a warhead, a recognition element and a reporter tag.[35,36] Linkers are often incorporated in the design of the probes, to minimise steric hindrance and impart the required levels of solubility and lipophilicity.[36]

The warhead allows irreversible binding to the protein of interest, and they are commonly electrophilic moieties susceptible to attack from nucleophiles in the active site. The choice of warhead is of paramount importance, with a balance required between the selectivity and reactivity of the ABPP probe.

The recognition element provides selectivity for the subset of enzymes studied, whilst the reporter tag allows for characterization. Reporter tags are commonly fluorophores, biotin or CuAAC precursors.[35]

An example of the use of ABPP is in the study of cysteine proteases. As shown in Figure 2.5, Bogyo's DCG-04 compound combined the 3 key structural elements of an ABPP probe.[37] The reactive warhead was an electrophilic epoxysuccinate moiety, which formed a covalent bond with the enzyme's active site through a nucleophilic cysteine residue. The probe was based on the natural product E-64, which provided the required recognition element, whilst the addition of a biotin group allowed detection.

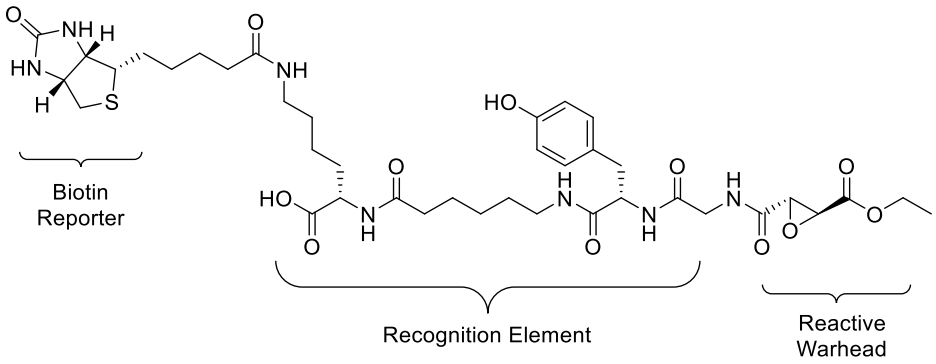


Figure 2.5: *Bogyo's ABBP probe DCG-O4 for the study of cysteine proteases.*[37]

Affinity labelling is a related technique to ABPP, however there are several key distinctions. The affinity probes are often analogues of tight-binding reversible inhibitors of proteins, with the incorporation of a chemical cross linker. Affinity labels require careful design and development to achieve a high level of specificity for the target protein without perturbing the natural binding events and modes of action.

Chemical cross-linkers are employed to form a covalent bond between the affinity probe and the protein of interest. However, unlike ABPP, which often uses an electrophilic warhead, affinity labelling generally utilises photo-reactive moieties (*vide infra*).

PROTEIN FOOTPRINTING

Protein footprinting is an approach where probes are employed to decorate the surface of a protein in a relatively non-specific manner. Analysis of the data collected allows information regarding the structure, conformation or dynamics of the protein studied to be inferred.[38]

The coupling of protein footprinting and mass spectrometry to measure the imparted mass increase has become a powerful technique in probing key biological questions.[39] A diverse range of strategies have been employed to label the protein surface, with techniques spanning from electrolysis to photochemistry.[39]

Undoubtedly, one of the key methods in this field is that of hydrogen-deuterium exchange. First conceived by Linderstrøm-Lang in the 1950's, the technique is based upon the continual exchange of labile NH peptide protons with bulk solution.[40] Therefore, the use of deuterated water as solvent results in the incorporation of deuterium into the protein structure.

Prior to the mid-1990's, the analysis of this technique was undertaken by NMR spectroscopy, however in more recent times this has been superseded in popularity by mass spectrometry.[40,41]

In comparison to NMR, the study of hydrogen-deuterium exchange by mass spectrometry has a series of advantages, notably the significant reduction in mass and concentration of protein required. Additionally, proteins of a substantially larger size can be studied through tandem hydrogen-deuterium exchange mass spectrometry.[42]

As illustrated in Figure 2.6, incubation in deuterated water achieves the desired hydrogen-deuterium exchange. Incorporation of deuterium alters

the mass of the protein by a single mass unit, which is detectable with high degrees of sensitivity through mass spectrometry.[43,44]

The environment of individual N-H bonds has a strong influence on their rate of exchange; solvent exposure and lack of hydrogen bonding results in rapid exchange, whilst N-H bonds in the protein interior can take months to fully deuterate. This results in a technique that is highly sensitive to the nature of the protein structure.[41]

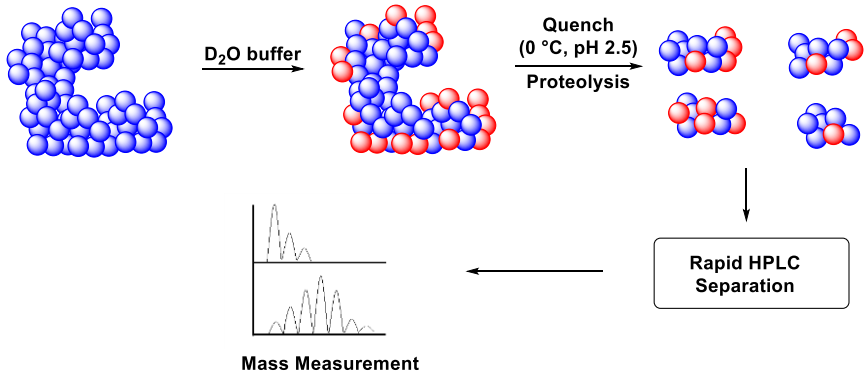


Figure 2.6: *Schematic of the process of hydrogen-deuterium exchange followed by mass spectrometric analysis.*[41]

The potential for back-exchange is a significant drawback to this methodology, however many modifications have been introduced to minimise this undesired effect. The rate of hydrogen-deuterium exchange is strongly dependant on both pH and temperature, and can effectively be "quenched" through cooling and acidification to pH 2.5.[41] Digestion in a protease active at low pH, followed by rapid separation and analysis by tandem HPLC/MS minimises the risk of back exchange.

The formation of stable covalent labels is an alternative to hydrogen-deuterium exchange. Once formed the covalent labels result in a permanent change to the protein structure, the location of which can be isolated and

information inferred. Multiple approaches to this strategy have been employed, varying from site selective to more general labelling techniques.[39,45,46]

The most popular method of achieving more promiscuous labelling is through the use of hydroxyl radicals.[38] This technique is widely used to study protein dynamics and interactions, along with their structure. In contrast to hydrogen-deuterium exchange which probes the peptide backbone, hydroxyl radical protein footprinting mostly labels side chains.[39]

Hydroxyl radicals oxidise amino acid residues that are surface accessible. The small size of the hydroxyl radical results in a similar van der Waal's radius to water, and so can provide high resolution structural information.[39]

Schematically, the work flow for hydroxyl radical footprinting is similar to that of hydrogen-deuterium exchange. The desired protein is first labelled, digested by an appropriate protease and subsequently separated and analysed by LC-MS (Figure 2.7). Crucially, this labelling is irreversible in nature and so no additional precautions regarding pH, temperature and protease selection are required.[38]

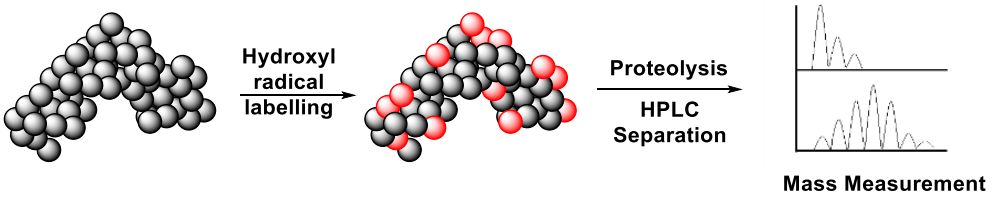


Figure 2.7: *Schematic of the process of hydroxyl-radical footprinting.*[39]

Key to this technique is the formation of the hydroxyl radicals, and a variety of methods have been developed. These include the photolysis of hydrogen peroxide,[20] radiolysis of water,[47] along with the use of chemical reagents.[39]

For example, Fenton's reagent can decompose hydrogen peroxide to hydroxyl radicals *via* transition metal catalysis, notably Fe(II).[48] Whilst this is a low cost experiment, the addition of chemicals such as ethylenediaminetetraacetic acid (EDTA) used in the Fenton system can alter the biological conditions of the samples, and long reaction times can result in undesired secondary reactions.[39]

The ability of hydroxyl radicals to modify amino acids through oxidation allows labelling of a far greater range of substrates than more selective approaches; however, it is not an approach without drawbacks. The rates of labelling vary significantly between amino acids, with glycine not being oxidised.[49] This demonstrates that this technique can't give an exact description of the surface, although it improves significantly on previous techniques. The lifetime of the hydroxyl radical is shorter than that of a conformational change in the protein structure which allows for accurate data on protein dynamics to be collected.[38]

PHOTOACTIVABLE LABELS

Alongside hydrogen-deuterium exchange and the use of hydroxyl radicals for protein footprinting, reagents comprising photo-activated functionality are finding increasing use in the study of protein-protein interactions.

The use of these reagents, upon activation, result in the formation of covalent bonds between probes and biomolecules. The requirements for these photoactivable labels are that they are chemically inert prior to activation, are rapidly activated and that the generated intermediates are highly reactive.[50]

Upon exposure to light, usually ultra-violet (UV), certain functionalities form reactive intermediates which are often radical, carbene or nitrene based.[51] A range of novel photoaffinity labels have been reported, with an early example being the use of *p*-nitrophenyldiazoacetate to label chymotrypsin in 1962.[52] Subsequent developments have included the use of aryl azides **2.01**, benzophenones **2.02** and diazirines **2.03** as the initial precursors, the structures of which are depicted in Figure 2.8.

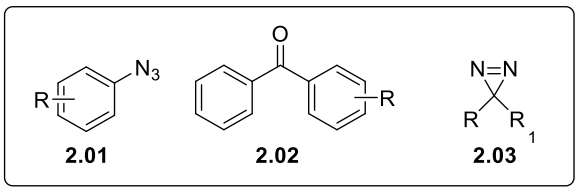
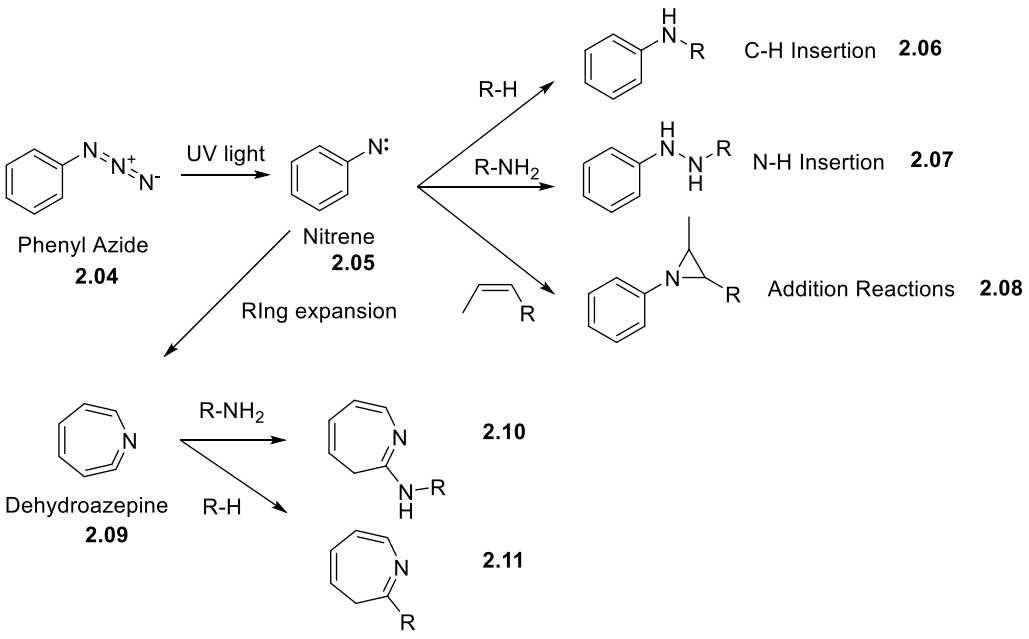


***Figure 2.8**: Photoactivatable labels.*

Upon irradiation, phenyl azide **2.04** initially loses a molecule of nitrogen gas to form a nitrene intermediate **2.05**, which then has the ability to undergo

a range of reactions, as shown in Scheme 2.1. For example, nitrene **2.05** can react directly with molecules containing C-H bonds, nucleophiles such as amines or alkenes, or ring expand to form a highly reactive dehydroazepine **2.09**, which can then react further.[53]

The photochemistry of aryl azides is complicated, with both singlet and triplet states of nitrenes reported.[53] The reaction pathways followed after irradiation are highly dependent on the substituents of the phenyl ring, with extensive investigations undertaken on the reactions of fluorinated analogues.[54]



***Scheme 2.1**: Formation and reactivity of aryl nitrene **2.05**.*

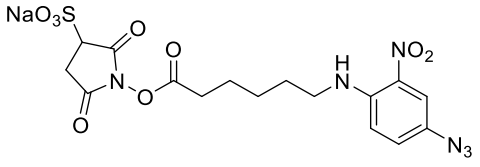
A significant disadvantage of the use of aryl azides for protein labelling are the wavelengths required to activate the compounds into generating the nitrene intermediates. Although the precise wavelength is dependent on the substituents on the aromatic ring, the general range is between 254-400

nm. The high energy nature of these short wavelengths has potential to damage structures of a biomolecular nature.[55]

It has been demonstrated that many aryl nitrenes have half-lives in the range of milliseconds, with insertion into C-H bonds being one of its slower reactions.[56] Additionally, it has been reported that aryl azides are converted to amines by thiols, a potential disadvantage in biochemical studies due to the presence of thiols in some buffer solutions.[57]

In spite of these limitations, aryl azides have still found considerable use in the field of protein labelling, in particular as bifunctional photo-reactive crosslinkers and as the photoactive component of photoaffinity probes.

The commercially available Sulfo-SANPAH (**2.12**) is a pertinent example of a photo-reactive crosslinker, with the small organic molecule containing both *N*-hydroxysuccinimide (NHS) ester and aryl azide functionality (Figure 2.9).

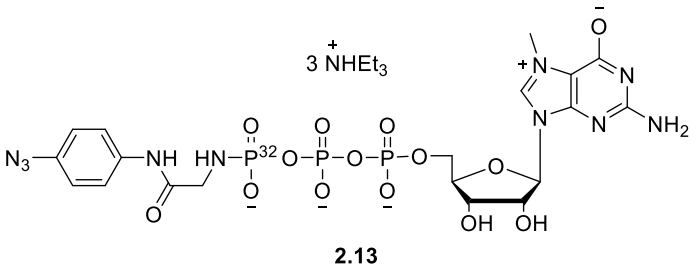


2.12

Figure 2.9: *Sulfo-SANPAH - a water soluble bifunctional photo-crosslinker.*

The NHS ester readily reacts with amino groups in proteins, forming stable amide bonds. Incubation of the formed photoactive precursor with the protein of interest, followed by irradiation, results in the formation of a nitrene, which can then react in a variety of manners described in Scheme 2.1, to form a crosslinked species.

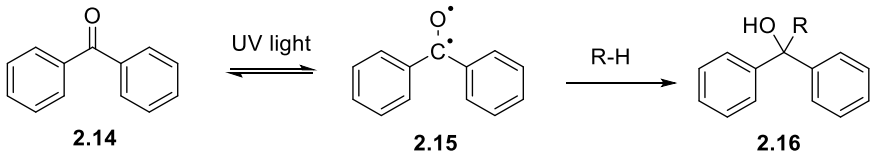
An alternative application of aryl azides is as the photo-reactive component of affinity probes. Rhoads *et al*. designed probe **2.13** for affinity labelling, in combination with a range of additional methodologies in their study of protein synthesis initiation factor eIF-4E.[58]



2.13

Figure 2.10: *Aryl azide ABPP probe utilised by Rhoads et al.[58]*

Of the commonly used photo-reactive groups, the benzophenones **2.14** are the most chemically stable and are known to selectivity abstract hydrogens from C-H bonds upon activation.[50] This advantageous property, combined with the reduced photo-reactivity of benzophenones with water makes it a powerful precursor for photolabelling.[50] However, the steric hindrance of the bulky benzophenone group is likely to perturb protein-protein interactions when in close proximity to the binding site. Additionally, benzophenones require prolonged irradiation times as compared to alternative photo-reactive groups due to a reversible activation mechanism (Scheme 2.2). The prolonged irradiation required has previously been suggested to cause undesired non-specific labelling.[59]

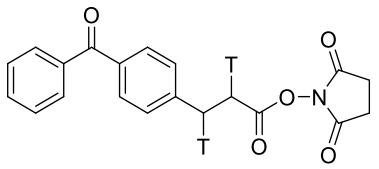


2.14 **2.15** **2.16**

Scheme 2.2*: Reactions of benzophenone* ***2.14****.*

Benzophenones typically form diyl species **2.15** upon irradiation with light in the wavelength range of 350-365 nm, a UV frequency, but of a low enough energy to not interact and disrupt the structure of biomolecules. During irradiation, a triplet excited state is formed *via* rapid inter system crossing from a singlet excited state.[60] The triplet excited state acts as a biradical species, centred on the carbon and oxygen atoms of the carbonyl group, due to its n → π* nature.[61] The formed diyl can then formally insert into an R-H bond through hydrogen abstraction followed by radical combination to form the new carbon-carbon bond, or relax back to the ground state **2.14**.

Benzophenones have been extensively used for a range of applications, for example, Prestwich *et al*. developed compound **2.17** as a photoactivatable cross-linker (Figure 2.11).[62] The incorporation of tritium into **2.17** allowed for the insertion reaction to be detected through radioactivity.



2.17

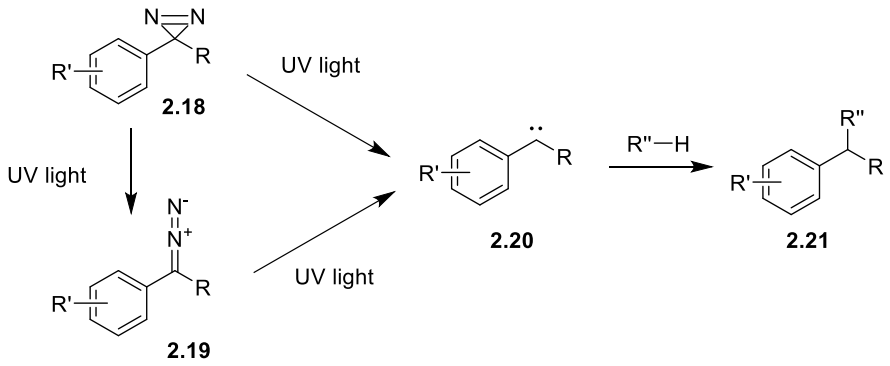
Figure 2.11: *Prestwich's tritium labelled benzophenone crosslinker* ***2.17****.*[62]

Schultz *et al.* demonstrated that, contrary to the requirements of photoactivable labels, benzophenones can react with protein residues prior to activation.[63] In a study unrelated to protein footprinting, Schiff-base formation was noted from the benzophenone ketone moiety, resulting in an increase of potency of the designed inhibitors.[63] Although a positive result

in the work undertaken, this highlighted the potential for undesired reactivity of benzophenones in the field of protein footprinting.

Alongside the use of aryl azides and benzophenones as photoactive labels, diazirines are a class of compounds that have also been the subject of significant research in this area and contain a characteristic three membered heterocyclic ring. The photo-induced reactivity of these molecules is strongly entropically driven, with the release of both ring strain and the formation of a molecule of nitrogen gas.

As Scheme 2.3 shows, absorption of UV light by diazirine **2.18** results in the formation of a reactive carbene **2.20**, either directly or through a diazo intermediate **2.19**. The carbene **2.20** can insert into reactive R-H bonds in a relatively non-specific manner.[64] Crucially, this UV light is at a wavelength above those which can damage proteins and other biomolecules.[65]



Scheme 2.3: *Activation of aryl diazirines.*[66]

Although diazirines are highly efficient photo-labels, there are some associated limitations. Due to the highly strained nature of diazirines both thermal decomposition pathways and sensitivity to ambient light conditions have been reported.[67] It is therefore vital that diazirines are carefully handled to prevent premature photolysis.

Two classes of diazirine containing molecules are described in the literature. Whereas alkyl diazirines offer the smallest steric size, aryl diazirines offer more reliable reactivity of the generated carbene, resulting in reduced intramolecular insertion due to the extra rigidity in the molecule.

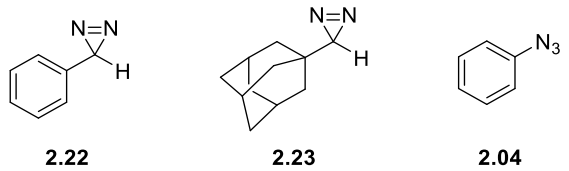
There are two major areas of research in the use of diazirines in bioconjugation. Their use in photoaffinity labels has been extensively reported with applications including the study of protein-protein, ligand-enzyme and ligand-receptor interactions.[55,68]

In addition to photoaffinity labelling, there has been research undertaken in employing diazirines as non-selective labels to helping to elucidate the characteristics of the surface area of proteins.

DEVELOPMENT OF DIAZIRINES FOR USE IN PHOTO-LABELLING

The diazirine moiety fits the previously discussed requirements for a photoactivable group for protein labelling: rapid activation occurs at non-harmful wavelengths, the generated intermediates are extremely reactive and the precursors are chemically stable prior to activation, providing the correct precautions are followed.

In 1978, Bayley and Knowles utilised two separate diazirines for their studies on the labelling of membrane bilayers: 3*H*,3-phenyldiazirine (**2.22**), and adamantanediazirine (**2.23**) (Figure 2.12).[69]



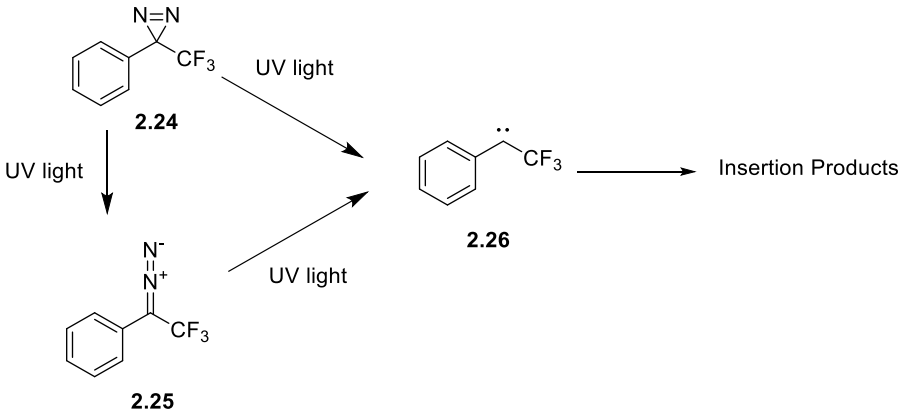
2.22 **2.23** **2.04**

Figure 2.12: *Diazirines utilised for membrane labelling.*[69]

The authors noted that phenylcarbene, formed through the photolysis of phenyldiazirine **2.22**, was a significantly more efficient labelling reagent than phenylnitrene, generated from phenylazide **2.04**.

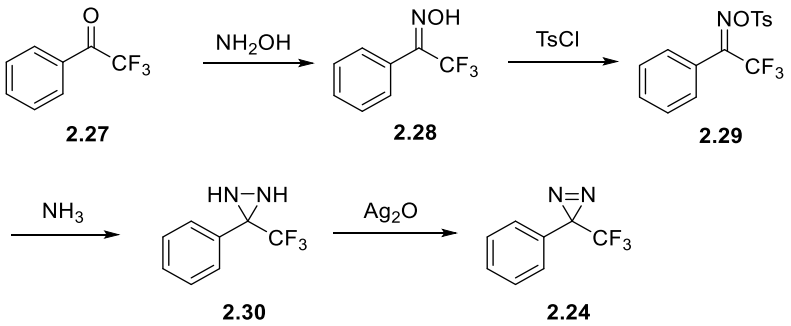
Although the two diazirine reagents successfully formed the carbene for insertion reactions, a significant observed disadvantage was the isomerisation into the linear diazo compound, with approximately 40% of the phenyldiazirine decomposing to the linear form.[69] Although diazo compounds can also be photolysed at a similar wavelength, they are strongly electrophilic and may lead to unwanted side reactions.

Brunner *et al*. investigated diazirines that led to diazo isomers which showed higher levels of stability than the phenyldiazomethane equivalent.[56,70] This led to the development of 3-trifluoromethyl-3-phenyldiazirine (**2.24**), as the diazo isomer, 1-phenyl-2,2,2-trifluorodiazoethane (**2.25**) was shown to have superior stability under acidic conditions as compared to the non-fluorinated analogue (Scheme 2.4).



***Scheme 2.4**: Reactivity of 3-trifluoromethyl-3-phenyldiazirine (**2.24**).*

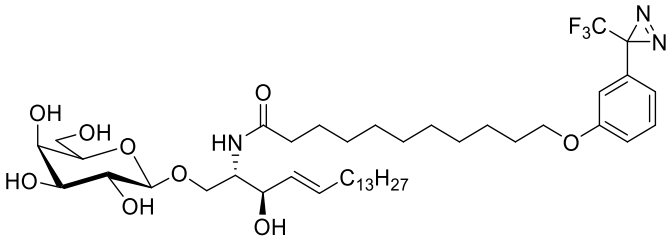
Although the photolysis of diazirine **2.24** doesn't inhibit the formation of the corresponding diazo isomer **2.25**, the increased stability of this species reduces the propensity of undesired side reactions. The reagent can be accessed through a multistep synthetic route as a depicted in Scheme 2.5.



***Scheme 2.5:** Brunner's synthesis of 3-trifluoromethyl-3-phenyldiazirine (**2.24**).[56]*

Brunner *et al*. demonstrated that trifluoroacetophenone **2.27** can be converted to the tosylated oxime **2.29** in two steps. Cyclisation with ammonia, followed by oxidation of the saturated diaziridine **2.30** with silver oxide generated the diazirine **2.24**. Studies revealed that **2.24** is stable at a range of pH and to a range of reaction conditions.[56]

The synthetic route to diazirine **2.24** in Scheme 2.4 has been adapted to allow functionalization of the aromatic ring for a host of applications by numerous groups. For example, Hatanaka and Hashimoto described a variety of reactions to impart additional functionality onto the aryltrifluoromethyldiazirine core and utilised this chemistry to synthesise the photo-reactive galactosylceramide analogue **2.31** as a photoaffinity probe (Figure 2.13).[71,72]



2.31

Figure 2.13: *Hatanaka and Hashimoto's photo-reactive galactosylceramide analogue* ***2.31****.*[72]

In a further investigation on the irradiation of diazirines, a photochemical study was performed by Crocker *et al*. to determine the nature of the generated carbene. The authors concluded that upon irradiation of *p*-tolyl(trifluoromethyl)carbene **2.32**, a triplet ground state **2.34** is formed (Figure 2.14).[73] However, further chemical trapping studies revealed that the carbene reacts through a low-lying singlet state **2.33**.

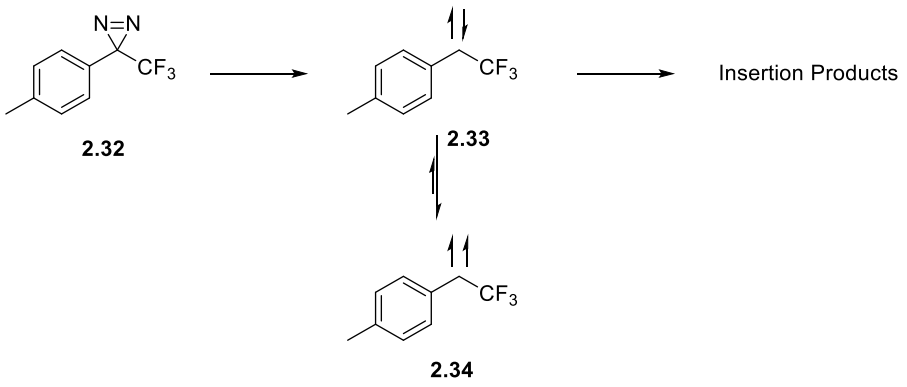


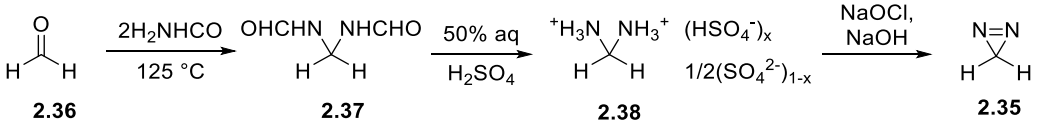
***Figure 2.14**: Photolysis of diazirine **2.32** to form carbenes **2.33** and **2.34**.*

DIAZIRINES IN PROTEIN FOOTPRINTING

Diazirines have also been employed in non-specific protein footprinting, where they are employed to decorate the solvent accessible protein surface. Although both hydrogen-deuterium exchange and hydroxyl radical labelling are highly effective techniques, a method that offers non-selective labelling without the disadvantage of back-exchange would be a useful development.

Delfino *et al*. explored the use of diazirine gas (**2.35**) as a potential protein-footprinting agent.[74] This photo-reactive gas generates the reactive methylene carbene upon irradiation. The size and shape of **2.35** are roughly analogous to those of water, and it was theorised that it may sample the same surface seen by water, and also label non-selectively.[75]

The synthesis of diazirine gas was achieved through a multistep synthetic route (Scheme 2.6). Prolonged heating of a 2:1 mixture of formamide and formaldehyde **2.36** yielded the crystalline methylene bisformamide **2.37**. Subsequent deformylation of **2.37** was achieved under acidic conditions to provide methylenediamine sulfate **2.38** in high yield, and this salt was used as a stable precursor to the final diazirine species.



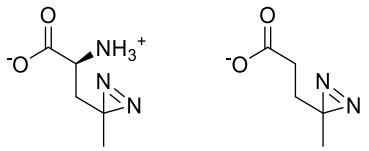
Scheme 2.6: *Delfino's synthesis of diazirine gas* ***2.32****.*[74]

The completion of the synthesis of diazirine gas (**2.35**) was achieved by exposing salt **2.38** to oxidative and basic conditions, with a range of intermediates suggested by Delfino *et al*.[74]

As a demonstration of the protein footprinting method, Delfino *et al*. utilised tritium labelled diazirine gas to study the protein-protein interactions between the complex formed between hen egg white lysozyme (HEWL) and MAb IgG1 D1.3. The study adopted a differential labelling approach, comparing the tryptic peptides of labelled HEWL, both in free form and in a complex and measuring their respective radioactivity. A further extension to this work by the same group utilised methylene labelling to study native and non-native conformation states of a protein.[76]

Unfortunately, labelling with diazirine gas could only be studied at a maximum concentration of 1 mM, and it is known that diazirine gas **2.32** is hampered by aqueous solubility issues.[77] To overcome this limitation, reagents that contained the diazirine moiety but with an enhanced level of water solubility were sought.

The development of the water soluble photo-leucine (**2.39**), a functionalised amino acid and the synthetic 4,4-azipentanoic acid **2.40** made it possible for protein footprinting with diazirines to be undertaken at higher concentrations (Figure 2.15).[68]



2.39 **2.40**

Figure 2.15: *Protein footprinting agents studied by Schreimer et al.*[68]

Schriemer *et al*. employed mass spectrometry to analyse the adducts formed through the irradiation of photoleucine (**2.39**) in the presence of myoglobin and also holo-calmodin (holo-CaM) (Figure 2.16).[68] Both proteins were labelled efficiently, with multiple labels incorporated into the protein structure. It was noteworthy the conformation of the proteins was not distorted upon labelling; a crucial characteristic when generating accurate representations of the protein surface.

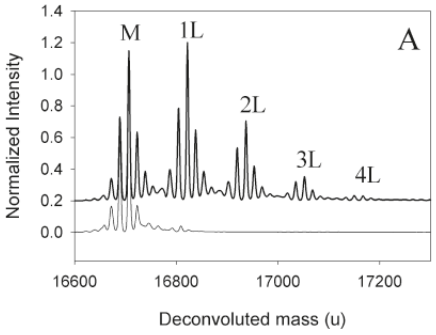


Figure 2.16: *Schriemer's labelling of myoglobin with photo-leucine (**2.39**). Each insertion of a label corresponds to a shift of 115.13 amu. Graphs reproduced from Schreimer et al.[68]*

Extending this study further, Schriemer *et al*. compared the labelling efficiency of photo-leucine (**2.39**) to those expected through methylene labelling.[76] It was concluded that the yield measured for the labelling of holo-CaM with photoleucine is 390 times greater than the equivalent labelling expected from the generation of methylene and the corresponding increase for labelling of myoglobin was 60 times higher.

Non-selective labelling was not achieved, due to the inherent zwitterionic nature of the reagent leading to a certain bias in areas on the protein surface pre-irradiation. However, the authors stated that, in principle, this may allow a range of carbene sources to be developed to give a tuneable selectivity over specific amino acid residues.

A subsequent publication by Schreimer *et al*. explored the concept of tuneable selectivity further, through comparison of the labelling behaviour of two different diazirine precursors: photoleucine (**2.39**) and the synthetic **2.40**.[78]

The authors hypothesised that higher labelling levels than expected had been achieved due to electrostatic interactions between photo-leucine (**2.39**) and amino acid residues resulting in "pre-concentration" on the protein surface prior to irradiation.[78] The amino acid residues where this was particularly marked were glutamate and aspartate residues, where electrostatic interactions between protein carboxylic acids and the amino groups of photoleucine are the cause of this "pre-concentration".

Comparison of the labelling behaviour of the two photo-labels **2.39** and **2.40** at a peptide level confirmed this hypothesis, with dramatically different labelling profiles observed (Figure 2.17). This implied that the substituents on the diazirine probe can be designed to induce changes in the labelling behaviour.

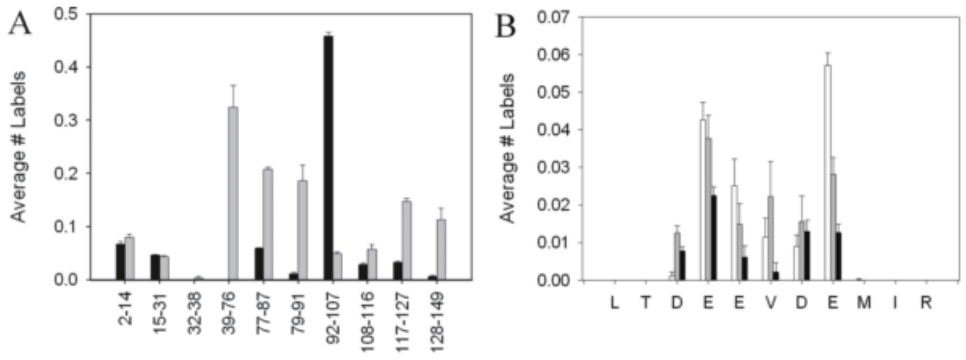


Figure 2.17: *A. Comparison of peptide labelling by differential diazirine labels: Photoleucine (grey bars), 4,4-azipentanoic acid (black bars). B. Influence of temperature on location of carbene labelling: All studies utilise photoleucine. 273 K – (white bars), 195 K – (grey bars), 77 k – (black bars). Graphs reproduced from Schreimer et al.*[78]

Schreimer *et al*. also studied the impact of temperature on protein footprinting. Utilising photoleucine (**2.39**) as the photoactive label, the temperature was varied between 273 and 77 K, with the yields of labelled peptide comparable across the temperature range (Figure 2.17).

It was noteworthy that the distribution of the labels varied considerably with temperature. This was most marked on the valine residue, with the level of labelling increasing significantly with higher temperatures. The authors proposed that this effect was due to the diffusion of the carbene label post-irradiation, suggesting that at higher temperatures, the lifetime of the carbene intermediate is comparable to that of the diffusion limit.[78]

PROJECT HYPOTHESIS AND AIMS

The aim of the work described in this chapter was to employ substituted aromatic diazirines as footprinting agents to elucidate information regarding the surface of proteins. Specifically, it was hypothesised that the use of diazirine probes based on aromatic cores may enhance the level of protein labelling that could be achieved, through a "pre-concentration" hydrophobic effect.

In order to explore the hypothesis of the project, firstly a suitable diazirine probe was needed to be synthesised. As a proof-of-concept study, the footprinting of ubiquitin would then be investigated (Figure 2.18). Solutions containing both the diazirine probe and ubiquitin were irradiated, and analysed by mass spectrometry. The location and extent of labelling could be ascertained, which would allow any labelling selectivity to be determined.

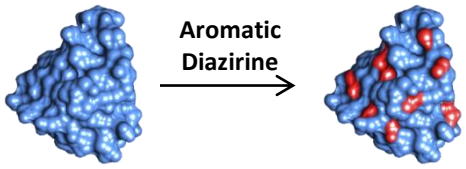


Figure 2.18: *Proposal of protein footprinting with aromatic diazirine probes. Labelling shown in red.*

Additionally, the protein footprinting technique would be extended to the study of protein-protein interactions. The distribution of labelling of the protein, both in its free form and in a complex, would be compared as illustrated in Figure 2.19 in a differential footprinting approach. By highlighting the location of reduced labelling information about the location of binding sites could be obtained.

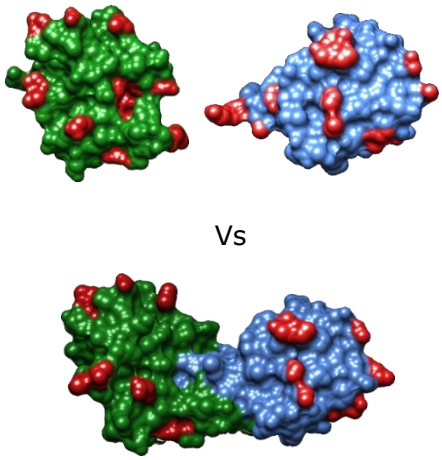


Figure 2.19: *Principle of differential footprinting - Hypothetical labelling reduction in complex (A + B), compared to labelling in protein A (green) and protein B (blue). Labelled regions shown in red.*

The effects of the structure of the diazirine containing label was also investigated. In order to explore how modifications alter labelling efficiency, a selection of aromatic diazirines with varying electronic and steric demands were to be synthesised.

RESULTS AND DISCUSSION

The initial stage of the project was to design and synthesise a diazirine probe that could be utilised for protein footprinting. It was theorised that aromatic diazirines may experience a similar "pre-concentration" effect on the protein surface, particularly around hydrophobic amino acid residues, similar to the effect previously postulated by Schriemer *et al*.[68]

Alongside the aromatic core, the probe design incorporated two additional elements (Figure 2.20). Substitution of the aromatic ring was required to impart the required levels of water-solubility. The trifluoromethyl moiety was also utilised, to reduce any intramolecular rearrangements from occurring during irradiation and to limit unwanted reactions from occurring through the electrophilic diazo isomer.

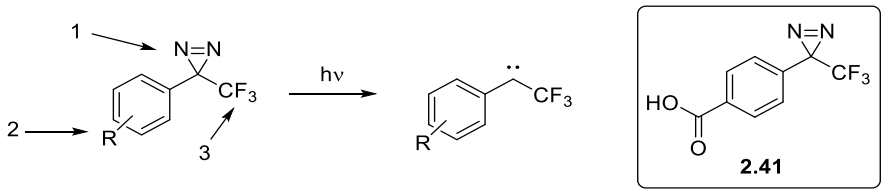
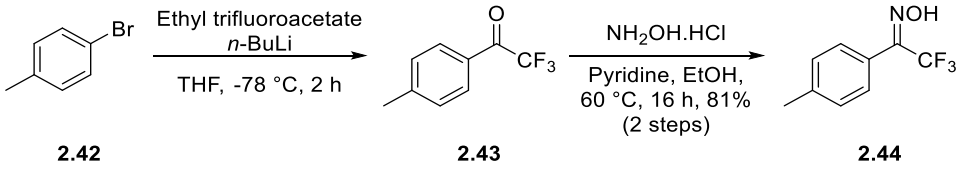


Figure 2.20: *Design of aromatic photo-label* ***2.41****. 1 – diazirine functionality, 2 – substitution to impart water solubility, 3 – trifluoromethyl moiety.*

It was reasoned that the benzoic acid derivative **2.41** would be suitably water soluble and therefore synthesis of this probe was undertaken.

SYNTHESIS OF AROMATIC DIAZIRINE LABEL

The synthesis began by the implementation of a lithium-halogen exchange using *n*-BuLi on 4-bromotoluene **2.42**, with the aryl lithium species trapped with ethyl trifluoroacetate, resulting in conversion to the trifluoromethylketone **2.43** (Scheme 2.7).[79]



***Scheme 2.7**: Two-step synthesis of oxime **2.44**.*

Interestingly, the use of ethyl trifluoroacetate to react with the aryl lithium species resulted in the formation of the ketone, whereas reactions of organometallic species with esters classically give tertiary alcohols.[80] Creary *et al*. proposed that the tetrahedral intermediate **2.46** formed is stabilised *via* inductive effects of the CF_3 group, either by raising the energy barrier for the displacement of the ethoxy group, or by reducing the net negative charge on the anionic oxygen.[80] (Figure 2.21).

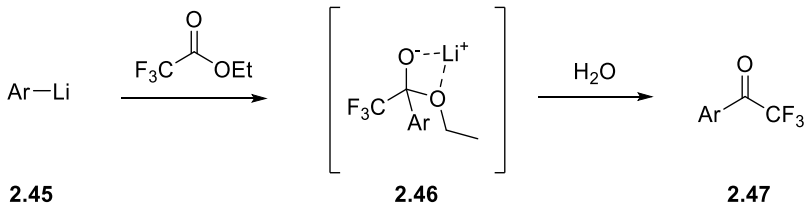
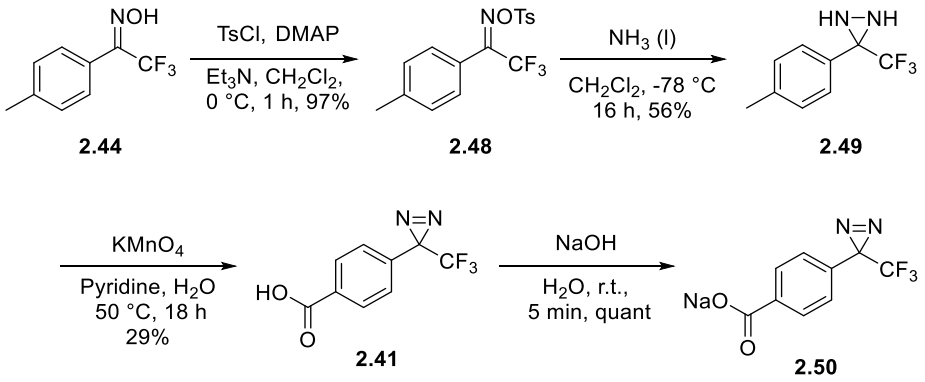


***Figure 2.21:** Formation of trifluoromethylketone **2.47** through a stabilised tetrahedral intermediate **2.46**.*

Purification of the trifluoromethylketone **2.43** proved problematic and so the crude ketone was directly converted into the corresponding oxime **2.44**, as a mixture of *E*- and *Z*- isomers.

Following Nassal's synthetic route to diaziridine **2.49**, oxime **2.44** was tosylated and the crude product **2.48** reacted directly with liquid ammonia to afford the diaziridine **2.49** (Scheme 2.8).[81]



Scheme 2.8: *Synthesis of carboxylic acid diazirine **2.50**, following a modification of Nassal's protocol.*[81]

Dual oxidation of the diaziridine and methyl moieties of **2.49** resulted in the formation of diazirine **2.41** in a modest yield (Scheme 2.8). To improve the water solubility of the diazirine for use in protein labelling, it was converted to the corresponding sodium salt **2.50**.

PROTEIN LABELLING WORK FLOW

The efficiency of diazirine **2.50** as a protein label was next studied. The work flow, as illustrated in Figure 2.22, highlights the key stages in the protein footprinting method.

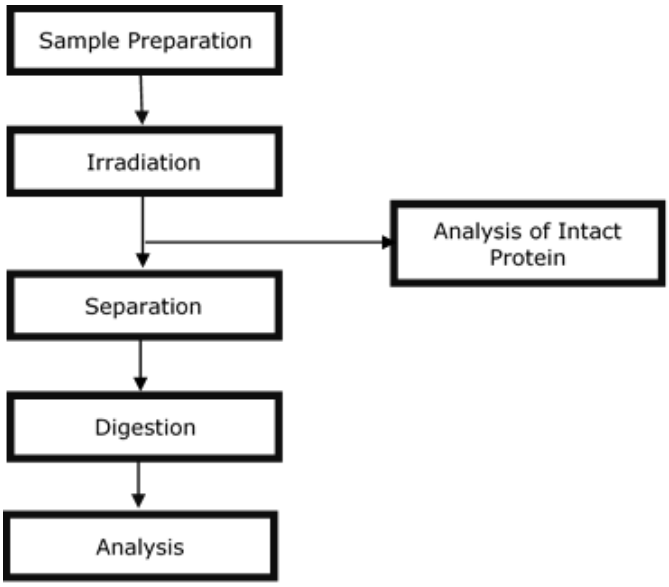


***Figure 2.22**: Protein footprinting work flow.*

Following the protocol developed by Schriemer, small volumes of solution containing both the target protein and diazirine **2.50** were prepared.[68] Typically, a large excess of the diazirine **2.50** (80 mM) was used in comparison to the protein (100 μM), in an attempt to generate high levels of labelling onto the protein surface.

Aliquots of the solution were subsequently flash frozen, to minimise migration of the *in situ* formed carbenes, and irradiation performed using a neodymium-doped yttrium lithium fluoride (Nd:YLF) laser. Dependant on the nature of the protein studied, two options were then available. If the

protein was of a sufficiently low molecular weight then mass spectroscopic analysis could be performed on the intact protein.

However, if further information about the location of labelling was required, then a purification and digestion stage were also needed. The purification and separation were performed over SDS-page and the spliced bands subsequently digested into their constituent peptides through selection of an appropriate protease.

Following digestion, analysis of the peptides was performed by mass spectrometry. Utilising tandem mass spectrometry, the labelling of a protein could be detected at an amino-acid level of resolution.

With both diazirine **2.50** and a suitable work flow developed, the labelling behaviour of **2.50** was next investigated. Ubiquitin was selected as a model protein, due to its well characterised nature allowing a comparison between known techniques and the developed diazirine technology.

UBIQUITIN LABELLING

Ubiquitin is an important 8.5 kDa regulatory protein, found in almost all eukaryotic cells, which performs a vast range of functions.[82] The small, 76 residue protein has a range of binding regions, which makes it a suitable substrate for investigations into protein footprinting (Figure 2.23).

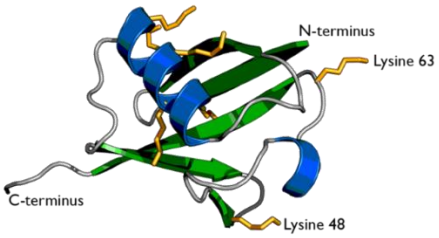


***Figure 2.23**: Structure of Ubiquitin.*

To determine whether protein footprinting of ubiquitin with diazirine **2.50** could be achieved, a stock solution was prepared, consisting of 80 mM of the diazirine **2.50** and 100 μM of ubiquitin. Following the previously described work-flow, 5 μL aliquots of the freshly prepared solution were flash-frozen and irradiated for 16 s with a Nd:YLF laser at 355 nm.

The irradiated samples were subsequently analysed by LC-MS, which confirmed successful labelling of the protein surface. The extent of labelling was determined through the study of the mass spectrum. Use of electrospray ionisation (ESI), resulted in ubiquitin appearing as a series of multiply charged peaks.

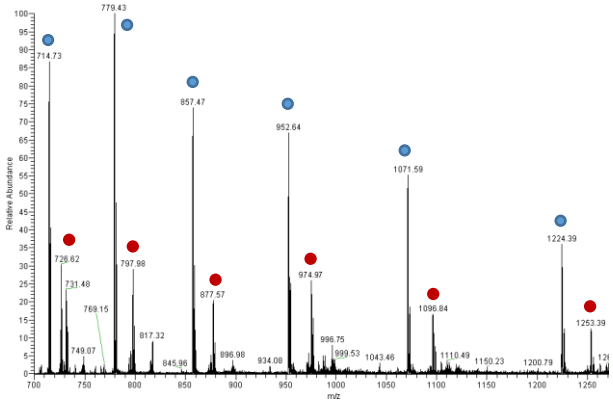


Figure 2.24: *Photo-labelling of ubiquitin with diazirine* ***2.50****. Blue = unlabelled ubiquitin; Red = labelled ubiquitin.*

Figure 2.24 clearly shows the charge states of ubiquitin, along with the corresponding labelled peaks, which indicated the incorporation of the footprinting label into the protein structure. The labelled peak is shifted from the non-labelled by a difference of +202.02 amu, corresponding to the mass of diazirine **2.50** after loss of N_2. Closer investigation of the 9+ charge state unveiled new information about the photo-labelling process.

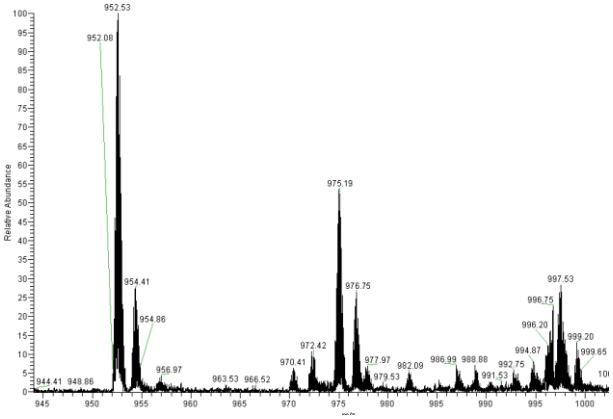


Figure 2.25: *Photolysis of diazirine* ***2.50*** *in the presence of ubiquitin. Figure displays the +9 charge state of ubiquitin.*

The peaks directly adjacent to both the ubiquitin and labelled ubiquitin peaks correspond to oxidation products. The amino acid methionine, of which there is one in the ubiquitin structure, contains a sulfide functional

group that can be oxidised to the corresponding sulfoxide. Whether the oxidation was caused directly by the presence of diazirine **2.50**, the photolysis conditions or due to other factors is unknown.

In order to map the level of labelling on various amino acid residues, first the protein needed to be digested into smaller peptides. This is due to the efficiency of MS/MS analysis diminishing further into the peptide; therefore a balance is required between a peptide being large enough to be distinguishable from the background noise, but small enough to generate data of an acceptable quality for analysis.

Asp-N was selected as a suitable protease for ubiquitin proteolysis, with the C-terminal peptide formed containing residues involved in 3 separate binding areas. Asp-N is an endoproteinase which selectively hydrolyses peptides on the *N*-terminal side of both cysteic and aspartic acid residues. Proteolysis of ubiquitin yields a C-terminal peptide of DYNIQKESTLHLVLRLRGG; a sequence containing 19 amino acid residues.

Samples of photolysed ubiquitin were purified by gel electrophoresis. The purified protein band was then digested using Asp-N and the peptides studied by LC-MS.[83]

Analysis of the spectra generated from the relevant section of the chromatogram, corresponding to the elution of the labelled and unlabelled peptides showed a major peak at 553.81. Upon closer inspection (Figure 2.26), this proved to correspond to the 4+ charge state of the target C-terminal peptide. The peak at 604.32 is the complementary labelled peptide, also in the 4+ charge state.

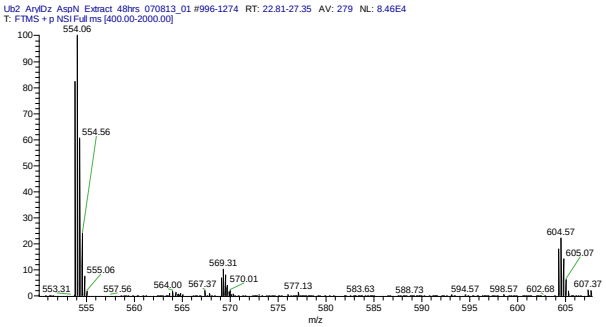


Figure 2.26: *The labelled and unlabelled C-terminal peptide of ubiquitin after photolysis with diazirine* ***2.50****.*

After confirmation that the C-terminal peptide in both its unlabelled and labelled forms could be easily visualised by LC-MS, LC-MS/MS was then undertaken on the labelled peak using electron-capture dissociation (ECD) as the method of fragmentation. As previously described, ECD is a method of fragmenting gas phase ions by the direct introduction of low energy electrons to trapped ions.[84]

The intensities of the labelled fragment peaks were compared to that of the corresponding unlabelled peaks for the z-ions of the peptide. This allowed the fraction of the peptide labelled to be determined at each point throughout the peptide (Table 2.1).

From this analysis, it was observed that the ratio of labelled to unlabelled peaks increased rapidly amongst the early leucine residues, with the fractional labelling not changing drastically towards the *N*-terminus of the peptide. At this point, it was noted that certain fragment ions did not appear in the mass spectrum, either in the labelled or unlabelled form and so these residues were combined with the adjacent amino acids.

Amino Acid Residue	***f(zi) mod***	***Labels/Residue***
D	1.00	0.00
Y	1.00	0.00
N	1.00	0.00
I	1.00	0.02
Q	0.98	0.01
K	0.97	-0.01
E	0.98	-0.01
S	0.99	0.02
T	0.97	-0.03
L	1.00	0.12
H	0.88	0.09
LV	0.78	0.50
L	0.28	-0.05
R	0.34	0.21
L	0.13	0.04
RG	0.09	0.09
G	0.00	0.00

Table 2.1: *Labels per residue on the C-terminal peptide of ubiquitin labelled with* ***2.50****.*

Further analysis of the data allowed the labels per residue to be plotted (Figure 2.27).[68] The graph highlighted that there is indeed selectivity over carbene insertion, with significant labelling around the basic histidine (H68) and arginine (R72 and R74) as well as the hydrophobic leucine (L69) and valine (V70) residues. Due to the acidic and aromatic nature of the diazirine label employed in this study, it is perhaps unsurprising that the basic and hydrophobic residues were preferentially labelled.

This result contrasted with the observations of Schriemer *et al*. where the use of photoleucine as a protein footprinting probe demonstrated preferential insertion into glutamic and aspartic acid residues.[78]

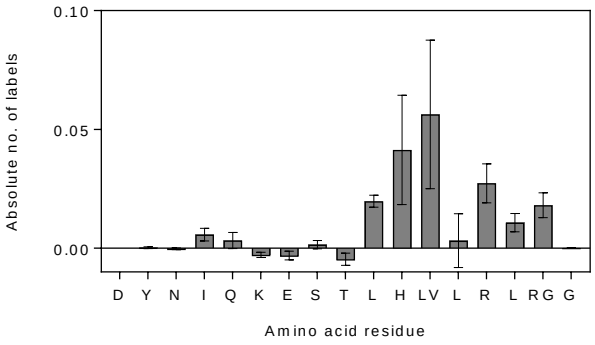


Figure 2.27: *Labels/residue for each amino acid residue in the C-terminal Ub peptide (58-76) highlighting preferred location of carbene insertion.*

DIFFERENTIAL LABELLING OF A UBIQUITIN COMPLEX

The C-terminal diglycine motif of ubiquitin is known to bind with the zinc finger ubiquitin binding domain (ZnF UBP) from isopeptidase T (IsoT) (Figure 2.28).[85] As it had been established that protein footprinting of ubiquitin with diazirine **2.50** showed labelling on the diglycine motif, it was hypothesised that the Ub-IsoT ZnF complex would be a suitable system to study further in a differential footprinting approach.

Binding at the C-terminal ubiquitin residues should lower the associated surface accessible area and subsequently inhibit the extent of footprinting with diazirine **2.50**. To investigate the interaction of the Ub-IsoT ZnF complex, the footprinting profile of the C-terminal peptide of ubiquitin in the free protein and the complex was compared.

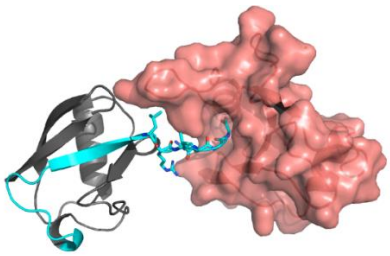


Figure 2.28: *X-ray crystal structure of Ub (grey/cyan) in complex with the IsoT ZnF UBP. PDB code: 2G45.*[85]

To generate the required labelled peptide, a solution of the Ub-IsoT ZnF complex (100 μM Ub, 100 μM ZnF UBD) was irradiated in the presence of diazirine **2.50** (80 mM). The photolysed samples were subsequently purified and digested by the previously established procedure to yield the required peptides.

Following analysis of the C-terminal labelled peptide peak by LC-MS/MS, the intensities of the labelled and unlabelled peaks for each fragment were studied, and the absolute labels per amino acid residue calculated (Figure 2.29).

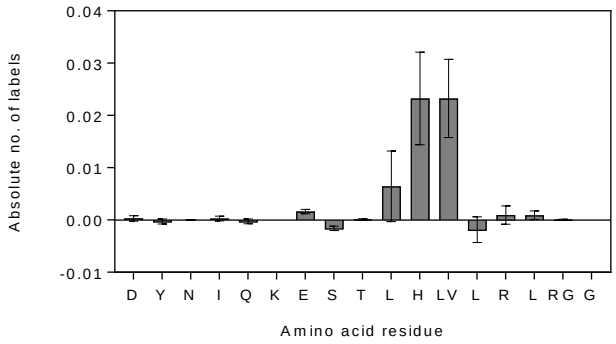


Figure 2.29: *Labels/residue for each amino acid in the C-terminal Ub peptide (58-76) highlighting preferred location of carbene insertion in an Ub-IsoT ZnF complex.*

The absolute level of labelling decreased compared to unbound ubiquitin, which is perhaps not surprising due to the lower surface accessible area in the Ub-IsoT ZnF complex. Plotting the absolute level of labels per residue for the ubiquitin peptide whilst photolysed in the presence of the IsoT ZnF, against the unbound ubiquitin gave Figure 2.30.

In this plot, it is clear that although the majority of the carbene label inserted into the central leucine, valine and histidine residues in both free and complexed ubiquitin, there was a significant decrease in the labelling seen towards the C-terminus of the peptide chain, strongly suggesting an obscuring of the surface accessible region of these residues caused by binding.

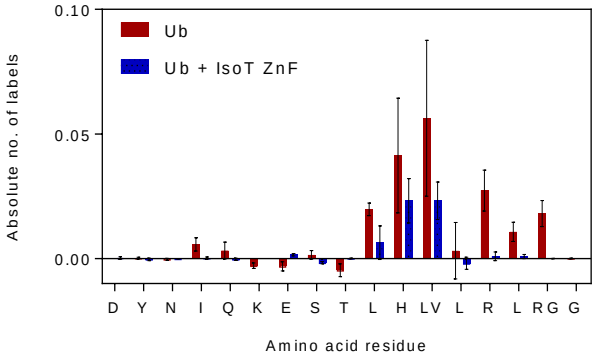


Figure 2.30: *Labels/residue for each amino acid in the C-terminal Ub peptide 58-76 Blue = Ub alone; Red = Ub + ZnF UBD from an initial concentration of 80 mM* ***2.50*** *and 100 μM ubiquitin.*

Plotting the data as the fractional difference in labelling highlighted the extent of the reduction of labelling in the known binding region (Figure 2.31). Although the overall labelling was diminished, the fractional level of modification only varied significantly on the C-terminal residues (L71-G76), indicating a masking of these positions in the Ub-IsoT ZnF complex.

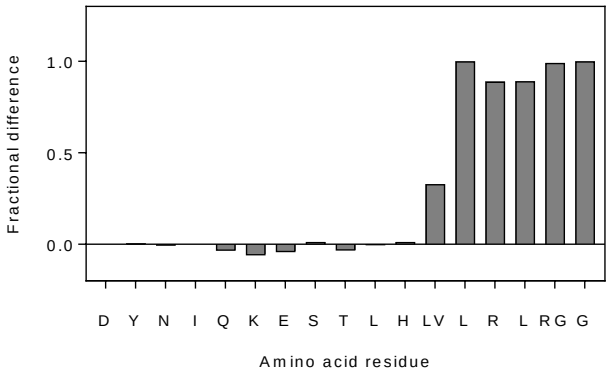


Figure 2.31: *Fractional differential labelling of Ub in the presence and absence of the ZnF UBD (C-terminal peptide, residues 58-76).*

The data collected correlated well with the crystal structure of this complex, which confirmed that the diazirine probe could be employed to study protein-protein interactions.[85] Having established that diazirine **2.50**

successfully footprinted the surface of ubiquitin, the next development was to optimise the labelling conditions.

OPTIMISATION OF LABELLING CONDITIONS

To improve the efficiency of the labelling procedure, the concentration of label **2.50** and length of irradiation were varied. Initially, the concentration of the diazirine label **2.50** was investigated. Previously, Schriemer *et al*. had found that the labelling of the protein holo-calmodulin with photoleucine (**2.39**) increased linearly with increasing concentrations of diazirine.[68] In this study, ubiquitin was employed as the protein, with irradiation occurring with varying concentrations of diazirine **2.50** (Figure 2.32).

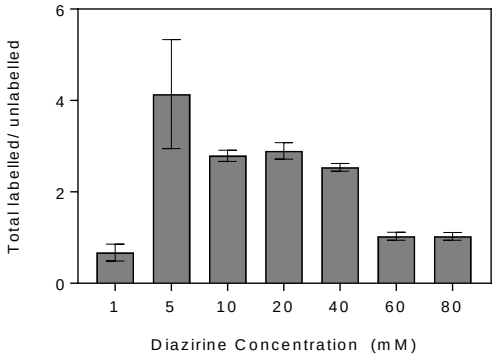


Figure 2.32: *The variation in labelling of Ub with concentration of diazirine* ***2.50****.*

The results obtained contrasted with those of Schriemer, with no linear increase in labelling observed.[68] Instead, a concentration curve was noted, with initial increase of label incorporation, peaking at 5 mM, before a gradual decrease of labelling with increasing concentration. It was postulated that although the expected initial increase was simply due to additional diazirine **2.50** being present, the subsequent decrease was caused through intermolecular interactions of **2.50**. The nature of these interactions is unknown, although π-stacking of the aromatic rings would result in stabilisation of the hydrophobic label in the aqueous solution.

The efficiency of the synthesised label **2.50** was compared against commercial photoleucine (**2.39**) at both 5 mM and 80 mM concentrations (Figure 2.33). The aromatic diazirine **2.50** was shown to label ubiquitin significantly more efficiently at both concentrations. It was theorised that this was due to a "pre-concentration" effect, where the diazirine probe **2.50** is closely associated to the hydrophobic regions on the protein surface before irradiation. Increased "pre-concentration" of the aromatic **2.50**, compared to photoleucine (**2.39**) would explain the substantial increase in labelling efficiency.

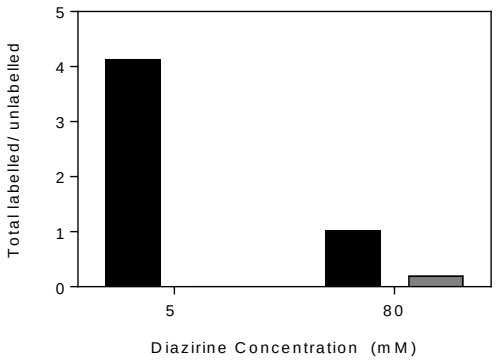


Figure 2.33: *The variation in labelling of Ub with concentration of diazirine* ***2.50*** *(black) and photoleucine (****2.39****) (grey).*

The duration of irradiation was next varied, with the extent of footprinting measured over a time frame of 2 to 16 seconds. Analysis of the generated spectra suggested that the previously utilised 16 seconds was sufficient to achieve maximum labelling, with no significant degradation of the covalent labels noted (Figure 2.34).

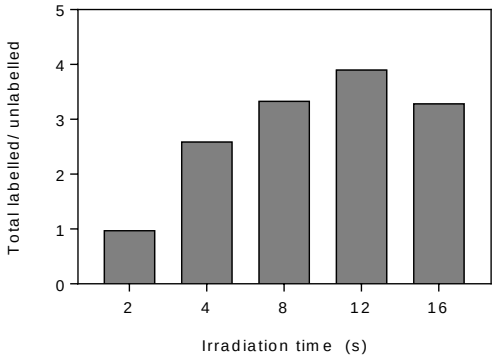


Figure 2.34: *Effect of varying irradiation time on the labelling of Ub with diazirine* ***2.50****.*

With confirmation that the level of label incorporation did not increase linearly with concentration of diazirine **2.50**, the study of the model Ub-IsoT ZnF (100 μM Ub, 100 μM ZnF UBD) was re-examined with 5 μM of diazirine **2.50**. Following the previously described workplan, the relevant C-terminal peptides of ubiquitin were analysed by tandem mass spectrometry, with ECD selected as the fragmentation method.

As illustrated in Figure 2.35, irradiation in the presence of a significantly lower concentration of diazirine **2.50** successfully highlighted the interaction at the C-terminal residues of ubiquitin. Although the general trend observed agreed with the data obtained for irradiation of 80 mM **2.50**, subtle differences in the labelling behaviour were noted.

For instance, the observed labelling at the histidine residue was markedly lower as compared to labelling at 80 mM, although the nearby leucine residues experienced a corresponding increase in label incorporation. Despite these subtle differences in labelling distribution, the fractional difference between the irradiation of free ubiquitin and the IsoT ZnF complex showed complete inhibition of labelling on the C-terminal residues, which corresponds to the known binding site of IsoT ZnF with ubiquitin.[85]

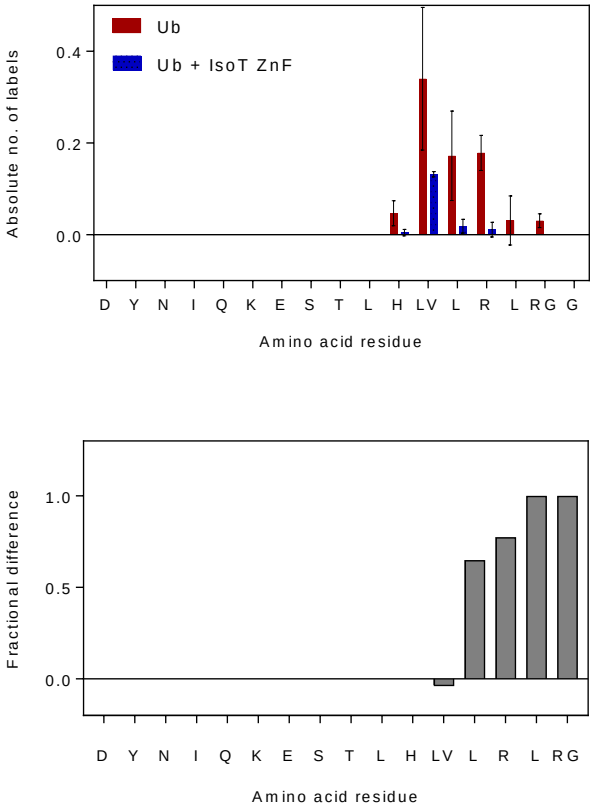


Figure 2.35: *Labels/residue for each amino acid in the C-terminal Ub peptide 58-76 Blue = Ub alone (3 repeats); Red = Ub + ZnF UBD (2 repeats) from an initial concentration of 5 mM* ***2.50*** *and 100 μM ubiquitin.*

Electron-capture dissociation (ECD) was used as the preferred fragmentation method for the tandem mass spectrometry undertaken in this study, allowing the determination of label incorporation at an amino-acid level of resolution. However, inefficient fragmentation of the labelled ubiquitin C-terminal peptide peak was noted during our studies (Figure 2.36). Although sufficient coverage of the peptide was achieved to determine the location of footprinting, the non-fragmented ion remained the most prominent in the mass spectrum.

Collision-induced dissociation (CID) is an alternative technique for tandem mass spectrometry.[33] The application of CID to the labelled C-terminal peptide of ubiquitin resulted in complete fragmentation of the precursor ion.

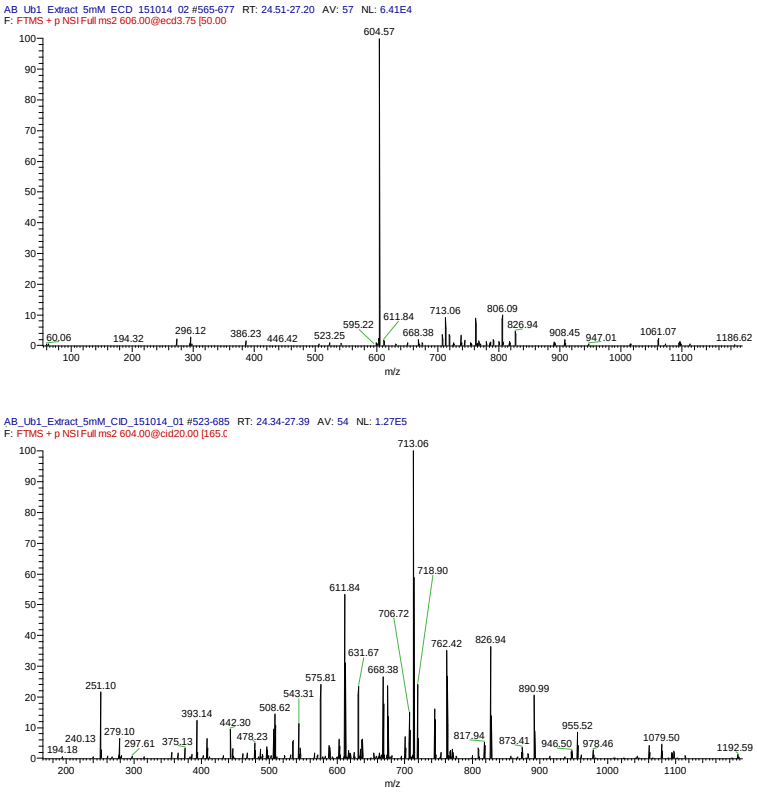


Figure 2.36: *Tandem mass spectrometry of the C-terminal peptide of ubiquitin after irradiation with diazirine* ***2.50****. Top) ECD fragmentation; Bottom) CID.*

The use of the CID technique generated fragment ions of a significantly higher intensity than ECD. CID is an 'ergodic' ion activation method, which results in the cleavage of the weakest bonds first, producing b and y ions, rather than the c and z ions formed through ECD.[34]

Figure 2.37 shows the distribution of label incorporation after analysis of the spectra generated through CID tandem mass spectrometry. Although the intensity of the fragment ions were substantially higher in magnitude than through the use of ECD, the coverage of the C-terminal peptide was diminished.

Minimal information could be extracted regarding the C-terminal peptides (RLRGG), due to the absence of the corresponding B and Y daughter ions in the mass spectrum. Attempted further fragmentation did not yield the

required daughter ions to probe the C-terminal residues. It was concluded that with the study of the Ub – IsoT ZnF complex, although the data from CID fragmentation did imply a reduction of labelling towards the C-terminus of the investigated peptide, the greater coverage provided by ECD resulted in a clearer analysis.

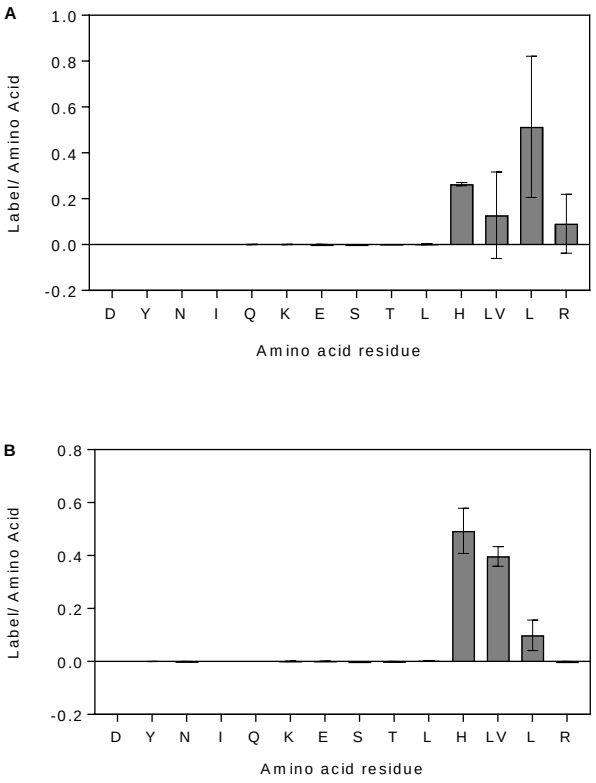


Figure 2.37: *Labels/residue for each amino acid in the C-terminal Ub peptide 58-76 irradiated in 5 mM* ***2.50*** *and 100 μM ubiquitin. A – Free Ub; B – Ub + IsoT ZnF. MS/MS analysis by CID, based on two repeats.*

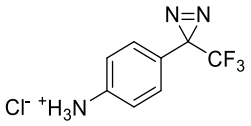
Although the use of CID did not provide the coverage needed to fully observe the binding of ubiquitin and IsoT ZnF, the information gained from CID was still informative. Neither of the employed fragmentation techniques resulted in cleavage of the label, suggesting that in future studies, both approaches can be used in a complementary approach to maximise coverage of the protein surface.

Having established that the synthesised anionic diazirine **2.50** was substantially more efficient than the amino acid derivative photoleucine (**2.39**), and that the probe could be utilised to study protein-protein interactions, the synthesis of alternative probes was next investigated.

It was proposed that variation of the electronics and sterics of aromatic diazirine probes could be used to improve labelling efficiency, and also alter the selectivity observed by **2.50** for basic, hydrophobic residues.

SYNTHESIS OF A CATIONIC DIAZIRINE LABEL

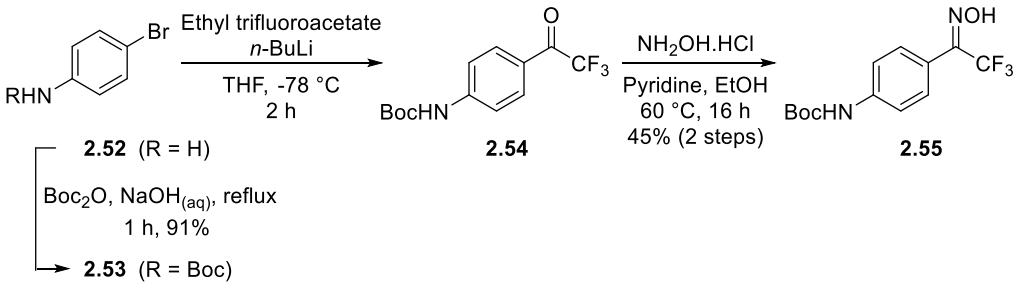
To complement the investigations undertaken with the anionic diazirine label **2.50**, a cationic equivalent was targeted. The initially pursued strategy involved the synthesis of an anilinium chloride derivative **2.51**.



2.51

***Figure 2.38**: Proposed cationic diazirine **2.51**.*

A substituted aniline was selected to improve the aqueous solubility of the diazirine label, however the use of this moiety required a protecting group. The synthesis of **2.51** began with the Boc protection of 4-bromoaniline (**2.52**) under basic conditions. Analogous to the synthesis of **2.50**, the aryl bromide **2.53** was lithiated with *n*-BuLi and quenched with ethyltrifluoroacetate, yielding the trifluoromethylketone **2.54** (Scheme 2.9).



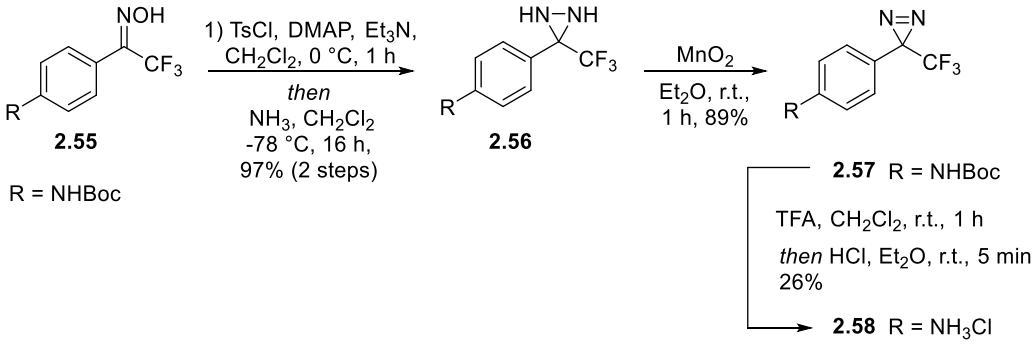
***Scheme 2.9**: Formation of oxime **2.55** from 4-bromoaniline **2.52**.*

To overcome the previously encountered issues with the purification of trifluoromethylketones, the crude ketone **2.54** was directly reacted with

hydroxylamine hydrochloride. The oxime **2.55** was isolated in a modest 45% yield over the two steps, suggesting poor initial conversion into the trifluoromethylketone **2.54**. It was likely that this was due to unwanted side reactions with the amine protecting group.

Tosylation of oxime **2.55** was followed by an ammonia-mediated cyclisation without purification of the intermediate tosylate. An excellent isolated yield was achieved over two steps, which provided the diaziridine **2.56** (Scheme 2.10).

Following the procedure of Barton *et al*., manganese dioxide was employed as the oxidant for the conversion of **2.56** into the diazirine **2.57**.[86] The simple purification and high yield obtained represented a significant improvement over the previously utilised *t*-BuOCl oxidation.



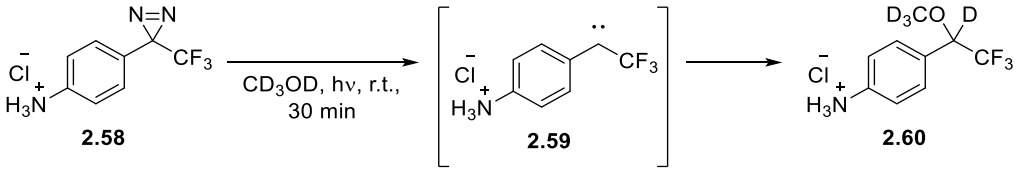
***Scheme 2.10**: Conversion of oxime **2.55** to diazirine **2.58**.*

Deprotection following the conventional trifluoroacetic acid/dichloromethane solvent system and subsequent salt formation using hydrogen chloride gave the water soluble diazirine **2.58**.

Next, the labelling behaviour of **2.58** was investigated. As an initial test, an aqueous solution of **2.58** (80 mM) and ubiquitin (100 μM) was prepared.

The solution was flash frozen, irradiated and analysed by LC-MS. Unfortunately, analysis of the mass spectrum showed no presence of labelled protein, with only unlabelled ubiquitin detected.

To investigate this surprising behaviour further, the irradiation of **2.58** in deuterated methanol was monitored by ^{1}H NMR spectroscopy. The irradiation of diazirine **2.58** in the presence of deuterated methanol should result in the rapid formation of carbene **2.59**, followed by insertion into the methanol O-D bond, forming the methyl ether **2.60** (Scheme 2.11).



***Scheme 2.11**: Proposed reactivity of **2.58** under ultraviolet irradiation.*

The ^{1}H NMR spectrum recorded pre-irradiation showed a set of roofing doublets in the aromatic region between 7.40 and 7.50 ppm (Figure 2.39). The sample was then irradiated with UV light for 30 minutes and analysed by ^{1}H NMR. An array of new aromatic proton environments were observed, suggesting that clean conversion into the methyl ether **2.60** had not been achieved.

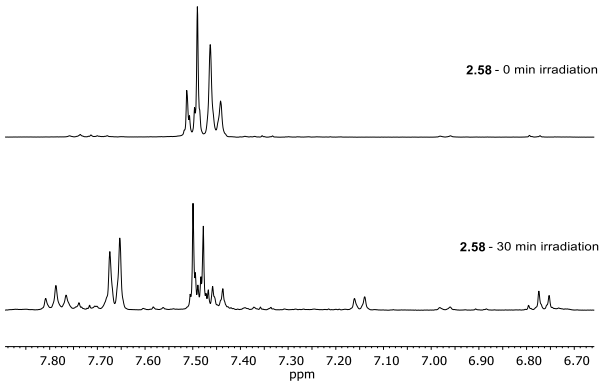
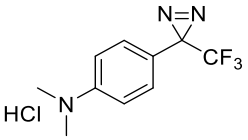


***Figure 2.39**: ^{1}H NMR study of irradiation of **2.58** in CD_3OD.*

A potential explanation for this undesired reactivity was the presence of free N-H bonds. In principle, it is possible for the carbene **2.59** to react with diazirine **2.58** to create unwanted oligomeric side-products. The proposed intermolecular reaction may have resulted in the lack of labelling onto the ubiquitin surface.

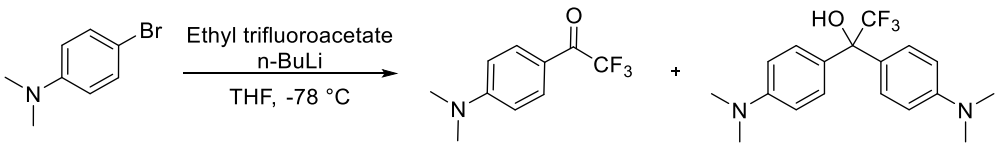
We therefore elected to synthesise an analogue of **2.58**, without free N-H bonds, based on a *N*,*N*-dimethylaniline moiety. The diazirine would be converted the hydrochloride salt **2.61** to increase water solubility (Figure 2.40).



2.61

Figure 2.40*: N-methylated aniline diazirine* ***2.61****.*

It was proposed that the diazirine **2.61** could be synthesised through an analogous reaction sequence to **2.58**, without the requirement of a protecting group. However, the conversion of bromoaniline **2.62** to the corresponding trifluoromethylketone **2.63** proved to be a difficult and capricious transformation. Under the conditions reported by Creavy (*n*-BuLi at −78 °C) the reaction proved unreliable, producing a mixture of mono **2.62** and double **2.63** addition products (Scheme 2.12).[80]

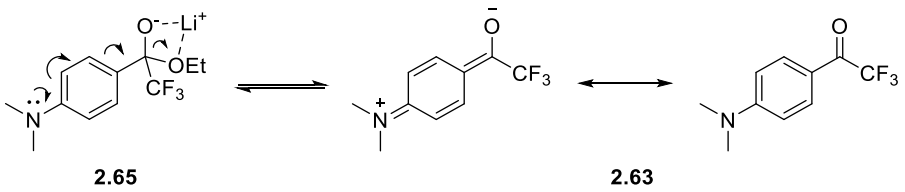


2.62 **2.63** **2.64**

Scheme 2.12: *Formation of unwanted byproduct* ***2.64*** *in formation of trifluoromethylketone* ***2.63****.*

It was reasoned that the electron-donating nature of the *N,N*-dimethyl moiety in the *para*-position destabilised the tetrahedral intermediate **2.65**, resulting in the elimination of ethanol, forming the trifluoromethylketone

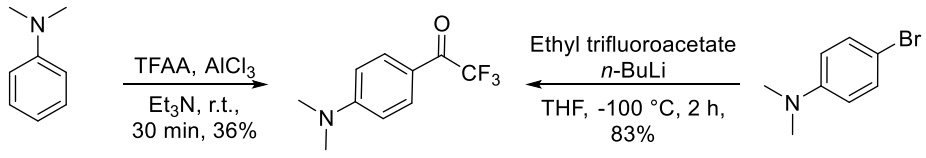
2.63 *in situ* (Scheme 2.13). A second addition of lithiated species then resulted in the formation of tertiary alcohol **2.64**.



2.65 **2.63**

Scheme 2.13*: Proposed destabilisation of tetrahedral intermediate* ***2.65****.*

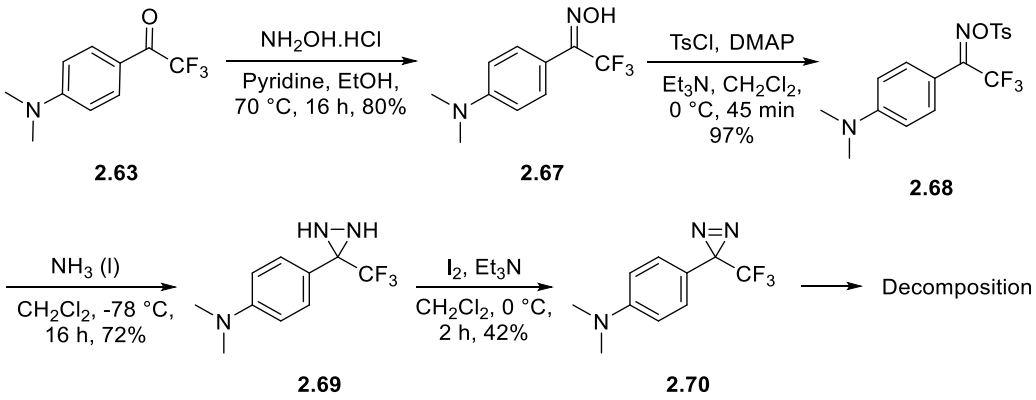
Two approaches were investigated to overcome this problem. Following Sheppard's conditions for the synthesis of the trifluoromethylketone **2.63** through a Friedel-Crafts reaction of *N,N*-dimethylaniline **2.66** and trifluoroacetic anhydride resulted in a disappointing yield.[87] Alternatively, cooling the lithiation reaction to -100 °C resulted in full conversion to the desired trifluoromethylketone **2.63** (Scheme 2.14). The improved yield of the reaction is presumably due to increased stabilisation of the tetrahedral intermediate **2.65**, preventing the formation of the double addition product **2.64**.



2.66 **2.63** **2.62**

Scheme 2.14*: Synthetic routes to trifluoromethylketone* ***2.63****.*

The conversion of trifluoromethylketone **2.63** to oxime **2.67** proceeded as planned. Although a near-quantitative yield to the tosylate **2.68** was achieved, the reaction proved to be highly capricious (Scheme 2.15).



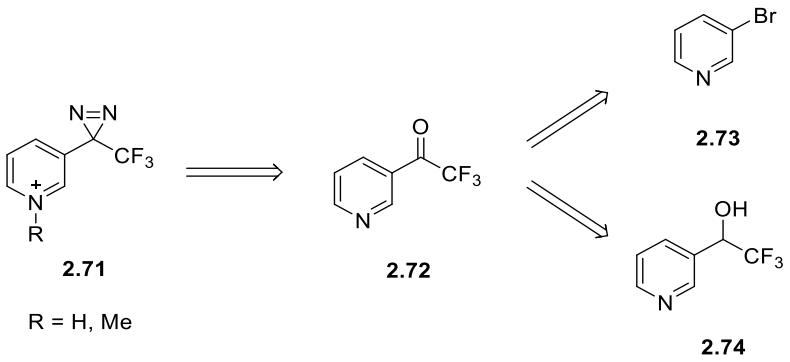
***Scheme 2.15**: Synthesis of diazirine **2.70**.*

Cyclisation followed by oxidation with iodine gave the diazirine **2.70** in a modest yield**.** It was noted that the diazirine **2.70** was unstable to both ambient light and increased temperature, with all further attempts to functionalise **2.70** to impart water solubility resulting in decomposition.

In a recent publication, Manetsch *et al*. demonstrated that reducing the electron-density on the aromatic ring resulted in an increase of the diazirine stability in ambient light.[65] This correlated well with our observations, which implied that the presence of electron-donating substituents on the aromatic ring led to destabilisation of the diazirine moiety.

SYNTHESIS OF A PYRIDINIUM DIAZIRINE LABEL

Considering the observed instability of electron-rich diazirines, a change in strategy was required. A pyridinium core was selected; the electron poor nature of pyridine-based molecules would improve stability, and water-solubility could be increased through protonation or methylation. It was reasoned that the water soluble diazirine **2.71** could be accessed from the trifluoromethylketone **2.72** (Scheme 2.16). Synthetically there are two logical precursors to this key intermediate: the bromopyridine **2.73** or the trifluoromethylcarbinol **2.74**.

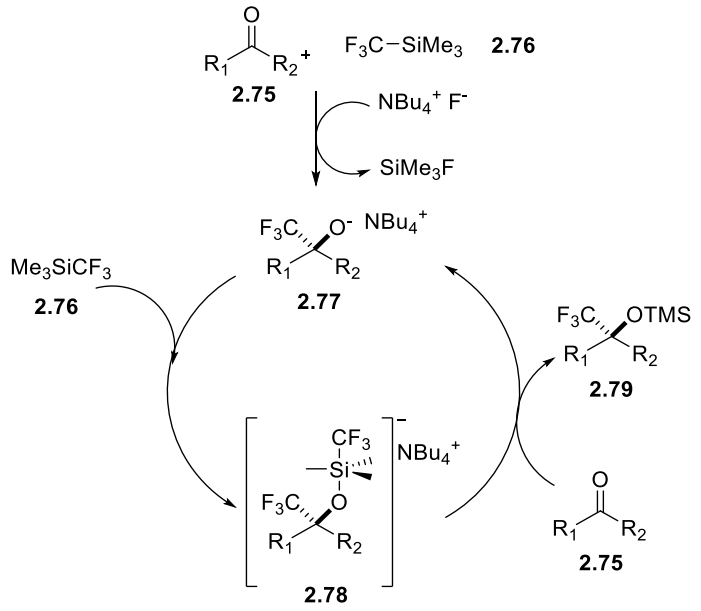


***Scheme 2.16**: Retrosynthetic analysis of cationic diazirine **2.71**.*

The first strategy pursued was the functionalisation of 3-bromopyridine (**2.73**). Both the Grignard formation and lithiation of 3-bromopyridines have been previously reported, however attempting to trap the lithiated species with ethyl trifluoroacetate proved unreliable in this case.[88–91]

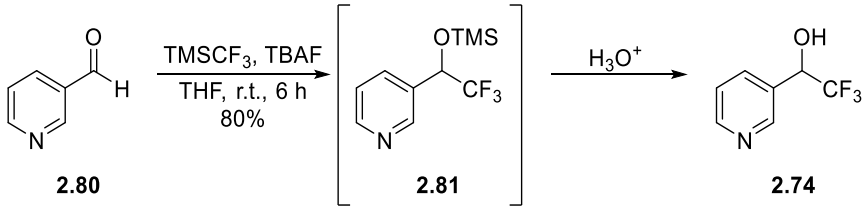
Due to an initial lack of encouraging results in functionalising bromopyridine **2.73**, an alternative strategy was developed. It was envisioned that a nucleophilic source of CF_3 could be incorporated into a carbonyl compound to yield the trifluoromethylcarbinol **2.74**. Although both CF_3Li and CF_3MgX

are unstable,[92,93] nucleophilic trifluoromethylation can be achieved using the Ruppert-Prakash reagent, trifluoromethyltrimethylsilane ($TMSCF_3$).[94–97]



Scheme 2.17: *Prakash and Olah's TBAF initiated trifluoromethylation of aldehydes and ketones.*[96]

Prakash and Olah's trifluoromethylation is initiated by the nucleophilic attack of a fluoride anion on $TMSCF_3$ **2.76**, which can subsequently attack the carbonyl compound **2.75**, forming alkoxide **2.77** (Scheme 2.17).[96] The alkoxide **2.77** reacts with another $TMSCF_3$ molecule, generating another anionic CF_3 species **2.78**, which can propagate the cycle, along with the production of the protected alcohol **2.79**.

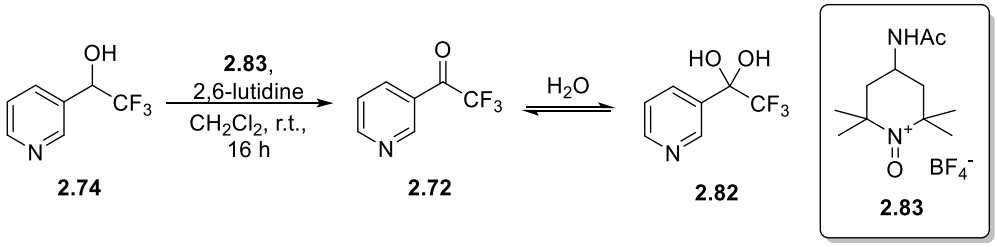


Scheme 2.18*: Formation of trifluoromethylcarbinol* ***2.74****.*

Application of Prakash and Olah's conditions on 3-nicotinaldehyde **2.80** yielded the trifluoromethylcarbinol **2.74** in good yield after deprotection (Scheme 2.18).[96] Oxidation of the alcohol to the ketone was now required to synthesise the key synthetic intermediate **2.72**. The oxidation of this moiety is notoriously difficult to accomplish,[98] with a range of methods known to be unsuccessful, and it has been proposed that this is due either to the diminished nucleophilicity of the alcohol, or an increase in the C-H bond enthalpy.[99] In metal-based oxidations, along with Swern conditions, the nucleophilicity of the alcohol is key, and so the reduced nucleophilicity of the alcohol in trifluoromethylcarbinols reduces the effectiveness of these methods.

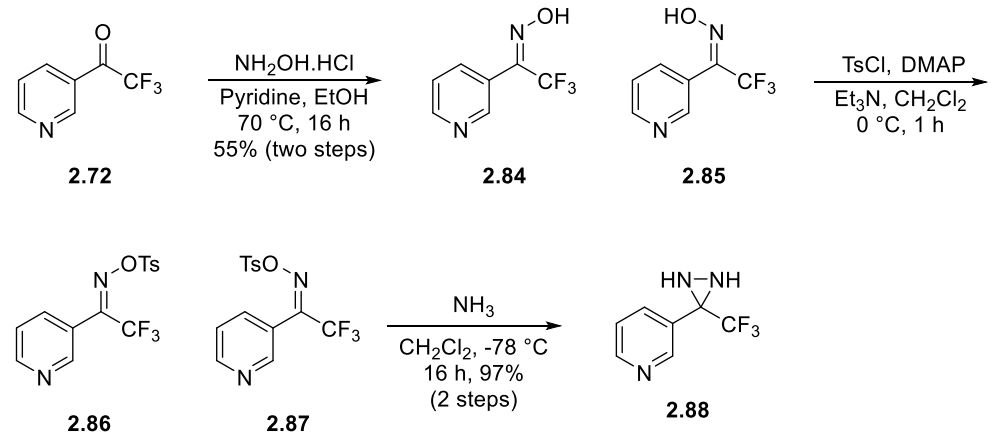
Despite this, there are several procedures that are known to allow this oxidation to occur. Conditions developed by Linderman *et al*. allow a range of trifluoromethylcarbinols to be converted to the corresponding ketone,[100] although 3.7 equivalents of Dess-Martin periodinane are required.

Another oxidant, "Bobbitt's Salt" proved to perform the required transformation, yielding a mixture of ketone **2.72** and hydrate **2.82** (Scheme 2.19). This oxidant, 4-acetamido-2,2,6,6-tetramethylpiperidine-1-oxoammonium tetrafluoroborate (**2.83**) has a similar mechanism of action to the well-known oxidant TEMPO.[101] The oxidant can be easily and economically synthesised from 4-amino-2,2,6,6-tetramethylpiperidine, and has the advantage that the generated byproduct is easily recycled.[102]



***Scheme 2.19**: Oxidation of trifluoromethylcarbinol **2.74** to the ketone **2.72** and hydrate **2.82**.*

Isolation of the target ketone **2.72** proved difficult due to the formation of the hydrate **2.82**. However, as these species exist in equilibrium, the crude material was directly reacted to form a mix of oxime isomers **2.84** and **2.85** (Scheme 2.20).

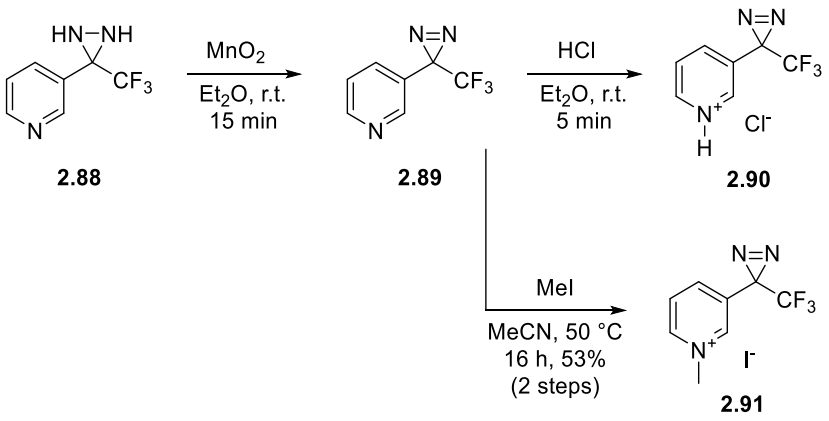


***Scheme 2.20**: Oxime formation from crude trifluoromethylketone **2.72**.*

Tosylation, catalysed by DMAP, occurred rapidly to yield both isomers of the tosylate **2.86** and **2.87**. Nucleophilic attack of the tosylated oximes **2.86** and **2.87** with ammonia gave the saturated diaziridine **2.88** in excellent yield. It was observed that these two steps could run without purification of the tosylated intermediates, with no decrease in yield.

Oxidation of the diaziridine **2.88** was conducted with manganese dioxide, affording the unsaturated diazirine **2.89** (Scheme 2.21). It was noted at this point that the pyridyl diazirine **2.89** was volatile. For ease of handling, upon formation of the diazirine **2.89**, salt formation was attempted immediately.

Addition of 1 M HCl in diethyl ether to an ethereal solution of **2.89** afforded the hydrochloride salt **2.90**, which was isolated by evaporation of the solvent. However, the salt proved to be highly hygroscopic, and therefore it was decided a methylated pyridinium salt would be a more suitable precursor for protein footprinting.



Scheme 2.21*: Formation of the hydrochloride salt.*

Methylation with methyl iodide in acetonitrile proved successful, with purification achieved through precipitation from diethyl ether. The water-soluble yellow salt **2.91** was then taken forward for investigations in protein footprinting.

LABELLING BEHAVIOUR OF THE CATIONIC DIAZIRINE PROBE

Previously, it was established that the carboxylate diazirine **2.50** showed efficient labelling of ubiquitin, with approximately 25% of the protein mono-labelled, with a lower percentage showing the presence of two labels (*vide supra*).

To compare the labelling behaviour of the anionic **2.50** and cationic **2.91** diazirines, the footprinting potential pyridinium based label **2.91** was investigated. The analysis of the irradiation of a solution of **2.91** (80 mM) and ubiquitin (100 μM) exhibited significantly higher labelling than had previously been observed with carboxylate **2.50** (Figure 2.41). Peaks corresponding up to the tri-labelled species were observed, which initially suggested that the label had great potential for future differential footprinting.

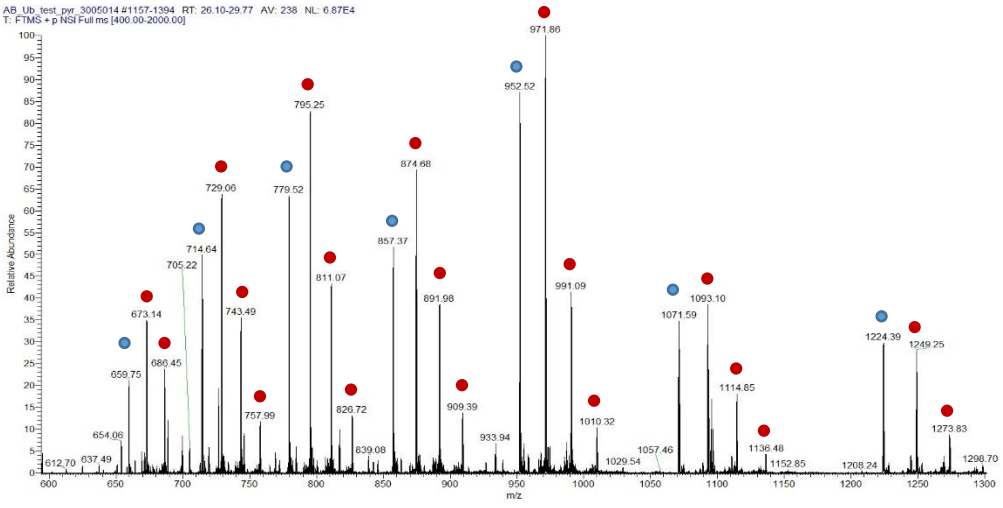


Figure 2.41: *Mass spectrum of ubiquitin (100 μM) labelled with* ***2.91*** *(80 mM). Blue = unlabelled ubiquitin; Red = labelled ubiquitin.*

Closer inspection of the +10 charge state of labelled ubiquitin with anionic **2.50** and cationic **2.91** highlighted the improved labelling behaviour exhibited by the pyridinium diazirine **2.91** (Figure 2.42).

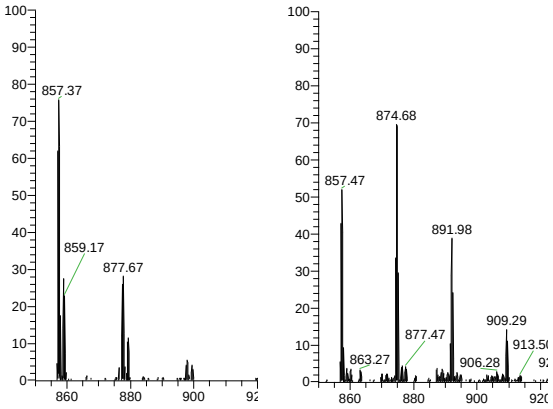


Figure 2.42: *Comparison of the labelling behaviour of* ***2.50*** *(left) and* ***2.91*** *(right) of ubiquitin (+10 charge state).*

To investigate the reactivity of the pyridine diazirine **2.91**, a solution of **2.91** was irradiated in deuterated methanol, and the pre- and post- irradiation ^{1}H NMR spectra compared. As previously noted with aniline **2.58**, clean conversion to the methyl ether **2.93** was not observed, with various unidentified byproducts present in the aromatic region of the ^{1}H NMR spectrum (Figure 2.43). Additionally, the ^{19}F NMR spectrum revealed a number of peaks, with one major singlet corresponding to the methyl ether **2.93**.

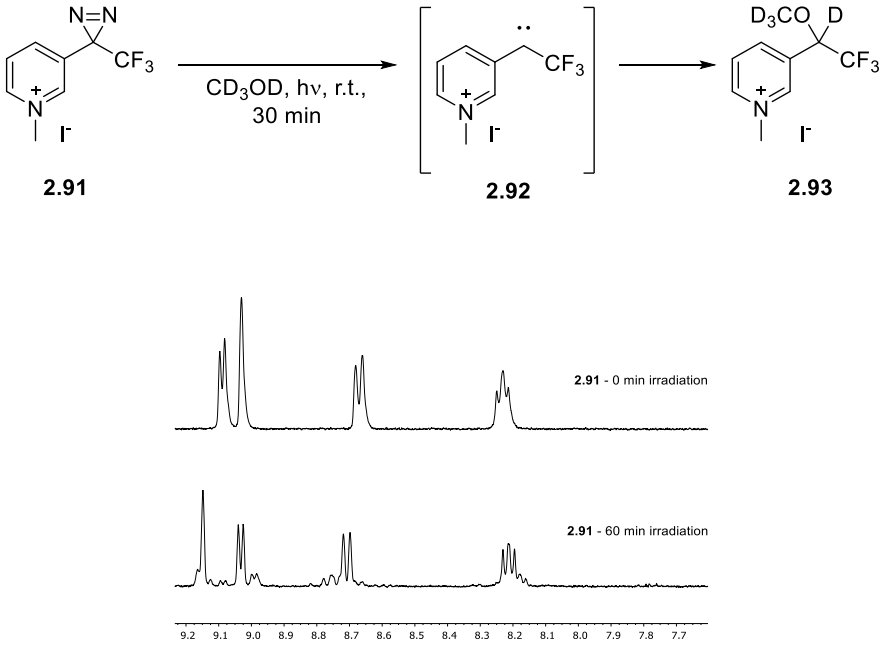


***Figure 2.43**: [1]H NMR analysis of irradiation of **2.91** in CD_3OD.*

SYNTHESIS OF A SELECTION OF ISOMERIC DIAZIRINE PROBES

Having confirmed that the anionic **2.50** and cationic **2.91** diazirines were both viable reagents for protein labelling, the effect of structural isomerism on labelling efficiency was next investigated. To achieve this, a full set of the isomers of **2.50** and **2.91** were targeted (Figure 2.44).

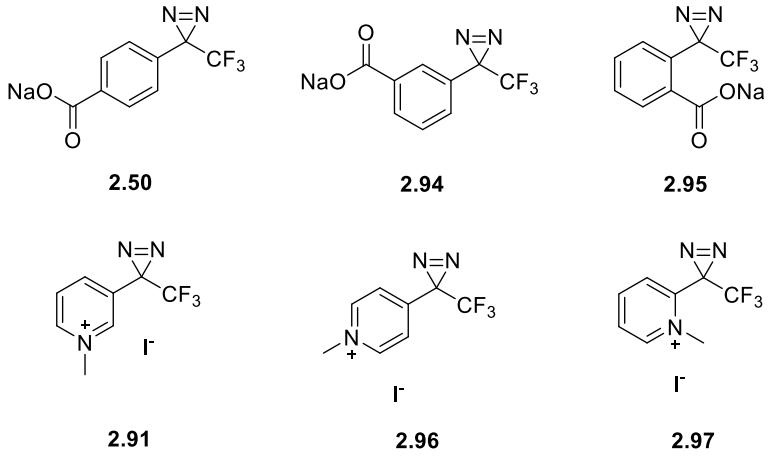
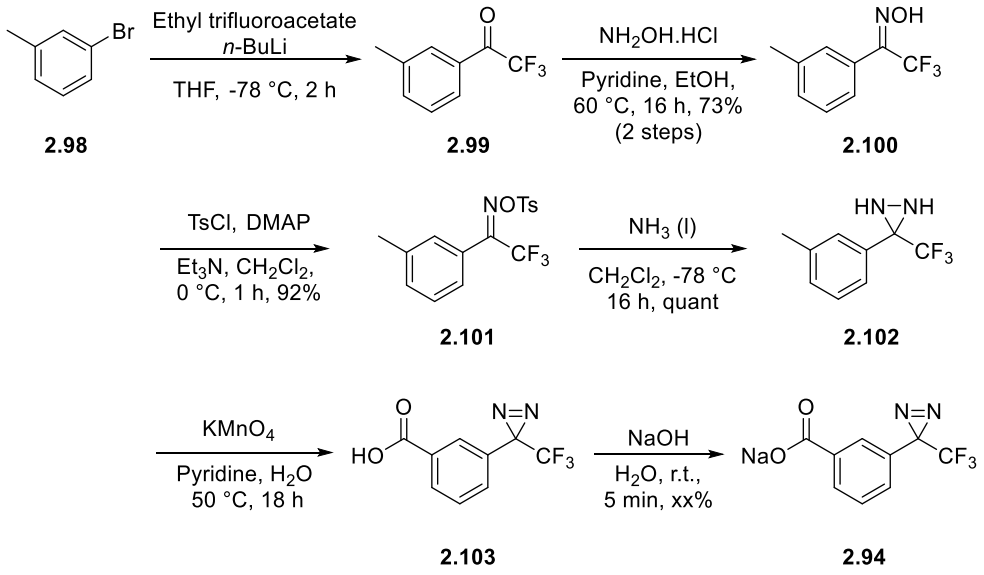


***Figure 2.44**: Structural isomers of synthesised diazirines **2.50** and **2.91**.*

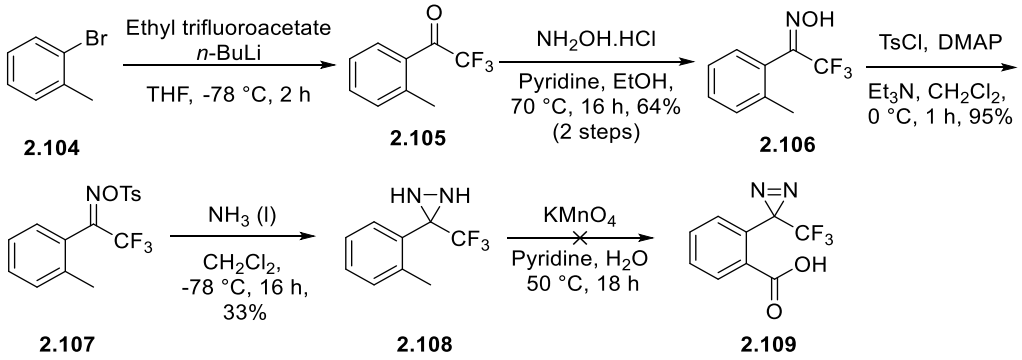
The carboxylate derivatives **2.94** and **2.95** were first synthesised, following an analogous synthetic scheme to the initial diazirine **2.50**. Starting from 3-bromotoluene, a lithiation, trifluoromethylation and oxime formation reaction sequence gave the oxime **2.100** in an isolated yield of 73% over two steps (Scheme 2.22).



***Scheme 2.22**: Completion of the synthesis of diazirine **2.94**.*

Tosylation and cyclisation to diaziridine **2.102** both proceeded in excellent yield, and dual-oxidation mediated by potassium permanganate resulted in the formation of diazirine **2.103**. As previously observed with the 4-carboxylate analogue **2.41**, the isolated yield was extremely poor, presumably due to decomposition of the diazirine ring. Reaction with sodium hydroxide provided the water soluble salt **2.94**.

The corresponding 2-carboxylate **2.95** was next targeted. As before, the bromotoluene **2.104** was converted to the oxime **2.105** through a two-step sequence. Tosylation of the mixture of oxime isomers proceeded in excellent yield as a mixture of chromatographically separable isomers (Scheme 2.23).



***Scheme 2.23**: Attempted synthesis of diazirine **2.109**.*

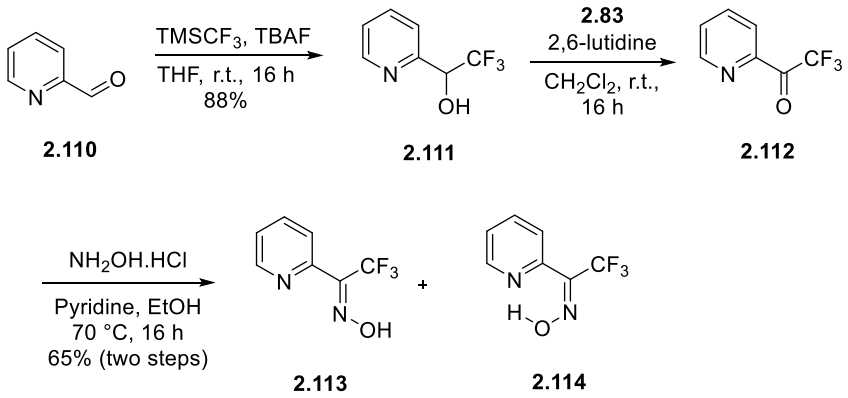
The cyclisation with ammonia did not proceed as expected, with significantly lower yields observed than with structural isomers **2.49** and **2.102**. It was hypothesised that this was a result of higher levels of steric hindrance due to the *ortho*-methyl moiety, which may restrict access for the initial nucleophilic attack of ammonia, and thus lowered the overall yield.

Unfortunately, attempts to oxidise diaziridine **2.108** to diazirine **2.109** resulted in a complex mixture of degradation products. The proximity of the carboxylic acid and diazirine was theorised to result in the formation of undesired byproducts, with no product isolated.

Next, the cationic diazirines **2.96** and **2.97** were targeted. It was reasoned that the 2-pyridyl analogue **2.97** could be synthesised following the same synthetic route as the 3-pyridyl **2.91**. Trifluoromethylcarbinol **2.111** was generated through the TBAF initiated reaction of $TMSCF_3$ and 2-pyridinecarboxaldehyde **2.110** followed by cleavage of the TMS ether in 88% isolated yield (Scheme 2.24).

Oxidation by **2.83** and 2,6-lutidine resulted in a mixture of ketone **2.112**, the corresponding hydrate and residual 2,6-lutidine after passing the reaction mixture through a short silica pad. It was noticeable that significantly more of the product was in the hydrate form than compared to

the analogous 3-pyridyl substrate. Due to the known issues in purification of electron-poor trifluoromethyl ketones, synthesis of the oxime was undertaken on the crude ketone **2.112**, resulting in the formation of isomers **2.113** and **2.114**.

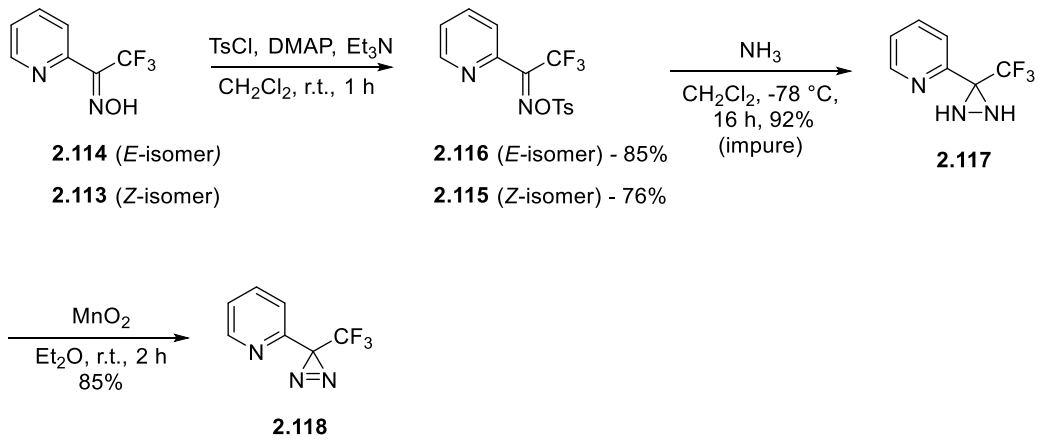


***Scheme 2.24**: Synthetic sequence to oximes **2.113** and **2.114**.*

As noted with previous substrates, the oxime was formed as a mixture of the *E*- and *Z*-isomers. Chromatographically, separation of the isomeric mixture proved facile, and this is likely due to the formation of an intramolecular hydrogen bond in **2.114**, resulting in a significantly lower polarity. Further evidence for this stabilised 6-membered ring was provided by the ^{1}H NMR spectrum, where the oxime proton of the *E*-isomer **2.114** was highly deshielded, appearing at 17.3 ppm, suggesting an interaction with the pyridine nitrogen.

Tosylation of both isomers of the formed oxime proceeded well, with yields of 85% and 76% achieved for **2.116** (*E*-isomer) and **2.115** (*Z*-isomer) respectively (Scheme 2.25). The cyclisation of both isomers with ammonia to form the saturated diaziridine **2.117** were successful, but coincided with the formation of a minor, unknown and inseparable byproduct. It was

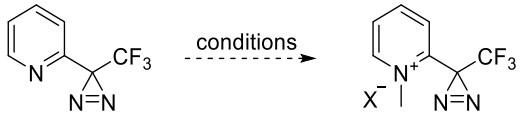
therefore decided to oxidise the impure material directly to diazirine **2.118** with manganese dioxide.



2.114 (*E*-isomer)
2.113 (*Z*-isomer)
2.116 (*E*-isomer) - 85%
2.115 (*Z*-isomer) - 76%
2.117
2.118

***Scheme 2.25**: Synthesis of diazirine **2.118**.*

Diazirine **2.118** in hand, methylation to install the required water solubility was investigated (Table 2.2). Firstly, the optimised conditions used for the previous formation of **2.91** were applied, with a large excess of methyl iodide in acetonitrile (Table 2.2, entry 1). Unfortunately after prolonged heating, analysis by TLC showed the presence of a significant quantity of the starting material **2.91**. Concentration of the reaction mixture resulted in complete degradation, and so alternative methylation conditions were explored.



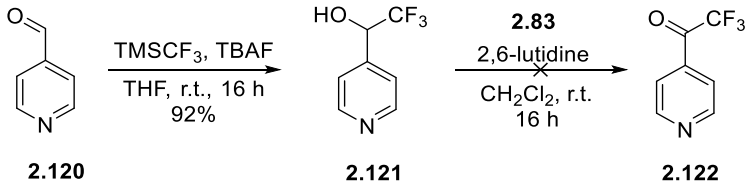
2.118 **2.119**

Entry	***Reagent***	***Temp (°C)***	***Solvent***	***Time (h)***	***Conversion (%)[a]***
1	MeI (10 equiv)	50	MeCN	72	Degradation
2	MeOTf (6 equiv)	−78	CH_2Cl_2	48	1:0.4 (**2.118** : **2.119**)
3	OMe_3BF_4 (1.1 equiv)	r.t.	CH_2Cl_2	16	1:0.66 (**2.118** : **2.119**)
4	OMe_3BF_4 (1.3 equiv)	r.t.	CH_2Cl_2	3	>95% (73%)[b]

Table 2.2: *Conditions for the methylation of diazirine* ***2.118****. [a] Conversion determined by NMR. [b] Isolated yield.*

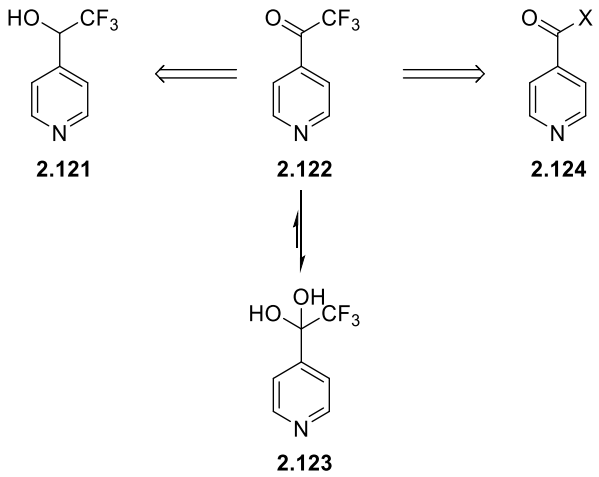
The use of highly electrophilic methyl triflate resulted in incomplete conversion to the desired methyl pyridinium salt **2.119** (Table 2.2, entry 2). Although more commonly utilised for *O*-selective alkylations, a trialkyloxonium salt was next investigated.[103] Trimethyloxonium tetrafluoroborate, an analogue of the more common triethyloxonium salt "Meerwein's salt", resulted in partial conversion into the pyridinium salt (Table 2.2, entry 3).[104] Increasing the loading of oxonium salt resulted in full conversion to the methyl pyridinium salt **2.119** in an acceptable isolated yield of 73% (Table 2.2, entry 4).

To complete the set of pyridine isomers, the synthesis of a 4-pyridyl diazirine was undertaken. Following the established synthetic sequence, 4-pyridinecarboxyaldehyde **2.120** was converted into the trifluoromethylcarbinol **2.121** in excellent yield (Scheme 2.26).



***Scheme 2.26**: Attempted formation of trifluoromethylketone **2.122**.*

Oxidation of the trifluoromethylcarbinol **2.121** proved problematic with the use of the Bobbitt reagent **2.83** in this instance resulting in no ketone **2.122** being isolated. Further reactions following Swern and Dess-Martin Periodiane conditions gave similar negative results. At this stage, it was theorised that the desired ketone **2.122** exists purely in the hydrated form **2.123**. This would significantly change the properties of the molecule, explaining the challenges experienced in attempted isolation. Further analysis of the literature suggested that the desired ketone **2.122**/ hydrate **2.123** could be accessed through a non-oxidative reaction from **2.124** (Scheme 2.27).

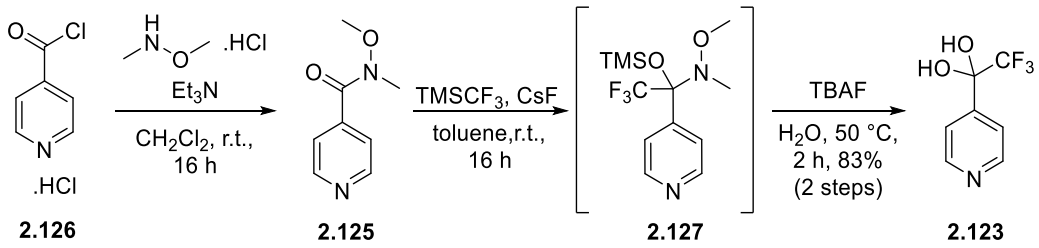


***Scheme 2.27**: Retrosynthesis of the required trifluoromethylketone **2.122**.*

Leadbeater *et al*. reported the synthesis of trifluoromethylketones from the corresponding Weinreb amides and $TMSCF_3$.[105] The substrates tested with their methodology included a 4-pyridyl derivative which was isolated as the corresponding hydrate **2.123**, rather than the trifluoromethylketone **2.124**.

Subsequently, the required Weinreb amide **2.125** was synthesised from the commercially available isonicotinyl chloride hydrochloride **2.126** with *N,O*-dimethylhydroxylamine hydrochloride (Scheme 2.28).

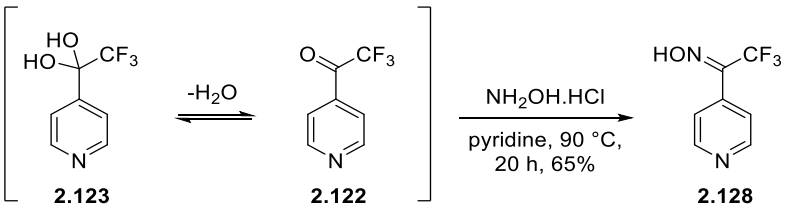
Applying Leadbeater's conditions, Weinreb amide **2.125** was exposed to $TMSCF_3$ with a sub-stoichiometric amount of caesium fluoride.[105] The silylated intermediate **2.127** was formed, and cleaved with aqueous TBAF to afford the hydrate **2.123**, which was used without further purification (Scheme 2.28).



2.126 **2.125** **2.127** **2.123**

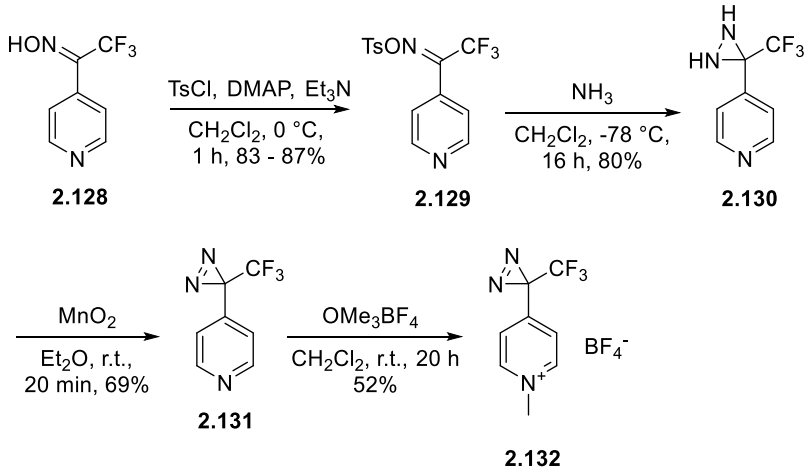
Scheme 2.28*: Trifluoromethylation of Weinreb amide* ***2.125*** *to yield hydrate* ***2.123****.*

Due to the ketone **2.122** existing predominantly in the form of hydrate **2.123**, forcing conditions were required for the conversion into the oxime **2.128**. Heating the reaction to 90 °C, and using 5 equivalents of hydroxylamine hydrochloride in pyridine generated a mixture of isomers in a total yield of 65% (Scheme 2.29).



***Scheme 2.29**: Oxime formation from hydrate **2.123**.*

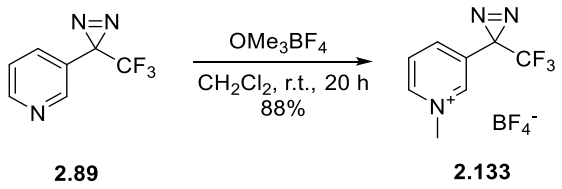
The isomers were separated by column chromatography, and individually tosylated in yields of 83% and 87%. Cyclisation to the diaziridine **2.130** proceeded in good yield from a mixture of the tosylated isomers **2.129** and subsequent oxidation with manganese dioxide then yielded the diazirine **2.131** in an acceptable yield (Scheme 2.30).



***Scheme 2.30**: Synthesis of diazirine **2.132**.*

To complete the synthesis of the water soluble diazirine label **2.132**, methylation was required. Due to the previous issues encountered with the methylation of the 2-pyridyl diazirine to **2.118** to form **2.97** with methyl iodide, the transformation was attempted with trimethyloxonium tetrafluoroborate. Pleasingly, the salt **2.132** was generated in an acceptable

yield, which allowed protein labelling studies to be undertaken. Additionally, the corresponding tetrafluoroborate salt of the isomeric 3-pyridyl diazirine **2.133** was synthesised (Scheme 2.31) to complete the set of isomeric diazirine tetrafluoroborate salts.



2.89 **2.133**

***Scheme 2.31**: Formation of tetrafluoroborate salt **2.133**.*

LABELLING STUDIES OF ADDITIONAL DIAZIRINES

Following the completion of the synthesis of a range of aromatic diazirines, their labelling efficiency of ubiquitin was examined. The carboxylate diazirines **2.50** and **2.94**, the iodide salt **2.91** and the three tetrafluoroborate pyridinium diazirines **2.132**, **2.133** and **2.119** were the diazirines studied (Figure 2.45).

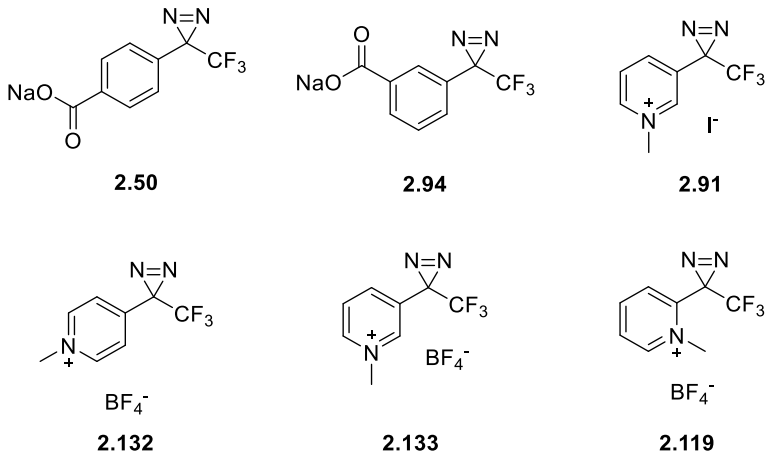


***Figure 2.45**: Synthesised diazirines for footprinting studies.*

The concentration of the diazirines was set at 10 mM and the spectra produced analysed to determine the level of incorporation of the various labels onto the protein surface (Figure 2.46).

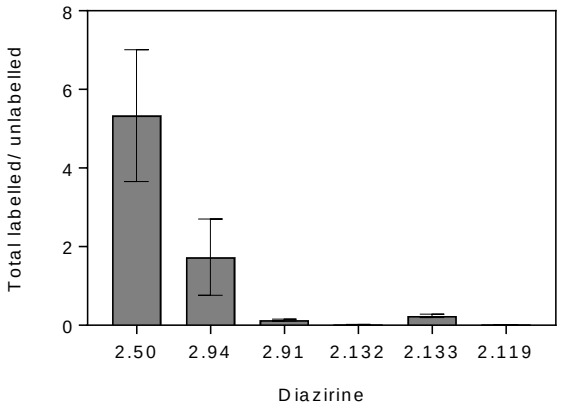


Figure 2.46: *The variation in labelling of Ub (27 μM) with a range of diazirines.*

The original carboxylate diazirine **2.50** was shown to exhibit the highest labelling efficiency, whilst the structural isomer **2.94** also labelled effectively. Disappointingly, the pyridinium based diazirines were significantly less efficient, with the 3-pyridyl diazirines **2.91** and **2.133** showing approximately an order of magnitude less labelling than the acid diazirines. The 2- and 4- pyridinium diazirines showed minor levels of labelling, however this was a further order of magnitude less than observed for **2.132** and **2.119**.

To complement the previous concentration studies, a similar study was undertaken with the most efficient pyridinium diazirine, **2.133**. Similar to the labelling observed for carboxylate **2.50**, a variation in label incorporation was noted in the concentration range investigated, with optimum labelling achieved at 5 mM of diazirine (Figure 2.47).

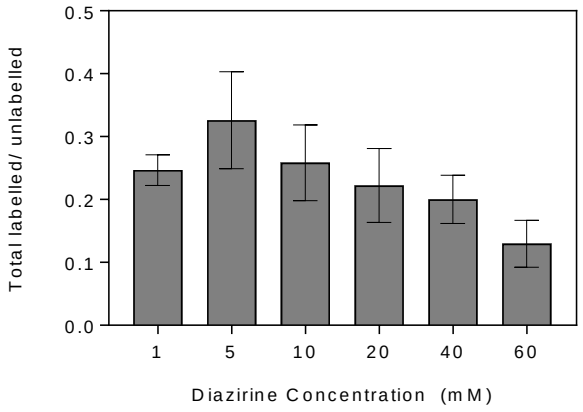


Figure 2.47: *The variation in labelling of Ub (27 μM) with concentration of diazirine* ***2.133****.*

To further probe the variation in labelling achieved with the isomeric pyridinium diazirines **2.132**, **2.133** and **2.119**, their respectively insertion into deuterated solvents were examined. Firstly, deuterated methanol was employed as solvent (Figure 2.48), with the 3-pyridyl diazirine **2.133** demonstrating the cleanest insertion into the solvent.

Over the 60 min irradiation period, all three diazirines were fully consumed, however it was noteworthy that a variety of unknown proton environments appeared in all spectra. The formation of side-products during the photolysis experiments implied either degradation, or reaction with another molecule of diazirine probe; both processes which are undesirable for efficient protein footprinting.

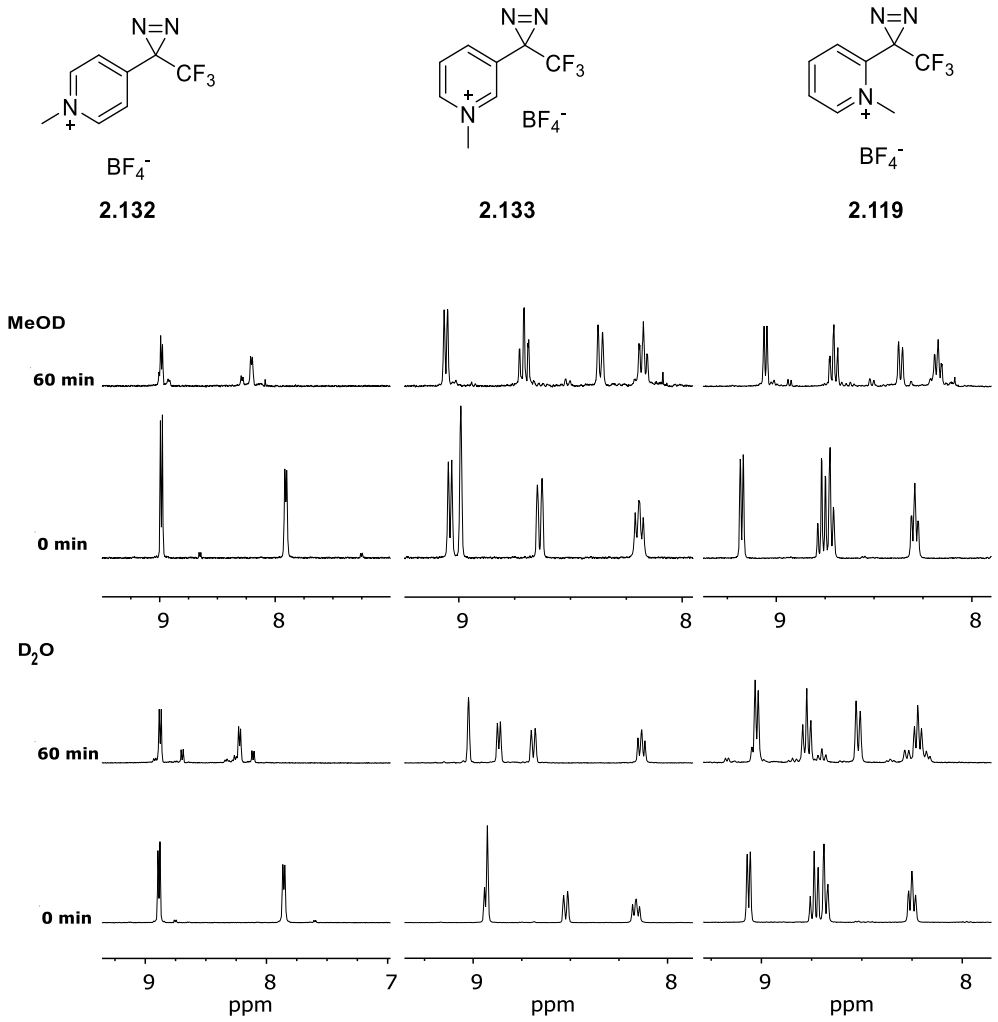


***Figure 2.48**: [1]H NMR spectra of the irradiation of diazirines **2.132**, **2.133** and **2.119** in deuterated methanol and deuterium oxide.*

Next, the photolysis of the collection of diazirines in deuterated water was examined. As before, side products were detected after irradiation of the 4-pyridyl **2.132** and 2-pyridyl **2.119** probes. In contrast, the 3-pyridyl diazirine **2.133** smoothly converted into the corresponding alcohol. It was reasoned that the increased labelling of ubiquitin with **2.133** over its isomeric analogues is a result of minimal self-reaction.

The poor efficiency of the pyridinium diazirines contrasted significantly with the initially promising preliminary data collected (*vide supra*), which implied that the irradiation of these species is capricious in nature. Further work is

evidently required to establish the cause of the irreproducibility, and to optimise the labelling conditions for the cationic diazirine probes.

CONCLUSIONS AND FUTURE WORK

In summary, a range of water soluble diazirines have been synthesised, and then investigated as potential protein footprinting agents to investigate protein-protein interactions.

A complex of ubiquitin and a ZnF UBD from Isopeptidase T has been utilised as a proof-of-concept for a differential footprinting approach. Ubiquitin was photolysed with a diazirine label both alone and as a complex with the IsoT ZnF, with analysis by mass spectroscopy showing a complete reduction of labelling in the binding pocket, showing full agreement with the crystal structure. This indicates that the application of diazirine labels to map protein surfaces and interactions has potential as an accurate, reproducible and viable tool for structural investigations.

The developed technique has proven to be amenable to analysis to tandem mass spectrometry through both ECD and CID techniques, without cleavage of the incorporated labels. ECD was demonstrated to provide higher coverage of the C-terminal peptide of ubiquitin, whilst CID generated daughter ions of a much higher resolution. We therefore propose that future applications of this technique utilise both fragmentation methods in a complementary fashion.

Of the synthesised diazirines, a benzoic derivative **2.50** proved to be a particularly efficient footprinting agent. As compared to the commercially available photo-leucine **2.39**, the aromatic diazirine **2.50** has been shown to be significantly more efficient at labelling the surface of ubiquitin. It was reasoned that this was due to a "pre-concentration" of the diazirine on the hydrophobic regions of the protein surface pre-irradiation.

A range of isomeric pyridinium based diazirines probes have also been prepared, and shown to act as footprinting agents, albeit less efficiently than the corresponding carboxylates. It was shown that the 3-pyridyl derivative **2.33** was the most efficient isomer for protein labelling, however the use of this particular reagent was demonstrated to be highly capricious.

To expand the project further, there are two major areas for research. Firstly, the labelling efficiency of the cationic probes would be investigated to improve incorporation.

It has been shown that the carboxylate based diazirine probes show selectivity for labelling around basic and hydrophobic residues, and it is envisioned that by altering the electronics and sterics of diazirine containing labels, that alternative labelling profiles could be achieved.

In addition to optimising the labelling conditions for the previously synthesised pyridinium diazirines, alternative cationic diazirines will be synthesised. Benzylic bromination of diazirine **2.134**, itself simply accessed from a previous synthetic route, followed by nucleophilic attack could be used to install a variety of amines onto the diazirine containing label (Figure 2.49). Further modification through salt formation or methylation would install the necessary water solubility to allow for protein footprinting studies to be undertaken.

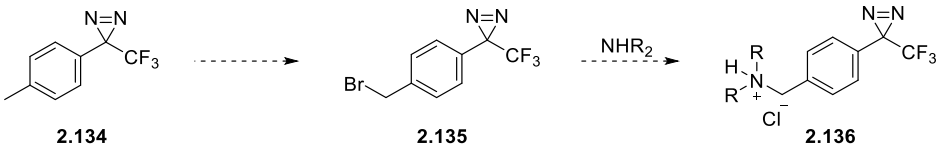


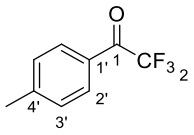
***Figure 2.49**: Proposed synthesis of alternative cationic diazirines.*

EXPERIMENTAL SECTION

Unless stated, reactions were carried out in flame-dried glassware, under an atmosphere of argon with magnetic stirring. THF was freshly distilled over sodium and benzophenone; CH_2Cl_2 was freshly distilled over CaH_2 under a nitrogen atmosphere. NEt_3 was distilled from CaH_2 and stored over 4 Å molecular sieves. All other reagents were obtained from commercial sources and used without further purification. Reactions were monitored using Thin Layer Chromatography (TLC), and visualised using UV light and stained using a basic $KMnO_4$ solution. Flash column chromatography was performed using Merck silica gel 60 as the stationary phase. Petrol refers to petroleum spirit (b.p. 40-60 °C). The lamp used in the irradiation experiments was a 125 W medium-pressure mercury lamp (model 3010; power supply 3110) purchased from Photochemical Reactors Ltd. Irradiation reactions were conducted in NMR tubes under an atmosphere of argon, with an approximate distance of 5 cm between sample and light source. Bobbitt's salt **2.83** was synthesised following a literature procedure.[101]

NMR spectra (^1H, ^{13}C and ^{19}F) were recorded on Bruker DPX300 (300 MHz), AV400 (400 MHz), DPX400 (400 MHz), AV3400 (400 MHz), AV3400HD (400 MHz) and AV3500 (500 MHz) spectrometers, in $CDCl_3$, D_2O, CD_3OD, DMSO-d^6 and acetone-d^6. Infra-red spectra were obtained using a Bruker Alpha FTIR spectrometer with a platinum ATR adaptor, with the peaks recorded as υ_{max} (cm^{-1}). HRMS were obtained using a Bruker MicroTOF mass spectrometer operating in electrospray ionisation (ESI) or electron ionisation (EI) mode. Attempts to ionise some diazirine containing molecules resulted in decomposition. Melting point data was collected using a Stuart SMP3. Where referenced, spectral data showed agreement with the literature.

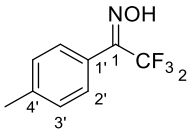
2,2,2-Trifluoro-1-(*p*-tolyl)ethanone[81] **(2.43)**



To a solution of 4-bromotoluene (**2.42**) (3.00 g, 17.5 mmol) in anhydrous THF (20 mL) at −78 °C was added *n*-BuLi (12.3 mL, 18.4 mmol of a 1.50 M solution in hexane) and the solution stirred for 15 min. Ethyl trifluoroacetate (2.30 mL, 19.3 mmol) was added dropwise over 5 min, the solution warmed to room temperature over 2 h before addition of 2M $HCl_{(aq)}$ (10 mL). Volatiles were removed under reduced pressure, and the product extracted between EtOAc (100 mL) and 2M $HCl_{(aq)}$ (100 mL). The organic layer was dried over $MgSO_4$, filtered, concentrated under reduced pressure and used without further purification.

υ_{max} (cm^{-1}): 1714 (C=O), 1608, 1176, 939; δ_H($CDCl_3$, 400 MHz): 8.02 – 7.97 (m, 2H, 2'-H), 7.38 – 7.34 (m, 2H, 3'-H), 2.47 (s, 3H, 4'-CH_3); δ_C($CDCl_3$, 101 MHz): 180.1 (q, *J* = 35 Hz, C-1), 147.0 (C-4'), 130.3 (Ar), 129.8 (Ar), 127.5 (C-1'), 116.8 (q, *J* = 291 Hz, C-2), 21.9 (4'-CH_3); δ_F($CDCl_3$, 377 MHz): −71.3; Does not ionise by ESI.

2,2,2-Trifluoro-1-(*p*-tolyl)ethanone oxime[81] **(2.44)**

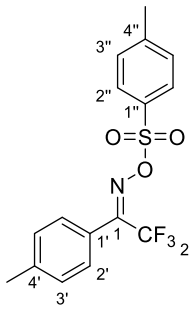


To a solution of crude 2,2,2-trifluoro-1-(*p*-tolyl)ethanone (**2.43**) (from previous step) in pyridine (10 mL) and ethanol (5 mL) was added hydroxylamine hydrochloride (1.22 g, 17.5 mmol). The reaction mixture was heated at 50 °C for 16 h, cooled, diluted with EtOAc (100 mL), washed with 2 M $HCl_{(aq)}$ (100 mL), dried over $MgSO_4$, filtered and concentrated under

reduced pressure. Purification by flash column chromatography (5% EtOAc/Petrol) yielded the title compound as a white solid (2.89 g, 81% over two steps). m.p. 77-80 °C (lit: 63-86 °C).[81]

υ_{max} (cm^{-1}): 3561 (OH), 1612 (C=N), 1516, 1381; δ_H($CDCl_3$, 400 MHz): 9.61 (s, 1H, OH), 7.54 - 7.52 (m, 2H, 2'-H), 7.36 - 7.32 (m, 2H, 3'-H), 2.41 (s, 3H, 4'-CH_3); δ_C($CDCl_3$, 101 MHz): 147.8 (q, *J* = 32 Hz, C-1), 141.1 (C-1'), 129.3 (Ar), 128.6 (Ar) 122.9 (C-4'), 120.6 (q, *J* = 275 Hz, C-2), 21.5 (4'-CH_3); δ_F($CDCl_3$, 377 MHz): −66.6; **HRMS** (EI) calculated for $C_9H_8F_3NO_2$ [M^+] 203.0558, found 203.0551.

2,2,2-Trifluoro-1-(*p*-tolyl)ethanone *O*-tosyl oxime[81] (2.48)

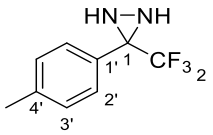


To a solution of 2,2,2-trifluoro-1-(*p*-tolyl)ethanone oxime (**2.44**) (1.30 g, 6.40 mmol) and DMAP (39 mg, 0.32 mmol) in anhydrous CH_2Cl_2 (30 mL) at 0 °C was added triethylamine (2.23 mL, 16.0 mmol) followed by tosyl chloride (1.46 g, 7.70 mmol). The reaction mixture was stirred at room temperature for 1 h before the organic layer was washed with H_2O (30 mL), dried over $MgSO_4$, filtered and concentrated under reduced pressure. Purification by flash column chromatography (5% EtOAc/Petrol) yielded the title compound as a white solid (2.21 g, 97%). m.p. 101 – 103 °C (lit: 104-105 °C).[81]

υ_{max} (cm^{-1}): 3043, 2926, 1598 (C=N), 1389; δ_H ($CDCl_3$, 400 MHz): 7.93 - 7.87 (m, 2H, 2'-H), 7.42 - 7.20 (m, 6H, Ar-H), 2.49 (s, 3H, 4''-CH_3), 2.41

(s, 3H, 4'-CH_3); δ_C($CDCl_3$, 101 MHz): 154.0 (d, *J* = 33 Hz, C-1), 146.1 (C-1''), 142.5 (C-4'), 131.3 (C-4''), 129.9 (Ar), 129.5 (Ar), 129.3 (Ar), 128.5 (Ar), 121.7 (C-1'), 119.7 (q, *J* = 278 Hz, C-2), 21.8 and 21.6 (4'-CH_3 and 4''-CH_3); δ_F($CDCl_3$, 377 MHz): −66.6; **HRMS** (ESI) calculated for $C_{16}H_{14}F_3NNaO_3S$ $[M+Na]^+$ 380.0539, found 380.0546.

3-(*p*-Tolyl)-3-(trifluoromethyl)diaziridine[81] (2.49)



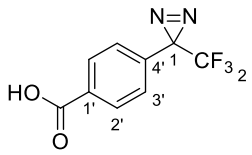
To a solution of 2,2,2-trifluoro-1-(*p*-tolyl)ethanone oxime (**2.48**) (2.50 g, 12.3 mmol) and DMAP (75 mg, 0.62 mmol) in anhydrous CH_2Cl_2 (30 mL) was added triethylamine (4.29 mL, 30.8 mmol) followed by tosyl chloride (2.82 g, 14.8 mmol) at 0 °C. The reaction mixture was stirred at room temperature for 1 h, washed with H_2O (30 mL), dried over $MgSO_4$, filtered and concentrated under reduced pressure. The crude tosylate was then dissolved in anhydrous CH_2Cl_2, added to liquid ammonia (3 mL) at −78 °C in a microwave tube, sealed and stirred for 16 h.

The vial was unsealed, excess ammonia evaporated, and the residue diluted in CH_2Cl_2 (50 mL). The organic phase washed with H_2O (50 mL), dried over $MgSO_4$, filtered and concentrated under reduced pressure. Purification by flash column chromatography (20% EtOAc/Petrol) yielded the title compound as a white solid (1.40 g, 56%). m.p. 42 – 44 °C (lit: 45-46 °C).[81]

υ_{max} (cm^{-1}): 3282 (NH), 3009 (NH), 1731, 1602, 1394; δ_H($CDCl_3$, 300 MHz): 7.51 – 7.48 (m, 2H, 2'-H), 7.26 - 7.20 (m, 2H, 3'-H), 2.77 (d, 1H, *J* = 8.6 Hz, NH), 2.39 (s, 3H, 4'-CH_3), 2.19 (d, 1H, *J* = 8.6 Hz, NH); δ_C($CDCl_3$, 75 MHz): 140.3 (C-1'), 129.4 (Ar), 129.1 (C-4'), 128.8 (Ar), 123.6 (q, *J* = 278

Hz, C-2), 57.9 (q, *J* = 36 Hz, C-1), 21.3 (4'-CH_3); δ_F($CDCl_3$, 377 MHz): −75.7; **HRMS** (EI) calculated for $C_9H_9F_3N_2$ [M^+] 202.0718, found 202.0719.

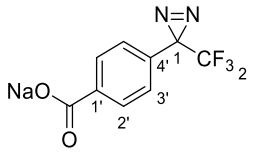
4-(3-(Trifluoromethyl)-3*H*-diazirin-3-yl)benzoic acid[81] (2.41)



To a homogenous solution of 3-(*p*-tolyl)-3-(trifluoromethyl)-3*H*-diaziridine (**2.49**) (600 mg, 2.97 mmol) in pyridine (10 mL) and H_2O (10 mL) was added $KMnO_4$ (1.90 g, 11.9 mmol) and the reaction stirred at 50 °C for 16 h. The solution was cooled, diluted with H_2O and acidified with 2 M $HCl_{(aq)}$ before the addition of 10% sodium $bisulfite_{(aq)}$ (40 mL). The product was extracted into Et_2O (50 mL), the organic layer was separated, basified with 2 M $NaOH_{(aq)}$, extracted into aqueous layer before being acidified once more and extracted into Et_2O (50 mL). The product was dried over $MgSO_4$, filtered and concentrated under reduced pressure to yield the title compound a white solid (200 mg, 29%). m.p. 121 – 122 °C (lit: 123-125 °C).[81]

υ_{max} (cm^{-1}): 3513 (OH), 3061, 1737 (C=O), 1700, 1611; δ_H($CDCl_3$, 400 MHz): 8.13 – 8.11 (m, 2H, 2'-H), 7.31 – 7.28 (m, 2H, 3'-H); δ_C($CDCl_3$, 101 MHz): 166.8 (COOH), 132.8 (Ar), 132.3 (Ar), 130.5 (C-2'), 127.1 (C-3'), 122.1 (q, *J* = 275 Hz, C-2), 28.5 (q, *J* = 41 Hz, C-1); δ_F($CDCl_3$, 377 MHz): −64.4; **HRMS** (ESI) calculated for $C_9H_4F_3N_2O_2$ [M−H]$^-$ 229.0230, found 229.0225.

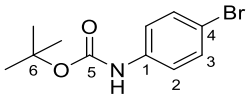
Sodium 4-(3-(trifluoromethyl)-3*H*-diazirin-3-yl)benzoate (2.50)



To a solution of sodium hydroxide (16 mg, 0.39 mmol) in H_2O (1 mL) was added 4-(3-(trifluoromethyl)-3*H*-diazirin-3-yl)benzoic acid (**2.41**) (100 mg, 0.430 mmol) and the suspension stirred for 5 min. The suspension was filtered, and the filtrate concentrated under reduced pressure to yield the title compound as a white solid (98 mg, 89%). m.p. 220 °C (decomposition).

υ_{max} (cm^{-1}): 1592 (C=O), 1546, 1418, 1343, 1144, 942, 777; δ_H(CD_3OD, 400 MHz): 8.02 – 7.98 (m, 2H, 2'-H), 7.25 – 7.20 (m, 2H, 3'-H); δ_C(CD_3OD, 101 MHz): 174.0 (CO_2Na), 141.1 (C-4'), 131.7 (C-1'), 131.0 (C-2'), 127.0 (C-3'), 123.8 (q, *J* = 274 Hz, C-2), 29.7 (q, *J* = 40 Hz, C-1); δ_F(CD_3OD, 377 MHz): −66.9; **HRMS** (ESI) calculated for $C_9H_4F_3N_2O_2$ $[M]^-$ 229.0230, found 229.0228.

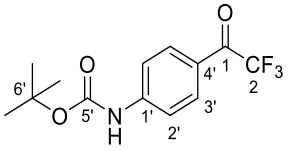
***tert*-Butyl (4-bromophenyl)carbamate[106] (2.53)**



To a suspension of 4-bromoaniline (**2.52**) (1.50 g, 8.72 mmol) in 2 M $NaOH_{(aq)}$ (20 mL) was added di-*tert*-butyl dicarbonate (1.90 g, 8.72 mmol) and refluxed for 1.5 h. The reaction was cooled and extracted into Et_2O (60 mL). The organic phase was separated, washed with sat. $NH_4Cl_{(aq)}$ (40 mL) and H_2O (40 mL), dried over $MgSO_4$, filtered and concentrated under reduced pressure to yield the title compound as a white solid (2.17 g, 91%). m.p. 104 – 105 °C (lit: 104 °C).[106]

υ_{max} (cm^{-1}): 3438 (NH), 2983, 1727 (C=O), 1588, 1513, 1395, 1157; δ_H($CDCl_3$, 400 MHz): 7.42 - 7.37 (m, 2H, Ar-H), 7.29 - 7.23 (m, 2H, Ar-H), 6.49 (br. s, 1H, NH), 1.52 (s, 9H, 6-CH_3); δ_C($CDCl_3$, 101 MHz): 152.5 (C-5), 137.5 (C-1), 131.9 (C-3), 120.0 (C-2), 115.4 (C-4), 80.9 (C-6), 28.3 (6-CH_3); **HRMS** (ESI) calculated for $C_{11}H_{14}BrNO_2Na$ $[M+Na]^+$ 294.0100, found 294.0086.

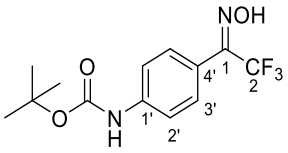
tert-Butyl (4-(2,2,2-trifluoroacetyl)phenyl)carbamate (2.54)



To a solution of *tert*-butyl (4-bromophenyl)carbamate (**2.53**) (1.08 g, 4.00 mmol) in anhydrous THF (30 mL) at −78 °C was added *n*-BuLi (4.54 mL, 10.0 mmol of a 2.20 M solution in hexane) and the resultant solution was stirred for 30 min. Ethyl trifluoroacetate (524 µL, 4.40 mmol) was added at −78 °C and the reaction stirred for 4 h, slowly warming to room temperature. H_2O (5 mL) was added, and volatiles removed under reduced pressure. The residue was extracted between EtOAc (100 mL) and H_2O (100 mL), the organic phase dried over $MgSO_4$, filtered and concentrated under reduced pressure to yield the crude title compound which was used without further purification. m.p. 98–100 °C.

υ_{max} (cm^{-1}): 3430 (NH), 2983, 1736 (C=O), 1709 (C=O), 1605, 1523, 1499, 1150 (C-O); δ_H ($CDCl_3$, 400 MHz): 8.05 – 8.03 (m, 2H, 3'-H), 7.57 - 7.52 (m, 2H, 2'-H), 6.79 (br. s, 1H, NH), 1.55 (s, 9H, s, $C(CH_3)_3$); δ_C($CDCl_3$, 101 MHz): 179.0 (q, *J* = 35 Hz, C-1), 151.8 (C-5'), 145.2 (C-1'), 132.0 (C-3'), 124.2 (C-4'), 117.6 (C-2'), 116.8 (q, *J* = 291 Hz, C-2), 81.9 ($\underline{C}(CH_3)_3$), 28.2 ($C(\underline{C}H_3)$);δ_F ($CDCl_3$, 377 MHz): −71.1; **HRMS** (ESI) calculated for $C_{13}H_{14}F_3NO_3$ $[M-H]^-$ 288.0855, found 288.0853.

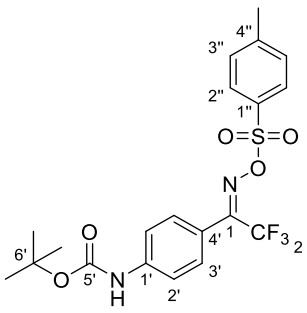
tert-Butyl (4-(2,2,2-trifluoro-1-(hydroxyimino)ethyl)phenyl)carbamate (2.55)



To a solution of crude *t*ert-butyl (4-(2,2,2-trifluoroacetyl)phenyl)carbamate (**2.54**) (from previous step) in ethanol (6 mL) was added hydroxylamine hydrochloride (278 mg, 4.00 mmol) and pyridine (2 mL). The reaction mixture was heated at 60 °C for 16 h, cooled and concentrated under reduced pressure. The residue was extracted between EtOAc (100 mL) and H_2O (100 mL), the organic phase dried over $MgSO_4$, filtered and concentrated under reduced pressure. Purification by flash column chromatography (5-20% EtOAc/Petrol) yielded the title compound as a white solid (551 mg, 45% over two steps). m.p. 141-142 °C

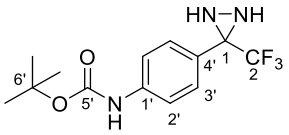
υ_{max} (cm^{-1}): 3556 (NH), 3436, 2983, 1731 (C=O), 1611 (C=N), 1586, 1184 (C-O); δ_H($CDCl_3$, 400 MHz): 9.34 (s, 1H, OH), 7.56 - 7.52 (m, 2H, 3'-H), 7.48 - 7.44 (m, 2H, 2'-H), 6.81 (br. s, 1H, NH), 1.55 (s, 9H, 6'-CH_3); δ_C($CDCl_3$, 101 MHz): 152.7 (C-5'), 146.8 (q, *J* = 32 Hz, C-1), 140.3 (C-1'), 129.8 (C-3'), 120.7 (q, *J* = 275 Hz, C-2), 120.2 (C-4'), 118.0 (C-2'), 81.5 (C-6'), 28.3 (6'-CH_3); δ_F($CDCl_3$, 377 MHz): −66.1; **HRMS** (ESI) calculated for $C_{13}H_{15}F_3N_2O_3Na$ $[M+Na]^+$ 327.0927, found 327.0917.

***tert*-Butyl (4-(2,2,2-trifluoro-1-((tosyloxy)imino)ethyl)phenyl)carbamate**



To a suspension of *tert*-butyl (4-(2,2,2-trifluoro-1-(hydroxyimino)ethyl)phenyl)carbamate (**2.55**) (600 mg, 1.97 mmol) and DMAP (12 mg, 0.10 mmol) in anhydrous CH_2Cl_2 (15 mL) at 0 °C was added triethylamine (687 µL, 4.93 mmol) followed by tosyl chloride (450 mg, 2.36 mmol). The reaction mixture was stirred for 16 h at room temperature, diluted with CH_2Cl_2 (50 mL) and washed with brine (50 mL). The organic phase was dried over $MgSO_4$, filtered and concentrated under reduced pressure to yield the crude title compound which was used without further purification.

***tert*-Butyl (4-(3-(trifluoromethyl)diaziridin-3-yl)phenyl)carbamate (2.56)**

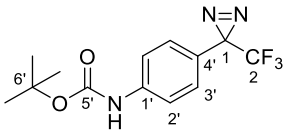


A solution of crude *tert*-butyl (4-(2,2,2-trifluoro-1-((tosyloxy)imino)ethyl)phenyl)carbamate (from previous step) in CH_2Cl_2 (3 mL) was added dropwise a microwave vial containing liquid ammonia (3 mL) at −78 °C. The vial was sealed, warmed to room temperature and stirred for 16 h. The reaction mixture was cooled to −78 °C, the vial unsealed and excess ammonia evaporated. The residue was diluted in CH_2Cl_2 (40 mL) and

washed with H_2O (2 x 20 mL). The organic layer was dried over $MgSO_4$, filtered and concentrated under reduced pressure. Purification by flash column chromatography (10-20% EtOAc/Petrol) yielded the title compound as a white solid (583 mg, 97% over 2 steps). m.p. 129 °C

υ_{max} (cm^{-1}): 3437 (NH), 3282 (NH), 2983, 1729 (C=O), 1615, 1592, 1527, 1155 (C-O); δ_H($CDCl_3$, 400 MHz): 7.55 – 7.53 (m, 2H, Ar-H), 7.43 – 7.41 (m, 2H, Ar-H), 6.60 (br. s, 1H, NH), 2.76 (m, 1H, NH), 2.18 (m, 1H, NH), 1.53 (s, 9H, 6'-CH_3); δ_C($CDCl_3$, 101 MHz): 152.4 (C-5'), 140.1 (C-1'), 128.9 (C-3'), 125.9 (C-4'), 123.5 (q, *J* = 278 Hz, C-2), 118.3 (C-2'), 81.0 (C-6'), 57.6 (q, *J* = 36 Hz, C-1), 28.3 (6'-CH_3); δ_F($CDCl_3$, 377 MHz): −75.6; **HRMS** (ESI) calculated for $C_{13}H_{16}F_3N_3NaO_2$ $[M+Na]^+$ 326.1087, found 326.1077.

tert-Butyl (4-(3-(trifluoromethyl)-3*H*-diazirin-3-yl)phenyl)carbamate (2.57)

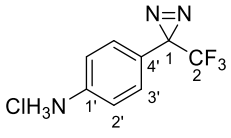


Activated manganese dioxide (**2.56**) (1.29 g, 14.8 mmol) was added to solution of *tert*-butyl (4-(3-(trifluoromethyl)diaziridin-3-yl)phenyl)carbamate (450 mg, 1.48 mmol) in Et_2O (30 mL) and stirred for 1 h. The reaction mixture was filtered through silica (Et_2O), and concentrated under reduced pressure to yield the title compound as a yellow solid (400 mg, 89%). m.p. 105 °C

υ_{max} (cm^{-1}): 3436 (NH), 2983, 1730 (C=O), 1616, 1526, 1156 (C-O); δ_H($CDCl_3$, 400 MHz): 7.41 – 7.39 (m, 2H, Ar), 7.15 – 7.13 (m, 2H, Ar), 6.58 (br. s, 1H, NH), 1.52 (s, 9H, 6'-CH_3); δ_C($CDCl_3$, 101 MHz): 152.3 (C-5'), 139.8 (C-1'), 127.4 (C-3'), 123.1 (C-4'), 122.2 (q, *J* = 275 Hz, C-2), 118.3 (C-2'), 81.1 (C-6'), 28.3 (6'-CH_3), 28.2 (q, *J* = 41 Hz, C-1'); δ_F($CDCl_3$, 377

MHz): −65.5; **HRMS** (ESI) calculated for $C_{13}H_{14}F_3N_3NaO_2$ $[M+Na]^+$ 324.0930, found 324.0940.

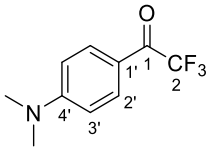
4-(3-(Trifluoromethyl)-3*H*-diazirin-3-yl)aniline hydrochloride (2.58)



To a solution of *tert*-butyl (4-(3-(trifluoromethyl)-3*H*-diazirin-3-yl)phenyl)carbamate (**2.57**) (100 mg, 0.330 mmol) in CH_2Cl_2 (0.5 mL) was added trifluoroacetic acid (0.5 mL) and the reaction was left to stir for 1 h. Volatiles were removed under reduced pressure, and the residue suspended in Et_2O (1 mL). To this solution was added HCl (2 M in Et_2O, 1 mL, 1 mmol) and the reaction stirred for 5 min. Volatiles were removed under reduced pressure to yield the title compound as an off-white solid (20 mg, 26%). m.p. 175 °C (decomposition).

υ_{max} (cm^{-1}): 2843, 1512, 1343, 1145, 939; δ_H(CD_3OD, 400 MHz): 7.56 - 7.52 (m, 2H, 2'-H), 7.48 - 7.44 (m, 2H, 3'-H); δ_C(CD_3OD, 101 MHz): 134.3 (Ar), 130.9 (Ar), 129.8 (C-3'), 125.3 (C-2'), 123.5 (q, *J* = 274 Hz, C-2), 29.4 (q, *J* = 41 Hz, C-1); δ_F(CD_3OD, 377 MHz): −67.2; **HRMS** (ESI) calculated for $C_8H_7F_3N_1$ $[M-N_2]^+$ 174.0525, found 174.0525.

1-(4-(Dimethylamino)phenyl)-2,2,2-trifluoroethanone[80] (2.63)

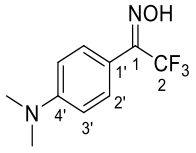


To a solution of 4-bromo-*N,N*-dimethylaniline (**2.62**) (2.00 g, 10.0 mmol) in anhydrous THF (40 mL) at −78 °C was added *n*-BuLi (4.40 mL, 11.0 mmol

of a 2.5 M solution in hexanes) and the solution stirred for 15 min. The reaction was cooled to -100 °C, and a solution of ethyl trifluoroacetate (1.31 mL, 11.0 mmol) in anhydrous THF (10 mL) at −78 °C was added *via* cannula. The solution was warmed to room temperature over 1.5 h, diluted with Et_2O (40 mL) and washed with sat. $NH_4Cl_{(aq)}$ (50 mL). The aqueous phase washed with Et_2O (40 mL), the organic phases combined, dried over $MgSO_4$, filtered and concentrated under reduced pressure. The crude material was slurried in cold hexane (30 mL) and filtered to yield the title compound as an off white solid (1.80 g, 83%). m.p. 73-74 °C (lit: 74-75 °C).[80]

υ_{max} (cm^{-1}): 2920, 1686 (C=O), 1598, 1380, 1164; δ_H($CDCl_3$, 400 MHz): 7.98 – 7.96 (m, 2H, 2'-H), 6.71 – 6.69 (m, 2H, 3'-H), 3.13 (s, 6H, $N(CH_3)_2$); δ_C($CDCl_3$, 101 MHz): 177.9 (q, *J* = 34 Hz, C-1), 154.7 (C-4'), 132.6 (C-2'), 117.5 (q, *J* = 291 Hz, C-2), 117.4 (C-1'), 110.9 (C-3'), 40.0 ($N(CH_3)_2$); δ_F(377 MHz, $CDCl_3$) −70.3. **HRMS** (EI) calculated for $C_{10}H_{10}F_3NO$ $[M]^+$ 217.07090 found 217.07100.

1-(4-(Dimethylamino)phenyl)-2,2,2-trifluoroethanone oxime (2.67)

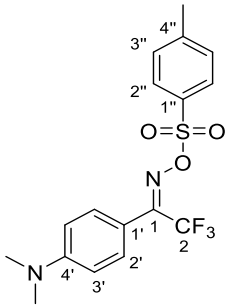


To a solution of 1-(4-(dimethylamino)phenyl)-2,2,2-trifluoroethanone (**2.63**) (1.50 g, 6.91 mmol) in ethanol (13 mL) was added hydroxylamine hydrochloride (721 mg, 10.4 mmol) and pyridine (4 mL). The resultant solution was heated at 70 °C for 16 h. The reaction mixture was concentrated under reduced pressure, extracted into Et_2O (60 mL) and washed with brine (60 mL). The aqueous phase was washed with Et_2O (40

mL), the organic phases combined, dried over $MgSO_4$, filtered and concentrated under reduced pressure. Purification by recrystallisation (EtOAc/hexane) yielded the title compound as a white solid as a mix of isomers (1.28 g, 80%). m.p. 180 °C

υ_{max} (cm^{-1}): 3244 (NH), 1615 (C=N), 1186, 1130; δ_H($CDCl_3$, 400 MHz): Isomer 1: 8.88 (s, 1H, N-OH), 7.60 – 7.58 (m, 2H, 2'-H), 6.77 – 6.67 (m, 2H, 3'-H), 3.03 (s, 6H, $N(CH_3)_2$); Isomer 2: 8.80 (s, 1H, N-OH), 7.41 – 7.39 (m, 2H, 2'-H), 6.77 – 6.67 (m, 2H, 3'-H), 3.02 (s, 6H, $N(CH_3)_2$); δ_C($CDCl_3$, 101 MHz) 151.4 (C-4'), 147.1 (q, *J* = 31 Hz, C-1), 130.3 (C-2'), 121.1 (q, *J* = 275 Hz, C-2), 112.7 (C-1'), 111.2 (C-3'), 40.1 ($N(CH_3)_2$); δ_F(377 MHz, $CDCl_3$) −65.5, −62.3; **HRMS** (ESI) calculated for $C_{10}H_{12}F_3N_2O_1$ $[M+H]^+$ 233.0896, found 233.0893.

1-(4-(Dimethylamino)phenyl)-2,2,2-trifluoroethanone *O*-tosyl oxime (2.68)

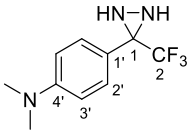


To a solution of 1-(4-(dimethylamino)phenyl)-2,2,2-trifluoroethanone oxime (**2.67**) (100 mg, 0.430 mmol) and DMAP (3 mg, 0.02 mmol) in CH_2Cl_2 (2 mL) at 0 °C was added triethylamine (150 µL, 1.08 mmol) followed by tosyl chloride (99 mg, 0.52 mmol). The reaction mixture warmed to room temperature, stirred for 45 min, diluted with CH_2Cl_2 (20 mL) and washed with water (20 mL). The organic layer was dried over $MgSO_4$, filtered and concentrated under reduced pressure. Purification by flash column

chromatography (5% EtOAc/Petrol) yielded the title compound as a yellow solid (161 mg, 97%). m.p. 127 °C

υ_{max} (cm^{-1}): 2918, 1596 (C=N), 1529, 1377, 1190; δ_H($CDCl_3$, 400 MHz): 7.92 – 7.90 (m, 2H, 2''-H), 7.53 – 7.51 (m, 2H, 2'-H), 7.38 – 7.36 (m, 2H, 3''-H), 6.70 – 6.68 (m, 2H, 3'-H), 3.05 (s, 6H, $N(CH_3)_2$), 2.47 (s, 3H, 4''-CH_3); δ_C($CDCl_3$, 101 MHz): 152.8 (q, *J* = 31 Hz, C-1), 152.1 (C-4'), 145.7 (C-1''), 131.6 (C-4''), 131.0 (C-2'), 129.7 (C-3''), 129.3 (C-2''), 120.3 (q, *J* = 278 Hz, C-2), 111.0 (C-3'), 110.8 (C-1'), 39.9 ($N(CH_3)_2$), 21.8 (4''-CH_3); δ_F(377 MHz, $CDCl_3$) −64.7; **HRMS** (ESI) calculated for $C_{17}H_{18}F_3N_2O_3Na$ $[M+H]^+$ 387.0985, found 387.0991.

N,*N*-Dimethyl-4-(3-(trifluoromethyl)diaziridin-3-yl)aniline (2.69)

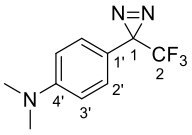


A solution of 1-(4-(dimethylamino)phenyl)-2,2,2-trifluoroethanone *O*-tosyl oxime (**2.68**) (100 mg, 0.260 mmol) in CH_2Cl_2 (3 mL) was added to liquid ammonia (3 mL) in a microwave vial at −78 °C. The vial was sealed and stirred for 16 h at room temperature. The vial was cooled to −78 °C, unsealed and excess ammonia evaporated. The reaction mixture was diluted with CH_2Cl_2 (20 mL), washed with brine (20 mL), dried over $MgSO_4$, filtered and concentrated under reduced pressure. Purification by flash column chromatography (7.5% EtOAc/Petrol) yielded the title compound as a yellow solid (43 mg, 72%). m.p. 56 °C.

υ_{max} (cm^{-1}): 3207 (NH), 2893, 1611, 1528, 1140; δ_H($CDCl_3$, 400 MHz,): 7.47 – 7.44 (m, 2H, 2'-H), 6.74 – 6.68 (m, 2H, 3'-H), 2.99 (s, 6H, $N(CH_3)_2$), 2.71 (d, *J* = 9.1 Hz, 1H, NH), 2.13 (d, *J* = 9.1 Hz, 1H, NH); δ_C($CDCl_3$, 101 MHz): 151.3 (C-4'), 128.9 (C-2'), 123.8 (q, *J* = 278 Hz, C-2), 118.5 (C-1'), 111.8

(C-3'), 57.7 (q, *J* = 36 Hz, C-1), 40.2 ($N(CH_3)_2$); δ_F($CDCl_3$, 282 MHz): −75.8; **HRMS** (ESI) calculated for $C_{10}H_{13}F_3N_3$ $[M+H]^+$ 232.1056, found 232.1053.

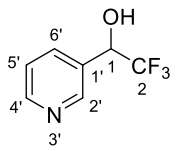
N,*N*-Dimethyl-4-(3-(trifluoromethyl)-3*H*-diazirin-3-yl)aniline (2.70)



To a solution of *N*,*N*-dimethyl-4-(3-(trifluoromethyl)diaziridin-3-yl)aniline (**2.69**) (140 mg, 0.610 mmol) and triethylamine (94 µL, 0.67 mmol) in anhydrous CH_2Cl_2 (3 mL) was added iodine (185 mg, 0.73 mmol) at 0 °C. The reaction mixture was stirred for 2 h, diluted with CH_2Cl_2 (20 mL) washed with 2M $HCl_{(aq)}$ (20 mL), dried over $MgSO_4$, filtered and concentrated under reduced pressure. Purification by flash column chromatography (2% EtOAc/Petrol) afforded the title compound as an unstable orange solid (58 mg, 42%).

δ_H($CDCl_3$, 400 MHz): 7.10 – 7.08 (m, 2H, 2'-H), 6.70 – 6.68 (m, 2H, 3'-H), 2.99 (s, 6H, $N(CH_3)_2$); δ_C($CDCl_3$, 101 MHz): 151.0 (C-4'), 127.6 (C-2'), 122.5 (q, *J* = 274 Hz, C-2), 115.7 (C-1'), 111.9 (C-3'), 40.1 ($N(CH_3)_2$), 28.4 (q, *J* = 40 Hz, C-1). δ_F($CDCl_3$, 377 MHz): −65.7.

(*rac*)-2,2,2-Trifluoro-1-(pyridin-3-yl)ethan-1-ol[107] (2.74)

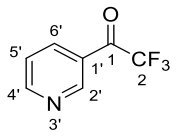


3-Pyridinecarboxaldehyde (**2.80**) (2.14 g, 20.0 mmol) was added to a solution of $TMSCF_3$ (3.25 mL, 22.0 mmol) in anhydrous THF (24 mL) at 0 °C. TBAF (1 M in THF, 0.2 mL, 0.2 mmol) was added and the reaction stirred

for 16 h at room temperature. The reaction mixture was cooled to 0 °C and H_2O (10 mL) then TBAF (1 M in THF, 2 mL, 2 mmol) was added. The reaction mixture was stirred for 10 min at 0 °C then at room temperature for 2 h. The reaction mixture was extracted between Et_2O (100 mL) and brine (100 mL), and the aqueous layer washed with Et_2O (2 x 50 mL). The organic layers were combined, dried over $MgSO_4$, filtered and concentrated under reduced pressure. Purification by flash column chromatography (10-50% EtOAc/Petrol) yielded the title compound as a white solid (2.82 g, 80%). m.p. 44-46 °C (lit: 45-47 °C).[108]

υ_{max} (cm^{-1}): 3605 (OH), 3096, 1601, 1584, 1431, 1270; δ_H($CDCl_3$, 400 MHz): 8.59 (d, *J* = 1.7 Hz, 1H, 2'-H), 8.54 (dd, *J* = 4.9, 1.7 Hz, 1H, 4'-H), 7.97 (dd, *J* = 7.9, 0.5 Hz, 1H, 6'-H), 7.41 (ddd, *J* = 7.9, 4.9, 0.5 Hz, 1H, 5'-H), 6.53 (br. s., 1H, OH), 5.11 (q, *J* = 6.8 Hz, 1H, 1-H); δ_C($CDCl_3$, 101 MHz): 149.6 (C-2'), 148.2 (C-4'), 136.1 (C-6'), 131.5 (C-1'), 124.2 (q, *J* = 283 Hz, C-2), 123.9 (C-5'), 70.3 (q, *J* = 32 Hz, C-1); δ_F($CDCl_3$, 377 MHz): −78.3 (d, *J* = 6.9 Hz); **HRMS** (ESI) calculated for $C_7H_7F_3N_1O_1$ $[M+H]^+$ 178.0474, found 178.0475.

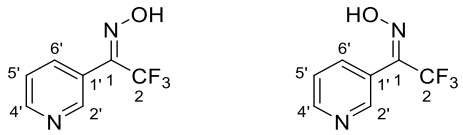
2,2,2-Trifluoro-1-(pyridin-3-yl)ethanone (2.72)



To a solution of 2,2,2-trifluoro-1-(pyridin-3-yl)ethan-1-ol (**2.74**) (2.50 g, 14.1 mmol) and "Bobbitt's" salt **2.83**[101] (10.0 g, 35.3 mmol) in anhydrous CH_2Cl_2 (40 mL) was added 2,6-lutidine (3.68 mL, 31.9 mmol) and the reaction mixture stirred for 16 h at room temperature. The solvent was removed under reduced pressure, Et_2O (50 mL) was added and the sides of the reaction flask scratched to induce full precipitation of the byproduct. The

resultant suspension was stirred for 10 min and filtered through a silica plug with Et_2O (3 x 50 mL) and concentrated under reduced pressure, yielding the crude title compound, which was used without further purification, as a colourless oil.

2,2,2-Trifluoro-1-(pyridin-3-yl)ethanone oxime (2.84 and 2.85)



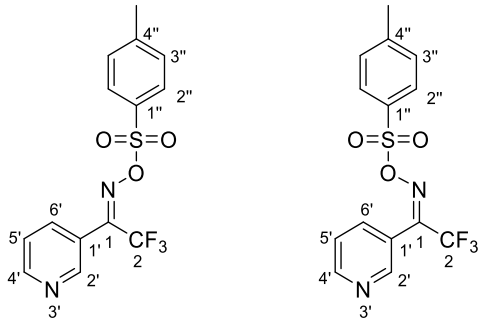
To a solution of crude 2,2,2-trifluoro-1-(pyridin-3-yl)ethanone (**2.72**) (from previous step) in ethanol (30 mL) and pyridine (4 mL) was added hydroxylamine hydrochloride (1.96 g, 28.3 mmol). The reaction mixture was stirred for 16 h at 70 °C. The reaction mixture was cooled, and concentrated under reduced pressure. The crude residue was extracted into Et_2O (100 mL) and washed with brine (100 mL). The aqueous phase was washed with Et_2O (2 x 50 mL), the organic phases combined, dried over $MgSO_4$, filtered and concentrated. Recrystallisation (EtOAc/Hexane) yielded the title compound as a mixture of separable isomers (1.48 g, 55% over two steps).

Isomer 1 (white solid, m.p. 138 °C): υ_{max} (cm^{-1}): 3556 (NH), 2779, 1595 (C=N), 1576, 1499, 1174, 964; δ_H($CDCl_3$, 400 MHz): 8.84 (d, *J* = 1.8 Hz, 1H, 2'-H), 8.66 (dd, *J* = 5.0, 1.8 Hz, 1H, 4'-H), 7.97 - 7.91 (m, 1H, 6'-H), 7.45 (ddd, *J* = 8.0, 5.0, 0.7 Hz, 1H, 5'-H); δ_C($CDCl_3$, 101 MHz): 149.1 (C-4'), 148.2 (C-2'), 143.2 (q, *J* = 31 Hz, C-1), 136.9 (C-6'), 128.2 (C-1'), 123.6 (C-5'), 118.4 (q, *J* = 283 Hz, C-2); δ_F($CDCl_3$, 377 MHz): −62.6; **HRMS** (ESI) calculated for $C_7H_6F_3N_2O_1$ $[M+H]^+$ 191.0427, found 191.0428.

Isomer 2 (white solid, 105 °C): υ_{max} (cm^{-1}): 3556 (NH), 2779, 1595 (C=N), 1576, 1499, 1174, 964; δ_H($CDCl_3$, 400 MHz): 8.90 (d, *J* = 1.5 Hz, 1H, 2'-H),

8.69 (dd, *J* = 5.1, 1.5 Hz, 1H, 4'-H), 7.97 - 7.91 (m, 1H, 6'-H), 7.52 (ddd, *J* = 8.0, 5.1, 1.2 Hz, 1H, 5'-H); δ_C($CDCl_3$, 101 MHz): 149.7 (C-4'), 149.3 (C-2'), 137.2 (C-6'), 143.2 (q, *J* = 31 Hz, C-1), 128.2 (C-1'), 123.9 (C-5'), 118.4 (q, *J* = 283 Hz, C-2); δ_F($CDCl_3$, 377 MHz): −66.0; **HRMS** (ESI) calculated for $C_7H_6F_3N_2O_1$ $[M+H]^+$ 191.0427, found 191.0428.

2,2,2-Trifluoro-1-(pyridin-3-yl)ethanone *O*-tosyl oxime (2.86 and 2.87)



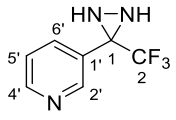
To a solution of 2,2,2-trifluoro-1-(pyridin-3-yl)ethanone oxime (**2.84** and **2.85**) (500 mg, 2.63 mmol) and DMAP (16 mg, 0.13 mmol) in anhydrous CH_2Cl_2 (15 mL) at 0 °C was added triethylamine (917 µL, 6.58 mmol) followed by tosyl chloride (604 mg, 3.16 mmol). The reaction mixture was stirred at room temperature for 2 h, diluted with CH_2Cl_2 (50 mL) and washed with brine (50 mL). The organic phase was dried over $MgSO_4$, filtered and concentrated under reduced pressure. Purification by flash column chromatography (20% EtOAc/Petrol) yielded the title compound as a mixture of separable isomers. (901 mg, 99%)

Isomer 1 (white solid, m.p. 87 °C): υ_{max} (cm^{-1}): 2989, 1597 (C=N), 1394, 1192, 1182, 889 (NO); δ_H($CDCl_3$, 400 MHz): 8.76 (dd, *J* = 4.8, 1.6 Hz, 1H, 4'-H), 8.64 (d, *J* = 1.6 Hz, 1H, 2'-H), 7.95 - 7.87 (m, 2H, 2''-H), 7.83 - 7.79 (m, 1H, 6'-H), 7.43 - 7.35 (m, 3H, 3''-H and 5'-H), 2.48 (s, 3H, 4''-CH_3); δ_C($CDCl_3$, 101 MHz): 152.5 (C-4'), 151.5 (q, *J* = 33 Hz, C-1), 149.1 (C-2'),

146.4 (C-1''), 136.2 (C-6'), 131.0 (C-4''), 130.0 (C-3''), 129.2 (C-2''), 124.4 (C-1'), 123.3 (C-5'), 117.0 (q, *J* = 284 Hz, C-2), 21.8 (4''-CH_3); δ_F($CDCl_3$, 377 MHz): −61.7; **HRMS** (ESI) calculated for $C_{14}H_{12}F_3N_2O_3S$ $[M+H]^+$ 345.0515, found 345.0500.

Isomer 2 (white solid, m.p. 108-110 °C): υ_{max} (cm^{-1}): 2992, 1597 (C=N), 1394, 1193, 1182, 899 (NO); δ_H($CDCl_3$, 400 MHz): 8.78 (dd, *J* = 4.9, 1.8 Hz, 1H, 4'-H), 8.64 (d, *J* = 1.8 Hz, 1H, 2'-H), 7.92 - 7.88 (m, 2H, 2''-H), 7.77 (m, 1H, 6'-H), 7.46 (ddd, *J* = 8.0, 4.9, 0.8 Hz, 1H, 5'-H), 7.43 - 7.39 (m, 2H, 3''-H), 2.50 (s, 3H, 4''-H_3); δ_C($CDCl_3$, 101 MHz): 152.4 (C-4'), 151.5 (q, *J* = 34 Hz, C-1), 148.7 (C-2'), 146.5 (C-1''), 136.1 (C-6'), 130.8 (C-4''), 130.0 (C-3''), 129.3 (C-2''), 123.5 (C-5'), 121.4 (C-1'), 119.4 (q, *J* = 277 Hz, C-2), 21.8 (4''-CH_3); δ_F($CDCl_3$, 377 MHz): −66.9; **HRMS** (ESI) calculated for $C_{14}H_{12}F_3N_2O_3S$ $[M+H]^+$ 345.0515, found 345.0500.

3-(3-(Trifluoromethyl)diaziridin-3-yl)pyridine (2.88)

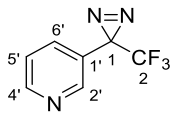


A solution of 2,2,2-trifluoro-1-(pyridin-3-yl)ethanone *O*-tosyl oxime (**2.86** and **2.87**) (267 mg, 0.780 mmol) in CH_2Cl_2 (2 mL) was added dropwise to a microwave vial at −78 °C containing liquid ammonia (3 mL). The vial was sealed and stirred for 16 h at room temperature. The vial was cooled to −78 °C, unsealed and excess ammonia evaporated. The residue was diluted in CH_2Cl_2 (40 mL) and washed with H_2O (2 x 20 mL). The organic phase was dried over $MgSO_4$, filtered and concentrated under reduced pressure, yielding the title compound as a white solid (126 mg, 85%). m.p. 91-92 °C.

υ_{max} (cm^{-1}): 3283 (NH), 2988, 1596, 1578, 1395, 1184, 1145; δ_H($CDCl_3$, 400 MHz): 8.87 (d, *J* = 1.7 Hz, 1H, 2'-H), 8.69 (dd, *J* = 4.9, 1.7 Hz, 1H, 4'-H),

7.94 (d, *J* = 8.0 Hz, 1H, 6′-H), 7.37 (ddd, *J* = 8.0, 4.9, 0.8 Hz, 1H, 5′-H), 2.89 (d, *J* = 8.5 Hz, 1H, NH), 2.33 (d, *J* = 8.5 Hz, 1H, NH); δ_C($CDCl_3$, 101 MHz): 151.3 (C-4′), 149.4 (C-2′), 135.9 (C-6′), 127.9 (C-1′), 123.4 (C-5′), 123.2 (q, *J* = 278 Hz, C-2), 56.6 (q, *J* = 37 Hz, C-1); δ_F($CDCl_3$, 377 MHz): −75.5; **HRMS** (ESI) calculated for $C_7H_7F_3N_3$ $[M+H]^+$ 190.0587, found 190.0591.

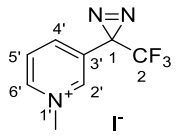
3-(3-(Trifluoromethyl)-3*H*-diazirin-3-yl)pyridine (2.89)



To a solution of 3-(3-(trifluoromethyl)diaziridin-3-yl)pyridine (**2.88**) (100 mg, 0.530 mmol) in Et_2O (10 mL) at room temperature, was added activated manganese dioxide (460 mg, 5.30 mmol). The reaction mixture was left to stir for 30 min, filtered through Celite® and washed with Et_2O (50 mL) and concentrated under reduced pressure, utilising an ice bath, yielding the title compound as a volatile yellow oil, which was used immediately in the next step.

υ_{max} (cm^{-1}): 2928, 1621, 1346, 1152; δ_H($CDCl_3$, 400 MHz): 8.69 (dd, *J* = 4.8, 1.8 Hz, 1H, 4′-H), 8.52 (d, *J* = 1.8 Hz, 1H, 2′-H), 7.60 - 7.54 (m, 1H, 6′-H), 7.36 (ddd, *J* = 8.0, 4.8, 0.9 Hz, 1H, 5′-H); δ_C($CDCl_3$, 101 MHz): 150.7 (C-4′), 147.9 (C-2′), 134.3 (C-6′), 125.4 (C-1′), 123.3 (C-5′), 121.7 (q, *J* = 275 Hz, C-2′), 27.1 (q, *J* = 41 Hz, C-1); δ_F($CDCl_3$, 377 MHz,): −65.5.

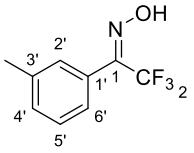
1-Methyl-3-(3-(trifluoromethyl)-3*H*-diazirin-3-yl)pyridin-1-ium iodide (2.91)



To a solution of 3-(3-(trifluoromethyl)-3*H*-diazirin-3-yl)pyridine (**2.89**) (from previous step) in acetonitrile (5 mL) was added methyl iodide (330 µL, 5.30 mmol) and the reaction heated at 50 °C for 16 h. The reaction mixture was concentrated under reduced pressure, suspended in Et_2O (15 mL) and filtered, washing with Et_2O (30 mL) to yield the title compound as a yellow solid (92 mg, 53% (over two steps)). m.p. 130 °C.

υ_{max} (cm^{-1}): 3035, 1644, 1517, 815; δ_H(CD_3OD, 400 MHz): 9.07 (d, *J* = 6.6 Hz, 1H, 6'-H), 9.00 (s, 1H, 2'-H), 8.64 (d, *J* = 7.8 Hz, 1H, 4'-H), 8.21 (dd, *J* = 7.8, 6.6 Hz, 1H, 5'-H), 4.46 (s, 3H, 1'-CH_3); δ_C(CD_3OD, 101 MHz): 148.5 (C-6'), 146.3 (C-2'), 145.2 (C-4'), 131.2 (C-3'), 129.8 (C-5'), 122.7 (q, *J* = 275 Hz, C-2), 28.0 (q, *J* = 43 Hz, C-1), (1-CH_3 not visible); δ_F(CD_3OD, 377 MHz) −67.3; **HRMS** (ESI) calculated for $C_8H_7F_3N_3$ $[M]^+$ 202.0587, found 202.0591.

(*E*)-2,2,2-Trifluoro-1-(*m*-tolyl)ethan-1-one oxime[109] **(2.100)**



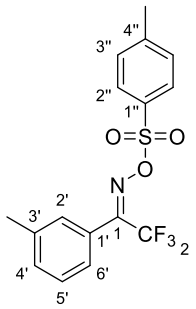
Step 1: To a solution of 3-bromotoluene (**2.98**) (3.00 g, 29.2 mmol) in anhydrous THF (50 mL) at −78 °C was added *n*-BuLi (2.87 mL, 32.2 mmol of a 2.5 M solution in hexane) and the solution stirred for 20 min. Ethyl trifluoroacetate (3.83 mL, 32.2 mmol) was added, the solution slowly warmed to room temperature over 2 h before the addition of sat. $NH_4Cl_{(aq)}$

(10 mL). Volatiles were removed under reduced pressure, and the product was extracted between Et_2O (80 mL) and sat. $NH_4Cl_{(aq)}$ (2 x 50 mL). The organic layer was dried over $MgSO_4$, filtered and concentrated under reduced pressure to yield the crude trifluoromethylketone as a clear oil, which was used without further purification.

Step 2: To a solution of crude trifluoromethylketone (from previous step) in ethanol (40 mL) and pyridine (2 mL) was added hydroxylamine hydrochloride (2.24 g, 32.2 mmol). The reaction mixture was heated to 70 °C for 16 h, cooled and diluted with Et_2O (80 mL) and washed with 2 M $HCl_{(aq)}$ (50 mL). The aqueous layer was then washed with Et_2O (2 x 50 mL) and the organic layers combined, dried over $MgSO_4$, filtered and concentrated under reduced pressure. Purification by recrystallisation from hexane yielded the title compound as a white solid (4.31 g, 73%). m.p. 62 °C

υ_{max} (cm^{-1}): 3311 (OH), 1336, 1132; δ_H($CDCl_3$, 400 MHz): 8.71 (s, 1H, N-OH), 7.42 – 7.36 (m, 1H, 2'-H), 7.34 – 7.29 (m, 3H, 4'-H, 5'-H and 6'-H), 2.42 (s, 3H, 3'-CH_3); δ_C ($CDCl_3$, 101 MHz): 148.1 (q, *J* = 32 Hz, C-1), 138.4 (Ar), 131.4 (Ar), 129.0 (Ar), 128.5 (Ar), 125.9 (Ar), 125.6 (Ar), 120.6 (q, *J* = 275 Hz, C-2), 21.4 (3'-CH_3); δ_F ($CDCl_3$, 377 MHz): −66.8. Does not ionise by ESI.

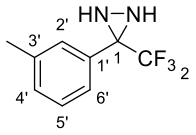
2,2,2-Trifluoro-1-(*m*-tolyl)ethan-1-one O-tosyl oxime[109] (2.101)



To a solution of 2,2,2-trifluoro-1-(*m*-tolyl)ethan-1-one oxime (**2.100**) (3.75 g, 18.5 mmol) and DMAP (112 mg, 0.924 mmol) in anhydrous CH_2Cl_2 (60 mL) at 0 °C was added triethylamine (6.44 mL, 46.2 mmol) followed by tosyl chloride (4.23 g, 22.2 mmol). The reaction was stirred at room temperature for 40 min, diluted with CH_2Cl_2 (40 mL) and washed with H_2O (60 mL). The organic layer was dried over $MgSO_4$, filtered and concentrated under reduced pressure. The crude residue was filtered through a silica pad using CH_2Cl_2 as the eluent to yield the title compound as a white solid (6.04 g, 92%). m.p. 100 °C

υ_{max} (cm^{-1}): 3045, 2923, 1598 (C=N), 1389, 1181, 1154; δ_H($CDCl_3$, 400 MHz): 7.93 - 7.88 (m, 2H, 2''-H), 7.42 - 7.39 (m, 2H, 3''-H), 7.39 – 7.33 (m, 2H, 2'-H and 6'-H), 7.21 - 7.16 (m, 2H, 4'-H and 5'-H), 2.49 (s, 3H, 4''-CH_3), 2.40 (s, 3H, 3'-CH_3); δ_C($CDCl_3$, 101 MHz): 154.3 (q, *J* = 34 Hz, C-1), 146.1 (C-1''), 138.8 (C-3'), 132.4 (Ar), 131.3 (C-4''), 129.9 (C-3''), 129.3 (C-2''), 128.7 (Ar), 128.6 (Ar), 125.5 (Ar), 124.6 (C-1'), 119.6 (q, *J* = 278 Hz, C-2), 21.8 (4''-CH_3), 21.4 (3'-CH_3); δ_F($CDCl_3$, 377 MHz): −66.9; **HRMS** (ESI) calculated for $C_{16}H_{14}F_3NNaO_3S$ $[M+Na]^+$ 380.0539, found 380.0541.

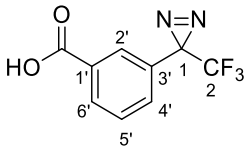
3-(*m*-Tolyl)-3-(trifluoromethyl)diaziridine[109] (2.102)



A solution of 2,2,2-trifluoro-1-(*m*-tolyl)ethan-1-one *O*-tosyl oxime (**2.101**) (1.50 g, 4.20 mmol) in CH_2Cl_2 (4 mL) was added dropwise to a microwave vial containing liquid ammonia (3 mL) at −78 °C. The vial was sealed and stirred for 16 h at room temperature. The vial was cooled to −78 °C, unsealed and excess ammonia evaporated. The residue was diluted in CH_2Cl_2 (40 mL) and washed with H_2O (2 x 20 mL). The organic layer was dried over $MgSO_4$, filtered and concentrated under reduced pressure to yield the pure title compound, which was used without further purification, as a colourless oil (848 mg, quant.).

υ_{max} (cm^{-1}): 3281 (NH), 3010, 1393, 1182, 1144; δ_H($CDCl_3$, 400 MHz): 7.47 – 7.42 (m, 2H, Ar), 7.34 (m, 1H, Ar), 7.31 – 7.26 (m, 1H, Ar), 2.78 (d, *J* = 8.2 Hz, 1H, NH), 2.40 (s, 3H, 3'-CH_3), 2.23 (d, *J* = 8.2 Hz, 1H, NH); δ_C($CDCl_3$, 101 MHz): 138.6 (C-3'), 131.6 (C-1'), 130.9 (Ar), 128.7 (Ar), 128.6 (Ar), 125.2 (Ar), 123.6 (q, *J* = 278 Hz, C-2), 58.1 (q, *J* = 36 Hz, C-1), 21.3 (3'-CH_3); δ_F($CDCl_3$, 377 MHz): −75.6. Does not ionise by ESI

3-(3-(Trifluoromethyl)-3*H*-diazirin-3-yl)benzoic acid[110] (2.103)

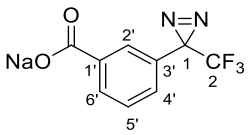


To a solution of 3-(*m*-tolyl)-3-(trifluoromethyl)diaziridine (**2.102**) (600 mg, 2.97 mmol) in pyridine (10 mL) and water (10 mL) was added $KMnO_4$ (1.90 g, 12.0 mmol). The solution was heated to 50 °C and stirred for 16 h. The reaction mixture was cooled, acidified with 6M HCl (aq) and excess $KMnO_4$

reduced with 10% $Na_2S_2O_{3(aq)}$. The solution was extracted into Et_2O (2 x 30 mL), the organics combined, dried over $MgSO_4$, filtered and concentrated under reduced pressure. The crude residue was dissolved in Et_2O (50 mL) and extracted into 2M $NaOH_{(aq)}$. The aqueous layer was acidified with 2M $HCl_{(aq)}$ and extracted with Et_2O (2 x 30 mL). The organic layers were combined, dried over $MgSO_4$, filtered and concentrated under reduced pressure to yield the title compound as a white solid (200 mg, 29%). m.p. 110 °C (lit: 85-87 °C decomposition).[110]

υ_{max} (cm^{-1}): 2987 (OH), 1691 (C=O), 1419, 1137; δ_H(CD_3OD, 400 MHz): 8.13 – 8.11 (m, 1H, 6'-H), 7.90 – 7.87 (m, 1H, 2'-H), 7.63 - 7.55 (m, 1H, 5'-H), 7.48 (m, 1H, 4'-H); δ_C(CD_3OD, 101 MHz): 168.2 (CO_2H), 133.1 (C-3'), 132.2 (Ar), 131.7 (Ar), 130.6 (Ar), 130.4 (C-1'), 128.6 (Ar), 123.5 (q, *J* = 274 Hz, C-2), 29.4 (q, *J* = 40 Hz, C-1); δ_F(CD_3OD, 377 MHz): −63.2; **HRMS** (ESI) calculated for $C_9H_4F_3N_2O_2$ $[M-H]^+$ 229.0230, found 229.0232.

Sodium 3-(3-(trifluoromethyl)-3*H*-diazirin-3-yl)benzoate (2.94)

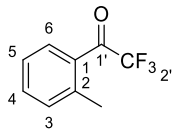


To a solution of sodium hydroxide (8 mg, 0.2 mmol) in H_2O (1 mL) was added 3-(3-(trifluoromethyl)-3*H*-diazirin-3-yl)benzoic acid (**2.103**) (50 mg, 0.22 mmol), and the suspension stirred for 5 min. The suspension was filtered, and the filtrate concentrated under reduced pressure to yield the title compound as a white solid (48 mg, 94%). m.p. 215 °C (decomposition).

υ_{max} (cm^{-1}): 1615 (C=O), 1557, 1397, 1146; δ_H(CD_3OD, 400 MHz): 8.04 (ddd, *J* = 7.8, 1.4, 1.4 Hz, 1H, 6'-H), 7.83 (s, 1H, 2'-H), 7.46 (dd, *J* = 7.8, 7.8, 1H, 5'-H), 7.33 (dd, *J* = 7.8, 1.4 Hz, 1H, 4'-H); δ_C(CD_3OD, 101 MHz): 173.5 (CO_2Na), 140.3 (C-3'), 131.8 (C-6'), 129.7 (C-5'), 129.5 (C-1'), 129.1

(C-4'), 128.3 (C-2'), 123.7 (q, *J* = 274 Hz, C-2), 29.6 (q, *J* = 40 Hz, C-1); δ_F(CD_3OD, 377 MHz): −67.1; **HRMS** (ESI) calculated for $C_9H_4F_3N_2O_2$ $[M-H]^+$ 229.0230, found 229.0237.

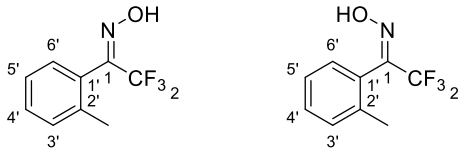
2,2,2-Trifluoro-1-(*o*-tolyl)ethan-1-one[111] (2.105)



To a solution of 2-bromotoluene (**2.104**) (1.50 g, 8.75 mmol) in anhydrous THF (15 mL) at −78 °C was added *n*-BuLi (3.91 mL, 9.19 mmol of a 2.35 M solution in hexane) dropwise. The solution was stirred for 10 min and ethyl trifluoroacetate (1.15 mL, 9.63 mmol) added. The reaction was stirred for 30 min and warmed to room temperature and water (10 mL) added. Volatiles were removed under reduced pressure and the product extracted between Et_2O (2 x 50 mL) and brine (50 mL). The organic phases were combined, dried over $MgSO_4$, filtered and concentrated under reduced pressure to yield the title compound as a clear oil (995 mg, 60%).

υ_{max} (cm^{-1}): 1713 (C=O), 1182, 1139; δ_H($CDCl_3$, 400 MHz): 7.90 – 7.88 (m, 1H, 6-H), 7.56 – 7.53 (m, 1H, 4-H), 7.41 – 7.33 (m, 2H, 5-H, 3-H), 2.60 (s, 3H); δ_C($CDCl_3$, 101MHz): 182.4 (q, *J* = 34 Hz, C-1'), 142.4 (C-2), 134.0 (C-4), 132.7 (C-3), 130.5 (q, *J* = 4 Hz, C-6), 129.2 (C-1), 126.0 (C-5), 116.5 (q, *J* = 293 Hz), 21.9 (2-CH_3); δ_F($CDCl_3$, 377 MHz): −71.3 (d, *J* = 2.0 Hz). **HRMS** (EI) calculated for $C_9H_7F_3O$ $[M]^+$ 188.04435, found 188.04378.

2,2,2-Trifluoro-1-(*o*-tolyl)ethan-1-one oxime (2.106)

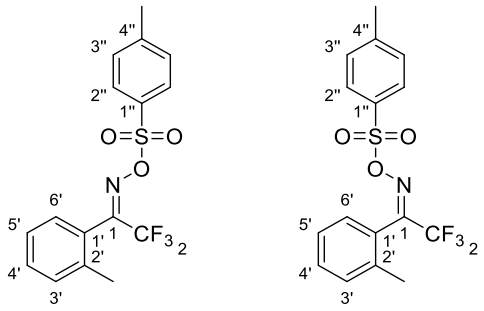


To a solution of 2,2,2-trifluoro-1-(*o*-tolyl)ethan-1-one (**2.105**) (733 mg, 3.90 mmol) in pyridine (2 mL) and ethanol (10 mL) was added hydroxylamine hydrochloride (325 mg, 4.68 mmol). The reaction mixture was heated at 70 °C for 16 h, cooled, diluted with Et_2O (100 mL), washed with 2M HCl (100 mL), dried over $MgSO_4$, filtered and concentrated under reduced pressure. Purification by flash column chromatography (0-5% Et_2O/Petrol) yielded the title compound as a mixture of two isomers (776 mg, 98%).

Isomer 1 (white solid, m.p. 72 °C). υ_{max} (cm^{-1}): 3238 (OH), 1329, 1148; δ_H($CDCl_3$, 400 MHz): 8.76 (s, 1H, N-OH), 7.40 (ddd, *J* = 7.6, 7.6, 1.5 Hz, 1H, Ar), 7.35 – 7.27 (m, 2H, Ar), 7.21 (d, *J* = 7.6 Hz, 1H, Ar), 2.31 (s, 3H, 2'-CH_3); δ_C($CDCl_3$, 101 MHz): 148.9 (q, *J* = 33 Hz, C-1), 137.3 (C-2'), 130.3 (Ar), 130.2 (Ar), 127.7 (Ar), 126.6 (C-1'), 125.9 (Ar), 120.6 (q, *J* = 275 Hz, C-2), 19.4 (2'-CH_3); δ_F ($CDCl_3$, 377 MHz): −68.2; **HRMS** (ESI) calculated for $C_9H_7F_3NO$ $[M-H]^-$ 202.0485, found 202.0486.

Isomer 2 (colourless oil). υ_{max} (cm^{-1}): 3321 (OH), 1331, 1185, 1133; δ_H($CDCl_3$, 400 MHz): 9.11 (s, 1H, N-OH), 7.45 – 7.36 (m, 1H, Ar), 7.32 – 7.24 (m, 3H, Ar), 2.36 (s, 3H, 2'-CH_3) ; δ_C($CDCl_3$, 101 MHz): 148.6 (q, *J* = 31 Hz), 137.7 (C-2'), 130.5 (Ar), 130.2 (Ar), 129.7 (Ar), 129.7 (C-1'), 125.8 (Ar), 118.0 (q, *J* = 283 Hz), 19.5 (2'-CH_3); δ_F ($CDCl_3$, 377 MHz): -64.1; **HRMS** (ESI) calculated for $C_9H_7F_3NO$ $[M-H]^-$ 202.0485, found 202.0487.

2,2,2-Trifluoro-1-(*o*-tolyl)ethan-1-one *O*-tosyl oxime (2.107)



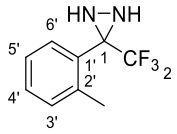
To a solution of 2,2,2-trifluoro-1-(*o*-tolyl)ethan-1-one oxime (**2.106**) (mix of isomers, 1.50 g, 7.38 mmol) and DMAP (90 mg, 0.74 mmol) in CH_2Cl_2 (30 mL) at 0 °C was added triethylamine (2.57 mL, 18.5 mmol) followed by tosyl chloride (1.55 g, 8.12 mmol). The reaction was stirred at room temperature for 1 h, diluted with CH_2Cl_2 (40 mL) and washed with H_2O (60 mL). The aqueous phase was washed with CH_2Cl_2 (50 mL), the organic phases combined, dried over $MgSO_4$, filtered and concentrated under reduced pressure. Purification by flash column chromatography (20% Et_2O/Petrol) yielded the title compound as a mix of isomers (2.51 g, 95%).

Isomer 1 (white solid, m.p. 96 °C). υ_{max} (cm^{-1}): 1597 (C=N), 1391, 1179; δ_H($CDCl_3$, 400 MHz): 7.94 – 7.82 (m, 2H, 2''-H), 7.43 – 7.36 (m, 3H, 6'-H and 3''-H), 7.31 – 7.23 (m, 2H, 4'-H and 5'-H), 7.07 (d, *J* = 7.7 Hz, 1H, 3'-H), 2.49 (s, 2H, 4''-CH_3), 2.14 (s, 3H, 2'-CH_3); δ_C($CDCl_3$, 101 MHz): 155.1 (q, *J* = 34 Hz, C-1), 146.1 (C-1''), 136.6 (C-2'), 131.2 (C-4''), 131.0 (C-6'), 130.6 (C-4'), 129.8 (C-3''), 129.2 (C-2''), 126.9 (C-3'), 126.0 (C-5'), 125.0 (C-1'), 119.5 (q, *J* = 277 Hz, C-2), 21.8 (4''-CH_3), 19.3 (2'-CH_3); δ_F ($CDCl_3$, 377 MHz): −68.4; **HRMS** (ESI) calculated for $C_{16}H_{14}F_3NNaO_3S$ $[M+Na]^+$ 380.0539, found 380.0535.

Isomer 2 (white solid, m.p. 65 °C). υ_{max} (cm^{-1}): 1597 (C=N), 1387, 1179; δ_H($CDCl_3$, 400 MHz): 7.89 – 7.86 (m, 2H, 2''-H), 7.42 – 7.34 (m, 3H, 6'-H and 3''-H), 7.28 – 7.20 (m, 2H, 4'-H and 5'-H), 7.15 – 7.10 (m, 1H, 3'-H),

2.47 (s, 3H, 4''-CH_3), 2.13 (s, 3H, 2'-CH_3).; δ_C($CDCl_3$, 101 MHz): 155.3 (q, *J* = 34 Hz, C-1), 145.9 (C-1''), 137.6 (C-2'), 131.6 (C-4''), 131.1 (C-6'), 130.7 (C-4'), 129.8 (C-3''), 129.4 (C-3'), 129.2 (C-1'), 129.1 (C-2''), 125.9 (C-5'), 116.9 (q, *J* = 284 Hz, C-2), 21.7 (4''-CH_3), 19.3 (2'-CH_3); δ_F ($CDCl_3$, 377 MHz): −63.2; **HRMS** (ESI) calculated for $C_{16}H_{14}F_3NNaO_3S$ $[M+Na]^+$ 380.0539, found 380.0535.

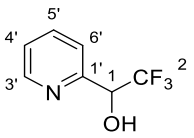
3-(*o*-Tolyl)-3-(trifluoromethyl)diaziridine (2.108)



A solution of 2,2,2-trifluoro-1-(*o*-tolyl)ethan-1-one *O*-tosyl oxime (**2.107**) (2.19 g, 6.13 mmol) in CH_2Cl_2 (3 mL) was added dropwise to a microwave vial containing liquid ammonia (3 mL) at −78 °C. The vial was sealed and stirred for 16 h at room temperature. The vial was cooled to −78 °C, unsealed and excess ammonia evaporated. The residue was diluted in CH_2Cl_2 (40 mL) and washed with H_2O (2 x 20 mL). The organic layer was dried over $MgSO_4$, filtered and concentrated under reduced pressure. Purification by flash column chromatography (20% EtOAc/Petrol) yielded the title compound as a colourless oil (409 mg, 33%).

υ_{max} (cm^{-1}): 3256 (NH), 1389, 1139; δ_H($CDCl_3$, 400 MHz): 7.48 – 7.45 (m, 1H, 6'-H), 7.37 (m, 1H, Ar), 7.28 – 7.26 (m, 2H, Ar), 2.85 (d, *J* = 8.9 Hz, 1H, NH), 2.50 (s, 3H, 2'-CH_3), 2.38 (d, *J* = 8.9 Hz, 1H, NH); δ_C($CDCl_3$, 101 MHz): 138.2 (C-2'), 130.8 (Ar), 130.1 (C-1'), 129.9 (Ar), 129.9 (Ar), 125.9 (Ar), 123.7 (q, *J* = 279 Hz, C-2), 57.8 (q, *J* = 37 Hz, C-1), 19.0 (q, *J* = 2 Hz, 2'-CH_3); δ_F ($CDCl_3$, 377 MHz): −76.6; **HRMS** (ESI) calculated for $[M+Na]^+$ 225.0610 , found 225.0608.

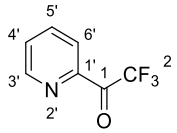
(*rac*)-2,2,2-Trifluoro-1-(pyridin-2-yl)ethan-1-ol[102] **(2.111)**



2-Pyridinecarboxaldehyde (**2.110**) (2.14 g, 20.0 mmol) was added to a solution of $TMSCF_3$ (3.25 mL, 22.0 mmol) in anhydrous THF (30 mL) at 0 °C. TBAF (1.0 M in THF, 0.20 mL, 0.20 mmol) was added and the reaction stirred for 16 h at room temperature. To the reaction mixture was added H_2O (10 mL) then TBAF (1 M in THF, 2 mL, 2 mmol) and the resultant solution stirred for 1 h at room temperature. The reaction mixture was concentrated under reduced pressure, and extracted between Et_2O (2 x 60 mL) and brine (60 mL). The organic layers were combined, dried over $MgSO_4$, filtered and concentrated under reduced pressure. Purification by flash column chromatography (50% Et_2O in petrol) yielded the title compound as a white solid (3.54 g, 88%). m.p. 44 °C (lit: 46 °C).[112]

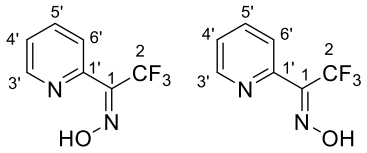
υ_{max} (cm^{-1}): 3065 (OH), 1596, 1439, 1258, 1124; δ_H($CDCl_3$, 400 MHz): 8.64 (ddd, *J* = 4.9, 1.5, 1.2 Hz, 1H, 3'-H), 7.81 (ddd, *J* = 7.9, 7.7, 1.5 Hz, 1H, 5'-H), 7.44 (ddd, *J* = 7.9, 1.6, 1.2 Hz, 1H, 6'-H), 7.40 (ddd, *J* = 7.7, 4.9, 1.6 Hz, 1H, 4'-H), 5.50 (s, 1H, OH), 5.04 (q, *J* = 6.7 Hz, 1H, 1-H); δ_C($CDCl_3$, 101 MHz); 151.0 (q, *J* = 2 Hz, C-1'), 148.3 (C-3'), 137.2 (C-5'), 124.5 (d, *J* = 283 Hz, C-2), 124.4 (C-4'), 122.6 (d, *J* = 3 Hz, C-6'), 70.6 (q, *J* = 32 Hz, C-1); δ_F($CDCl_3$, 377 MHz): −78.0 (dd, *J* = 6.6, 1.1 Hz); **HRMS** (ESI) calculated for $C_7H_7F_3N_1O_1$ $[M+H]^+$ 178.0474, found 178.0476.

2,2,2-Trifluoro-1-(pyridin-2-yl)ethan-1-one (2.112)



To a solution of 2,2,2-trifluoro-1-(pyridin-2-yl)ethan-1-ol (**2.111**) (1.20 g, 6.78 mmol) and "Bobbitt's" salt **2.83**[101] (4.82 g, 16.9 mmol) anhydrous CH_2Cl_2 (17 mL) was added 2,6-lutidine (1.77 mL, 15.2 mmol) and the reaction mixture was stirred for 16 h at room temperature The solvent was removed under reduced pressure, Et_2O (50 mL) was added, and the sides of the reaction flask scratched to induce full precipitation of the byproduct. The resultant suspension was stirred for 10 min and filtered through a silica plug, eluting with Et_2O (3 x 50 mL) and concentrated under reduced pressure, yielding the crude title compound as a mixture of ketone and hydrate, which was used without further purification, as a colourless oil.

2,2,2-Trifluoro-1-(pyridin-2-yl)ethan-1-one oxime (2.113 and 2.114)



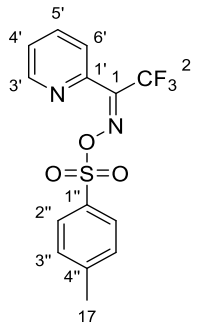
To a solution of crude 2,2,2-trifluoro-1-(pyridin-2-yl)ethan-1-one (**2.112**) (from previous step) in ethanol (10 mL) and pyridine (2 mL) was added hydroxylamine hydrochloride (519 mg, 7.47 mmol). The reaction mixture was stirred for 16 h at 70 °C. The reaction mixture was cooled, and concentrated under reduced pressure. The crude residue was extracted into EtOAc (100 mL) and washed with brine (100 mL). The aqueous phase was washed with EtOAc (2 x 50 mL), the organic phases combined, dried over $MgSO_4$, filtered and concentrated. Purification by flash column

chromatography (10-30% EtOAc/Petrol) yielded the title compound as a mixture of separable isomers (843 mg, 65%).

E-Isomer (determined by ^{1}H NMR) **2.114** (white solid, m.p. 99 °C): υ_{max} (cm^{-1}): 2808 (NH), 1596 (C=N), 1353, 1187, 1118; δ_{H}($CDCl_3$, 400 MHz): 17.30 (s, 1H, N-OH), 8.62 (ddd, *J* = 5.1, 2.0, 1.0 Hz, 1H, 3'-H), 8.03 (dddd, *J* = 8.2, 7.9, 2.1, 2.0 Hz, 1H, 5'-H), 7.65 (m, 1H, 6'-H), 7.59 (dd, *J* = 7.9, 5.1 Hz, 1H, 4'-H); δ_{C}($CDCl_3$, 101 MHz): 147.7 (C-1'), 145.9 (C-3'), 139.5 (q, *J* = 32 Hz, C-1), 138.8 (C-5'), 126.0 (C-4'), 121.9 (q, *J* = 3 Hz, C-6'), 121.2 (q, *J* = 275 Hz, C-2); δ_{F}(377 MHz, $CDCl_3$): −64.6 (d, *J* = 2 Hz); **HRMS** (ESI) calculated for $C_7H_6F_3N_2O_1$ $[M+H]^+$ 191.0427, found 191.0428.

Z-isomer (determined by ^{1}H NMR) **2.113** (white solid, m.p. 89-90 °C): υ_{max} (cm^{-1}): 2692 (NH), 1632 (C=N), 1494, 1224, 1143; δ_{H}($CDCl_3$, 400 MHz): 11.92 (s, 1H), 8.70 (d, *J* = 4.9 Hz, 1H, 3'-H), 7.82 (ddd, *J* = 7.8, 7.8, 1.8 Hz, 1H, 5'-H), 7.59 (dddd, *J* = 7.9, 1.0, 1.0, 1.0 Hz, 1H, 6'-H), 7.42 (ddd, *J* = 7.6, 5.0, 1.2 Hz, 1H, 4'-H); δ_{C}($CDCl_3$, 101 MHz): 149.3 (C-3'), 148.2 (C-1'), 144.5 (q, *J* = 30 Hz, C-1), 137.3 (C-5'), 124.6 (C-4'), 124.0 (C-6'), 118.2 (q, *J* = 283 Hz, C-2); δ_{F}(377 MHz, $CDCl_3$): −64.1; **HRMS** (ESI) calculated for $C_7H_6F_3N_2O_1$ $[M+H]^+$ 191.0427, found 191.0431.

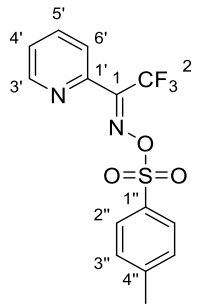
(*E*)-2,2,2-Trifluoro-1-(pyridin-2-yl)ethan-1-one *O*-tosyl oxime (2.116)



To a solution of *E*-2,2,2-trifluoro-1-(pyridin-2-yl)ethanone oxime (**2.114**) (200 mg, 1.05 mmol) and DMAP (13 mg, 0.11 mmol) in anhydrous CH_2Cl_2 (10 mL) at 0 °C was added triethylamine (367 µL, 2.63 mmol) followed by tosyl chloride (221 mg, 1.16 mmol). The reaction mixture was stirred at room temperature for 1 h, diluted with CH_2Cl_2 (50 mL) and washed with brine (50 mL). The organic phase was dried over $MgSO_4$, filtered and concentrated under reduced pressure. Purification by flash column chromatography (10-20% EtOAc/Petrol) yielded the title compound as a white solid (309 mg, 85%). m.p. 69 °C.

υ_{max} (cm^{-1}): 1584 (C=N), 1388, 1194; δ_H($CDCl_3$, 400 MHz): 8.76 – 8.72 (m, 1H, 3'-H), 7.93 – 7.83 (m, 3H, 2''-H and 5'-H), 7.66 (ddd, *J* = 7.9, 1.1, 1.1 Hz, 1H, 6'-H), 7.45 (ddd, *J* = 7.8, 4.8, 1.1 Hz, 1H, 4'-H), 7.42 – 7.38 (m, 2H, 3''-H), 2.48 (s, 3H, 4''-CH_3); δ_C($CDCl_3$, 101 MHz): 152.2 (q, *J* = 33 Hz, C-1), 150.1 (C-3'), 146.3 (C-1''), 144.2 (C-1), 136.8 (C-5'), 130.9 (C-4''), 129.9 (C-3''), 129.3 (C-2''), 126.1 (C-6'), 125.8 (C-4'), 119.3 (q, *J* = 278 Hz, C-2), 21.8 (4''-CH_3); δ_F($CDCl_3$, 377 MHz): −65.5 (d, *J* = 1.6 Hz); **HRMS** (ESI) calculated for $C_{14}H_{12}F_3N_2O_3S$ $[M+H]^+$ 345.0515, found 345.0519.

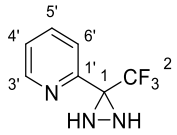
(*Z*)-2,2,2-Trifluoro-1-(pyridin-2-yl)ethan-1-one *O*-tosyl oxime (2.115)



To a solution of *Z*-2,2,2-trifluoro-1-(pyridin-2-yl)ethanone oxime (**2.113**) (200 mg, 1.05 mmol) and DMAP (13 mg, 0.11 mmol) in anhydrous CH_2Cl_2 (10 mL) at 0 °C was added triethylamine (367 µL, 2.63 mmol) followed by tosyl chloride (221 mg, 1.16 mmol). The reaction mixture was stirred at room temperature for 1 h, diluted with CH_2Cl_2 (50 mL) and washed with brine (50 mL). The organic phase was dried over $MgSO_4$, filtered and concentrated under reduced pressure. Purification by flash column chromatography (20% EtOAc/Petrol) yielded the title compound as a white solid (275 mg, 76%). m.p. 75 °C.

υ_{max} (cm^{-1}): 1596 (C=N), 1391, 1180; δ_H($CDCl_3$, 400 MHz): 8.68 (ddd, *J* = 4.8, 1.8, 0.9 Hz, 1H, 3'-H), 7.92 – 7.86 (m, 2H, 2''-H), 7.80 (ddd, *J* = 7.9, 7.8, 1.8 Hz, 1H, 5'-H), 7.54 (ddd, *J* = 7.9, 1.1, 1.1 Hz, 1H, 6'-H), 7.43 (ddd, *J* = 7.8, 4.8, 1.1 Hz, 1H, 4'-H), 7.40 – 7.34 (m, 2H, 3''-H), 2.46 (s, 3H, 4''-CH_3); δ_C($CDCl_3$, 101 MHz): 152.0 (q, *J* = 32 Hz, C-1), 149.7 (C-3'), 147.7 (C-1'), 146.2 (C-1''), 137.1 (C-5'), 131.2 (C-4''), 130.0 (C-3''), 129.1 (C-2''), 125.6 (C-4'), 124.1 (C-6'), 117.0 (q, *J* = 284 Hz, C-2), 21.7 (4''-CH_3); δ_F($CDCl_3$, 377 MHz): −61.4 (d, *J* = 0.9 Hz); **HRMS** (ESI) calculated for $C_{14}H_{12}F_3N_2O_3S$ $[M+H]^+$ 345.0515, found 345.0510.

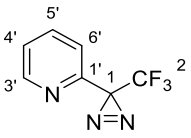
2-(3-(Trifluoromethyl)diaziridin-3-yl)pyridine (2.117)



A solution of (*Z*)-2,2,2-trifluoro-1-(pyridin-2-yl)ethan-1-one *O*-tosyl oxime (**2.115**) (232 mg, 0.670 mmol) in CH_2Cl_2 (2 mL) was added dropwise to a microwave vial at −78 °C containing liquid ammonia (3 mL). The vial was sealed and stirred for 16 h at room temperature. The vial was cooled to −78 °C, unsealed and excess ammonia evaporated. The residue was diluted in CH_2Cl_2 (30 mL) and washed with H_2O (30 mL). The organic phase was dried over $MgSO_4$, filtered and concentrated under reduced pressure, yielding the title compound as an impure white solid (117 mg, 92%). m.p. 35 °C.

υ_{max} (cm^{-1}): 3207 (NH), 1591, 1137; δ_H($CDCl_3$, 400 MHz): 8.63 (ddd, *J* = 4.9, 1.4, 1.4 Hz, 1H, 3'-H), 7.85 – 7.74 (m, 2H, 5'-H and 6'-H), 7.38 (ddd, *J* = 6.9, 4.9, 1.6 Hz, 1H, 4'-H), 3.64 (d, *J* = 9.1 Hz, 1H, NH), 2.82 (d, *J* = 9.1 Hz, 1H, NH); δ_C($CDCl_3$, 101 MHz): 149.8 (C-3'), 137.1 (C-5'), 124.7 (C-4'), 123.6 (q, *J* = 278 Hz, C-2), 123.1 (q, *J* = 3 Hz, C-6'), 56.9 (q, *J* = 35 Hz, C-1), C-1' not visible; δ_F($CDCl_3$, 377 MHz): −73.4 (q, *J* = 1 Hz); **HRMS** (ESI) calculated for $C_7H_7F_3N_3$ $[M+H]^+$ 190.0587, found 190.0587.

2-(3-(Trifluoromethyl)-3*H*-diazirin-3-yl)pyridine (2.118)

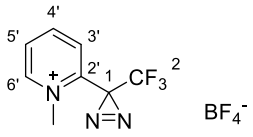


To a solution of 2-(3-(trifluoromethyl)diaziridin-3-yl)pyridine (**2.117**) (100 mg, 0.530 mmol) in Et_2O (10 mL) at room temperature, was added activated manganese dioxide (460 mg, 5.30 mmol). The reaction mixture was stirred for 30 min, filtered through Celite®, washed with Et_2O (50 mL)

and concentrated under reduced pressure, yielding the title compound as a volatile yellow oil (84 mg, 85%).

υ_{max} (cm^{-1}): 1590, 1474, 1348, 1150; δ_H($CDCl_3$, 400 MHz): 8.58 (ddd, *J* = 4.8, 1.8, 1.0 Hz, 1H, 3'-H), 7.76 (ddd, *J* = 8.0, 8.0, 1.8 Hz, 1H. 5'-H), 7.42 (dddd, *J* = 8.0, 1.0, 1.0, 1.0 Hz, 1H, 6'-H), 7.33 (ddd, *J* = 8.0, 4.8, 1.0 Hz, 1H, 4'-H); δ_C($CDCl_3$, 101 MHz): 149.5 (C-3'), 148.8 (C-1'), 136.6 (C-5'), 123.7 (C-4'), 121.9 (q, *J* = 274 Hz, C-1), 121.7 (C-6'), 29.4 (q, *J* = 40 Hz, C-2). δ_F($CDCl_3$, 377 MHz): −64.8 (d, *J* = 1.0 Hz).

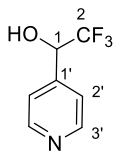
1-Methyl-2-(3-(trifluoromethyl)-3*H*-diazirin-3-yl)pyridin-1-ium tetrafluoroborate (2.119)



To a solution of 2-(3-(trifluoromethyl)-3*H*-diazirin-3-yl)pyridine (**2.118**) (200 mg, 1.07 mmol) in CH_2Cl_2 (10 mL) was added trimethyloxonium tetrafluoroborate (237 mg, 1.60 mmol) and the resultant mixture stirred for 3 h. Methanol (2 mL) was added and the solution concentrated under reduced pressure. Et_2O (20 mL) was added, and the product was collected by filtration as a white solid (227 mg, 73%). m.p. 126 °C (decomposition).

υ_{max} (cm^{-1}): 3074, 1627, 1335, 1213, 1032; δ_H(CD_3OD, 400 MHz): 9.18 – 9.13 (m, 1H, 6'-H), 8.76 (ddd, *J* = 7.9, 7.9, 1.4 Hz, 1H, 4'-H), 8.69 (dd, *J* = 7.9, 1.7 Hz, 1H, 3'-H), 8.28 (ddd, *J* = 7.9, 6.1, 1.7 Hz, 1H, 5'-H), 4.69 (s, 3H, 1'-CH_3); δ_C(CD_3OD, 101 MHz): 151.3 (C-6'), 148.8 (C-4'), 142.7 (C-2'), 133.8 (C-3'), 131.8 (C-5'), 122.0 (q, *J* = 275 Hz, C-2), 47.5 (CH_3), 26.5 (q, *J* = 45 Hz, C-1); δ_F ($CDCl_3$, 377 MHz): −68.7, −154.8; **HRMS** (ESI) calculated for $C_8H_7F_3N_3$ $[M]^+$ 202.0587, found 202.0598.

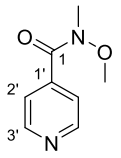
(*rac*)-2,2,2-Trifluoro-1-(pyridin-4-yl)ethan-1-ol[113] **(2.121)**



4-Pyridinecarboxaldehyde (**2.120**) (2.14 g, 20.0 mmol) was added to a solution of $TMSCF_3$ (3.25 mL, 22.0 mmol) in anhydrous THF (30 mL) at 0 °C. TBAF (1 M in THF, 0.2 mL, 0.2 mmol) was added and the reaction stirred for 16 h at room temperature. The reaction mixture was cooled to 0 °C and water (10 mL) then TBAF (1 M in THF, 2 mL, 2 mmol) added and stirred for 30 min at room temperature. The reaction mixture was concentrated under reduced pressure and extracted between EtOAc (50 mL) and brine (50 mL). The aqueous layer was washed with EtOAc (2 x 50 mL), the organic phases combined, dried over $MgSO_4$, filtered and concentrated under reduced pressure. Purification through a short silica pad (50% EtOAc/Petrol) yielded the title compound as a white solid (3.24 g, 92%). m.p. 79-80 °C (lit: 76-77 °C).[113]

υ_{max} (cm^{-1}): 3056 (OH), 1609, 1419, 1262, 1127; δ_H($CDCl_3$, 400 MHz): 8.57 – 8.53 (m, 2H, 3'-H), 7.53 – 7.48 (m, 2H, 2'-H), 6.32 (s, 1H, OH), 5.08 (q, *J* = 6.7 Hz, 1H, 1-H); δ_C($CDCl_3$, 101 MHz): 149.2 (C-3'), 144.6 (C-1'), 124.0 (q, *J* = 283 Hz, C-2), 122.7 (C-2'), 71.0 (q, *J* = 32 Hz, C-1); δ_F($CDCl_3$, 377 MHz): −77.8 (d, *J* = 6.7 Hz); **HRMS** (ESI) calculated for $C_7H_7F_3N_1O_1$ $[M+H]^+$ 178.0474, found 178.0478.

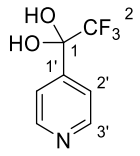
N-Methoxy-*N*-methylisonicotinamide[105] (2.125)



To a suspension of isonicotinoyl chloride hydrochloride (**2.126**) (3.00 g, 16.9 mmol) in CH_2Cl_2 (40 mL) was added pyridine (4.75 mL, 59.0 mmol) followed by *N*,*O*-dimethylhydroxylamine hydrochloride (2.14 g, 21.9 mmol). The resultant suspension was stirred for 2 h at room temperature. The reaction mixture was diluted with CH_2Cl_2 (60 mL) and washed with brine (60 mL). The aqueous layer was washed with CH_2Cl_2 (60 mL), the organic phases combined, dried over $MgSO_4$, filtered and concentrated under reduced pressure to yield the title compound as a yellow oil (2.62 g, 94%).

υ_{max} (cm^{-1}): 3425, 1640 (C=O), 1383; δ_H($CDCl_3$, 400 MHz): 8.76 – 8.62 (m, 2H, 3'-H), 7.58 – 7.44 (m, 2H, 2'-H), 3.53 (s, 3H, OCH_3), 3.36 (s, 3H, NCH_3). δ_C($CDCl_3$, 101 MHz): 167.5 (C-1), 149.6 (C-3'), 142.0 (C-1'), 122.1 (C-2'), 61.4 (OCH_3), 33.1 (NCH_3); **HRMS** (ESI) calculated for $C_8H_{11}N_2O_2$ $[M+H]^+$ 167.0815, found 167.0816.

2,2,2-Trifluoro-1-(pyridin-4-yl)ethane-1,1-diol[105] (2.123)

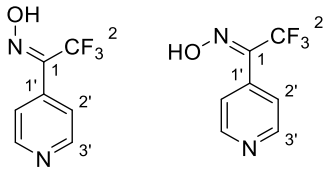


To a solution of *N*-methoxy-*N*-methylisonicotinamide (**2.125**) (606 mg, 3.65 mmol) in anhydrous toluene (2 mL) was added caesium fluoride (110 mg, 0.730 mmol). The resultant suspension was cooled to 0 °C and trifluoromethyltrimethylsilane (1.08 mL, 7.29 mmol) was added dropwise over 10 min. The solution was stirred for 16 h at room temperature, cooled

to 0 °C and water (5.00 mL) and TBAF (20.0 mL, 0.25 M in THF) added sequentially. The reaction mixture was heated at 50 °C for 2 h, cooled to room temperature and diluted with Et_2O (150 mL). The organic phase was washed with water (2 x 50 mL) and brine (50 mL), dried over $MgSO_4$, filtered and concentrated under reduced pressure to yield the title compound as a tan solid (586 mg, 83%) which was used without further purification. m.p. 154 °C.

υ_{max} (cm^{-1}): 3292 (OH), 1610, 1262, 1170; δ_H($(CD_3)_2CO$, 400 MHz): 8.69 – 8.64 (m, 2H, 3'-H), 7.70 – 7.68 (m, 2H, 2'-H), 7.00 (s, 2H, OH); δ_C($(CD_3)_2CO$, 101 MHz): 150.5 (C-3'), 147.5 (C-1'), 124.1 (q, *J* = 288 Hz, C-2), 122.9 (C-2'), 93.4 (q, *J* = 32 Hz, C-1); δ_F ($(CD_3)_2CO$, 377 MHz): −84.7; **HRMS** (ESI) calculated for $C_7H_7F_3NO_2$ $[M+H]^+$ 194.0423, found 194.0414.

2,2,2-Trifluoro-1-(pyridin-4-yl)ethan-1-one oxime (2.128)

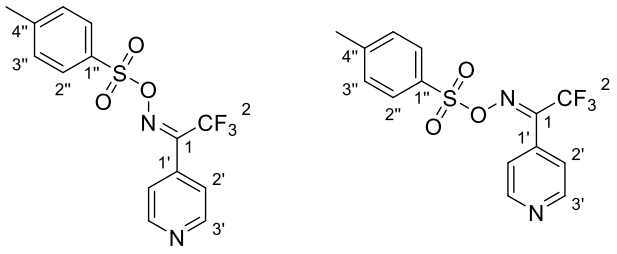


To a solution of 2,2,2-trifluoro-1-(pyridin-4-yl)ethane-1,1-diol (**2.123**) (1.00 g, 5.18 mmol) in pyridine (10 mL) was added hydroxylamine hydrochloride (1.80 g, 25.9 mmol) and the resultant mixture heated to 90 °C for 20 h. The solution was cooled and concentrated under reduced pressure. The residue was extracted into EtOAc (100 mL) and washed with brine (2 x 50 mL). The organic phase was dried over $MgSO_4$, filtered and concentrated under reduced pressure. Purification by flash column chromatography (50% EtOAc/Petrol) to yield the title compound as a mixture of separable isomers (636 mg, 65%).

Isomer 1 (white solid, m.p. 149 °C). υ_{max} (cm^{-1}): 2577, 1605 (C=N), 1351, 1189, 1124; δ_H(DMSO-d^6, 400 MHz): 13.15 (s, 1H, OH), 8.77 – 8.72 (m, 2H, 3'-H), 7.51 – 7.45 (m, 2H, 2'-H); δ_C(DMSO-d^6, 101 MHz): 150.3 (C-3'), 142.7 (q, J = 32 Hz, C-1), 134.2 (C-1'), 122.9 (C-2'), 120.7 (q, J = 274 Hz, C-2); δ_F(DMSO-d^6, 377 MHz): −64.9; **HRMS** (ESI) calculated for $C_7H_6F_3N_2O$ $[M+H]^+$ 191.0427, found 191.0416.

Isomer 2 (white solid, m.p. 158 °C). υ_{max} (cm^{-1}): 2445, 1603 (C=N), 1215, 1129; δ_H(DMSO-d^6, 400 MHz): 13.59 (s, 1H), 8.71 – 8.66 (m, 2H), 7.52 – 7.49 (m, 2H); δ_C(DMSO-d^6, 101 MHz): 150.1 (C-3'), 142.9 (q, J = 29 Hz, C-1), 137.9 (C-1'), 122.3 (C-2'), 118.1 (q, J = 283 Hz, C-2); δ_F(DMSO-d^6, 377 MHz): −61.8; **HRMS** (ESI) calculated for $C_7H_6F_3N_2O$ $[M+H]^+$ 191.0427, found 191.0417.

2,2,2-Trifluoro-1-(pyridin-4-yl)ethan-1-one *O*-tosyl oxime (2.129)



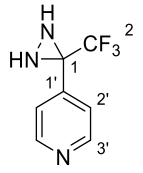
To a solution of 2,2,2-trifluoro-1-(pyridin-4-yl)ethan-1-one oxime (**2.128**) (100 mg, 0.530 mmol) and DMAP (6 mg , 0.05 mmol) in CH_2Cl_2 (5 mL) at 0 °C was added triethylamine (183 µL, 1.31 mmol) followed by tosyl chloride (120 mg, 0.630 mmol). The reaction was stirred for 1 h at room temperature, diluted with CH_2Cl_2 (50 mL) and washed with water (50 mL). The organic phase was dried over $MgSO_4$, filtered and concentrated under reduced pressure to yield the title compound.

Isomer 1 - (White solid, 158 mg, 87%, m.p. 86 °C): υ_{max} (cm^{-1}): 1594 (C=N), 1390, 1195; δ_H($CDCl_3$, 400 MHz): 8.82 – 8.77 (m, 2H, 3'-H), 7.93 –

7.84 (m, 2H, 2''-H), 7.42 – 7.40 (m, 2H, 3''-H), 7.32 – 7.24 (m, 2H, 2''-H), 2.50 (s, 3H, 4''-CH_3); δ_C($CDCl_3$, 101 MHz): 151.7 (q, *J* = 34 Hz, C-1), 150.6 (C-3'), 146.6 (C-1''), 132.3 (C-1'), 130.7 (C-4''), 130.0 (C-3''), 129.3 (C-2''), 122.1 (C-2'), 119.1 (q, *J* = 277 Hz, C-2), 21.8 (4''-CH_3); δ_F ($CDCl_3$, 377 MHz): −66.9; **HRMS** (ESI) calculated for $C_{14}H_{12}F_3N_2O_3S$ $[M+H]^+$ 345.0515, found 345.0513.

Isomer 2 – (White solid, 151 mg, 83%, m.p. 65 °C): υ_{max} (cm^{-1}): 1594 (C=N), 1389, 1194; δ_H($CDCl_3$, 400 MHz): 8.78 – 8.71 (m, 2H, 3'-H), 7.94 – 7.88 (m, 2H, 2''-H), 7.41 – 7.38 (m, 2H, 3''-H), 7.38 – 7.33 (m, 2H, 2'-H), 2.48 (s, 3H, 4''-CH_3); δ_C($CDCl_3$, 101 MHz): 151.6 (q, *J* = 33 Hz, C-1), 150.4 (C-3'), 146.5 (C-1''), 135.5 (C-1'), 131.0 (C-4''), 130.0 (C-3''), 129.2 (C-2''), 122.4 (C-2'), 116.9 (q, *J* = 284 Hz, C-2), 21.8 (4''-CH_3); δ_F ($CDCl_3$, 377 MHz): −61.5; **HRMS** (ESI) calculated for $C_{14}H_{12}F_3N_2O_3S$ $[M+H]^+$ 345.0515, found 345.0516.

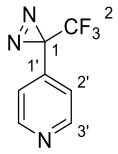
4-(3-(Trifluoromethyl)diaziridin-3-yl)pyridine (2.130)



A solution of 2,2,2-trifluoro-1-(pyridin-4-yl)ethan-1-one O-tosyl oxime (**2.129**) (200 mg, 0.570 mmol) in CH_2Cl_2 (3 mL) was added dropwise to a microwave vial containing liquid ammonia (3 mL) at −78 °C. The vial was sealed, and stirred for 16 h at room temperature. The vial was cooled to −78 °C, unsealed and excess ammonia evaporated. The residue was diluted with CH_2Cl_2 (50 mL) and washed with water (50 mL). The organic phase was dried over $MgSO_4$, filtered and concentrated under reduced pressure. Purification by flash column chromatography (40% EtOAc/Petrol) yielded the title compound as a white solid (110 mg, quant).

υ_{max} (cm^{-1}): 3130 (NH), 1605, 1151; δ_H($CDCl_3$, 400 MHz): 8.73 – 8.66 (m, 2H, 3'-H), 7.57 – 7.51 (m, 2H, 2'-H), 2.92 (d, *J* = 8.9 Hz, 1H, NH), 2.32 (d, *J* = 8.9 Hz, 1H, NH); δ_C($CDCl_3$, 101 MHz): 150.5 (C-3'), 140.2 (C-1'), 123.0 (q, *J* = 278 Hz, C-2), 122.3 (C-2'), 56.9 (q, *J* = 37 Hz, C-1); δ_F ($CDCl_3$, 377 MHz): −74.7; **HRMS** (ESI) calculated for $C_7H_7F_3N_3$ $[M+H]^+$ 190.0587, found 190.0574.

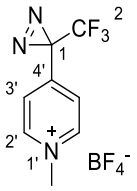
4-(3-(Trifluoromethyl)-3*H*-diazirin-3-yl)pyridine (2.131)



To a solution of 4-(3-(trifluoromethyl)diaziridin-3-yl)pyridine (**2.130**) (80 mg, 0.42 mmol) in Et_2O (5 mL) was added activated manganese dioxide (368 mg, 4.23 mmol). The reaction mixture was stirred for 20 min, filtered through Celite® and washed with Et_2O (50 mL). The solution was concentrated under reduced pressure, yielding the title compound as a volatile yellow oil, which was used immediately (55 mg, 69%).

υ_{max} (cm^{-1}): 1597, 1353, 1152; δ_H($CDCl_3$, 400 MHz): 8.69 – 8.64 (m, 2H, 3'-H), 7.06 – 7.02 (m, 2H, 2-H); δ_C($CDCl_3$, 101 MHz): 150.1 (C-3'), 138.0 (C-1'), 121.5 (q, *J* = 275 Hz, C-2), 120.3 (C-2'), 27.7 (q, *J* = 41 Hz, C-1); δ_F ($CDCl_3$, 377 MHz): −64.8.

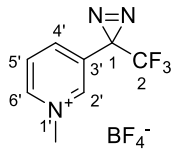
1-Methyl-4-(3-(trifluoromethyl)-3*H*-diazirin-3-yl)pyridin-1-ium tetrafluoroborate (2.132)



To a solution of 4-(3-(trifluoromethyl)-3*H*-diazirin-3-yl)pyridine (**2.130**) (250 mg, 1.34 mmol) in CH_2Cl_2 (10 mL) was added trimethyloxonium tetrafluoroborate (296 mg, 2.00 mmol) and the resultant mixture stirred for 3 h. Methanol (2 mL) was added and the solution concentrated under reduced pressure. Et_2O (20 mL) was added, and the product was collected by filtration as a white solid (201 mg, 52%). m.p. 120 °C (decomposition).

υ_{max} (cm^{-1}): 3069, 1640, 1342, 1154, 1026; δ_H(CD_3OD, 400 MHz): 9.03 – 8.90 (m, 2H, 2'-H), 7.92 – 7.88 (m, 2H, 3'-H), 4.43 (s, 3H, 1'-CH_3); δ_C(CD_3OD, 101 MHz): 148.3 (C-4'), 147.3 (C-2'), 125.8 (C-3'), 122.3 (q, *J* = 274 Hz, C-2), 29.5 (q, *J* = 42 Hz, C-1), 1'-CH_3 not visible; δ_F ($CDCl_3$, 377 MHz): −66.2, −154.8; **HRMS** (ESI) calculated for $C_8H_7F_3N_3$ $[M]^+$ 202.0587, found 202.0590.

1-Methyl-3-(3-(trifluoromethyl)-3*H*-diazirin-3-yl)pyridin-1-ium tetrafluoroborate (2.133)



To a solution of 3-(3-(trifluoromethyl)-3*H*-diazirin-3-yl)pyridine (**2.89**) (243 mg, 1.30 mmol) in CH_2Cl_2 (10 mL) was added trimethyloxonium tetrafluoroborate (288 mg, 1.95 mmol) and the resultant mixture stirred for 3 h. Methanol (2 mL) was added and the solution concentrated under

reduced pressure. Et_2O (20 mL) was added, and the product was collected by filtration as a white solid (331 mg, 88%). m.p. 130 °C (decomposition).

υ_{max} (cm^{-1}): 3095, 1522, 1377, 1155, 1028; δ_H(CD_3OD, 400 MHz): 9.01 (d, *J* = 6.1 Hz, 1H, 6'-H), 8.93 (dd, *J* = 1.5, 1.5 Hz, 1H, 2'-H), 8.66 – 8.58 (m, 1H, 4'-H), 8.18 (dd, *J* = 8.4, 6.1 Hz, 1H, 5'-H), 4.45 (s, 3H, 1'-CH_3); δ_C(CD_3OD, 101 MHz): 148.3 (C-6'), 146.0 (C-2'), 144.9 (C-4'), 131.1 (C-3'), 129.5 (C-5'), 122.5 (q, *J* = 274 Hz, C-2), 49.5 (1'-CH_3), 27.9 (q, *J* = 43 Hz, C-1); δ_F ($CDCl_3$, 377 MHz): −67.3, −154.8; **HRMS** (ESI) calculated for $C_8H_7F_3N_3$ $[M]^+$ 202.0587, found 202.0593.

Sample Preparation

Stock solution of ubiquitin prepared (1 mM Ubiquitin in Tris buffer (50 mM Tris in 500 mM NaCl)).

5 µL aliquots taken in tapered LCMS vials, flash frozen using liquid nitrogen and photolysed for 16 s at 355nm using Nd:YLF laser.

Protein Preparation

Ubiquitin and Asp-N were purchased from Sigma Aldrich.

Expression of IsoT (ZnF UBD) and SDS-PAGE purification of samples was carried out and gifted by Daniel Scott.

In Gel Digestion Protocol of Ubiquitin

Adapted from a literature procedure.[83]

Destain gel pieces

1) Add 100 µL of 100 mM ammonium bicarbonate/acetonitrile (1:1, vol/vol) to excised protein bands. Incubated for 1 h at 37 °C.
2) Supernatant removed. 200 µL of Acetonitrile/100 mM ammonium bicarbonate (9:1, vol/vol) added. Gel pieces shrink and become white and opaque. Supernatant removed.

In-gel digestion with Asp-N

1) 2 µg of lyophilized Asp-N reconstituted in 50 µL ultra-pure water. Split into 10 aliquots. Aliquot diluted to 50 µL.
2) Enough Asp-N solution added to cover dry gel pieces. Incubated for 30 minutes at 37 °C, at which point more Asp-N solution is added to cover gel pieces if necessary.
3) Incubated at 37 °C for 18 h.
4) Supernatant removed. Gel pieces extracted via incubation with extraction buffer (5% Formic Acid/ Acetonitrile (1:2, vol/vol) at 37 °C for 1 h.
5) Both supernatant and extract analysed – strongest sample used for analysis. (Extract for Ub alone, Supernatant for Ub IsoT mix).

The labeling reaction was initiated by irradiation (16 s) of the mixture using a Spectra Physics Explorer 349 laser (an actively Q-switched Nd:YLF laser operating at 349 nm, with a repetition frequency of 1000 Hz, and a pulse energy of 125 µJ, Newport, Didcot, UK). The laser beam was directed into the open top of the sample vial using a small 45° mirror.

LC-MS Analysis

Measurement of intact mono-ubiquitin or protein digests was carried out on a Dionex Ultimate 3000 Nano LC (Dionex, Camberley, UK) system using a commercially available C4 trapping column (Dionex) and a custom packed WP C4 column (5µm, 100Å, Phenomenex, Macclesfield, UK) with a Picofrit tip (75 µM i.d. x 150 mm, New Objective, supplied by Aquilant, Basingstoke, UK). The mobile phases A and B consisted of 95/5 water/acetonitrile (v/v) and 5/95 water/acetonitrile (v/v), respectively, and both contained 0.1% formic acid. The samples (1 µL) were injected in load-trapping mode.

Peptides were eluted using a 30 minutes linear gradient of mobile phase B from 0% to 70% at a flow rate of 0.3 µL/min followed by column equilibration. The HPLC system was coupled to a Thermo Scientific (Hemel Hempstead, UK) LTQ FT Ultra mass spectrometer equipped with a commercial nanoelectrospray ionization source. A 1.7 kV voltage was applied to a coated PicoTip emitter (New Objective). The capillary temperature was set at 275 °C, with inner capillary voltage value set on 37 V and tube lens value of 145 V. Spectra were acquired in positive ion mode over a 400-2000 *m/z* range at a nominal resolution of 100000 (at *m/z* 400). The instrument was controlled by Xcalibur software (Thermo Fisher).

Chapter 3 : Synthesis of Sulfonyl Azides Through SuFEx

The work is this chapter is partially described in the following publication:

Barrow, A. S.; Moses, J. E. *Synlett* **2016**, *27* (12), 1840–1843

AIMS AND OBJECTIVES

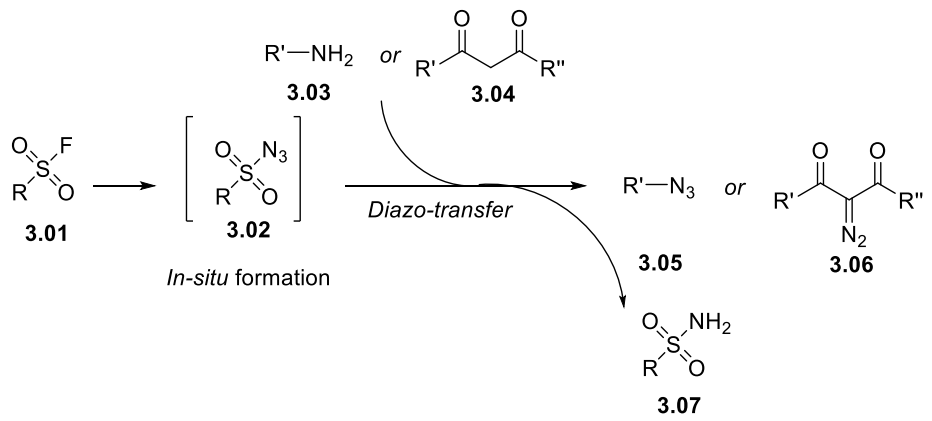
In Chapter 1 of this thesis, the concepts and philosophical origins of Click Chemistry were introduced, highlighting the stringent criteria that a reaction must attain to achieve Click status.

The recent development of Sulfur(VI) Fluoride Exchange (SuFEx), was also introduced, which included a discussion about the advantages of sulfur(VI) fluorides over their unstable chloride counterparts. It is therefore logical that, in reactions where sulfonyl chlorides prove capricious, it is desirable to develop alternative sulfonyl fluoride protocols.

One such instance is the use of sulfonyl chlorides as precursors to sulfonyl azides, which are highly useful reagents and substrates for a range of organic methodologies. The instability of the chloride precursors hamper the formation of more functionalised sulfonyl azides, since it is difficult to carry sulfonyl chlorides through multistep syntheses without degradation.

Diazo-transfer is another method for the production of sulfonyl azides; a procedure that is often performed using a distinct sulfonyl azide reagent. Despite significant advances in the development of these reagents, there are issues regarding their safety and stability, and so the development of an alternative methodology would potentially be synthetically valuable.

The aim of the work described in this chapter was to develop a SuFEx activated synthesis of sulfonyl azides from the corresponding sulfonyl fluoride and to employ these azides as reagents for *in situ* diazo-transfer reactions, in order to overcome two issues: the unstable nature of the precursors to sulfonyl azides and the concerns regarding the isolation of diazo-transfer reagents (Scheme 3.1).



Scheme 3.1: *Proposed in situ diazo-transfer reaction from sulfonyl fluoride precursor.*

The enhanced stability of sulfonyl fluorides would facilitate the synthesis of more functionalised sulfonyl azide precursors. Following this, SuFEx activation could be employed to facilitate fluoride-azide exchange.

Additionally, the proposed *in situ* diazo-transfer would help avoid some of the stability issues associated with diazo-transfer reagents, as the reaction could be performed, in principle, without isolation of the sulfonyl azide intermediate.

INTRODUCTION

The following section is split into two distinct areas of research, namely a more in-depth discussion of the recently developed SuFEx chemistry and also an introduction into the generation and reactivity of sulfonyl azides.

ACTIVATION AND REACTIONS OF SULFONYL FLUORIDES

The power of SuFEx hinges on the activation of the S^{VI}-F bond, which allows exchange reactions to occur in a controllable manner. It is therefore important that the activation and subsequent reactivity of this moiety is discussed in more detail.

A key feature of SuFEx chemistry is the requirement to stabilise the developing fluoride ion during the course of the substitution reaction. Currently, two modes of activation are known: i) hydrogen bonding to protons and ii) the presence of proximal silicon centres.[12]

Aqueous environments can strongly stabilise the fluoride ion generated during a substitution reaction through the formation of the bifluoride (HF_2^-) ion. This species is stabilised by an extremely strong 4-electron, 3-centre hydrogen bond worth 163 kJ mol^{-1} (Figure 3.1).[114]

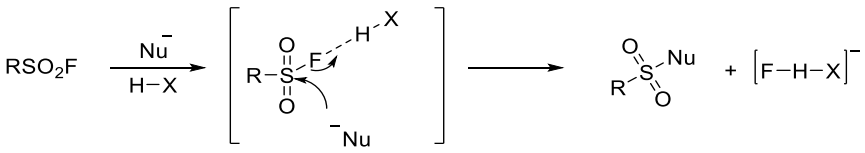
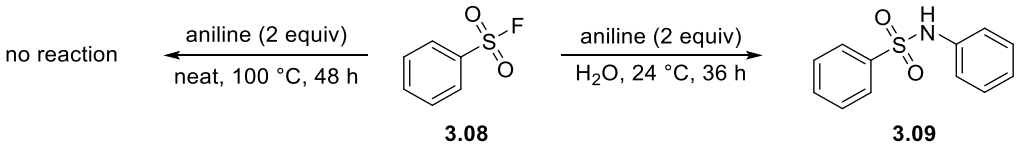


Figure 3.1: *Hydrogen-bonding activation of sulfonyl fluorides.*

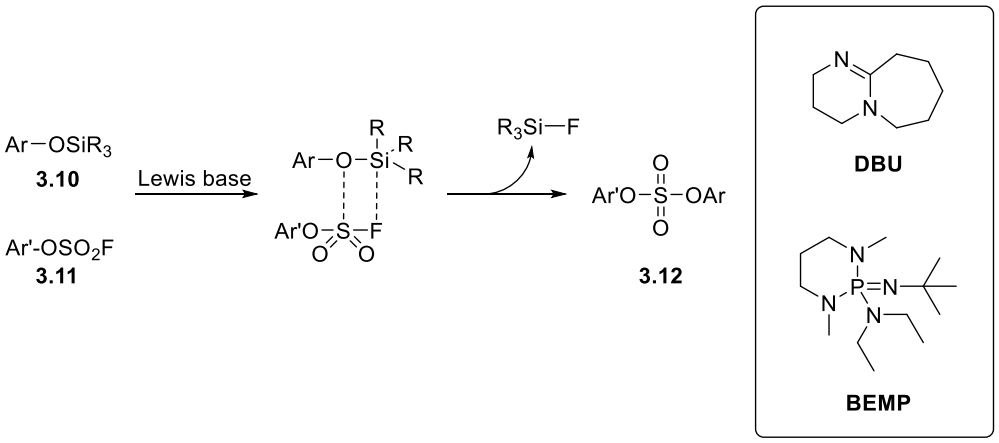
This activation mode has previously been illustrated using the reaction of benzenesulfonyl fluoride **3.08** with aniline (Scheme 3.2). In the absence of

activation, no reaction occurs even after exposure to heat for prolonged reaction periods. However, performing the reaction "on-water",[115] utilising hydrogen-bonding activation, gave the sulfonamide **3.09** at room temperature, demonstrating the power of SuFEx Click Chemistry.[12]



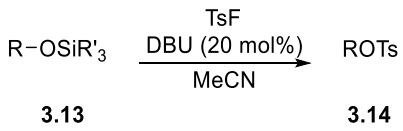
Scheme 3.2: *On-water activation of sulfonyl fluorides.*[12]

Aside from hydrogen bonding in aqueous environments, the S^{VI}-F bond can be activated by silicon centres. Sharpless *et al*. studied this activating effect with arylfluorosulfates (Ar-OSO_2F), and found that the addition of Lewis basic amines e.g. DBU or BEMP to a solution of an arylfluorosulfate **3.11** and silyl-protected alcohol **3.10** catalysed the formation of the arylsulfate product **3.12** (Scheme 3.3). The reaction proved to be tolerant of a wide variety of functionality, with the only limitations being substrates with acidic protons, which quench the catalyst, and those with sterically hindered silyl groups.[12]



Scheme 3.3: *Silyl activation of arylfluorosulfates. Dotted lines are to demonstrate connectivity, not mechanism.*

The exact role that the Lewis base plays in the mechanism has not yet been fully elucidated; however, nucleophilic bases have been reported to deprotect aryl silyl ethers.[116] In 2008, Gembus *et al*. developed a protocol for the interconversion of silyl protected alcohols to tosylates utilising tosyl fluoride and catalytic levels of DBU (Scheme 3.4). The methodology was successfully applied to substrates containing trimethylsilyl (TMS), triethylsilyl (TES) and even the hindered *tert*-butyldimethylsilyl (TBDMS) ethers.[117]



Scheme 3.4: *Gembus' protocol for the interconversion of silyl ethers to tosylates.*[117]

The most important aspect of the Gembus protocol was that reactions could proceed in the absence of an extra fluoride source to activate and cleave the silyl protecting group, which suggested a role for DBU. It is noteworthy that DBU was vital in this particular transformation, with alternative nucleophilic bases resulting in no formation of the tosylated alcohol **3.14**. This observation contrasts with similar methodology published by Levacher *et al*., in which case DMAP was employed in the transprotection of silyl protected alcohols to the corresponding benzoate esters.[118] Considering the reactivity of DBU, Gembus provided a working hypothesis to account for the reaction mechanism.

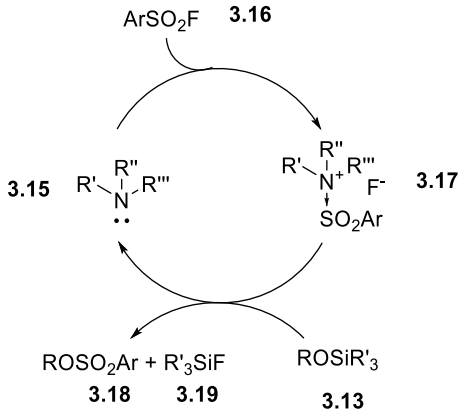


Figure 3.2: *Gembus' mechanistic hypothesis for the interconversion of silyl ethers and tosylates.*[117]

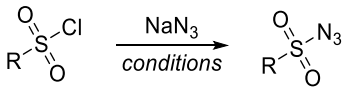
The proposed mechanism proceeds through the interaction of the sulfonyl fluoride **3.16** and DBU, resulting in the formation of the aryl sulfonyl ammonium fluoride salt **3.17** (Figure 3.2). The key intermediate **3.17** is then assumed to interact with the silyl species, thereby promoting arylsulfonyl transfer and simultaneously regenerating the catalytic base **3.15**.

Although the proposed mechanism accounts for the observed products, the exact involvement of the uniquely reactive DBU is unclear and warrants further mechanistic studies. Fully elucidating the nature of the interaction would allow the potential of SuFEx chemistry to be maximised, allowing enhanced reactivity of sulfonyl fluorides and fluorosulfates.

The second section of this introduction focuses on the generation and reactivity of the synthetically valuable sulfonyl azides.

SYNTHESIS OF SULFONYL AZIDES

Sulfonyl azides are versatile reagents and building blocks for organic synthesis, having wide application and scope. Subsequently, numerous methods have been developed to enable the synthesis of this valuable functionality. Probably the most convenient and practical method, given the wide availability of the starting materials, involves the reaction of sodium azide and a sulfonyl chloride in wet acetone (Scheme 3.5).[119]

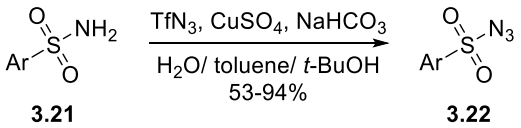


3.20 **3.02**

Scheme 3.5: *Conversion of sulfonyl chlorides into sulfonyl azides.*

However, as earlier described, sulfonyl chlorides are not always convenient as they have limited functional group compatibility due to their electrophilic and hydrolytically unstable nature.[12] For this reason, the inclusion of sulfonyl chlorides in functionalised substrates can be problematic when there is a need to carry the functionality through a multistep synthesis. In such cases, alternative strategies must be employed.

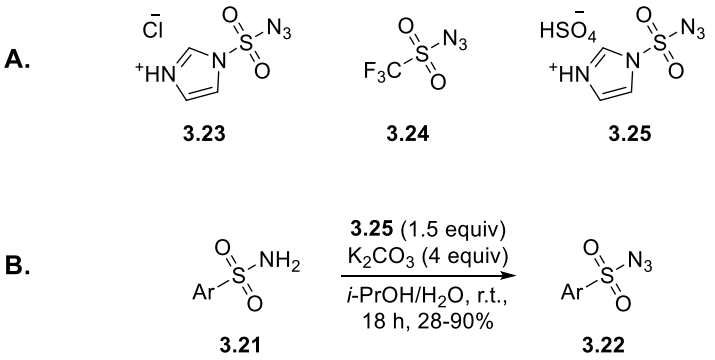
To circumvent some of the inherent issues with sulfonyl chlorides, the diazo-transfer reaction from the corresponding sulfonamide has been extensively developed. Sulfonamides are significantly more stable than their chloride counterparts; have higher functional group tolerance and are readily available. Fokin and co-workers pioneered the diazo-transfer reaction utilising sulfonamides as substrates with triflic azide **3.24** (Scheme 3.6).[120]



Scheme 3.6: *Fokin's protocol for the conversion of sulfonamides to sulfonyl azides with TfN_3.*[120]

Fokin's method was used to synthesise a range of aromatic sulfonyl azides in high yields.[120] However, the protocol is disadvantaged by the use of triflic azide as it is costly, shock-sensitive and requires preparation immediately prior to addition.

In an attempt to overcome the issues associated with triflic azide, a range of alternative reagents have been developed (Scheme 3.7.A). In 2007, Goddard-Berger introduced imidazole-1-sulfonyl azide hydrochloride **3.23**;[121] the analogous hydrogen sulfate salt **3.25** has been used by Odell *et al*. in the synthesis of a range of aryl sulfonyl azides (Scheme 3.7.B).[122]



Scheme 3.7: *A. Selection of diazo-transfer reagents; B Odell's synthesis of aryl sulfonyl azides*[122]

Odell's reaction demonstrated broad scope, with a range of aryl and heteroaryl sulfonamides, however alkyl sulfonamides substrates were not tolerated under the optimised conditions.[122] Experiments to probe the mechanism of the reaction were performed using ^{15}N NMR spectroscopy.

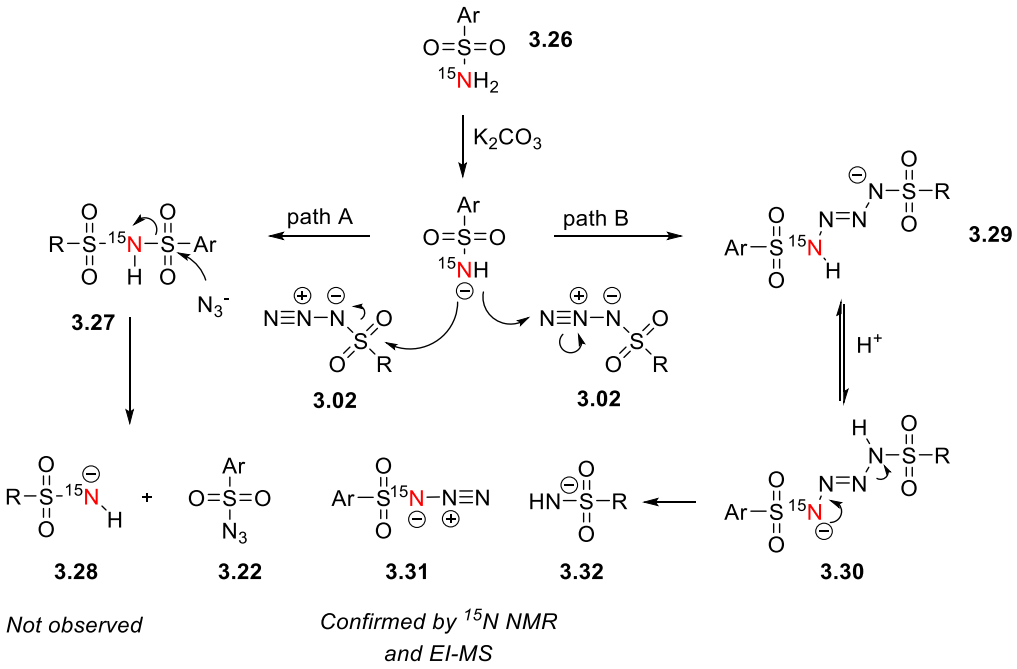


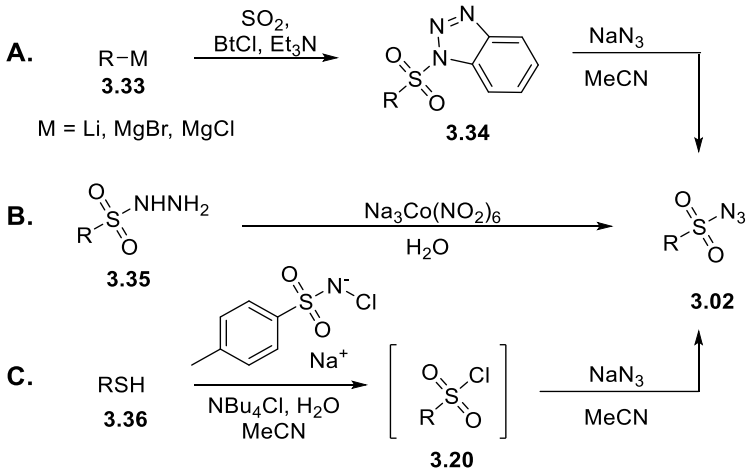
Figure 3.3: *Odell's mechanistic NMR experiment to confirm diazo-transfer.*[122]

As shown in Figure 3.3, Odell suggested two mechanisms for the formation of sulfonyl azides.[122] Path A followed an azide-transfer mechanism, whereas Path B proceeded through diazo-transfer. An isotopically labelled sulfonamide **3.26** was used to unequivocally demonstrate the diazo-transfer mechanism. The labelled sulfonyl azide product **3.31** was detected by ^{15}N NMR spectroscopy and mass spectrometry, whilst the ^{15}N containing sulfonamide **3.28** was absent.

Although imidazole-1-sulfonyl azide salts are effective diazo transfer agents, concerns about their stability have been reported by Goddard-Berger and Klapötke. They concluded that, whilst the hydrogen sulfate analogue **3.25** was the most stable tested, each of the salts hydrolysed over time, forming the dangerous hydrazoic acid.[123,124]

Aside from diazo-transfer reactions, several alternative and less commonly used methodologies for the production of sulfonyl azides have also been developed, utilising a range of reactive precursors.

Katritzky *et al.* reported the formation of sulfonyl azides from the corresponding 1-sulfonyl benzotriazole.[125] This procedure involved the addition of Grignard or alkyllithium reagents to sulfur dioxide and 1-chlorobenzotriazole, forming the key 1-sulfonylbenzotriazole motif **3.34**. The reaction of the isolable intermediates with sodium azide in refluxing acetonitrile gave the sulfonyl azide products in good yields (Scheme 3.8. A).



Scheme 3.8: *A. Katritzy's synthesis of sulfonyl azides through a benzotriazole intermediate;*[126] *B. Polanc's protocol for the nitrosation of sulfonyl hydrazines;*[127] *C. Maleki's one-pot conversion of thiols to sulfonyl azides.*[128]

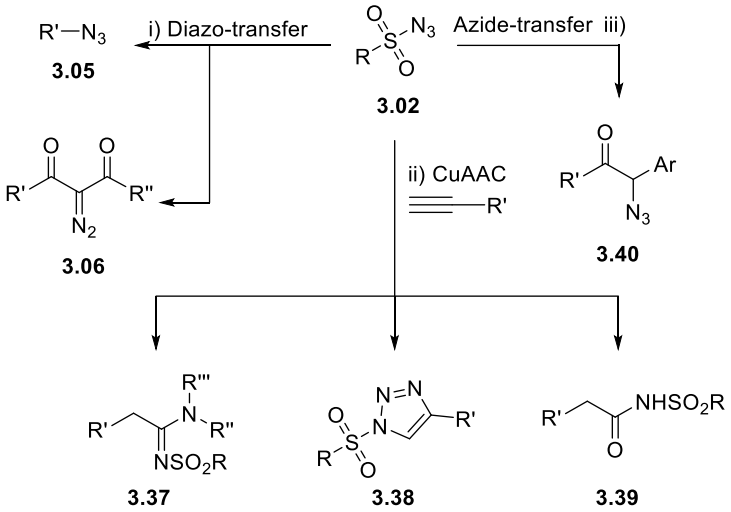
The conversion of sulfonyl hydrazines to sulfonyl azides *via* nitrosation with sodium hexanitrocobaltate(III) has been reported by Polanc *et al*., in yields of 60-85% (Scheme 3.8. B).[127]

Additionally, in 2013, Maleki *et al*. reported a one-pot method for the preparation of sulfonyl azides, which involved the oxidation of thiols in the presence of a chloride source to generate sulfonyl chlorides, which were then reacted with sodium azide without isolation (Scheme 3.8.C).[128]

APPLICATIONS OF SULFONYL AZIDES IN SYNTHESIS

As illustrated in Scheme 3.9, some of the most commonly encountered applications of sulfonyl azides have been as substrates and reagents for:

i) Diazo-transfer reactions
ii) Click Chemistry (CuACC)
iii) Electrophilic azide transfer



***Scheme 3.9**: Summary of the reactivity of sulfonyl azides.*

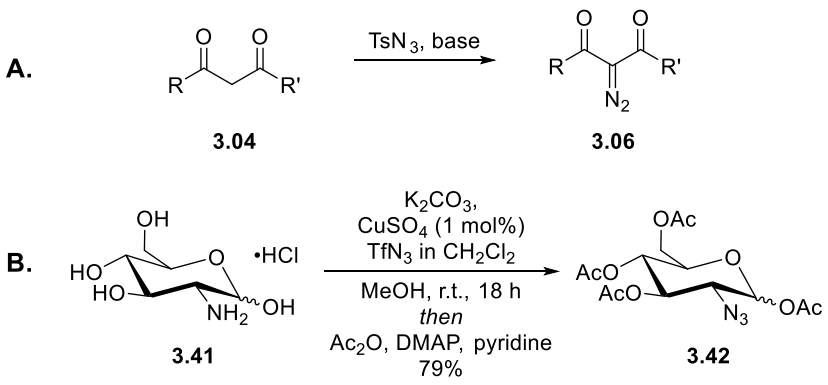
I) DIAZO-TRANSFER

Perhaps the most well described application of sulfonyl azides is as diazo-transfer reagents, which was first reported by Regitz in 1967.[129] The diazo-transfer reaction is a powerful synthetic tool, allowing the transfer of "N_2" onto a variety of substrates, notable 1,3-diones and primary amines, as well as the previously discussed sulfonamide (*vide supra)*.

The diazo and azide products formed through the diazo-transfer reaction are commonly utilised in synthetic chemistry. The bio-orthogonal nature of the azide moiety has led to its extensive use in bioconjugation, along with a whole host of other CuAAC directed applications.[130] Azides have also been used as photoaffinity labels (see Chapter 2), amine-protecting groups and as precursors of highly reactive nitrenes, which can form a collection of biologically relevant heterocycles.[131]

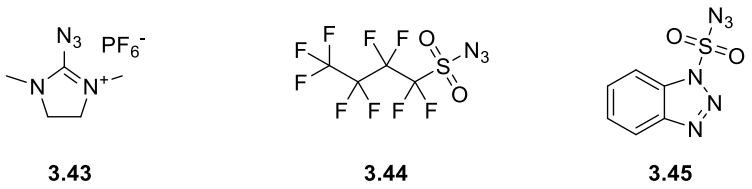
Diazo compounds are equally as useful, frequently used as precursors for the Wolff rearrangement,[132] and a wide range of metal-catalysed cyclopropanation and insertion reactions.[133,134]

In his seminal report on the diazo-transfer reaction, Regitz described the use of tosyl azide to convert 1,3-diones into their corresponding diazo compounds (Scheme 3.10.A).[129] Shiner *et al*. subsequently demonstrated the conversion of primary amines to azides in 1972, with triflic azide used as the transfer reagent.[135] The addition of a catalytic copper species was introduced by Wong *et al*., which resulted in a significant rate-enhancement. This allowed the reaction to proceed in good yield, without the requirement for freshly distilled triflic azide **3.24**.[136] The robust protocol was exemplified through the synthesis of the acetylated azido sugar **3.42** (Scheme 3.10.B).



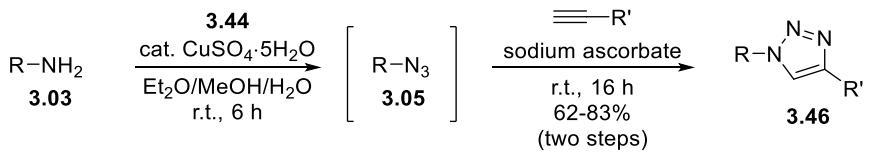
Scheme 3.10: *Early examples of diazo-transfer methodology A. Regitz's diazo-transfer reaction with 1,3-diones[129]; B. Wong's copper-catalysed synthesis of protected azido sugar* ***3.42****.[136]*

Due to the difficulties in the synthesis and the need to handle the explosive triflic azide, numerous alternative reagents have been developed, including: 2-azido-1,3-dimethylimidazolinium hexafluorophosphate (**3.43**),[137] nonafluorobutanesulfonyl azide (**3.44**)[138] and benzotriazol-1-yl-sulfonyl azide **3.45** (Scheme 3.11).[126]



Scheme 3.11: *Alternative diazo-transfer reagents for the formation of primary azides.*

In 2010, Chiara *et al*. reported that the combination of **3.44** and copper(II) sulfate catalysed the conversion of primary amines into their azido counterparts (Scheme 3.12).[138] This general method exhibited a wide scope with alkyl, benzyl and electron deficient aryl amines all efficient substrates, and the reaction conditions were also amenable to a subsequent one-pot cycloaddition reaction.



Scheme 3.12: *Chiara's method for the synthesis of primary azides.*[138]

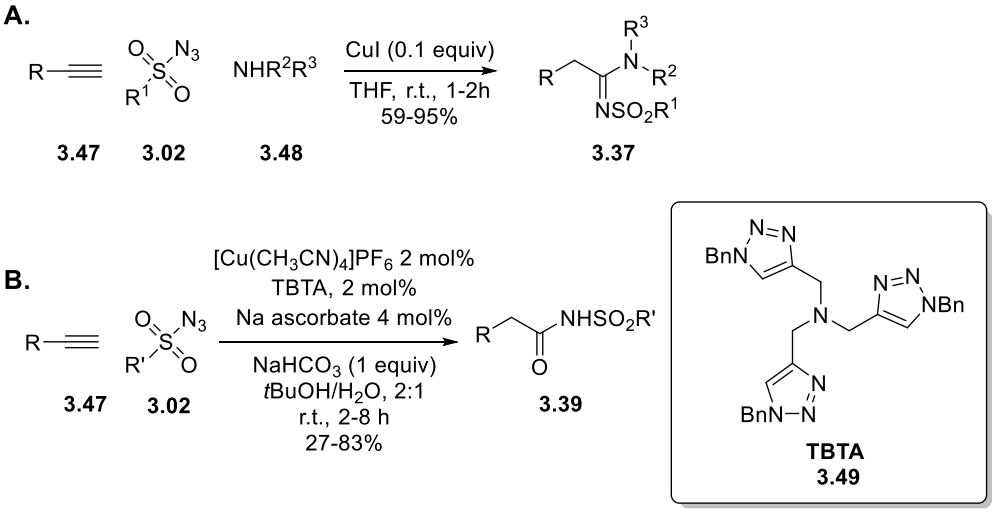
Due to the significant development in this field over the years, it is evident that the diazo-transfer reaction has become a powerful synthetic tool for the installation of azide and diazo functionality. However, as previously mentioned, safety concerns persist over isolated sulfonyl azide reagents and therefore a new protocol for an *in situ* formation of azides and diazo-compounds would be a potentially welcome addition to the field.

II) SULFONYL AZIDES IN CLICK CHEMISTRY

Sulfonyl azides have also been extensively studied as substrates for the CuAAC reaction. Interestingly, compared to the well-defined CuAAC reaction of alkyl and aryl azides (*vide supra*), several different products are possible from the electron-deficient sulfonyl azides through judicious choice of reaction conditions including *N*-sulfonylamidines, *N*-sulfonyl amides and *N*-sulfonyltriazoles.

In recent years, significant research has been undertaken on the use of *N*-sulfonyltriazoles as precursors to a range of nitrogen heterocycles. Under metal catalysis, *N*-sulfonyltriazoles have been shown to convert into imidazoles,[139] pyrroles[140] and pyrroloindolines.[141]

In 2005, Chang *et al*. reported a copper-catalysed multicomponent reaction of sulfonyl azides, alkynes and amines which directly yielded *N*-sulfonylamidines (Scheme 3.13.A).[142]

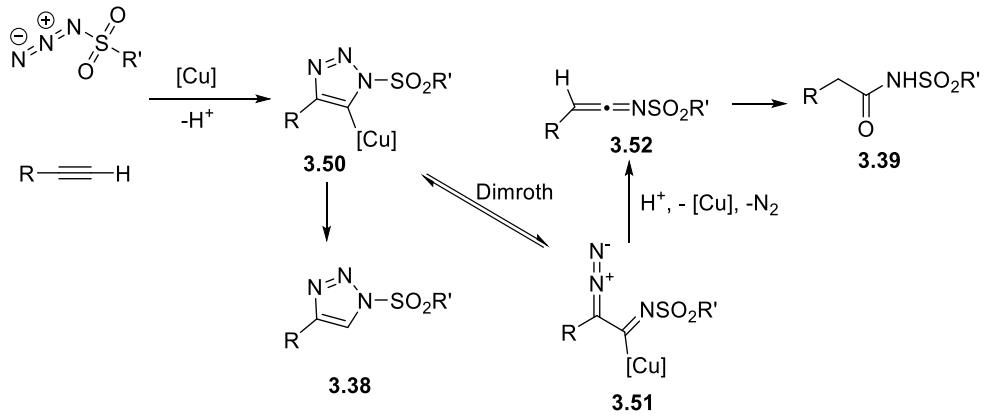


Scheme 3.13: *A. Chang's multicomponent synthesis of N-sulfonylamidines;[142] B: Fokin's conditions for the synthesis of N-sulfonyl amides.[143]*

The differing reactivity profile of sulfonyl azides and aryl/alkyl azides under CuAAC conditions was proposed to originate from the dissimilar interactions of the azide moieties with the active copper acetylide species.[142]

In late 2005 and early 2006 respectively, the groups of Chang[144] and Fokin[143], independently reported a variation of this reaction, substituting the amine for water to give the corresponding *N*-sulfonyl amides in good yield. Fokin's group discovered that the addition of 2 mol% of the ligand tris(benzyltriazolylmethyl)amine (TBTA; Tim's ligand **3.49**) resulted in a significant rate enhancement (Scheme 3.13.B).[143]

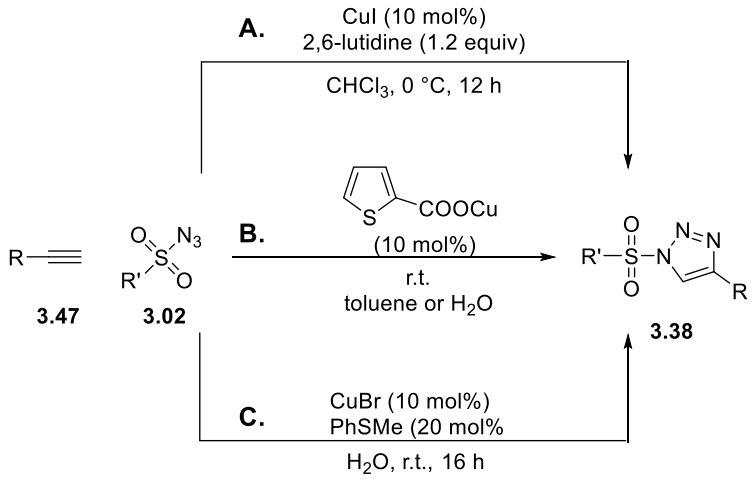
A collaborative effort by Fokin and Chang subsequently led to a more detailed understanding of the reaction mechanism. As Scheme 3.14 illustrates, computational modelling indicated the initial formation of a copper triazole **3.50**, followed by a Dimroth-type ring opening.[145,146] Extrusion of nitrogen followed by hydration and rearrangement yielded the *N*-sulfonyl amide **3.39**.



Scheme 3.14: *Fokin and Chang's collaborative proposed mechanism for the synthesis of N-sulfonyl amides.*[146]

The mechanistic insight gained allowed conditions to be developed to provide *N*-sulfonyl triazoles **3.38** under anhydrous conditions, through

proteolysis of the copper-triazole species **3.50** (Scheme 3.15.A).[146] Fu *et al*. later reported an "on-water" variation of this method, involving a CuBr/PhSMe catalyst system (Scheme 3.15.C).[147] Additionally, in 2010, Fokin *et al*. reported a general procedure using catalytic copper(I) thiophene-2-carboxylate (Liebeskind's reagent).[148] This publication was notable as *N*-sulfonyl triazoles could be formed in anhydrous conditions and also as a heterogeneous suspension in water (Scheme 3.15.B).[149]



Scheme 3.15: *Procedures for the formation of N-sulfonyl amides, reported by A) Chang and Fokin[146]; B) Fokin[149] and C) Fu.[147]*

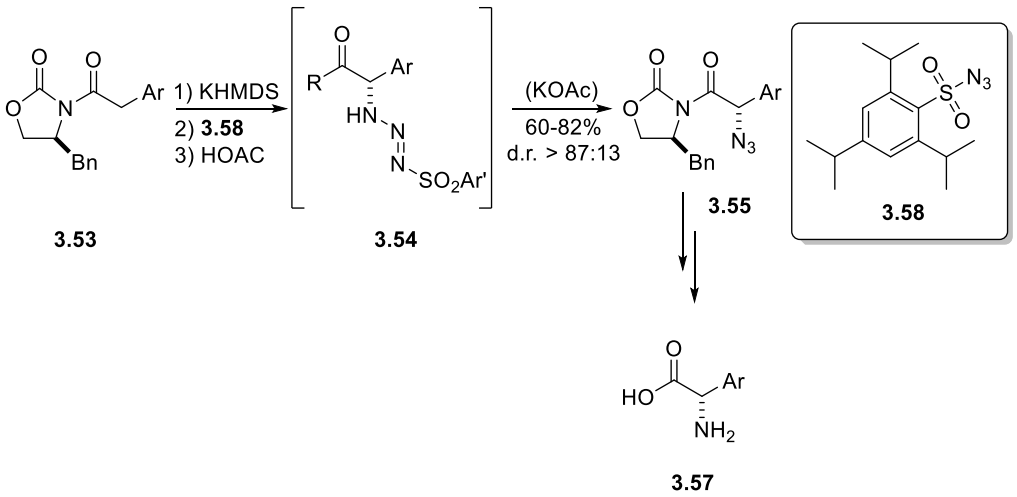
These studies, which focussed on just one class of reaction, nevertheless highlighted the versatility of sulfonyl azides in Click Chemistry. The modification of reaction conditions, ligands and additives led to host of synthetically useful products.

III) AZIDE TRANSFER

Alongside their use in Click Chemistry and as diazo-transfer reagents, sulfonyl azides can also be useful sources of electrophilic azide, although this application is far less common than other uses.

In 1987, the Evans group published a systematic study of the reaction of enolates with sulfonyl azides.[150] By altering key reaction parameters including metal enolate structure, azide source and quench reagent, it was possible to control the outcome of the reaction, generating either the diazo or the alkyl azide product. Electron-rich and sterically demanding sulfonyl azides were shown to increase the yield of the azidation product, along with larger, more electropositive enolate counterions.[151] The quench reagent, usually acetic acid, was important for the decomposition of the triazene intermediate **3.54** to form the target primary azides (Scheme 3.16).

The synthetic utility of Evans' reaction was illustrated through the reduction of the product's azido moiety, followed by cleavage of the chiral auxiliary, which resulted in the formation of useful α-amino acids.[152]



Scheme 3.16: *Evans' protocol for the direct, asymmetric azidation of enolates.*[152]

In summary, the reactivity of sulfonyl azides can be split into two major subsets. As a substrate, sulfonyl azides can exhibit properties analogous to aryl and alkyl azides, however this is not usually the case. This differing reactivity allows the synthesis of amides, amidines and triazoles through copper-catalysed transformations, simply by modifying reaction conditions.

The application of sulfonyl azides as chemical reagents was also discussed, with the electronic nature of the functional group able to act not only as a diazo-transfer reagent, but also as a source of electrophilic azide (Scheme 3.9).

RESULTS AND DISCUSSION

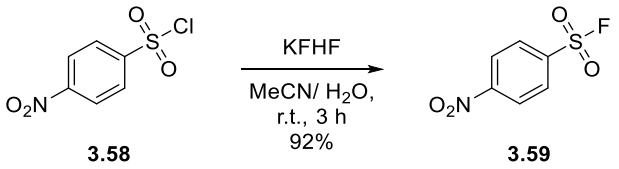
DEVELOPMENT OF METHODOLOGY TO FORM SULFONYL AZIDES

In the original report on SuFEx Click Chemistry, Sharpless *et al*. demonstrated that silyl-functionalised ethers reacted with S^{VI}-F bonds to form the corresponding sulfonate or sulfate species.[12]

With this in mind, we elected to investigate the conceptually similar exchange of fluoride with azide. It was hypothesised that the silicon based trimethylsilyl azide ($TMSN_3$) was a suitable reagent for this transformation. $TMSN_3$ is known to be a convenient, easy to handle reagent and has been extensively used by the Moses group for the azidation of anilines and one-pot cycloadditions.[153]

$TMSN_3$ is produced on tonne-scale annually and, although potentially hazardous, is frequently employed as an alternative to the shock sensitive and highly volatile hydrazoic acid (HN_3).[154] Unlike sodium azide, which is soluble only in highly polar solvents, $TMSN_3$ is a thermally stable liquid that is miscible and stable in a range of aprotic organic solvents, making it a suitable choice for the target study.

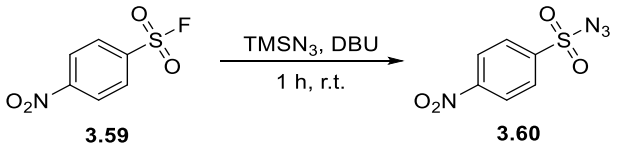
Focus was initially centred upon on the development of a methodology to form sulfonyl azides. The study began with 4-nitrobenzenesulfonyl fluoride (**3.59**) as a model substrate, which was readily prepared from the corresponding sulfonyl chloride (**3.58**) utilising potassium bifluoride (Scheme 3.17).[12,155]



3.58 **3.59**

Scheme 3.17: *Preparation of model substrate* ***3.59****.*

In early attempts, adding $TMSN_3$ to a solution of **3.59** in acetonitrile resulted in no conversion to the target sulfonyl azide **3.60** (Table 3.1). However, in the presence of a sub-stoichiometric amount of DBU (0.3 eq.) the sulfonyl azide **3.60** was observed in 81% conversion (Table 3.1, Entry 2). Varying the solvent medium resulted in lower conversions and in the case of methanol, ethanol and THF a significant amount of side products were observed. The use of methanol and ethanol as solvent resulted in the formation of the corresponding sulfonates, whereas THF gave a complex mixture of unidentified species.



3.59 **3.60**

Entry	***Solvent***	***$TMSN_3$ (eq.)***	***DBU (eq.)***	***Conversion (%)[a]***
1	MeCN	1	0	n/r
2	MeCN	1	0.3	81
3	EtOAc	1	0.3	75
4	MeOH	1	0.3	76[b]
5	THF	1	0.3	61[b]
6	EtOH	1	0.3	67[b]
7[c]	MeCN	1	0.3	73
8	MeCN	1	1	54
9	MeCN	1.5	0.3	96
10[d]	MeCN	1.5	0.3	>99
11	MeCN	1.5[e]	0	3
12	MeCN	1.5[e]	0.3	>99

[a] 0.5 mmol scale, conversion determined by ^1H NMR. [b] Reactions showed significant levels of other by-products by ^1H NMR. [c] Reaction run over 4 h. [d] $TMSN_3$ was added in 2 portions. [e] NaN_3 was used instead of $TMSN_3$.

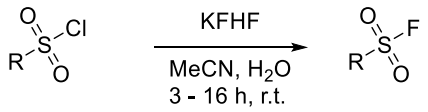
Table 3.1: *Reaction optimisation by variation of solvent and reagent loadings*

Extending the reaction time to 4 hours did not improve the conversion (Table 3.1, entry 6), whereas utilising stoichiometric levels of DBU was detrimental (Table 3.1, entry 7). Kim *et al*. reported the application of DBU as a catalyst for the deprotection of silyl-protected alcohols, suggesting an interaction between DBU and the silicon centre.[156] It was proposed that the lower conversion observed could be explained through an analogous DBU-mediated degradation of $TMSN_3$.

Increasing the quantity of $TMSN_3$ to 1.5 eq. greatly improved conversion to 96% (Table 3.1, entry 9), whereas splitting the addition of azide into two equal portions, at 15 minute intervals, resulted in full conversion to the target sulfonyl azide **3.60** (Table 3.1, entry 10).

Interestingly, under the same reaction conditions, sodium azide performed equally as well as $TMSN_3$ (Table 3.1, entries 11 and 12). This is in contrast to observations of Offort *et al*. who used wet acetone as solvent, and this may be attributed to the different solubility of sodium azide in the different solvents.[157] Although both $TMSN_3$ and sodium azide were valid reagents for further optimisation, $TMSN_3$ was more convenient for the reasons described earlier.

Having found optimal reaction conditions (Table 3.1, entry 10), the scope of the transformation was next explored. A selection of aromatic sulfonyl fluorides were prepared from the corresponding chlorides, with varying electronic and steric demands (Table 3.2).[12]

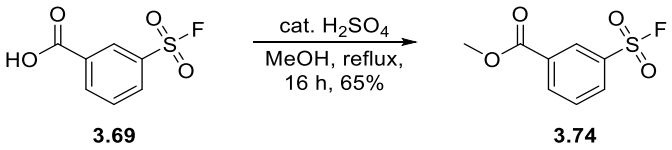


Entry	*R*	*Product*	*Yield (%)[a]*
1	4-NO_2-C_6H_4	**3.59**	84
2	2-NO_2-C_6H_4	**3.61**	95
3	4-CN-C_6H_4	**3.62**	85
4	4-CH_3CO-C_6H_4	**3.63**	90
5	4-CF_3-C_6H_4	**3.64**	85
6	4-Br-C_6H_4	**3.65**	87
7	4-CH_3-C_6H_4	**3.66**	94
8	2,4,6-CH_3-C_6H_2	**3.67**	92
9	C_6H_5	**3.08**	96
10	4-OCH_3-C_6H_4	**3.68**	95
11	3-COOH-C_6H_4	**3.69**	89
12	$PhCH_2$	**3.70**	70
13	2,4,6-^{I}Pr-C_6H_2	**3.71**	91
14	4-F-C_6H_4	**3.72**	86
15	3-F-C_6H_4	**3.73**	93

[a] Isolated yields, 2.3 eq of KFHF required.

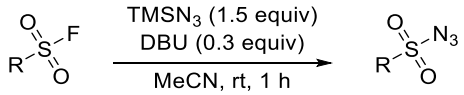
***Table 3.2**: Preparation of sulfonyl fluorides.*

The benzyl derivative **3.70** was also synthesised to determine the scope of the methodology outside of purely aromatic compounds. Each of the substrates were synthesised in high yield with no purification required after aqueous workup. Alongside the benzoic acid sulfonyl fluoride **3.69**, the corresponding methyl ester **3.74** was generated *via* a Fischer esterification, again demonstrating the robust nature of the S^{VI}-F bond (Scheme 3.18).



***Scheme 3.18:** Fischer esterification of **3.69**.*

Having synthesised a range of precursors, the conversion of substrates containing electron-withdrawing substituents were first studied under the optimised conditions (Table 3.1, entry 10).



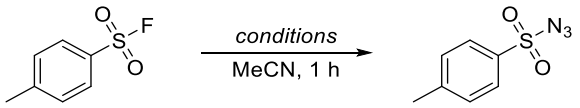
3.01 **3.02**

Entry	*R*	*Product*	*Yield (%)[a]*
1	4-NO_2-C_6H_4	**3.60**	92
2	2-NO_2-C_6H_4	**3.75**	99
3	4-CN-C_6H_4	**3.76**	90
4	4-CH_3CO-C_6H_4	**3.77**	89
5	3-CO_2Me-C_6H_4	**3.78**	99
6	4-CF_3-C_6H_4	**3.79**	88
7	4-Br-C_6H_4	**3.80**	79

[a]0.5 mmol scale, 0.5 M in MeCN, $TMSN_3$ was added in 2 portions, isolated yield reported.

Table 3.3: *Formation of electron deficient sulfonyl azides.*

Each of the electron-deficient sulfonyl fluorides investigated reacted efficiently, generating the corresponding sulfonyl azide in excellent yield, with only minimal purification required (Table 3.3). Under these conditions, poor conversion of tosyl fluoride **3.66** to sulfonyl azide **3.80** was noted (Table 3.4, entry 1). To improve this conversion, a short optimisation sequence was performed (Table 3.4).



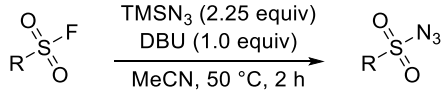
3.66 **3.80**

Entry	***Temp (°C)***	***$TMSN_3$ (eq.)***	***DBU (eq.)***	***Conversion (%)[a]***
1	r.t	1.5[b]	0.3	29
2	r.t.	1.5[b]	1	55
3	50	1.5[b]	1	78
4	r.t.	2.25[c]	1	49
5	50	2.25[c]	1	>99

[a] - 0.5 mmol scale, 0.5 M in MeCN, ratio of product to starting material as determined by ^1H NMR. [b] – $TMSN_3$ added into two 15 minute intervals. [c] – $TMSN_3$ added in three 15 minute intervals and run for 2 h.

Table 3.4: *Optimisation of reaction conditions for the formation of tosyl azide* ***3.80****.*

Both increased reagent loading and reaction temperature were required to achieve good yields in a comparable time frame to the electron-poor substrates. The modified conditions (Table 3.4, entry 5) were used to convert the remaining sulfonyl fluorides into sulfonyl azides (Table 3.5).



3.01 **3.02**

Entry	***R***	***Product***	***Yield (%)[a]***
1	4-Me-C_6H_4	**3.81**	93
2	2,4,6-Me-C_6H_2	**3.82**	91
3	C_6H_5	**3.83**	72
4	4-OCH_3-C_6H_4	**3.84**	94
5	3-COOH-C_6H_4	**3.85**	-
6	$PhCH_2$	**3.86**	-
7	2,4,6-^{I}Pr-C_6H_2	**3.57**	99
8	4-F-C_6H_4	**3.87**	47[b]
9	3-F-C_6H_4	**3.88**	95[c]

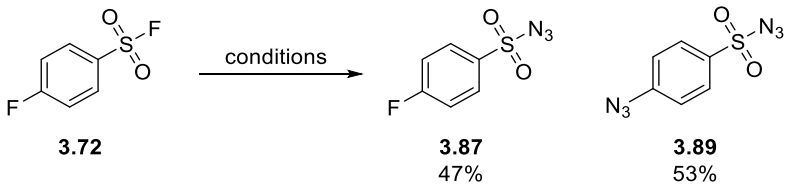
0.5 mmol scale, 0.5 M in MeCN, isolated yields: $TMSN_3$ (2.25 eq.), DBU (1.0 eq.), 2 h, 50 °C .[b] Conversion by NMR. [c] – Run at r.t.

Table 3.5: *Synthesis of sulfonyl azides.*

These improved conditions worked well with the electro-neutral substrate **3.66**, to provide sulfonyl azide **3.81** (Table 3.5, entry 1) with the lower yield of **3.83** explained by the volatility of the product (Table 3.5, entry 3). Sterically encumbered substrates such as **3.67** and **3.71** (Table 3.5, entries 2 and 7) were also amenable to the reaction conditions, with the tri-isopropyl derivative **3.57** formed in a near quantitative yield.

The electron-rich, and therefore deactivated, 4-methoxybenzenesulfonyl fluoride (**3.68**) also underwent the fluoride-azide exchange reaction cleanly, resulting in 94% product (**3.84**) (Table 3.5, entry 4).

The fluoro-substituted aromatic sulfonyl fluoride **3.72** generated a mixture of two products: the target sulfonyl azide **3.87**, and a side product, proposed to be the diazide **3.89**. The formation of **3.89** can be explained by a S_NAr reaction of the electron deficient **3.87**, resulting in substitution of the fluoride by azide (Scheme 3.19).



3.72 | **3.87** 47% | **3.89** 53%

Scheme 3.19: *Formation of a S_NAr generated di-azide side product.*

Repeating the reaction at a reduced temperature resulted in a mixture of the two products, although with a different ratio. Whereas incomplete consumption of the sulfonyl fluoride **3.72** was noted, integration of the ^1H NMR spectrum showed a mixture of **3.72**, **3.87** and **3.89** in a 5:86:9 ratio.

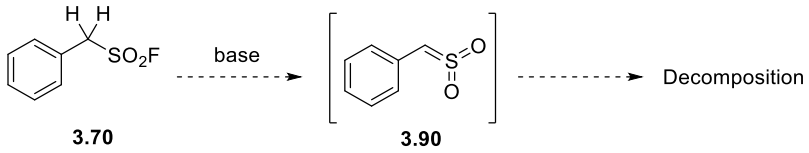
Conversely, the reaction of the isomeric 3-fluoro isomer **3.73**, which is not activated towards S_NAr, gave the corresponding azido compound **3.88** in 95% yield at room temperature.

Unfortunately, not all substrates tested demonstrated the desired reactivity. The aliphatic sulfonyl fluoride **3.70** and benzoic acid derivative **3.69** proved to be particularly challenging substrates with no conversion noted under the optimised conditions. The benzoic acid **3.69** proved inert under the standard conditions, which may be a result of deprotonation of the acid moiety removing DBU from the reaction.

It was observed that the aliphatic substrate **3.70** partially degraded into a complex mixture of unidentified side products and therefore additional optimisation of the reaction conditions was required.

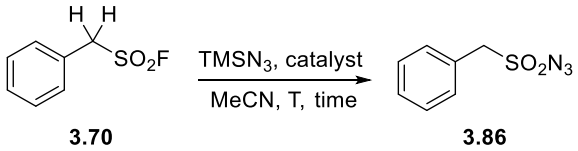
OPTIMISATION OF CONDITIONS FOR BASE-SENSITIVE SUBSTRATES

The acidic phenylmethylsulfonyl fluoride **3.70** was incompatible with the standard conditions for the fluoride-azide exchange reaction. It was proposed that deprotonation of the sulfonyl fluoride **3.70** generated the reactive sulfene **3.90**, which subsequently decomposed under the reaction conditions (Scheme 3.20). The generation of sulfene **3.90** has previously been achieved from the analogous sulfonyl chloride in the presence of a tertiary amine, which supports the proposed degradation pathway.[158]



Scheme 3.20: *Proposed deprotonation of **3.70** to form **3.90**.*

The initial attempt to prevent decomposition and provide the target sulfonyl azide **3.86** employed DBU under a range of less forcing conditions (Table 3.6).



Entry	***catalyst (eq.)***	***temp (°C)***	***TMSN₃ (eq.)***	***time (h)***	***Conversion (%)[a]***
1	DBU (1)	50	2.25	1	Decomposition
2	DBU (1)	r.t.	2.25	1	Decomposition
3	DBU (0.3)	r.t.	1.5	1	51
4	DBU (0.15)	r.t	1.5	16	59
5	DBU (0.3)	50	2.25	1	81

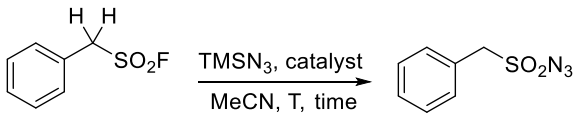
[a]0.5 mmol scale, ratio of product to starting material as determined by ^{1}H NMR.

Table 3.6*: DBU promoted formation of phenylmethylsulfonyl azide **3.86**.*

Stoichiometric loading of DBU resulted in decomposition with several new environments in the benzylic region of the ^{1}H NMR spectra (Table 3.6, entries 1 and 2). Reducing the concentration of DBU inhibited the degradation pathways with the use of 0.3 eq. of base resulting in 51% conversion into sulfonyl azide **3.86** (Table 3.6, entry 3). Lowering the DBU concentration further, but increasing the reaction duration, resulted in a modest increase in conversion (Table 3.6, entry 4).

Performing the reaction at 50 °C with an increasing loading of $TMSN_3$ resulted in 81% conversion into the product **3.86** after 1 h (Table 3.6, entry 5). This demonstrated that it was the stoichiometric loading of DBU that resulted in degradation, rather than the increased temperature.

Encouraged by this result, a selection of weaker bases were explored (Table 3.7). The nucleophilic DMAP (pK_aH (MeCN) = 17.95) and DABCO pK_aH (H_2O) = 8.82) were trialled as potential amine catalysts.[159]



3.70 **3.86**

Entry	***catalyst (eq.)***	***temp (°C)***	***$TMSN_3$ (eq.)***	***time (h)***	***Conversion (%)[a]***
1	DMAP (1)	r.t.	2.25	1	15
2	DMAP (1)	50	1.5	1	84
3	DMAP (1)	50	2	1	91
4	DMAP (1)	50	3	2	98
5	DABCO (1)	50	2.25	2	92

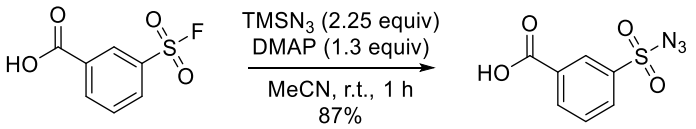
[a]0.5 mmol scale, 0.5 M in MeCN, ratio of product to starting material as determined by ^{1}H NMR.

Table 3.7: *Alternative bases of sulfonyl azide formation*

Using a stoichiometric quantity of DMAP, at room temperature, gave 15% conversion into the sulfonyl azide **3.86**, however no degradation was noted (Table 3.7, entry 1). Increasing the temperature and equivalents of $TMSN_3$

significantly improved conversion (Table 3.7, entries 2 and 3). A further increase in the loading of $TMSN_3$ resulted in an impressive 98% conversion after 2 hours. (Table 3.7, entry 4). DABCO was not as effective as DMAP, with azide **3.86** generated in 92% conversion (Table 3.7, entry 5).

The benzoic acid sulfonyl fluoride **3.69** was also converted to the corresponding azide **3.85** in good yield, with an excess of both $TMSN_3$ and DMAP (Scheme 3.21).



3.69 **3.85**

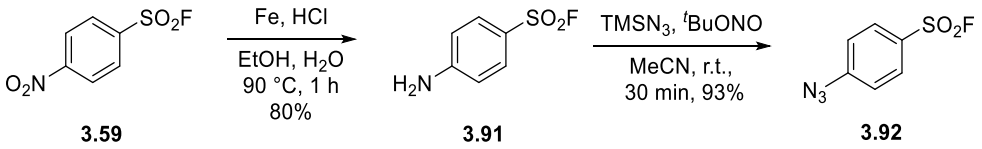
Scheme 3.21: *Optimised conversion of* ***3.69*** *to* ***3.85****.*

DEVELOPMENT OF A MORE COMPLEX SUBSTRATE

As previously discussed, the key advantage of using sulfonyl fluorides over their chloride counterparts is their stability. We were therefore keen to demonstrate that sulfonyl fluorides are compatible in a multistep synthesis, by generating a functionalised substrate inaccessible through sulfonyl chloride chemistry.

Sulfonyl chlorides, unlike sulfonyl fluorides, are known to be unstable under reductive conditions.[12] It was therefore fitting that a reduction would begin the synthetic sequence.

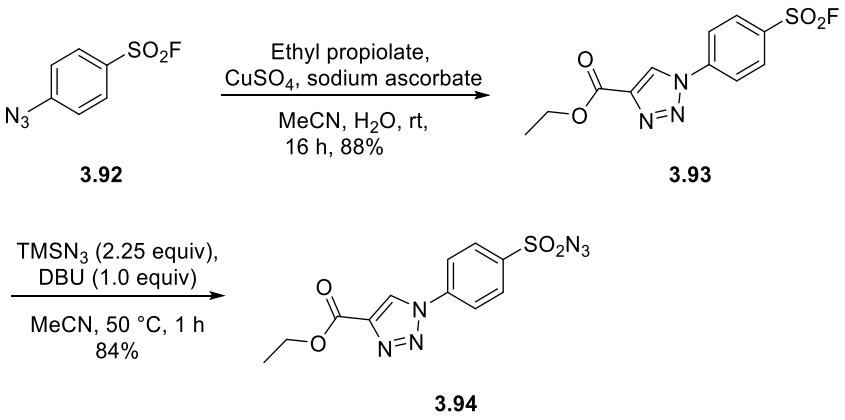
Exposing 4-nitrobenzenesulfonyl fluoride (**3.59**) to iron fillings and hydrochloric acid in refluxing aqueous ethanol resulted in the clean conversion to the aniline **3.91** in 80% yield. In our hands, under the same conditions, the corresponding sulfonyl chloride decomposed. Following a procedure previously developed in the Moses group, the aniline **3.91** was then converted to azide **3.92** through a diazotisation-azidation sequence in an excellent 93% (Scheme 3.22).[153]



Scheme 3.22: *Synthesis of aromatic azide* ***3.92****.*

This reaction was particularly notable due to the use of $TMSN_3$ as the azide source, with no sulfonyl azide detected during the course of the reaction. Next, the CuAAC reaction of the azide **3.92** and ethyl propiolate was

investigated, with the target triazole **3.93** synthesised in a good yield of 84% with no chromatographic purification required (Scheme 3.23).[153]



Scheme 3.23: *Completion of synthesis of functionalised sulfonyl azide* ***3.94****.*

Finally, the functionalised sulfonyl fluoride **3.93** was subjected to the optimised conditions for the synthesis of sulfonyl azides, utilising 2.25 eq. of $TMSN_3$ and 1.0 eq. of the Lewis basic DBU to generate the functionalised sulfonyl azide **3.94** in an excellent 84% yield (Scheme 3.23).

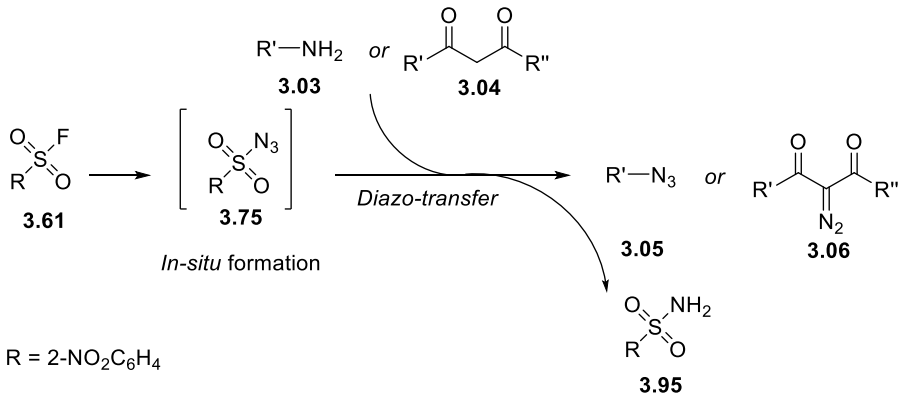
This short synthetic sequence demonstrated the advantages of sulfonyl fluorides over chlorides. The robust sulfonyl fluoride could be carried through a multistep sequence without degradation, thereby enabling access to more complex intermediates than is accessible with the sulfonyl chloride.

DEVELOPMENT OF AN *IN SITU* DIAZO-TRANSFER REACTION

As demonstrated by the groups of Fokin,[115] Goddard-Borger,[116] Kitamura[106] and Suarez[107] amongst others, the diazo-transfer reaction converting sulfonamides into their corresponding sulfonyl azides is a useful synthetic transformation. A major drawback of these protocols is that the sulfonyl azide reagents are isolated, which presents significant safety issues.

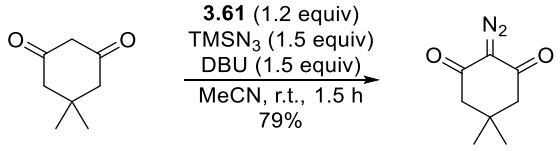
Having developed a method for the synthesis of sulfonyl azides from the corresponding fluoride, the possibility of using these reagents *in situ* was intriguing. The development of a diazo-transfer reagent that is formed and then used *in situ* would offer several benefits, notably removing the need to isolate the potentially unstable sulfonyl azide.

It was reasoned that the sulfonyl azides generated from sulfonyl fluorides could be utilised to install diazo moieties onto 1,3-diones as well as converting primary amines into the corresponding azides. During the course of this diazo-transfer, the sulfonyl azide would be converted to the corresponding sulfonamide **3.95** (Scheme 3.24).



Scheme 3.24: *Proposed in situ sulfonyl azide formation and diazo transfer reaction.*

Our investigations began with 2-nitrobenzenesulfonyl fluoride (**3.61**), which was selected as the transfer reagent of choice, due to the efficient conversion of the substrate into the corresponding sulfonyl azide **3.75**. Initially, the diazo-transfer with 1,3-diones as substrates was investigated and for this reaction, base was required to deprotonate the substrate. With 5,5-dimethylcyclohexyl-1,3-dione **3.96** as the substrate, the use of 1.2 eq. of sulfonyl fluoride **3.61** and 1.5 eq. of DBU resulted in 79% isolated yield of the diazo compound **3.97** (Scheme 3.25).

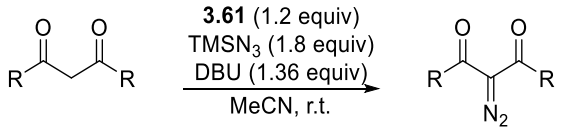


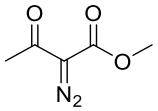
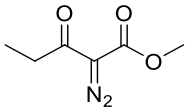
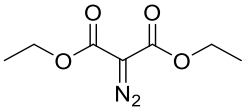
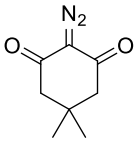
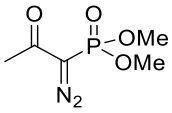
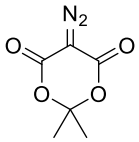
3.96 **3.97**

Scheme 3.25: *Initial attempt at the in situ diazo-transfer reaction.*

The sulfonyl azide intermediate **3.75** was allowed to form for 30 minutes before the addition of the 1,3-dione substrate. It was previously noted that increased levels of DBU hindered the formation of the sulfonyl azide and therefore it was reasoned that by adding the base in two separate portions, higher yields could be obtained. Subsequently, the conditions optimised for electron deficient sulfonyl fluorides (Table 3.1, entry 10) were adopted for the formation of the sulfonyl azide **3.75**, followed by a 1.0 eq. of base upon addition of the 1,3-dione substrate. This resulted in a corresponding increase in yield of the model reaction to 90%.

A selection of 1,3-diones were then subjected to these conditions, with good to excellent yields obtained in most cases (Table 3.8). The Ohira-Bestmann reagent **3.101** was synthesised in an acceptable 57% isolated yield without further optimisation (Table 3.8, entry 5).[160]



Entry	*Product*		*Time (h)*	*Yield (%)*
1		**3.98**	2	68
2		**3.99**	16	77
3		**3.100**	16	89
4		**3.97**	1	90
5		**3.101**	3	57
6		**3.102**	2	-

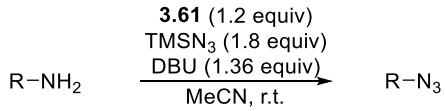
[a] 0.5 mmol scale, 0.5 M in MeCN: RSO_2F (1.2 eq.) $TMSN_3$ (1.8 eq.), DBU (1.36 eq.), r.t.

Table 3.8: *One-pot synthesis of diazo-compounds utilizing sulfonyl fluorides as precursors.*

Attempts to synthesise the diazo derivative of Meldrum's acid **3.102** were unsuccessful, with no target product isolated. It is noteworthy that only sulfonamide **3.95** was isolated from the reaction, suggesting the diazo-transfer occurred, but that the product most likely degraded under the reaction conditions.

Extending the methodology further, the diazo-transfer onto primary amines to form the corresponding azide was investigated. The same conditions

employed for the 1,3-diones substrates were adopted for a selection of amines (Table 3.9).



Entry	*R*	*Product*	*Yield (%)[a]*
1	4-OMe-C_6H_4	**3.103**	50
2	4-Br-C_6H_4	**3.104**	-
3	1-NapthylCH_2	**3.105**	71
4	4-Cl-Bn	**3.106**	67
5	Ph$CH(CH_3)$	**3.107**	63
6	PhCH_2CH_2	**3.108**	67

[a] 0.5 mmol scale, 0.5 M in MeCN: RSO_2F (1.2 eq.) $TMSN_3$ (1.8 eq.), DBU (1.36 eq.), r.t.

Table 3.9: *Diazo-transfer onto primary amines.*

As expected, the electronics of the substrates affected the yields obtained; the weakly nucleophilic 4-methoxyaniline gave azide **3.103** in a modest 50%, with no product detected with less nucleophilic anilines (Table 3.9, entries 1 and 2).

Alkyl and benzylic amines generated higher isolated yields of the corresponding azide (Table 3.9, entries 3 – 6), however the yields were generally lower than those achieved when 1,3-diones were employed as substrates. This is presumably due to the lower nucleophilicity of amines as compared to deprotonated 1,3-diones, which would inhibit the initial nucleophilic attack onto the sulfonyl azide moiety.

Having established the utility of sulfonyl fluorides as precursors of sulfonyl azides and *in situ* diazo-transfer reagents, it was decided to investigate the mechanism of the sulfonyl azide formation.

MECHANISTIC STUDIES

The activation of sulfonyl fluorides has been discussed at length in the literature, with various mechanisms of activation proposed. As previously described, Sharpless has highlighted that hydrogen bonding can promote nucleophilic substitution at the sulfur centre, in both aqueous solutions and biphasic mixtures.[12]

We postulated that the mechanism of the fluoride-azide exchange reaction followed that proposed by Gembus *et al*., involving the formation of an intermediate sulfonyl ammonium fluoride salt **3.17**.[21] The fluoride ion activates the $TMSN_3$ towards nucleophilic attack through the formation of a charged silicate species. This silicate species then reacts with the proposed intermediate sulfonyl salt **3.17**, thereby yielding the desired sulfonyl azide **3.02**, TMSF and regenerating the catalytic tertiary amine **3.15** (Figure 3.4).

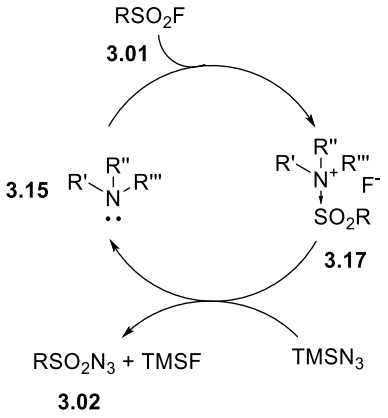


Figure 3.4: *Proposed mechanism for activation of sulfonyl fluorides to fluoride-azide exchange.*

The reactivity pattern is consistent with that previously reported by Vorbrüggen[161] and Kim;[116] that organic bases activate both sulfonyl

fluorides and silyl groups in the conversion of hydroxyl groups to fluorides and the hydrolysis of silyl ethers.

To understand the proposed activation step in more detail, a series of NMR experiments were undertaken. DBU was added to solutions of sulfonyl fluorides in deuterated acetonitrile, with ^{1}H NMR spectroscopy used to detect the formation of new species.

The first experiment performed used 4-acetylbenzenesulfonyl fluoride (**3.63**) as the substrate (Figure 3.5). Analysis of the aromatic region of the ^{1}H NMR spectrum showed only sulfonyl fluoride **3.63** in the absence of DBU; however after the addition of 0.3 eq. of base, two new aromatic multiplets appeared at around 7.82 and 7.94 ppm, suggesting the formation of a new, more shielded proton environments.

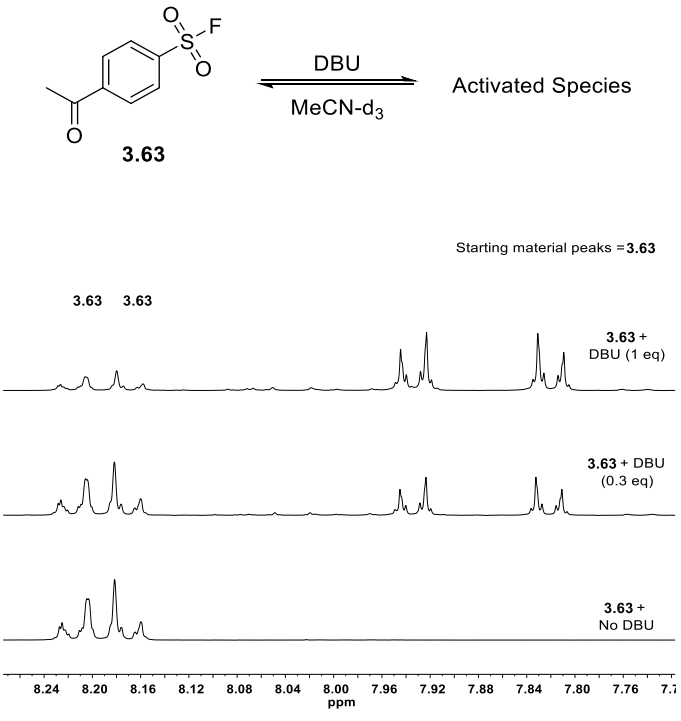


Figure 3.5: *NMR experiment illustrating the DBU mediated formation of an activated species of* ***3.63****.*

It was reasoned that the new aromatic environments could be formed due to the deprotonation of the acetyl moiety by DBU, however no substantial enolic environments were observed by ^{1}H NMR.

The NMR study was repeated with 4-nitrobenzenesulfonyl fluoride (**3.59**), with a similar result obtained (Figure 3.6). Intriguingly, further addition of DBU did not appear to significantly shift the ratio between **3.59** and the newly generated peaks, unlike the previous study where the ratio of the 'activated species' increased substantially (Figure 3.5).

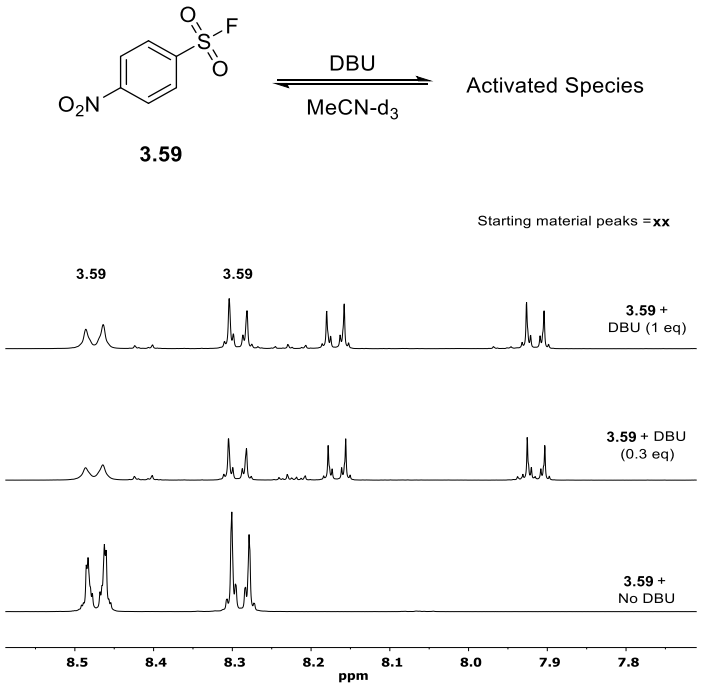
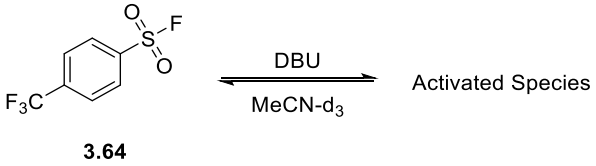


Figure 3.6: *Formation of an activated species of **3.59** through the addition of DBU.*

The ratio of the activated species formed from **3.63** increased from 0.7:1 to 3.1:1 upon the addition of extra base, however in the case of 4-nitrobenzenesulfonyl fluoride (**3.59**), the ratio stayed at approximately 0.7:1. This was a surprising result, as it would be expected that any interaction at the sulfur centre would be enhanced by the strongly electron-withdrawing nitro moiety.

To conclude the NMR experiments, the study was repeated with 4-trifluoromethylbenzenesulfonyl fluoride (**3.64**), which allowed both the ^{1}H and ^{19}F spectra to be analysed. The ^{1}H NMR study of **3.64** followed the same trend as previously observed, with a new set of aromatic multiplets appearing after the addition of DBU, the proportion of which didn't increase with higher concentration of base, with the ratio of activated species to starting material 0.56:1 (Figure 3.7).



3.64

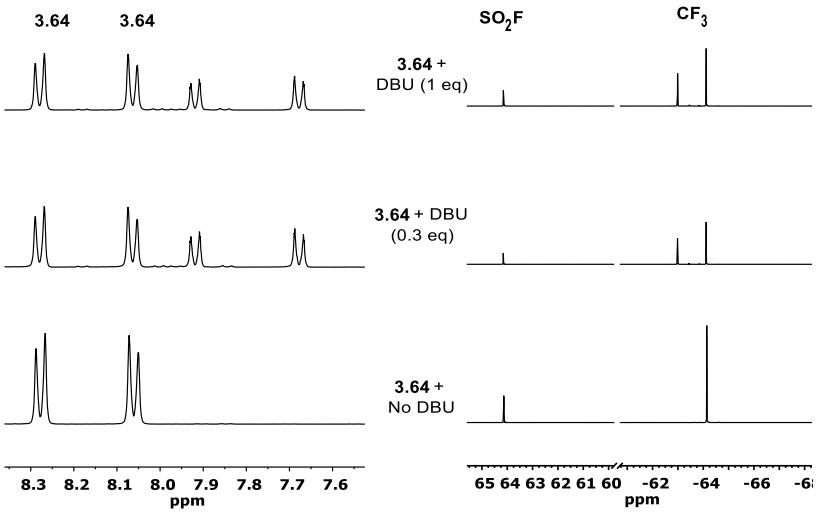


Figure 3.7: *Activation of **3.64** by DBU. Left: ^{1}H NMR spectrum; Right: Truncated ^{19}F NMR spectrum.*

Integration of the ^{19}F NMR spectrum of **3.64** showed the expected 1:3 ratio between the $-SO_2F$ (+64.2 ppm) and $-CF_3$ (-64.1 ppm) peaks. Upon addition of DBU, two differences were noted: the appearance of a new CF_3 environment, and the corresponding drop in the integral of the SO_2F peak (Table 3.10).

Collectively, the combined data indicate that the interaction of **3.64** and DBU resulted in the formation of a new intermediate that has a significantly different environment at the sulfur centre.

DBU (eq.)	***Integral of SO_2F***	***Integral of combined CF_3 peaks***	***Integral of 3.64 CF_3 peak***
0	1.02	3.00	3.00
0.3	0.66	3.00	1.94
1	0.65	3.00	1.99

Table 3.10: *Integral values of ^{19}F NMR peaks from the interaction of* ***3.64*** *and DBU.*

It is unclear whether a direct displacement of the fluoride ion had occurred, or whether the mechanism is subtler. The increased electron density at the sulfur centre from a proposed nucleophilic addition also aids the explanation of the formation of the new, more highly shielded aromatic proton environments observed.

Further studies are required to fully elucidate the nature of the interaction of sulfonyl fluorides and DBU. The current proposed model accounts for the formation of sulfonyl azides, however the cause of the reactivity of DBU is still unknown.

CONCLUSIONS AND FUTURE WORK

Sulfonyl azides are important synthetic compounds, having found application as both substrates in copper-catalysed transformations and also as reagents for both diazo- and azide-transfer. The most common protocol for the synthesis of these moieties is from the corresponding sulfonyl chlorides, which are known to be unstable under a range of conditions.

We have developed an operationally simple procedure for the formation of sulfonyl azides, from the significant more robust sulfonyl fluorides. The reaction occurs *via* SuFEx activation, providing consistently high yields with a range of functional groups and minimal purification. Conditions have also been developed for base-sensitive substrates, utilising alternative nucleophilic Lewis bases, which further expanded the scope of the transformation.

Sulfonyl azides are often employed as diazo-transfer reagents, however concerns persist regarding their stability. With this in mind, the methodology was extended to allow for *in situ* diazo-transfer reactions to be performed, generating diazo and azide in moderate to excellent yields. This modification removes the requirement of the isolation and handling of the unstable sulfonyl azide reagents.

NMR experiments were undertaken in an attempt to elucidate details about the nature of the activation of the sulfonyl fluoride moiety by DBU, following the mechanism previously proposed Gembus *et al*. These experiments suggested the formation of a new, more shielded sulfur environment, however the precise structure of this intermediate is still unknown.

To further extend our methodology, a one-pot azidation-copper catalysed cycloaddition procedure would be pursued, theoretically allowing access to *N*-sulfonyl triazole cores. The formation of these species from pre-formed sulfonyl azide reagents is known to require careful selection of reagents, with the formation of *N*-sulfonyl amides and *N*-sulfonylamidines also observed.

Additionally, further mechanistic studies would be undertaken to attempt to determine the true nature of the proposed "activated species" in our reaction, which would help elucidate the precise role of DBU. In particular, NMR experiments would be performed to determine the effect, if any, that the presence of water has on the formation of the postulated activated species.

EXPERIMENTAL SECTION

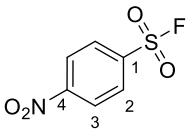
All reagents were obtained from commercial sources and used without further purification. Reactions were monitored using Thin Layer Chromatography (TLC), and visualised using UV light and stained using a basic $KMnO_4$ (potassium permanganate) solution. Flash column chromatography was performed using Merck silica gel 60 as the stationary phase. Petrol refers to petroleum spirit (b.p. 40-60 °C).

NMR spectra (^{1}H, ^{13}C and ^{19}F) were recorded on Bruker DPX300 (300 MHz), AV400 (400 MHz), DPX400 (400 MHz), AV3400 (400 MHz), AV3400HD (400 MHz) and AV3500 (500 MHz) spectrometers, in $CDCl_3$, D_2O, CD_3OD, DMSO-d^6 and Acetone-d^6. Infra-red spectra were obtained using a Bruker Alpha FTIR spectrometer with a platinum ATR adaptor, with the peaks recorded as υ_{max} (cm^{-1}). HRMS were obtained using a Bruker MicroTOF mass spectrometer operating in electrospray ionisation (ESI) or electron ionisation (EI) mode. Melting point data was collected using a Stuart SMP3. Where referenced, spectral data showed agreement with the literature.

General Procedure for Formation of Sulfonyl Fluorides

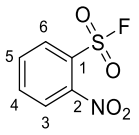
KFHF (2.3 mol eq.) was dissolved in H_2O to make a 4.6 M saturated solution. To this solution was added the sulfonyl chloride (1 mol eq., 1 M solution) in MeCN. The reaction mixture was stirred at room temperature for between 3 and 16 h. The mixture was extracted between EtOAc (2 x 50 mL) and brine (50 mL), the organic phases combined, dried over $MgSO_4$, filtered and concentrated under reduced pressure to yield the title compound.

4-Nitrobenzenesulfonyl fluoride[12] **(3.59)**



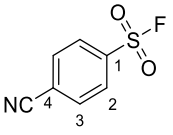
Yellow solid (1.35 g, 84%). m.p. 78 °C (lit: 75-76 °C).[12] υ_{max} (cm^{-1}): 1611, 1539 (NO_2), 1424, 1349; δ_H($CDCl_3$, 400 MHz): 8.52 – 8.48 (m, 2H, 3-H), 8.28 – 8.23 (m, 2H, 2-H); δ_C($CDCl_3$, 101 MHz): 151.8 (C-4), 138.3 (d, *J* = 27 Hz, C-1), 130.0 (C-2), 124.9 (C-3); δ_F($CDCl_3$, 377 MHz): 66.2; **HRMS** (EI) calculated for $C_6H_4FNO_4S$ $[M]^+$ 204.9840, found 204.9837.

2-Nitrobenzenesulfonyl fluoride[12] **(3.61)**



White solid (1.52 g, 95%). m.p. 61 °C (lit: 55-57 °C).[12] υ_{max} (cm^{-1}): 1551 (NO_2), 1446, 1422, 1358; δ_H($CDCl_3$, 400 MHz): 8.27 (dd, *J* = 7.8, 1.5 Hz, 1H, 3-H), 8.07 (d, *J* = 7.9 Hz, 1H, 6-H), 8.00 (ddd, *J* = 7.9, 7.7, 1.5 Hz, 1H, 5-H), 7.92 (dd, *J* = 7.8, 7.7, 1H, 4-H); δ_C($CDCl_3$, 101 MHz): 148.1 (C-2), 136.6 (C-5), 133.3 (C-4), 131.8 (C-3), 127.0 (d, *J* = 29 Hz, C-1), 125.9 (C-6); δ_F($CDCl_3$, 377 MHz): 65.0; **HRMS** (EI) calculated for $C_6H_4FNO_4S$ [M]+ 204.9840, found 204.9843.

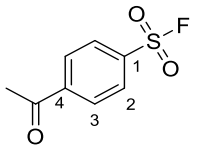
4-Cyanobenzenesulfonyl fluoride (3.62)



White solid (315 mg, 85%). m.p. 91 °C. υ_{max} (cm^{-1}): 2240 (CN), 1421; δ_H($CDCl_3$, 400 MHz): 8.19 – 8.14 (m, 2H, 3-H), 7.98 – 7.94 (m, 2H, 2-H); δ_C($CDCl_3$, 101 MHz): 136.9 (d, *J* = 27 Hz, C-1), 133.4 (C-2), 129.1 (C-3),

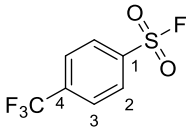
119.4 (C-4), 116.4 (CN); δ_F($CDCl_3$, 377 MHz): 66.0; **HRMS** (EI) calculated for $C_7H_4FNO_2S$ $[M]^+$ 184.9941, found 184.9940.

4-Acetylbenzenesulfonyl fluoride (3.63)



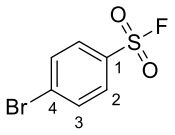
White solid (181 mg, 90%). m.p. 90 °C. υ_{max} (cm^{-1}): 1697 (C=O), 1417, 1259; δ_H($CDCl_3$, 400 MHz): 8.20 – 8.16 (m, 2H, 3-H), 8.15 – 8.12 (m, 2H, 2-H), 2.70 (s, 3H, CH_3); δ_C($CDCl_3$, 101 MHz): 196.1 ($COCH_3$), 142.2 (C-4), 136.6 (d, *J* = 25 Hz, C-1), 129.2 (C-3), 128.9 (C-2), 26.9 ($COCH_3$); δ_F($CDCl_3$, 377 MHz): 65.8; **HRMS** (EI) calculated for $C_8H_7FO_3S$ $[M]^+$ 202.0100, found 202.0103.

4-(Trifluoromethyl)benzenesulfonyl fluoride[12] (3.64)



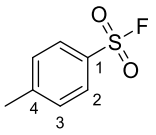
White solid (1.52 g, 85%). m.p. 69 °C (lit: 68-69 °C).[12] υ_{max} (cm^{-1}): 1420, 1322, 1181, 1147; δ_H($CDCl_3$, 400 MHz): 8.20 – 8.16 (m, 2H, 2-H), 7.94 – 7.91 (m, 2H, 3-H); δ_C($CDCl_3$, 101 MHz): 137.2 (q, *J* = 34 Hz, C-4), 136.5 (d, *J* = 26 Hz, C-1), 129.1 (C-2), 126.9 (q, *J* = 4 Hz, C-3), 122.7 (q, *J* = 273 Hz, CF_3); δ_F($CDCl_3$, 377 MHz): 65.8 (SO_2F), −63.6 (CF_3); **HRMS** (EI) calculated for $C_7H_4F_4O_2S$ $[M]^+$ 227.9868, found 227.9862.

4-Bromobenzenesulfonyl fluoride[12] **(3.65)**



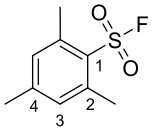
White solid (1.63 g, 87%). m.p. 64 °C (lit: 63-64 °C).[12] υ_{max} (cm^{-1}): 1578, 1472, 1416; δ_H($CDCl_3$, 400 MHz): 7.91 – 7.86 (m, 2H, Ar), 7.83 – 7.76 (m, 2H, Ar); δ_C($CDCl_3$, 101 MHz): 133.1 (Ar), 131.9 (d, *J* = 26 Hz, C-1), 131.3 (C-4), 129.8 (Ar); δ_F($CDCl_3$, 377 MHz): 66.4; **HRMS** (EI) calculated for $C_6H_4BrFO_2S$ $[M]^+$ 237.9094, found 237.9090.

4-Methylbenzenesulfonyl fluoride[162] **(3.66)**



White solid (1.29 g, 94%). m.p. 42 °C (lit: 41-43 °C).[163] υ_{max} (cm^{-1}): 1598, 1409; δ_H($CDCl_3$, 400 MHz): 7.92 – 7.88 (m, 2H, 2-H), 7.44 – 7.41 (m, 2H, 3-H), 2.50 (s, 3H, 4-CH_3); δ_C($CDCl_3$, 101 MHz): 147.1 (C-4), 130.2 (C-3), 130.0 (d, *J* = 24 Hz, C-1), 128.4 (C-2), 21.8 (4-CH_3); δ_F($CDCl_3$, 377 MHz): 66.3; **HRMS** (EI) calculated for $C_7H_7FO_2S$ $[M]^+$ 174.0157, found 174.0151.

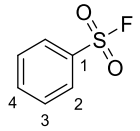
2,4,6-Trimethylbenzenesulfonyl fluoride[162] **(3.67)**



White solid (1.47 g, 92%). m.p. 72 °C (lit: 71-73 °C).[164] υ_{max} (cm^{-1}): 1605, 1569, 1394; δ_H($CDCl_3$, 400 MHz): 7.04 (s, 2H, 3-H), 2.65 (d, *J* = 1.8 Hz, 6H, 2-CH_3), 2.36 (s, 3H, 4-CH_3); δ_C($CDCl_3$, 101 MHz): 145.0 (C-4), 140.0 (C-2), 131.8 (C-3), 129.1 (d, *J* = 20 Hz, C-1), 22.3 (d, *J* = 2 Hz, 2-CH_3),

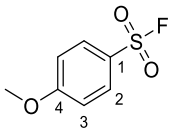
21.2 (4-CH_3); δ_F($CDCl_3$, 377 MHz): 68.2; **HRMS** (EI) calculated for $C_9H_{11}FO_2S$ $[M]^+$ 202.0458, found 202.0455.

Benzenesulfonyl fluoride[162] **(3.08)**



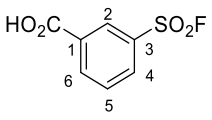
Colourless oil (1.20 g, 96%). υ_{max} (cm^{-1}): 1482, 1411; δ_H($CDCl_3$, 400 MHz): 8.06 – 8.00 (m, 2H, 2-H), 7.83 – 7.77 (m, 1H, 4-H), 7.69 - 7.62 (m, 2H, 3-H); δ_C($CDCl_3$, 101 MHz): 135.5 (C-4), 133.1 (d, *J* = 25 Hz, C-1), 129.6 (C-3), 128.4 (C-2); δ_F($CDCl_3$, 377 MHz): 65.9; **HRMS** (EI) calculated for $C_6H_5FO_2S$ $[M]^+$ 159.9994, found 159.9989.

4-Methoxybenzenesulfonyl fluoride[162] **(3.68)**



Colourless oil (1.42 g, 95%). υ_{max} (cm^{-1}): 1598, 1502, 1407, 1269 (C-O); δ_H($CDCl_3$, 400 MHz): 7.97 – 7.93 (m, 2H, 2-H), 7.09 – 7.05 (m, 2H, 3-H), 3.93 (s, 3H, OCH_3); δ_C($CDCl_3$, 101 MHz): 165.2 (C-4), 130.8 (C-2), 124.1 (d, *J* = 25 Hz, C-1), 114.9 (C-3), 55.9 (OCH_3); δ_F($CDCl_3$, 377 MHz): 67.3; **HRMS** (EI) calculated for $C_7H_7FO_3S$ $[M]^+$ 190.0100, found 190.0104.

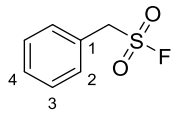
3-(Fluorosulfonyl)benzoic acid[12] **(3.69)**



White solid (1.42 g, 89%). m.p. 152 °C (lit: 152-154 °C).[12] υ_{max} (cm^{-1}): 3080 (OH), 1708 (C=O), 1418; δ_H($CDCl_3$, 400 MHz): 10.28 (s, 1H), 8.77 (dd, *J* = 1.9, 1.6 Hz, 1H, 2-H), 8.53 (ddd, *J* = 7.9, 1.6, 1.3 Hz, 1H, 6-H),

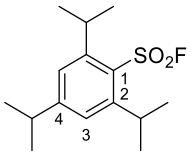
8.28 (ddd, *J* = 7.9, 1.9, 1.3 Hz, 1H, 4-H), 7.83 (dd, *J* = 7.9, 7.9 Hz, 1H, 5-H); δ_C($CDCl_3$, 101 MHz): 169.7 (COOH), 136.8 (C-6), 134.1 (d, *J* = 26 Hz, C-3), 133.1 (C-4), 131.1 (C-1), 130.3 (C-5), 130.2 (C-2); δ_F($CDCl_3$, 377 MHz): 66.0; **HRMS** (ESI) calculated for $C_7H_4FO_3S$ $[M-H]^-$ 202.9820, found 202.9821.

Phenylmethylsulfonyl fluoride[12] **(3.70)**



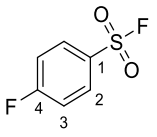
White solid (1.20 g, 80%). m.p. 92 °C (lit: 90 °C).[163] υ_{max} (cm^{-1}): 1497, 1458, 1411; δ_H($CDCl_3$, 400 MHz): 7.49 – 7.43 (m, 5H, Ar), 4.61 (d, *J* = 3.2 Hz, 2H, CH_2); δ_C($CDCl_3$, 101 MHz): 130.6 (Ar), 129.9 (Ar), 129.3 (Ar), 125.5 (C-1), 56.8 (d, *J* = 18 Hz, CH_2); δ_F($CDCl_3$, 377 MHz): 51.4; **HRMS** (EI) calculated for $C_7H_7FO_2S$ $[M]^+$ 174.0151, found 174.0152.

2,4,6-Triisopropylbenzenesulfonyl fluoride[164] **(3.71)**



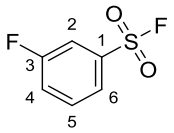
White solid (1.02 g, 91%). m.p. 67 °C (lit: 68-69 °C).[164] υ_{max} (cm^{-1}): 2961, 1599, 1398, 1204; δ_H($CDCl_3$, 400 MHz): 7.24 (s, 2H), 3.96 (heptd, *J* = 6.8, 2.5 Hz, 2H, 2-CH), 2.95 (hept, *J* = 6.9 Hz, 1H, 4-CH), 1.30 (d, *J* = 6.8 Hz, 12H, 2-^{i}Pr), 1.28 (d, *J* = 6.9 Hz, 6H, 4-^{i}Pr); δ_C($CDCl_3$, 101 MHz): 155.3 (C-4), 150.8 (C-2), 128.0 (d, *J* = 19 Hz, C-1), 124.0 (C-3), 34.4 (4-CH), 30.1 (d, *J* = 2 Hz, 2-CH), 24.5 (2-^{i}Pr), 23.5 (4-^{i}Pr); δ_F($CDCl_3$, 377 MHz): 73.4 (d, *J* = 2.5 Hz); **HRMS** (EI) calculated for $C_{15}H_{23}FO_2S$ $[M]^+$ 286.1397, found 286.1400.

4-Fluorobenzenesulfonyl fluoride[162] **(3.72)**



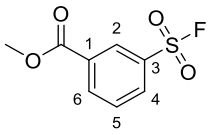
Colourless oil (1.20 g, 86%). υ_{max} (cm^{-1}): 1595, 1499, 1418; δ_H($CDCl_3$, 400 MHz): 8.10 – 8.03 (m, 2H, 2-H), 7.37 – 7.29 (m, 2H, 3-H); δ_C($CDCl_3$, 101 MHz): 166.9 (d, *J* = 260 Hz, C-4), 131.5 (d, *J* = 10 Hz, C-2), 129.0 (d, *J* = 26 Hz, C-1), 117.2 (d, *J* = 23 Hz, C-3); δ_F($CDCl_3$, 377 MHz): 66.8 (SO_2F), −99.3 (dd, *J* = 4.7, 3.2 Hz, 4-F); **HRMS** (EI) calculated for $C_6H_4F_2O_2S$ $[M]^+$ 177.9900, found 177.9901.

3-Fluorobenzenesulfonyl fluoride (3.73)



Yellow oil (1.30 g, 93%). υ_{max} (cm^{-1}): 1599, 1410, 1204; δ_H($CDCl_3$, 400 MHz): 7.86 (ddd, *J* = 8.0, 1.7, 0.8 Hz, 1H, 6-H), 7.74 (ddd, *J* = 7.6, 2.5, 1.7 Hz, 1H, 2-H), 7.66 (dddd, *J* = 8.1, 8.0, 5.1, 1.2 Hz, 1H, 5-H), 7.51 (dddd, *J* = 8.3, 8.1, 2.5, 0.8 Hz, 1H, 4-H); δ_C($CDCl_3$, 101 MHz): 162.3 (d, *J* = 254 Hz, C-3), 134.7 (dd, *J* = 26, 7 Hz, C-1), 131.6 (d, *J* = 8 Hz, C-5), 124.3 (d, *J* = 4 Hz, C-6), 123.0 (d, *J* = 21 Hz, C-4), 115.9 (d, *J* = 25 Hz, C-2); δ_F($CDCl_3$, 377 MHz): 65.9, −107.7 (dddd, *J* = 8.2, 8.2, 4.1, 4.1 Hz); **HRMS** (EI) calculated for $C_6H_4F_2O_2S$ $[M]^+$ 177.9895, found 177.9900.

Methyl 3-(fluorosulfonyl)benzoate[165] **(3.74)**



To a solution of 3-(fluorosulfonyl)benzoic acid (**3.69**) (436 mg, 2.00 mmol) in MeOH (10 mL) was added a few drops of conc. H_2SO_4. The resultant solution was refluxed for 16 hours, cooled, then extracted between EtOAc (2 x 40 mL) and sat. $NaHCO_{3(aq)}$ (40 mL). The organic phases were combined, dried over $MgSO_4$, filtered and volatile solvent removed under reduced pressure to yield a white solid (283 mg, 65%). m.p. 65 °C.

υ_{max} (cm^{-1}): 1732 (C=O), 1415, 1305, 1276 (C-O); δ_H($CDCl_3$, 400 MHz): 8.68 (dd, *J* = 1.7, 1.7 Hz, 1H, 2-H), 8.45 (ddd, *J* = 7.9, 1.7, 1.5 Hz, 1H, 6-H), 8.21 (ddd, *J* = 7.9, 1.7, 1.5 Hz, 1H, 4-H), 7.76 (dd, *J* = 7.9, 7.9 Hz, 1H, 5-H), 4.00 (s, 3H, OCH_3); δ_C($CDCl_3$, 101 MHz): 164.6 (CO_2CH_3), 136.3 (C-6), 133.8 (d, *J* = 26 Hz, C-3), 132.1 (C-4), 132.1 (C-1), 130.0 (C-5), 129.6 (C-2), 52.9 (CO_2CH_3); δ_F($CDCl_3$, 377 MHz): 66.0; **HRMS** (ESI) calculated for $C_8H_8F_1O_4S_1$ $[M+H]^+$ 219.0122, found 219.0128.

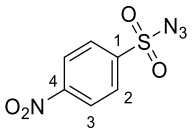
General Procedures

General Procedure 1: To a solution of sulfonyl fluoride (0.50 mmol) in MeCN (1 mL) was added DBU (22 µL, 0.15 mmol) followed by $TMSN_3$ (50 µL, 0.38 mmol). The resultant solution was stirred at room temperature for 15 min, then a further portion of $TMSN_3$ (50 µL, 0.38 mmol) was added. The solution was stirred for a further 45 min, filtered through a silica plug, eluted with EtOAc (50 mL) and volatiles removed under reduced pressure to yield the desired sulfonyl azide.

General Procedure 2: To a solution of sulfonyl fluoride (0.50 mmol) in MeCN (1 mL) was added DBU (75 µL, 0.50 mmol) followed by $TMSN_3$ (50 µL, 0.38 mmol). The resultant solution was stirred at 50 °C for 15 min, then further two portions of $TMSN_3$ (50 µL, 0.38 mmol) were added at 15 min intervals. The solution was stirred for a further 45 min, filtered through a silica plug, eluted with EtOAc (50 mL) and volatiles removed under reduced pressure to yield the desired sulfonyl azide.

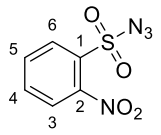
General Procedure 3: To a solution of 2-nitrobenzenesulfonyl fluoride (123 mg, 0.600 mmol) was added DBU (0.18 mmol) and $TMSN_3$ (0.45 mmol). The resultant solution was stirred for 15 minutes, before the addition of further $TMSN_3$ (0.45 mmol, 0.9 eq.). The solution was again stirred for 15 minutes, before the required aniline or di-one was added (0.5 mmol), along with additional DBU (0.5 mmol, 1 eq.). The reaction mixture was then left to stir for the stated time and extracted between EtOAc (2 x 50 mL) and brine (50 mL). The organic phases were combined, dried over $MgSO_4$ and volatiles removed under reduced pressure. Purification by flash column chromatography yielded the desired products.

4-Nitrobenzenesulfonyl azide[166] **(3.60)**



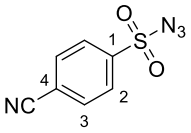
Prepared with **General Procedure 1**. White solid (105 mg, 92%). m.p. 102 °C (lit: 97-100 °C).[167] υ_{max} (cm^{-1}): 2134 (N_3), 1537 (NO_2), 1177; δ_H($CDCl_3$, 400 MHz): 8.49 – 8.46 (m, 2H, 3-H), 8.20 – 8.16 (m, 2H, 2-H); δ_C($CDCl_3$, 101 MHz): 151.2 (C-4), 143.7 (C-1), 128.9 (C-2), 124.9 (C-3); **HRMS** (EI) calculated for $C_6H_4N_4O_4S$ $[M]^+$ 227.9953, found 227.9960.

2-Nitrobenzenesulfonyl azide[166] **(3.75)**



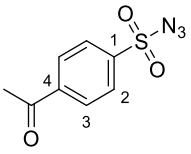
Prepared with **General Procedure 1**. White solid (113 mg, 99%). m.p. 70 °C (lit: 68-70 °C).[168] υ_{max} (cm^{-1}): 2126 (N_3), 1603 (NO_2), 1364; δ_H($CDCl_3$, 400 MHz): 8.22 – 8.18 (m, 1H, 3-H), 7.95 – 7.81 (m, 3H, Ar); δ_C($CDCl_3$, 101 MHz): 147.7 (C-2), 135.7 (Ar), 133.1 (Ar), 132.6 (C-1), 131.7 (C-6), 125.4 (Ar); **HRMS** (ESI) calculated for $C_6H_4N_4O_4SNa$ $[M+Na]^+$ 250.9845, found 250.9849.

4-Cyanobenzenesulfonyl azide[122] **(3.76)**



Prepared with **General Procedure 1**. White solid (94 mg, 90%). m.p. 114 °C. υ_{max} (cm^{-1}): 2134 (N_3), 1383, 1171; δ_H($CDCl_3$, 400 MHz): 8.12 – 8.08 (m, 2H, Ar), 7.95 – 7.92 (m, 2H, Ar); δ_C($CDCl_3$, 101 MHz): 142.3 (C-1), 133.4 (Ar), 128.1 (Ar), 118.5 (C-4), 116.7 (CN). Does not ionise by ESI.

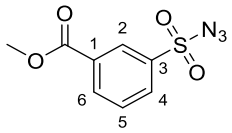
4-Acetylbenzenesulfonyl azide[122] **(3.77)**



Prepared following **General Procedure 1**. White solid (100 mg, 89%). m.p. 98 °C. υ_{max} (cm^{-1}): 2132 (N_3), 1696 (C=O), 1400; δ_H($CDCl_3$, 400 MHz): 8.19 – 8.15 (m, 2H, 3-H), 8.09 – 8.06 (m, 2H, 2-H), 2.69 (s, 3H, CH_3); δ_C($CDCl_3$, 101 MHz): 196.2 (CO), 142.0 (C-1), 141.6 (C-4), 129.4 (C-3) , 127.8 (C-

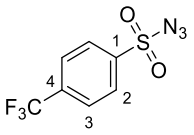
2), 26.9 (CH_3); **HRMS** (ESI) calculated for $C_8H_7N_3O_3SNa$ $[M+Na]^+$ 248.0100, found 248.0115.

Methyl 3-(azidosulfonyl)benzoate[165] **(3.78)**



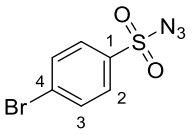
Prepared following **General Procedure 1**. White solid (115 mg, 95%). m.p. 40 °C. υ_{max} (cm^{-1}): 2132 (N_3), 1730 (C=O), 1379 (C-O); δ_H($CDCl_3$, 400 MHz): 8.62 (ddd, *J* = 2.0, 1.6, 0.5 Hz, 1H, 2-H), 8.40 (ddd, *J* = 7.9, 1.6, 1.2 Hz, 1H, 6-H), 8.15 (ddd, *J* = 7.9, 2.0, 1.2 Hz, 1H, 4-H), 7.74 (ddd, *J* = 7.9, 7.9, 0.5 Hz, 1H, 5-H), 4.00 (s, 3H, $CO_2\underline{C}H_3$); δ_C($CDCl_3$, 101 MHz): 164.8 (CO_2CH_3), 139.1 (C-3), 135.5 (C-6), 132.0 (C-1), 131.3 (C-4), 130.0 (C-5), 128.5 (C-2), 52.8 (CO_2CH_3); **HRMS** (ESI) calculated for $C_8H_8N_3O_4S_1$ $[M+H]^+$ 242.0230, found 242.0229.

4-(Trifluoromethyl)benzenesulfonyl azide[122] **(3.79)**



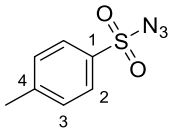
Prepared with **General Procedure 1**. White solid (110 mg, 88%). m.p. 50 °C (lit: 51-54 °C).[167] υ_{max} (cm^{-1}): 2133 (N_3), 1381, 1323; δ_H($CDCl_3$, 400 MHz): 8.13 – 8.10 (m, 2H, Ar), 7.93 – 7.89 (m, 2H, Ar); δ_C($CDCl_3$, 101 MHz): 141.8 (C-1), 136.3 (q, *J* = 34 Hz, C-4), 128.1 (C-2), 126.9 (q, *J* = 4 Hz, C-3), 122.8 (q, *J* = 273 Hz, CF_3); δ_F($CDCl_3$, 377 MHz): −63.4; Does not ionise by ESI.

4-Bromobenzenesulfonyl azide[122] **(3.80)**



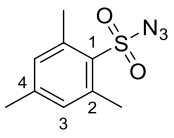
Prepared with **General Procedure 1**. White solid (104 mg, 79%). m.p. 50 °C (lit: 53-53.5 °C).[120] υ_{max} (cm^{-1}): 2131 (N_3), 1575, 1378; δ_H($CDCl_3$, 400 MHz): 7.86 – 7.81 (m, 2H, Ar), 7.79 – 7.75 (m, 2H, Ar); δ_C($CDCl_3$, 101 MHz): 137.4 (C-1), 133.1 (Ar), 130.3 (C-3), 128.9 (Ar); Does not ionise by ESI.

4-Methylbenzenesulfonyl azide[122] **(3.81)**



Prepared with **General Procedure 2**, heating for 1.5 h. Colourless oil (97 mg, 98%). υ_{max} (cm^{-1}): 2129 (N_3), 1597, 1373; δ_H($CDCl_3$, 400 MHz): 7.88 – 7.83 (m, 2H, 2-H), 7.44 – 7.39 (m, 2H, 3-H), 2.49 (s, 3H, CH_3); δ_C($CDCl_3$, 101 MHz): 146.2 (C-4), 135.5 (C-1), 130.3 (Ar), 127.5 (Ar), 21.7 (4-CH_3); **HRMS** (ESI) calculated for $C_7H_7N_3O_2SNa$ $[M+Na]^+$ 220.0151, found 220.0143.

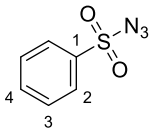
2,4,6-Trimethylbenzenesulfonyl azide[120] **(3.82)**



Prepared with **General Procedure 2**, heating for 2 h. White solid (103 mg, 91%). m.p. 35 °C. υ_{max} (cm^{-1}): 2126 (N_3), 1603, 1364; δ_H($CDCl_3$, 400 MHz): 7.03 (s, 2H, 3-H), 2.67 (s, 6H, 2-CH_3), 2.35 (s, 3H, 4-CH_3); δ_C($CDCl_3$, 101 MHz): 144.6 (C-4), 140.0 (C-2), 133.2 (C-1), 132.1 (C-3), 22.8 (2-CH_3),

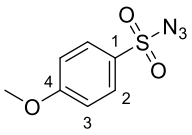
21.1 (4-CH_3); **HRMS** (ESI) calculated for $C_9H_{11}N_3O_2SNa$ $[M+Na]^+$ 248.0464, found 248.0463.

Benzenesulfonyl azide[167] **(3.83)**



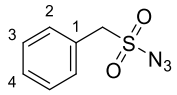
Prepared with **General Procedure 2**, heating for 1 h. Colourless oil (66 mg, 72%). υ_{max} (cm^{-1}): 2130 (N_3), 1450, 1374; δ_H($CDCl_3$, 400 MHz): 8.00 – 7.95 (m, 2H, 2-H), 7.78 – 7.72 (m, 1H, 4-H), 7.67 – 7.60 (m, 2H, 3-H); δ_C($CDCl_3$, 101 MHz): 138.5 (C-1), 134.8 (C-4), 129.7 (C-3), 127.5 (C-2); **HRMS** (ESI) calculated for $C_6H_5N_3O_2SNa$ $[M+Na]^+$ 205.9995, found 206.0011.

4-Methoxybenzenesulfonyl azide[122] **(3.84)**



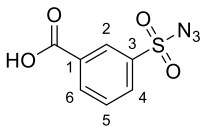
Prepared with **General Procedure 2**, heating for 2 h. White solid (100 mg, 94%). m.p. 52 °C (lit: 57-60 °C).[167] υ_{max} (cm^{-1}): 2128 (N_3), 1596, 1499, 1372 (C-O); δ_H($CDCl_3$, 400 MHz): 7.93 - 7.88 (m, 2H, 2-H), 7.09 - 7.04 (m, 2H, 3-H), 3.92 (s, 3H, OCH_3); δ_C($CDCl_3$, 101 MHz): 164.6 (C-4), 129.9 (C-2), 129.8 (C-1), 114.8 (C-3), 55.9 (OCH_3); **HRMS** (ESI) calculated for $C_7H_7N_3O_3SNa$ $[M+Na]^+$ 236.0100, found 236.0092.

Phenylmethanesulfonyl azide[167] **(3.86)**



To a solution of phenylmethanesulfonyl fluoride (**3.70**) (87 mg, 0.50 mmol) in MeCN (1 mL) at 50 °C was added DMAP (91 mg, 0.75 mmol) followed by $TMSN_3$ (50 µL, 0.38 mmol). The resultant solution was stirred at 50 °C for 15 min, then further two portions of $TMSN_3$ (50 µL, 0.38 mmol) were added at intervals of 15 min. The solution was stirred for a further 90 min, filtered through a silica plug, eluting with EtOAc (50 mL) and volatiles removed under reduced pressure to yield the target sulfonyl azide as a 97:3 mixture of product to starting material (by ^{1}H NMR integration) as a white solid (96 mg, 97%). m.p. 52 °C (lit: 52-59 °C).[167] υ_{max} (cm^{-1}): 2138 (N_3), 1370; δ_H($CDCl_3$, 400 MHz): 7.51 - 7.43 (m, 5H, Ar), 4.55 (s, 2H, CH_2); δ_C($CDCl_3$, 101 MHz): 131.0 (Ar), 129.9 (Ar), 129.3 (Ar), 126.6 (Ar), 62.0 (CH_2); Does not ionise by ESI.

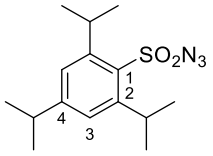
3-(Azidosulfonyl)benzoic acid[169] **(3.85)**



To a solution of 3-(fluorosulfonyl)benzoic acid (**3.69**) (109 mg, 0.500 mmol) in MeCN (1 mL) was added DMAP (79 mg, 0.65 mmol) followed by $TMSN_3$ (50 µL, 0.38 mmol). The resultant solution was stirred at room temperature for 15 min, then $TMSN_3$ (50 µL, 0.38 mmol) was added. After a further 15 min, $TMSN_3$ (50 µL, 0.38 mmol) was added and the solution stirred for 30 min, filtered through a silica plug, eluting with EtOAc (50 mL) and volatiles removed under reduced pressure to yield an off-white solid (112 mg, 99%). m.p. 126 °C (lit: 90-92 °C).[170] υ_{max} (cm^{-1}): 2155 (N_3), 1687 (C=O), 1370,

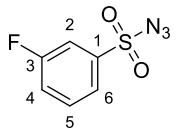
1176; δ_H($CDCl_3$, 400 MHz): 8.71 (t, *J* = 1.9, 1.6 Hz, 1H, 2-H), 8.48 (ddd, *J* = 7.9, 1.6, 1.3 Hz, 1H, 6-H), 8.22 (ddd, *J* = 8.0, 1.9, 1.3 Hz, 1H, 4-H), 7.79 (dd, *J* = 8.0, 7.9 Hz, 1H, 5-H); δ_C($CDCl_3$, 101 MHz): 169.3 (COOH), 139.5 (C-3), 136.0 (C-6), 132.2 (C-1), 131.0 (C-4), 130.2 (C-5), 129.2 (C-2); **HRMS** (ESI) calculated for $C_7H_4N_3O_4S_1$ $[M-H]^-$ 225.9928, found 225.9941.

2,4,6-Triisopropylbenzenesulfonyl azide (3.57)



Prepared with **General Procedure 2**. White solid (153 mg, 99%). m.p. 41 °C. υ_{max} (cm^{-1}): 2960, 2117 (N_3), 1351, 1165; δ_H($CDCl_3$, 400 MHz): 7.23 (s, 2H, 3-H), 4.07 (hept, *J* = 6.7 Hz, 2H, 2-CH), 2.94 (hept, *J* = 6.8 Hz, 1H, 4-CH), 1.30 (d, *J* = 6.7 Hz, 12H, 2-^{i}Pr), 1.28 (d, *J* = 6.8 Hz, 6H, 4-^{i}Pr); δ_C($CDCl_3$, 101 MHz): 154.8 (C-4), 150.9 (C-2), 132.0 (C-1), 124.1 (C-3), 34.3 (4-CH), 29.9 (2-CH), 24.8 (2-^{i}Pr), 23.5 (4-^{i}Pr); **HRMS** (ESI) calculated for $C_{15}H_{23}N_3O_2SNa$ $[M+Na]^+$ 332.1403, found 332.1405.

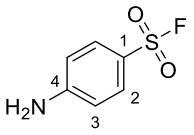
3-Fluorobenzenesulfonyl azide (3.88)



Prepared with **General Procedure 2**, stirred at room temperature. Colourless oil (191 mg, 95%). υ_{max} (cm^{-1}): 2126 (N_3), 1476, 1371, 1156; δ_H($CDCl_3$, 400 MHz): 7.78 (ddd, *J* = 7.9, 1.8, 1.0 Hz, 1H, 6-H), 7.68 (ddd, *J* = 8.0, 2.7, 1.8 Hz, 1H, 2-H), 7.63 (ddd, *J* = 8.1, 7.9, 5.1 Hz, 1H, 5-H), 7.45 (dddd, *J* = 8.2, 8.1, 2.7, 0.9 Hz, 1H, 4-H); δ_C($CDCl_3$, 101 MHz): 162.5 (d, *J* = 254 Hz, C-3), 140.2 (d, *J* = 7 Hz, C-1), 131.6 (d, *J* = 8 Hz, C-5), 123.3 (d, *J* = 4 Hz, C-6), 122.1 (d, *J* = 21 Hz, C-4), 114.9 (d, *J* = 25

Hz, C-2); δ_F($CDCl_3$, 377 MHz): −107.8 (dddd, *J* = 8.2, 8.0, 4.1, 4.1 Hz); Does not ionise by ESI.

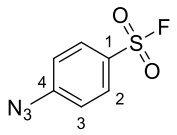
4-Aminobenzenesulfonyl fluoride[171] **(3.91)**



To a solution of 4-nitrobenzenesulfonyl fluoride (**3.59**) (1.03 g, 5.00 mmol) in ethanol (60 mL) and water (15 mL) was added conc. hydrochloric acid (3 mL) and iron fillings (1.40 g, 25.0 mmol). The suspension was heated to 90 °C for 1 h, cooled and filtered through a short pad of silica, washing with ethanol (100 mL). The solution was concentrated under reduced pressure and the residue extracted between EtOAc (80 mL) and 1M $NaOH_{(aq)}$ (80 mL). The organic layer was dried over $MgSO_4$, filtered and concentrated under reduced pressure. Purification by flash column chromatography (20% EtOAc/Petrol) yielded the title compound as an off white solid (702 mg, 80%). m.p. 69 °C (lit: 70 °C).[171]

υ_{max} (cm^{-1}): 3419 (NH_2), 1624, 1596, 1401, 1180; δ_H($CDCl_3$, 400 MHz): 7.79 - 7.74 (m, 2H, 2-H), 6.75 - 6.71 (m, 2H, 3-H), 4.41 (br. s, 2H, NH_2); δ_C($CDCl_3$, 101 MHz): 153.0 (C-4), 130.8 (C-2), 119.6 (d, *J* = 24 Hz, C-1), 113.9 (C-3); δ_F($CDCl_3$, 376 MHz): 67.7; **HRMS** (ESI) calculated for $C_6H_6FNO_2SNa$ $[M+Na]^+$ 197.9995, found 198.0006.

4-Azidobenzenesulfonyl fluoride[165] **(3.92)**

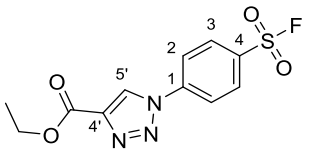


To a solution of 4-aminobenzenesulfonyl fluoride (**3.91**) (525 mg, 3.00 mmol) in MeCN (10 mL) at 0 °C was added *tert*-butyl nitrite (435 µL, 3.30

mmol) followed by $TMSN_3$ (540 µL, 4.50 mmol). The reaction was stirred for 30 min at room temperature and then concentrated under reduced pressure. Purification by flash column chromatography (4% Et_2O/Petrol) yielded a white solid (559 mg, 93%). m.p. 65 °C.

υ_{max} (cm^{-1}): 2109 (N_3), 1590, 1419, 1288; δ_H($CDCl_3$, 400 MHz): 8.03 - 7.98 (m, 2H, 2-H), 7.26 – 7.24 (m, 2H, 3-H); δ_C($CDCl_3$, 101 MHz): 148.0 (C-4), 130.5 (C-2), 128.6 (d, *J* = 25 Hz, C-1), 119.9 (C-3); δ_F($CDCl_3$, 376 MHz): 66.8; **HRMS** (EI) calculated for $C_6H_4N_3O_2FS$ $[M]^+$ requires 201.0002, found 200.9999.

Ethyl 1-(4-(fluorosulfonyl)phenyl)-1*H*-1,2,3-triazole-4-carboxylate[165] **(3.93)**

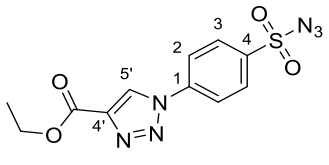


To a solution of 4-azidobenzenesulfonyl fluoride (**3.92**) (502 mg, 2.50 mmol) in MeCN (5 mL) was added ethyl propiolate (385 µL, 3.75 mmol), followed by a solution of $CuSO_4 \cdot 5H_2O$ (75 mg, 0.30 mmol) and sodium ascorbate (297 mg, 1.50 mmol) in H_2O (2.5 mL). The resultant biphasic solution was stirred for 16 h at room temperature, diluted with H_2O (50 mL) and filtered. The resultant solid was washed with H_2O (20 mL), then petrol (50 mL) and dried under reduced pressure to yield a pale yellow solid (660 mg, 88%). m.p. 181 °C.

υ_{max} (cm^{-1}): 1724 (C=O), 1420, 1261 (C-O), 1035; δ_H($CDCl_3$, 400 MHz): 8.67 (s, 1H, 5'-H), 8.28 – 8.22 (m, 2H, 2-H), 8.16 – 8.10 (m, 2H, 3-H), 4.50 (q, *J* = 7.1 Hz, 2H, $OC\underline{H}_2CH_3$), 1.46 (t, *J* = 7.1 Hz, 3H, $OCH_2C\underline{H}_3$); δ_C($CDCl_3$, 101 MHz): 160.0 (C=O), 141.7 (C-4'), 141.3 (C-1), 133.5 (d, *J* = 26.4 Hz, C-4'), 130.7 (C-2), 125.3 (C-5'), 121.2 (C-3), 61.9 ($O\underline{C}H_2CH_3$),

14.3 ($OCH_2\underline{C}H_3$); δ_F($CDCl_3$, 376 MHz): 66.6; **HRMS** (ESI) calculated for $C_{11}H_{11}FN_3O_4S$ $[M+H]^+$ 300.0449, found 300.0448.

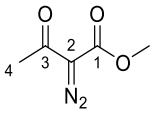
Ethyl 1-(4-(azidosulfonyl)phenyl)-1*H*-1,2,3-triazole-4-carboxylate[165] (3.94)



Prepared following **General Procedure 2** for 1 h, on a 0.33 mmol scale from ethyl 1-(4-(fluorosulfonyl)phenyl)-1*H*-1,2,3-triazole-4-carboxylate (**3.93**). Reaction was extracted between EtOAc (2 x 30 mL) and brine (30 mL), organics combined, dried over $MgSO_4$, filtered and concentrated under reduced pressure to yield the title compound as a pale yellow solid (90 mg, 84%). m.p. 170 °C (decomposition).

υ_{max} (cm^{-1}): 2132 (N_3), 1724 (C=O), 1378 (C-O), 1171; δ_H($CDCl_3$, 400 MHz): 8.65 (s, 1H, 5'-H), 8.23 – 8.15 (m, 2H, Ar), 8.12 - 8.07 (m, 2H, Ar), 4.50 (q, *J* = 7.1 Hz, 2H, $OC\underline{H}_2CH_3$), 1.46 (t, *J* = 7.1 Hz, 3H, $OCH_2C\underline{H}_3$); δ_C($CDCl_3$, 101 MHz): 160.1 (C=O), 141.7 (C-4'), 140.6 (Ar), 139.0 (Ar), 129.7 (Ar), 125.3 (C-5'), 121.3 (Ar), 61.9 ($O\underline{C}H_2CH_3$), 14.3 ($O\underline{C}H_2CH_3$); **HRMS** (ESI) calculated for $C_{11}H_{11}N_6O_4S$ $[M+H]^+$ 323.0557, found 323.0553.

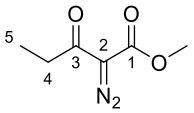
Methyl 2-diazo-3-oxobutanoate[172] (3.98)



Prepared with **General Procedure 3**, eluting with 20% EtOAc/Petrol to yield the title compound as a yellow oil (48 mg, 68%). υ_{max} (cm^{-1}): 2958, 2145 (N_2), 1719 (C=O), 1654 (C=O); δ_H($CDCl_3$, 400 MHz): 3.85 (s, 3H, OCH_3), 2.49 (s, 3H, 4-H); δ_C($CDCl_3$, 101 MHz): 190.0 (C-3), 161.8 (C-1),

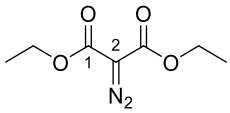
52.2 (OCH_3), 28.2 (CH_3) (C-2 not visible); **HRMS** (ESI) calculated for $C_5H_6N_2O_3Na$ $[M+Na]^+$ requires 165.0271, found 165.0274.

Methyl 2-diazo-3-oxopentanoate[173] **(3.99)**



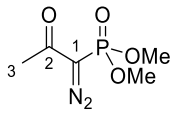
Prepared with **General Procedure 3**, eluting with 20% EtOAc/Petrol to yield the title compound as a yellow oil (60 mg, 77%). υ_{max} (cm^{-1}): 2957, 2147 (N_2), 1719 (C=O), 1652 (C=O); δ_H($CDCl_3$, 400 MHz): 3.84 (s, 3H, OCH_3), 2.87 (q, *J* = 7.3 Hz, 2H, 4-H), 1.14 (t, *J* = 7.3 Hz, 3H, 5-H); δ_C($CDCl_3$, 101 MHz): 193.4 (C-3), 161.8 (C-1), 52.1 (OCH_3), 33.7 ($\underline{C}H_2CH_3$), 8.2 ($CH_2\underline{C}H_3$) (C-2 not visible); **HRMS** (ESI) calculated for $C_6H_8N_2O_3Na$ $[M+Na]^+$ requires 179.0427, found 179.0434.

Diethyl diazomalonate[172] **(3.100)**



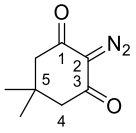
Prepared with **General Procedure 3**, eluting with 20% EtOAc/Petrol to yield the title compound as a yellow oil (83 mg, 89%). υ_{max} (cm^{-1}): 2986, 2142 (N_2), 1750 (C=O), 1687 (C=O); δ_H($CDCl_3$, 400 MHz): 4.31 (q, *J* = 7.2 Hz, 4H, $OC\underline{H}_2CH_3$), 1.32 (t, *J* = 7.2 Hz, 6H, $OCH_2C\underline{H}_3$); δ_C($CDCl_3$, 101 MHz): 161.1 (C-1), 61.6 ($\underline{C}H_2CH_3$), 14.3 ($CH_2\underline{C}H_3$) (C-2 not visible); **HRMS** (ESI) calculated for $C_7H_{10}N_2O_4$ $[M+H]^+$ requires 159.0400, found 159.0402.

Dimethyl (1-diazo-2-oxopropyl)phosphonate[174] **(3.101)**



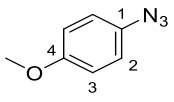
Prepared with **General Procedure 3**, eluting with 20% EtOAc/Petrol to yield the title compound as a yellow oil (55 mg, 57%). υ_{max} (cm^{-1}): 2119 (N_2), 1655 (C=O), 1265; δ_H($CDCl_3$, 400 MHz): 3.88 (s, 3H, OCH_3), 3.85 (s, 3H, OCH_3), 2.29 (s, 3H, 3-H); δ_C($CDCl_3$, 101 MHz): 189.9 (d, *J* = 13 Hz, C-2), 53.6 (OCH_3), 27.1 (C-3) (C-1 not visible); **HRMS** (ESI) calculated for $C_5H_{10}N_2O_4P$ $[M+H]^+$ requires 193.0373, found 193.0369.

2-Diazo-5,5-dimethylcyclohexane-1,3-dione[172] **(3.97)**



Prepared with **General Procedure 3** (stirring for 1 h), eluting with 20 – 30% EtOAc/Petrol to yield the title compound as a white solid (75 mg, 90%) m.p. 104 °C (lit: 103-106 °C).[172] υ_{max} (cm^{-1}): 2184 (N_2), 2140, 1645 (C=O), 1305; δ_H($CDCl_3$, 400 MHz): 2.45 (s, 4H, 4-H_2 and 6-H_2), 1.12 (s, 6H, 5-CH_3); δ_C($CDCl_3$, 101 MHz): 180.9 (C-1 and C-3), 50.5 (C-4), 31.1 (C-5), 28.3 (5-CH_3) (C-2 not visible); **HRMS** (ESI) calculated for $C_8H_{10}N_2O_2Na$ $[M+Na]^+$ requires 189.0634, found 189.0624.

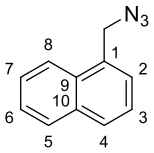
1-Azido-4-methoxybenzene[153] **(3.103)**



Prepared with **General Procedure 3**, eluting with 5% Et_2O/Petrol to yield the title compound as a yellow oil (37 mg, 50%). υ_{max} (cm^{-1}): 2108 (N_3), 1602, 1506; δ_H($CDCl_3$, 400 MHz): 6.99 – 6.95 (m, 2H, Ar), 6.92 – 6.88 (m,

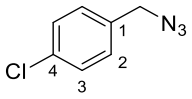
2H, Ar), 3.81 (s, 3H); δ_C($CDCl_3$, 101 MHz): 157.0 (C-4), 132.3 (Ar), 120.0 (Ar), 115.1 (Ar), 55.6 (OCH_3).

1-(Azidomethyl)naphthalene[175] **(3.105)**



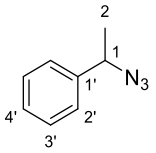
Prepared with **General Procedure 3**, eluting with 5% Et_2O/Petrol to yield the title compound as a colourless oil (65 mg, 71%). υ_{max} (cm^{-1}): 3011, 2103 (N_3); δ_H($CDCl_3$, 400 MHz): 8.08 - 8.02 (m, 1H, 8-H), 7.94 – 7.85 (m, 2H, Ar), 7.63 – 7.52 (m, 2H, Ar), 7.51 – 7.45 (m, 2H, Ar), 4.79 (s, 2H, CH_2); δ_C($CDCl_3$, 101 MHz): 133.9 (Ar), 131.3 (Ar), 131.0 (Ar), 129.4 (Ar), 128.8 (Ar), 127.3 (Ar), 126.7 (Ar), 126.2 (Ar), 125.2 (Ar), 123.5 (Ar), 53.0 (CH_2).

4-Chlorobenzylazide[175] **(3.106)**



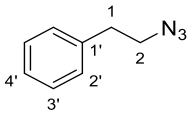
Prepared with **General Procedure 3**, eluting with 5% Et_2O/Petrol to yield the title compound as a colourless oil (56 mg, 67%). υ_{max} (cm^{-1}): 2102 (N_3), 1493; δ_H($CDCl_3$, 400 MHz): 7.39 – 7.35 (m, 2H, Ar), 7.29 – 7.25 (m, 2H, Ar), 4.33 (s, 2H, CH_2); δ_C($CDCl_3$, 101 MHz): 134.2 (Ar), 133.9 (Ar), 129.5 (Ar), 129.0 (Ar), 54.0 (CH_2).

(1-Azidoethyl)benzene[137] **(3.107)**



Prepared with **General Procedure 3**, eluting with 5% Et_2O/Petrol to yield the title compound as a colourless oil (46 mg, 63%). υ_{max} (cm^{-1}): 2983, 2108 (N_3), 1454; δ_H($CDCl_3$, 400 MHz): 7.45–7.30 (m, 5H), 4.63 (q, *J* = 6.8 Hz, 1H), 1.55 (d, *J* = 6.8 Hz, 3H); δ_C($CDCl_3$, 101 MHz): 140.8 (Ar), 128.8 (Ar), 128.1 (Ar), 126.4 (Ar), 61.1 (C-1), 21.6 (C-2).

(2-Azidoethyl)benzene[137] **(3.108)**



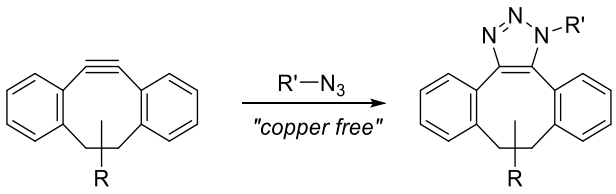
Prepared with **General Procedure 3**, eluting with 5% Et_2O/Petrol to yield the title compound as a colourless oil (49 mg, 67%). υ_{max} (cm^{-1}): 3011, 2100 (N_3), 1455; δ_H($CDCl_3$, 400 MHz): 7.37 – 7.31 (m, 2H, Ar), 7.29 – 7.21 (m, 3H, Ar), 3.52 (t, *J* = 7.3 Hz, 2H, 2-H), 2.91 (t, *J* = 7.3 Hz, 2H, 1-H); δ_C($CDCl_3$, 101 MHz): 138.0 (C-1'), 128.7 (Ar), 128.6 (Ar), 126.8 (Ar), 52.5 (C-2), 35.3 (C-1).

Chapter 4 : Radical Cation Initiated Enyne Hydration

BACKGROUND

As discussed in Chapter 1, the Huisgen 1,3-dipolar cycloaddition reaction of azides and alkynes has found wide application in a host of disciplines.[176] The copper-catalysed reaction (CuAAC) is regarded as the premier example of Click Chemistry, however there are drawbacks with this method.[177] The cytotoxicity of the copper catalyst limits the application of the CuAAC in living systems, which has resulted in the development of alternative protocols.[177,178,179]

An example of copper-free version of this transformation is the strain-promoted azide-alkyne cycloaddition (SPAAC), developed by Bertozzi *et al*.[177] which utilises strain-relief of a cyclo-octyne as the driving force to promote cyclisation (Scheme 4.1).



Scheme 4.1: *Bertozzi's SPAAC proposal.*[177]

Stimulated by related studies in the Moses group on radical cation activated cycloaddition reactions, the possibility of promoting azide-alkyne cycloadditions through a single electron oxidation was intriguing. There is substantial literature precedent for radical cation promoted cycloadditions,[180–182] with a pertinent example being the radical cation induced Diels-Alder reaction extensively developed by Bauld *et al*., utilising aminium salt **4.01** (Figure 4.1).[180]

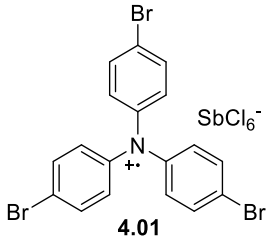
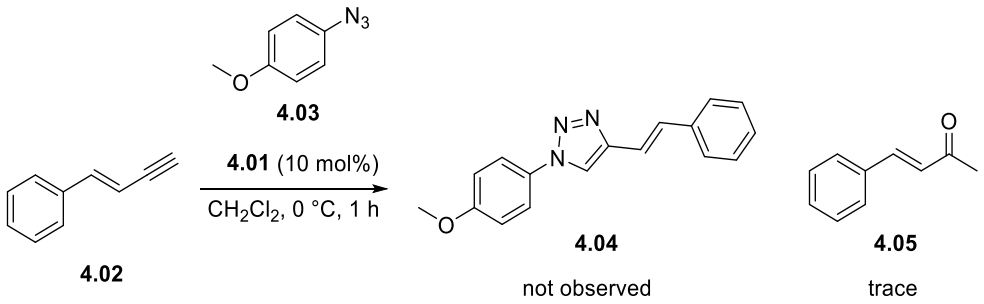


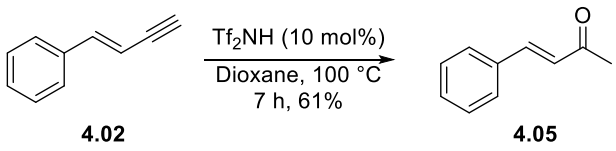
***Figure 4.1**: Tris-(p-bromophenyl)aminium hexachloroantimonate **4.01**.*

The reaction between aryl azide **4.03** and enyne **4.02** was investigated, adapting conditions from Bauld and co-workers initial reports (Scheme 4.2).[180] The conjugated enyne **4.02** was used, in an attempt to facilitate single electron oxidation in order to promote the desired cycloaddition. The proposed reaction involved the oxidation of **4.02**, to generate a reactive radical cation intermediate which would undergo cycloaddition with azide **4.03** to produce triazole **4.04**.



***Scheme 4.2:** Attempted radical cation induced azide-alkyne cycloaddition.*

Although no target triazole **4.04** was detected in the model study, a trace amount of the enone **4.05** was isolated. The enone **4.05** is the formal hydration product of enyne **4.02**, a transformation that is normally achieved through the use of forcing conditions such as acid catalysis and high temperature, or with catalytic mercury salts (Scheme 4.3).[183,184]



Scheme 4.3: *Shirakawa's acid-catalysed hydration of enyne* ***4.02****.*[183]

Enones are useful functional groups that participate in a range of transformations. The development of a methodology to convert the relatively inert enynes into reactive enones was therefore appealing. It was therefore decided to investigate this new transformation in more detail.

INTRODUCTION

RADICAL CATIONS

Radical cations are highly reactive species, possessing both a positive charge and an unpaired electron.[185] Upon oxidation of an organic substrate, a singly occupied molecular orbital (SOMO) can be formed. This high energy molecular orbital opens up potential reaction pathways that would otherwise be inaccessible to the neutral species.

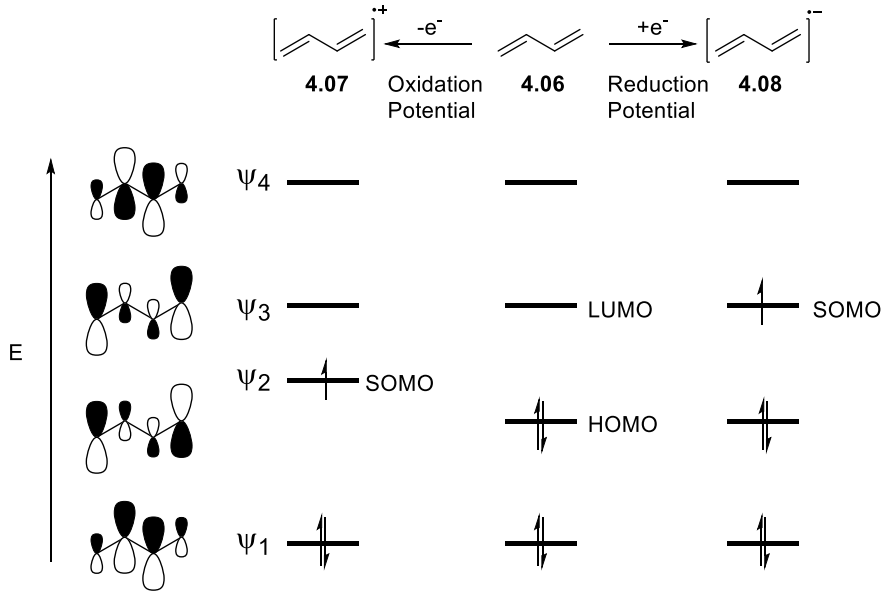


Figure 4.2: *Molecular orbital diagram of the radical ions of 1,3-butadiene.*

The nature of the radical cation moiety can be illustrated by studying the molecular orbitals of 1,3-butadiene (Figure 4.2). In the neutral molecule, the lowest two molecular orbitals are filled. Single electron oxidation to form the radical cation **4.07** removes an electron from the highest occupied molecular orbital (HOMO). The oxidation has a destabilising effect, resulting in a high energy SOMO. On the other hand, reduction of 1,3-butadiene forms

the radical anion **4.08**, with the lowest unoccupied molecular orbital (LUMO) of the neutral species populated by the additional electron.

Both radical cations and radical anions have substantially different molecular orbital energies than the corresponding neutral species, resulting in unusual umpolung reactivity.[186] For example, a single electron oxidation of a nucleophilic moiety renders it electrophilic, whilst reduction of an electrophile provides nucleophilic character.[186]

These species are of significant interest and a wide range of methodologies and applications have been developed to exploit this reactivity.[186]

Radical cations are predominantly formed through three major modes of activation:

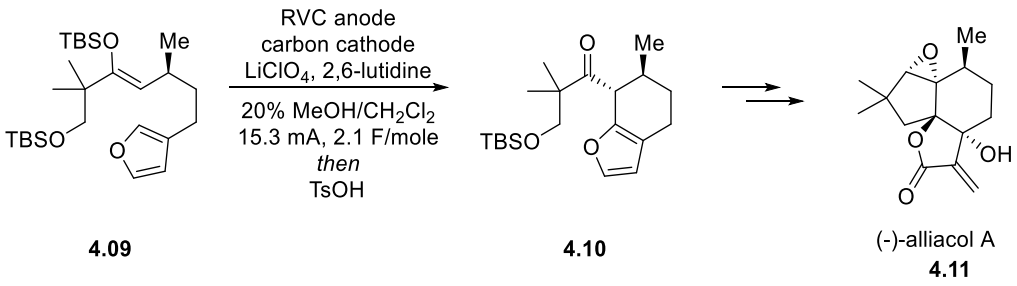
i) electrochemical oxidation
ii) photoinduced electron transfer (PET)
iii) chemical oxidation

To best demonstrate the generation of radical cations, a discussion of the applications of the species formed through these methods is warranted.

ELECTROCHEMICAL OXIDATION

Anodic oxidation involves the electrochemically induced abstraction of an electron to form radical cations. This is a particularly useful technique because electrochemistry allows selective oxidations of a wide range of functionality by modifying the electro-potential applied across the reaction.[187] This control is practically achieved through the application of a potentiostat, which allows the voltage applied across a system to be accurately tuned to the oxidation potential of the substrate.[188]

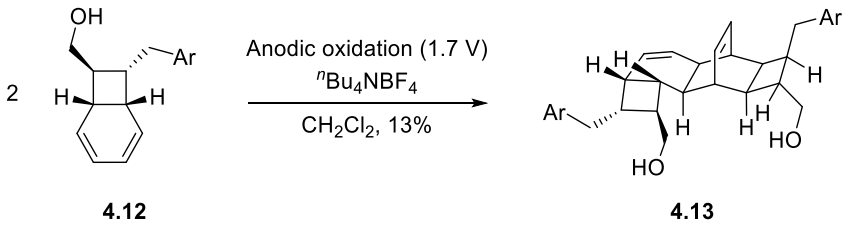
The high level of control under relatively mild conditions has been exploited in natural product synthesis on several occasions. Moeller *et al*. employed an elegant example of this technique for the formation of a substituted cyclohexane **4.10** during their synthesis of (–)-alliacol A (Scheme 4.4).[189] Oxidation of the silyl enol **4.09** generated an electrophilic radical cation, which induced ring closure through the nucleophilic attack of a pendant furan. Acidic workup gave the bicycle **4.10** and further modification post-cyclisation yielded the natural product **4.11**.



Scheme 4.4: *Moeller's anodic cyclisation of* ***4.09****.*[189]

Another example of the application of anodic oxidation in the field of natural product synthesis is the radical cation dimerisation *en route* to the formal synthesis of kingianin A, as described by Moses *et al*. (Scheme 4.5).[188]

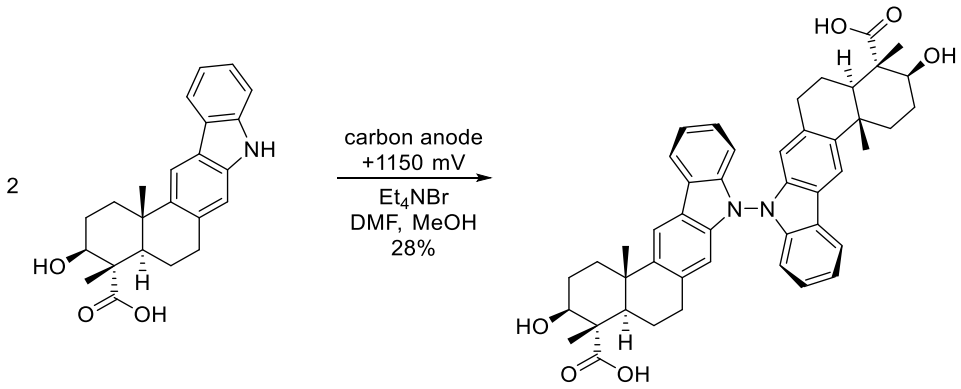
Oxidation of the diene moiety of monomer **4.12** resulted in the formation of a radical cation, which in turn underwent a Diels-Alder cycloaddition with another molecule of the monomer **4.12**, yielding the dimeric product **4.13**. In convergence with the work of Parker *et al*., the synthesis of **4.13** constituted the formal synthesis of the natural product.[190]



4.12 **4.13**

Scheme 4.5: *Moses' electrochemical Diels-Alder cycloaddition in the formal synthesis of kingianin A.*[188]

Baran *et al*. employed electrochemistry to perform a late stage *N-N* dimerisation in the synthesis of dixiamycin B (**4.15**) (Scheme 4.6).[191] This convergent approach employed a unique *N-N* dimerisation with molecules containing the rare *N-N* bond more traditionally synthesised from a hydrazine core.[192]



4.14 **4.15**

Scheme 4.6: *Baran's electrochemical N-N dimerisation in the synthesis of dixiamycin* ***4.15****.*[191]

PHOTOINDUCED ELECTRON TRANSFER

Photoinduced electron transfer (PET) involves the promotion of a photochemical sensitizer into its excited state, which is subsequent quenched by the desired substrate. Dependant on the nature of the substrate, this results in the formation of either a radical cation or a radical anion, and allows a variety of chemical transformations to be accessed.

This concept is illustrated in Figure 4.3, the irradiation of **4.16** results in the excitation of an electron to a higher energy level. The excited state **4.17** then acts as an electron acceptor, removing an electron from substrate **4.18** to form the radical anion of the photosensitizer along with radical cation **4.20**.

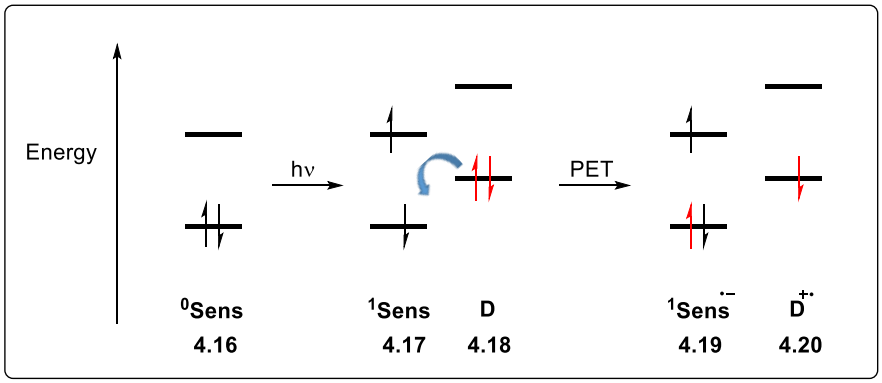
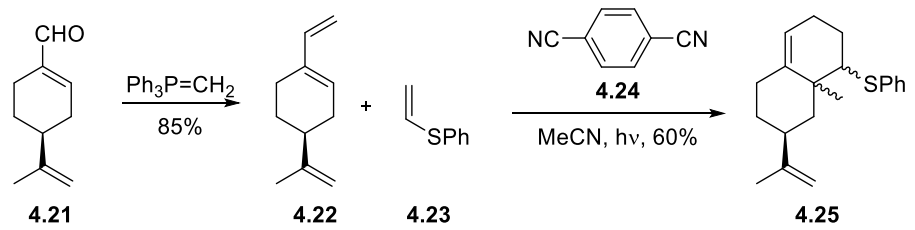


***Figure 4.3**: Photo-induced formation of a radical cation.*

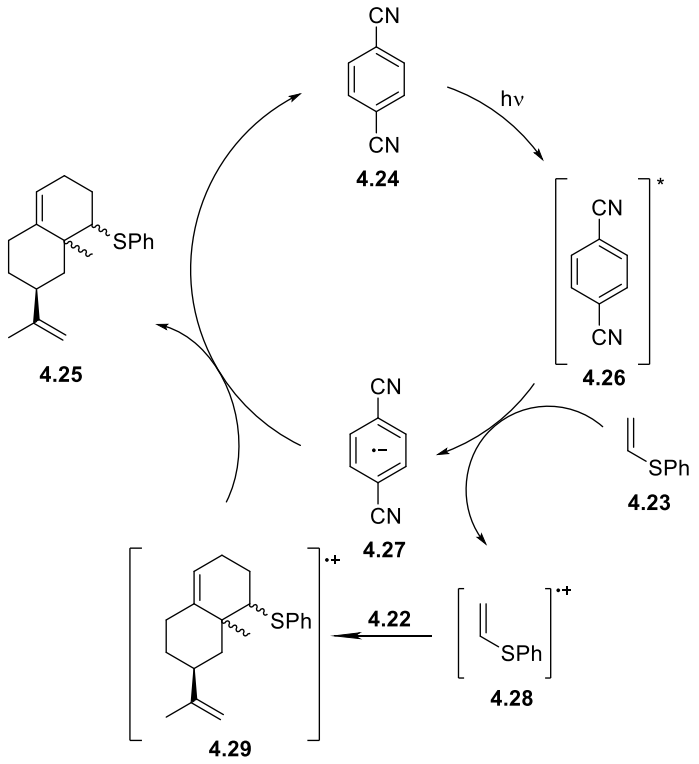
An early example where this methodology was used was in the formal synthesis of (−)-*β*-selinene by Bauld *et al*. (Scheme 4.7).[181] The key transformation in the synthesis was the radical cation Diels-Alder reaction between diene **4.22**, prepared from (−)-perillaldehyde **4.21**, and phenyl vinyl sulfide **4.23**. Catalytic quantities of 1,4-dicyanobenzene **4.24**, in the

presence of UV light, gave product **4.25** as a mixture of diastereoisomers in good yield.



Scheme 4.7: *Bauld's synthesis of* ***4.25*** *by a radical cation Diels-Alder reaction.*[181]

The irradiation of 1,4-dicyanobenzene **4.24** promotes the formation of an electronically excited state (Scheme 4.8). The excited state is a strong electron acceptor, which is quenched through a single-electron oxidation of vinyl sulfide **4.23**. A radical cation of the vinyl sulfide is formed, which gives rise to a high energy SOMO. The enhanced overlap between the LUMO of the diene **4.22** and the SOMO of the vinyl sulfide radical cation **4.28** promotes the Diels-Alder reaction to form **4.29**. Subsequent single electron reduction of **4.29** regenerates the photocatalyst **4.24** and liberates the product **4.25**.

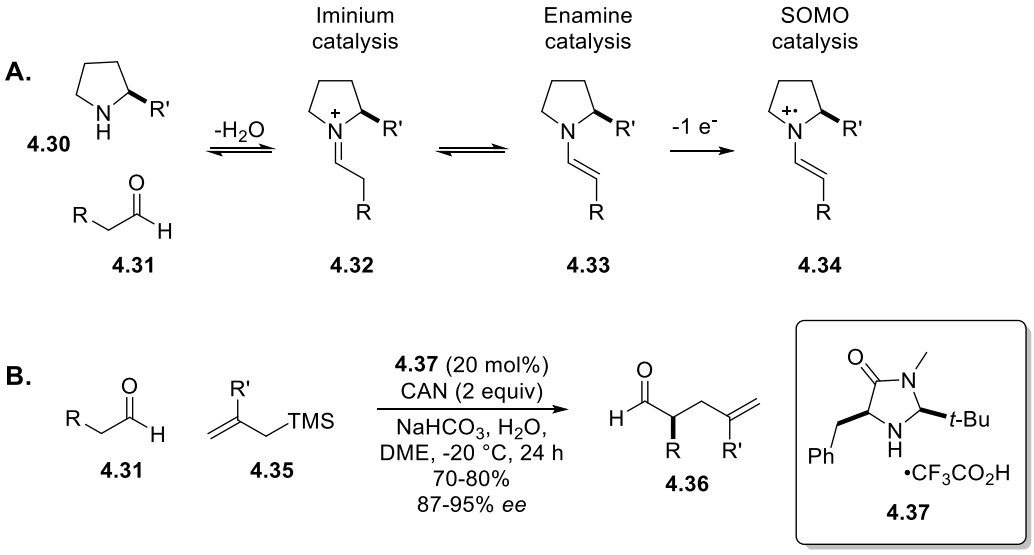


Scheme 4.8: *Bauld's photochemically catalysed Diels-Alder reaction.*[181]

CHEMICAL OXIDATION

Chemical oxidants are also important reagents for the generation of radical cation species. For example, MacMillan *et al.* used stoichiometric amounts of cerium ammonium nitrate (CAN) as a single electron oxidant in their research on SOMO activation.[193,194]

The condensation of an aldehyde **4.31** with an amine catalyst **4.30** forms the intermediate iminium ion **4.32**, which rapidly interconverts with an enamine species **4.33**. Macmillan *et al*. proposed that this equilibrium could be interrupted by a single electron oxidation to access an amine-centred electrophilic radical cation, capable of SOMO catalysis (Scheme 4.9 A).[194] The effectiveness of SOMO catalysis was demonstrated through the enantioselective α-allylation of aldehydes with allyl silanes **4.35** (Scheme 4.9 B).[194]



Scheme 4.9: *A. SOMO catalysis proposal; B. Macmillan's enantioselective α-allylation of aldehydes.*[194]

Radical cation salts are perhaps the most common reagents for the generation of radical cations, with these species often based on substituted

triarylamine cores.[186] The stability of these species can be explained through the delocalisation of the radical cation through the three aromatic rings (Figure 4.4).

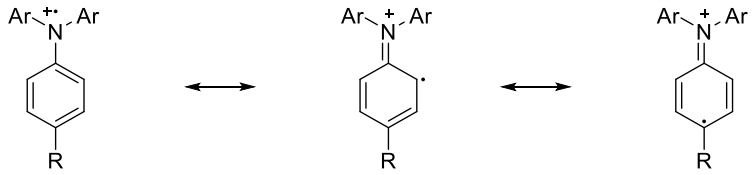
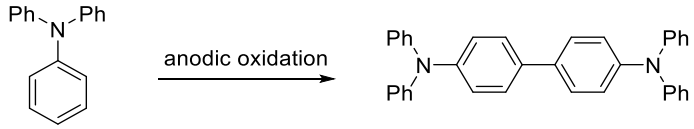


Figure 4.4*: Resonance stabilisation of triarylamine radical cations.*

A requirement for the formation of stable radical cation salts of triarylamines is the presence of *para*-substituents. In the absence of these substituents, single electron oxidation of triphenylamine **4.38** results in dimerisation to *N*,*N*,*N′*,*N′*-tetraphenylbenzidene **4.39**, with the loss of two protons (Scheme 4.10).[195]



4.38 **4.39**

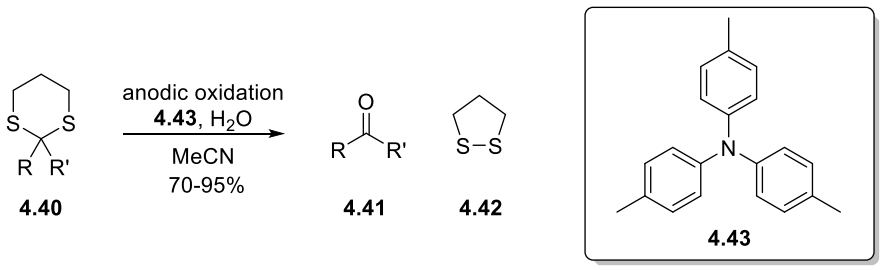
Scheme 4.10*: Oxidative anodic dimerisation of triphenylamine* ***4.38****.*

Through substitution of the triarylamine, particularly in the *para* position, the oxidation potential can be modified. The electrochemical behaviour of various triarylamines has been extensively studied, with both experimental and theoretical reports of their oxidation potentials.[195–198] A key consequence of these studies is that with careful selection of radical cation salt, it is possible to selectively oxidise substrates in a range of reactions.

APPLICATIONS OF TRIARYLAMINE RADICAL CATIONS

Triarylamine radical cations have been used extensively to effect a range of transformations.[181,196] The radical cation species can either be generated *in situ* through anodic oxidation, or used as pre-formed perchlorate or hexachloroantimonate salts.

Steckhan and co-workers employed tris-(*p*-tolyl)amine **4.43** for the deprotection of 1,3-dithianes to yield the parent ketone (Scheme 4.11).[199] The protecting group cleavage was equally effective whether the radical cation was generated electrochemically or the corresponding hexachloroantimonate salt was used.[199]

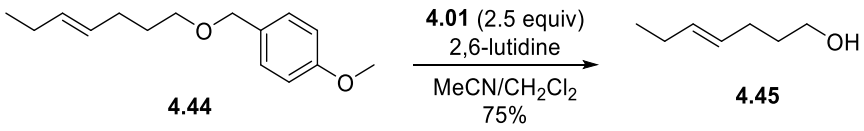


Scheme 4.11: *Steckhan's radical cation initiated cleavage of 1,3-dithiane protecting groups.*[199]

The authors noted that use of the more powerful oxidant, tris-(*p*-bromophenyl)aminium hexachloroantimonate (TBPA, **4.01**), accelerated the reaction. Additionally, compound **4.01** was shown to deprotect 1,3-dithiolanes, a species that was resistant to oxidation by tris-(*p*-tolyl)amine **4.43**, thereby highlighting the tuneable nature of radical cation salts.

Steckhan also reported that **4.01** mediated the selective cleavage of *p*-methoxybenzyl ethers (PMB) and benzyl ester protecting groups in a mild and selective manner.[200,201] A pertinent example that demonstrates the

chemoselectivity of the methodology is the deprotection of the PMB ether of *E*-4-hepten-1-ol (**4.44**). Both hydrogenation and sodium dissolved in ammonia are commonly used for PMB deprotections, however, under these conditions, the alkene is also susceptible to reduction. Deprotection with 2.5 equivalents of **4.01** effected the deprotection whilst leaving the double bond intact (Scheme 4.12).[200]



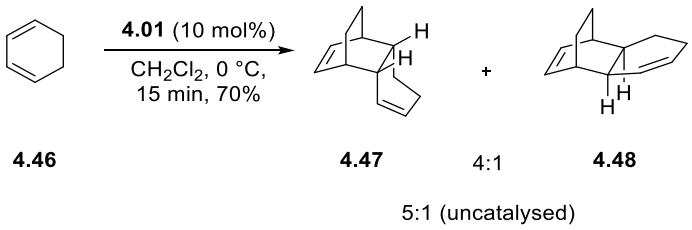
Scheme 4.12: *The selective radical cation initiated deprotection of PMB-ethers.*[200]

In the case of benzyl ester deprotection, it was demonstrated that **4.01** could selectively cleave both 4-methoxybenzyl and 2,4-dimethoxybenzyl esters in the presence of acid-labile Boc and *tert*-butyl esters.[201] Highlighting the tuneable nature of this chemistry, the stronger oxidant, tris-(2,4-dibromophenyl)aminium hexachloroantimonate, was required to cleave unsubstituted benzyl esters.

Radical cation salts have also been used as sub-stoichiometric reaction initiators. The classic example is the dimerisation of 1,3-cyclohexadiene **4.46**. This formal Diels-Alder reaction has a high barrier to activation due to the poor overlap of 1,3-cyclohexadiene's **4.46** HOMO and LUMO. Under thermal conditions, the dimerisation is low yielding, with only 30% product isolated even after heating at 200 °C for 20 hours.

The addition of a radical cation salt has a profound effect on the rate of the reaction. Treatment of 1,3-cyclohexadiene **4.46** with 10 mol% of TBPA (**4.01**) gave the cycloadduct products **4.47** and **4.48** in 70% yield after just

15 minutes at 0 °C (Scheme 4.13).[180] The phenomenal rate enhancement can be explained by the single electron oxidation of **4.46** resulting in a destabilised, higher energy SOMO. This molecular orbital has significantly improved overlap with the LUMO of another molecule of **4.46**, reducing the activation barrier and allowing good conversion into the Diels-Alder cycloadduct products.



Scheme 4.13: *Radical cation initiated dimerisation of 1,3-cyclohexadiene* ***4.46****.*[180]

The reactions developed by Bauld and Steckhan highlight the utility of radical cation salts in organic synthesis, however, these reagents do suffer some drawbacks. TBPA **4.01** is only a moderately stable salt, and decomposes slowly over time. It has been reported that the major mode of decomposition is through reaction with water to form the corresponding neutral triarylamine.[202]

ALKYNE HYDRATION

The formation of carbon-oxygen bonds is a fundamentally important transformation in organic chemistry, with the hydration of unsaturated compounds conceptually the most straightforward. In particular, the acid-catalysed hydration of alkynes to install the carbonyl moiety has been extensively studied. First reported in the 1800's, the hydration of terminal alkynes can result in two isomeric products.[203,204]

Markovnikov addition of water results in the formation of a methyl ketone, whereas anti-Markovnikov addition generates an aldehyde. If the substrate is an internal alkyne, the formation of two regioisomeric ketones is possible (Figure 4.5).

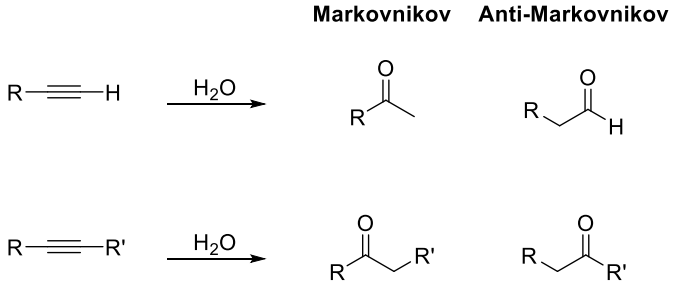


***Figure 4.5**: Regiomeric products of alkyne hydration.*

The conversion of the relatively inert alkyne to the reactive ketone moiety is a useful transformation, allowing functionality to be carried through multistep syntheses without unwanted reactivity.

The hydration reaction of alkynes is atom-economic and strongly exergonic, with the conversion of acetylene to acetaldehyde having ΔG = -105.8 $kJmol^{-1}$.[184] Although the reaction is thermodynamically favourable, alkynes

are kinetically stable to hydration, with the half-life of alkyl alkynes in acetone estimated to be in excess of 20000 years at 70°C.[205]

For the reaction to overcome this high activation barrier, a catalyst is required. In 1881, Kucherov reported that mercury(II) salts were efficient catalysts for alkyne hydration.[206] The mechanism is thought to proceed through the formation of a π-complex between the cationic mercury and nucleophilic alkyne substrate (Figure 4.6). Nucleophilic attack of water at the more highly substituted position of the activated alkyne **4.50**, produces a *β*-hydroxyethynylmercury species **4.51**. Hydrodemercuration regenerates the mercury(II) catalyst and produces enol **4.53**, which then tautomerises to give the Markovnikov ketone **4.54**.

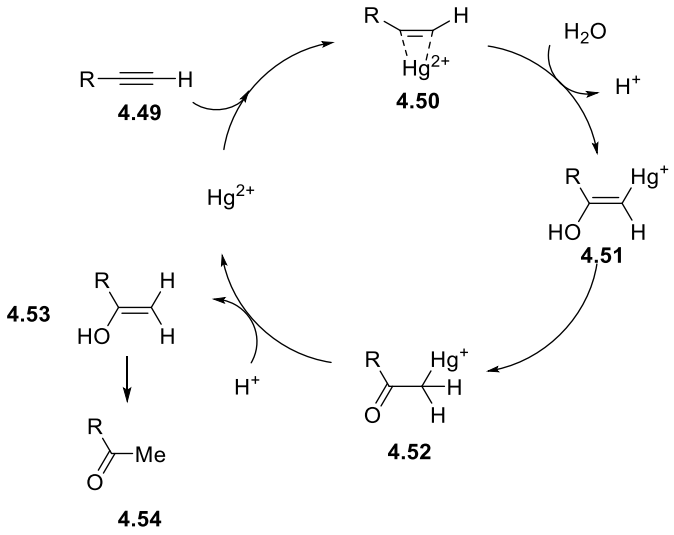


Figure 4.6: *Mechanism of the mercury mediated Kucherov reaction.[184]*

Since Kucherov's initial report, the alkyne hydration reaction has been developed with a number of counterions, additives and solvents.[184] Mercury(II) sulfate in acidic solution in the most common used catalyst, and

this reaction is very robust, but the use of toxic mercury salts poses a safety hazard, which has led to the development of alternative methods.

For example, heating terminal alkynes in water results in the formation of the Markovnikov products, although this transformation often requires very high temperatures. Kappe *et al*. demonstrated the conversion of phenylacetylene to acetophenone with near-critical water at 295 °C with microwave irradiation.[207] Similarly, Vasudevan *et al*. have shown that electron rich aromatic alkynes could be hydrated when heated to 200 °C under microwave conditions, which most likely arises as a result of the improved nucleophilicity of these compounds.[208] Hintermann and Labonne proposed that H_3O^+ can perform as a catalyst in these reactions; the concentration of which is increased at a higher temperature.[184]

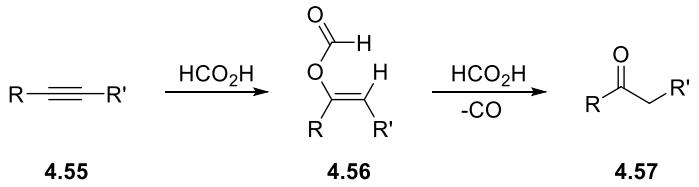
A range of acids have since been demonstrated as useful alkyne hydration catalysts. Strauss *et al*. demonstrated that hydration of phenylacetylene can be promoted by 0.5 M H_2SO_4 under microwave heating (Table 4.1, entry 1).[209] Aqueous trifluoroacetic acid was also reported to be an effective catalyst by Waldmann *et al*. (Table 4.1, entry 2).[210]

The selection of solvent is important for the alkyne hydration reaction with catalytic triflic acid. In 2000, Kawakami reported that 10 mol% of triflic acid hydrated various alkynes at 100 °C in dioxane, and this was followed by a report in 2016 which employed trifluoroethanol as solvent at room temperature (Table 4.1, entries 3 and 4).[183,211]

Entry	***Catalyst/Reagent***	***Conditions***
1[209]	H_2SO_4	H_2O, 280 °C, 1 h
2[210]	CF_3CO_2H (>100 mol%)	H_2O, r.t. to 60 °C
3[183]	TfOH (10 mol%)	dioxane, H_2O, 100 °C, 48 h
4[211]	TfOH (20 mol%)	H_2O, CF_3CH_2OH, 25 °C
5[212]	HCO_2H (100 mol%)	100 °C, 0.5 – 10 h

Table 4.1: *Selection of Brønsted acid catalysts for alkyne hydration.*

A particularly interesting example is the use of formic acid, reported by Shvo, which catalyses its own addition to the alkyne, giving the Markovnikov ketone **4.57** upon subsequent decarbonylation (Table 4.1, entry 5 and Scheme 4.14).[212]

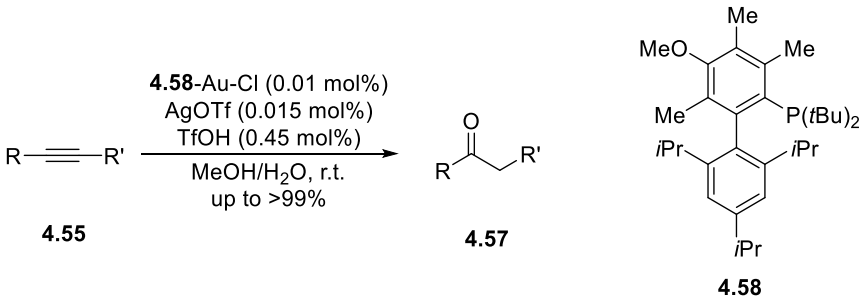


4.55 **4.56** **4.57**

Scheme 4.14: *Shvo's protocol for the formic acid catalysed hydration of alkynes.*[212]

A range of transition metal species have also been used as hydration catalysts, with most established catalysts based on copper, silver and particularly gold complexes.[184] An early report by Thomas and co-workers in 1976 described the hydration of alkynes by $HAuCl_4$.[213] In a more recent publication, Hayashi and Tanaka developed an Au^I-acid reagent combination for alkyne hydration which displayed impressively high catalytic efficiency with a turnover frequency of 14000 h^{-1} reported with 0.005 mol% catalyst loading.[214]

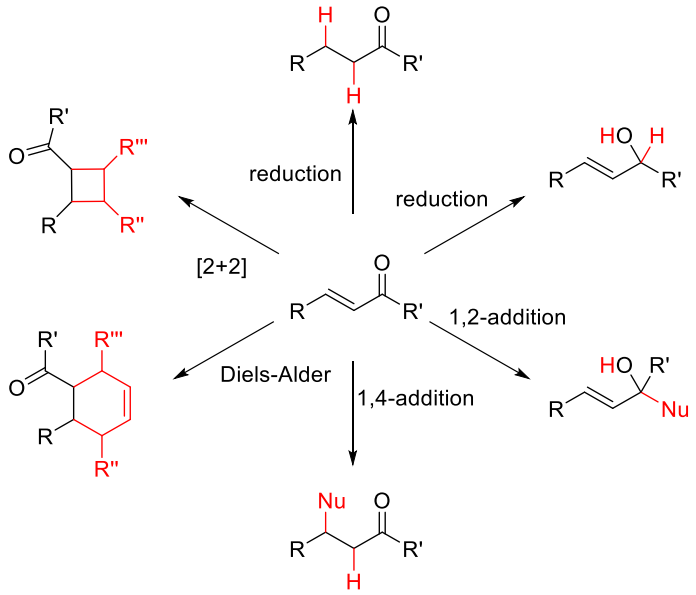
A recent report by Xu and Hammond explored the effects of ligands in the gold catalysed hydration of alkynes.[215] Modification of the phosphine ligand's electronic properties only had a minor effect on the kinetics on the hydration reaction, whereas the steric properties of the ligands studied were crucial. Subsequently, the sterically demanding ligand **4.58** enabled the hydration of a range of alkynes to be performed under mild conditions at room temperature, when used in combination with an acid co-catalyst (Scheme 4.15).



***Scheme 4.15**: Xu and Hammond's protocol for the hydration of alkynes under gold and acid co-catalysis.*

HYDRATION OF ENYNES

The hydration of enynes is particularly attractive, since the enone products can undergo a wide range of reactions including, but not limited to those illustrated in Scheme 4.16.

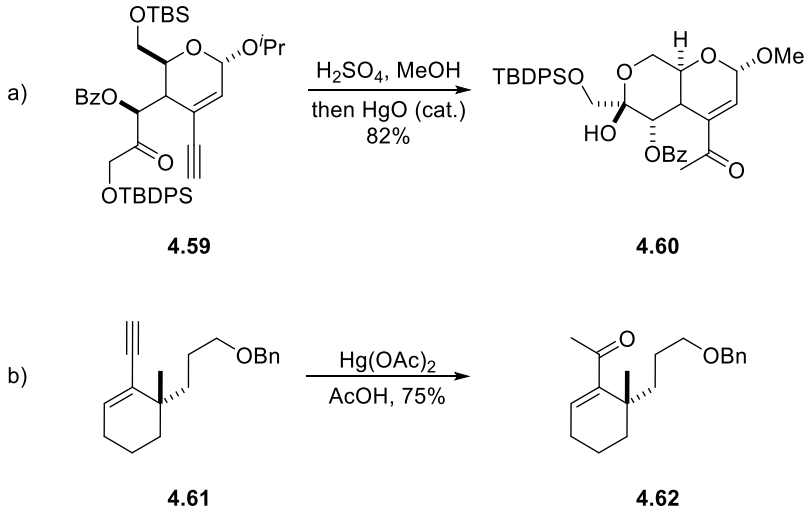


***Scheme 4.16**: Synthetic utility of the enone moiety.*

Given the potential of this transformation, it is perhaps surprising that examples of enyne hydration are relatively sparse in the literature. Typically, mercury salts are used to effect the desired transformation.[184]

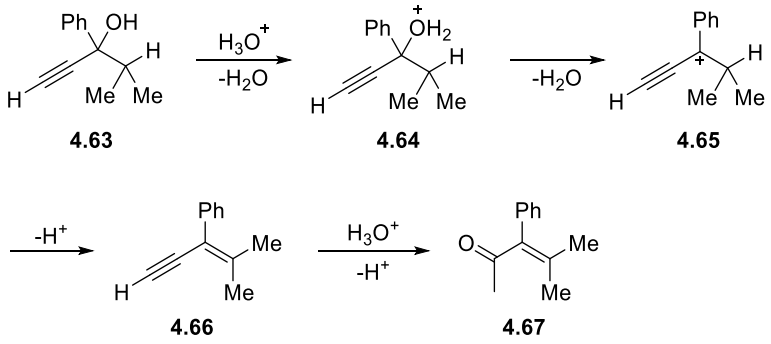
Enyne hydration of complex substrates has successfully been employed in natural product total synthesis. Pertinent examples appear in the syntheses of tetrodotoxine and dysidiolide (Scheme 4.17).[216,217] Isobe *et al*. utilised mercuric oxide in a tandem deprotection-cyclisation-hydration sequence to convert silyl ether **4.59** into enone **4.60** as part of their synthesis of

tetrodotoxine, whilst mercury acetate was employed by Jung to generate enone **4.62**, an intermediate *en route* to dysidiolide.



Scheme 4.17: *Enyne hydration of intermediates in the total synthesis of a) tetrodotoxine and b) dysidiolide.*[216,217]

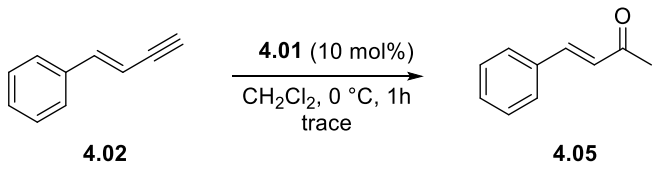
This reaction, in principle, can be mediated by acid catalysis. The Rupe rearrangement converts propargylic tertiary alcohols to *α*,*β*-unsaturated ketones through an enyne intermediate (Scheme 4.18).[218] The mechanism involves protonation of the alcohol **4.63**, followed by E_1 elimination resulting in the formation of enyne **4.66**, which is subsequently hydrated to the corresponding enone **4.67**.



Scheme 4.18: *Mechanism of the acid-catalysed Rupe rearrangement.*[218]

RESULTS AND DISCUSSION

As described earlier, an attempted radical cation induced click reaction led to the serendipitous discovery that radical cation **4.01** initiated the hydration of enyne **4.02**. To confirm the conversion of the enyne **4.02** into enone **4.05**, the hydration reaction was repeated in the absence of the aromatic azide, with the enone **4.05** again produced in trace quantities (Scheme 4.19). It was reasoned that the majority of the enyne **4.02** had been converted to polymeric byproducts, generated through the chain reaction of an activated enyne with a molecule of unactivated starting material.

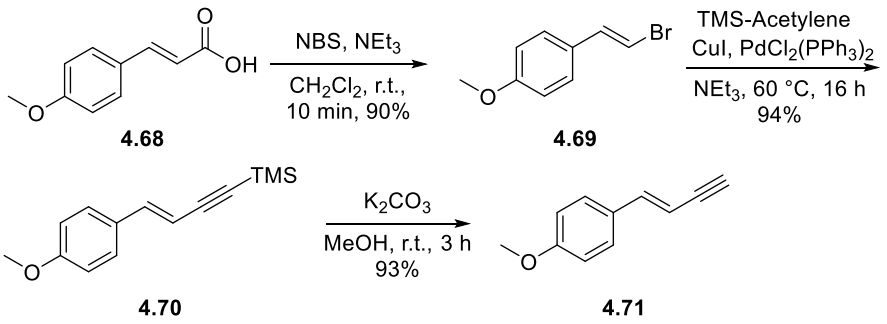


***Scheme 4.19**: Preliminary reaction of enyne hydration.*

The initial synthetic efforts were directed towards increasing the formation of the target enone product **4.05** and minimising side reactions. The (*E*)-1-(but-1-en-3-yn-1-yl)-4-methoxybenzene (**4.71**) was selected as the model substrate for this study, with the electron-rich methoxy moiety proposed to facilitate the required oxidation.

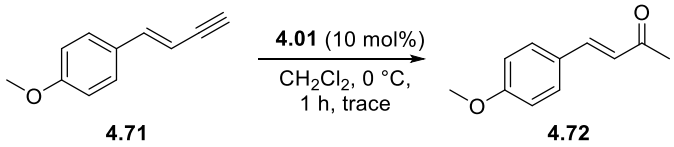
The synthesis of enyne **4.71** began with the commercially available 4-methoxycinnamic acid **4.68**. A Hunsdiecker reaction using *N*-bromosuccinimide and catalytic triethylamine generated the required bromostyrene **4.69** in excellent yield.[219] A palladium-catalysed Sonogashira coupling with trimethylsilyl acetylene, followed by TMS deprotection under

basic conditions yielded the required terminal enyne **4.71** (Scheme 4.20). This route proved to be both high yielding and scalable.



***Scheme 4.20**: Synthetic route to model enyne substrate **4.71**.*

To confirm the reactivity of the electron rich enyne **4.71,** a test reaction was performed. Pleasingly, the enone **4.72** was identified in the ^{1}H NMR spectra of the crude product, albeit with significant amounts of polymeric side products (Scheme 4.21).



***Scheme 4.21:** Hydration of electron rich enyne **4.71** with catalytic quantities of radical cation salt **4.01**.*

Optimisation of the reaction conditions began by varying the amount of the radical cation initiator **4.01** (Table 4.2). Minimal consumption of the enyne was observed at 1 and 2 mol % loading of the radical cation salt (Table 4.2, entries 1 and 2). Increasing the concentration to 5 and 10% resulted in complete consumption of the enyne **4.71**, with traces of the target enone

4.72 and an unidentified aldehyde detected alongside the polymeric by-products (Table 4.2, entries 3 and 4).

Entry	***4.01 (mol %)***	***4.71 (mM)***	***Water eq.***	***Conversion[a]***
1	1	200	-	Trace
2	2	200	-	Trace
3	5	200	-	Trace[b]
4	10	200	-	Trace[b]
5	10	400	-	Trace[b]
6	10	100	-	Trace[b]
7	10	75	-	Trace[b]
8	10	50	-	Trace[b]
9	10	200	10	Trace[b]
10	5	200	20	-

[a] Reaction run for 1h and concentrated. Conversion determined by ^{1}H NMR.[b] Full consumption of starting material noted.

Table 4.2: *Effects of initiator loading on enyne hydration reaction.*

Next, the concentration of the enyne with respect to initiator **4.01** was varied, with lower concentrations expected to restrict polymer formation. In each reaction performed, full consumption of the enyne **4.71** was observed, however, altering the concentration only had a minor effect on reaction outcome (Table 4.2, entries 4 to 8).

The amount of water present in the reaction mixture was also studied. Full consumption of starting material was observed with up to 10 equivalents of water, however, only trace amounts of enone **4.72** were detected. Higher loadings resulted only in recovery of starting material (Table 4.2, entry 10), presumably due to deactivation of the radical cation salt **4.01**.[220]

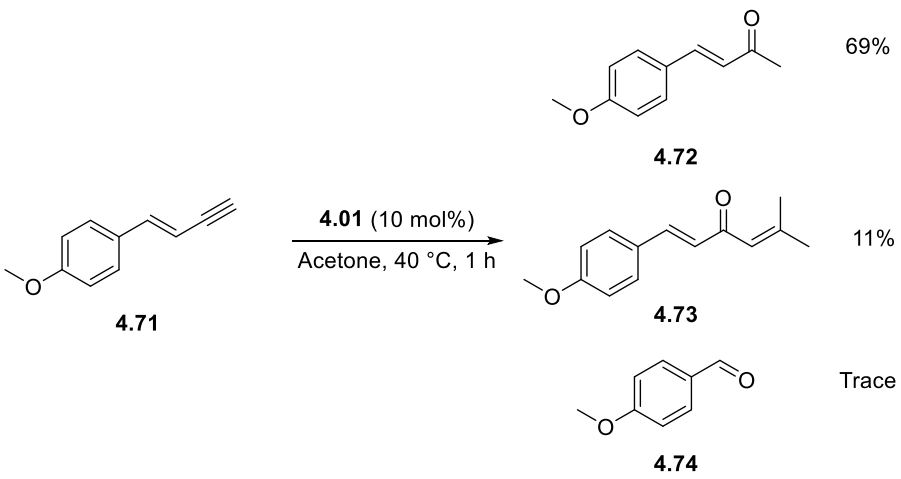
A solvent screen was also performed; a simple stability test for radical cation salt **4.01** is the persistence of its characteristic blue colour in solution, and therefore the initial solvent screen just involved **4.01** and the solvent (Table 4.3).

Entry	***Solvent***	***Observation***
1	CH_2Cl_2	Persistent colour
2	MeCN	Persistent colour
3	THF	Instant decolourisation
4	THF/CH_2Cl_2	Instant decolourisation
5	DMSO	Decolourisation over 2 minutes
6	Dioxane	Instant decolourisation
7	DMF	Slow decolourisation over 5 minutes
8	Acetone	Persistent colour

***Table 4.3**: Solvent screen for stability of **4.01**.*

Of the solvents surveyed, the intense blue colour of the radical cation salt **4.01** only persisted in dichloromethane, acetonitrile and acetone (Table 4.3, entries 1,2 and 8). The use of acetonitrile is well established in radical cation chemistry,[201] however no enone **4.72** was detected when acetonitrile was trialled as solvent.

Acetone was next selected as solvent (Table 4.3, entry 8 and Scheme 4.22), with the enone **4.72** formed as the major product at 40 °C, with no polymeric side products detected. Two products were isolated upon purification: the enone **4.72** in 69% yield, and the corresponding aldol condensation product **4.73**. Analysis of the ^{1}H NMR spectra of the crude product revealed the presence of a trace amount of anisaldehyde **4.74**, however, even after purification, this could not be isolated. It seems likely, given the presence of **4.73**, that anisaldehyde **4.74** was formed from a retro-aldol reaction of enone **4.72**.



***Scheme 4.22**: Radical cation initiated hydration of **4.71** in acetone.*

MECHANISTIC STUDIES

In order to elucidate mechanistic information of the hydration of enynes, and in particular the nature of any observable intermediates, the progression of the reaction in deuterated acetone was monitored by ^{1}H NMR. Analysis of the ^{1}H NMR spectra showed that the reaction was near completion after 10 min. A further ^{1}H NMR spectra recorded after 45 min confirmed full consumption of the starting material **4.71** (Figure 4.7).

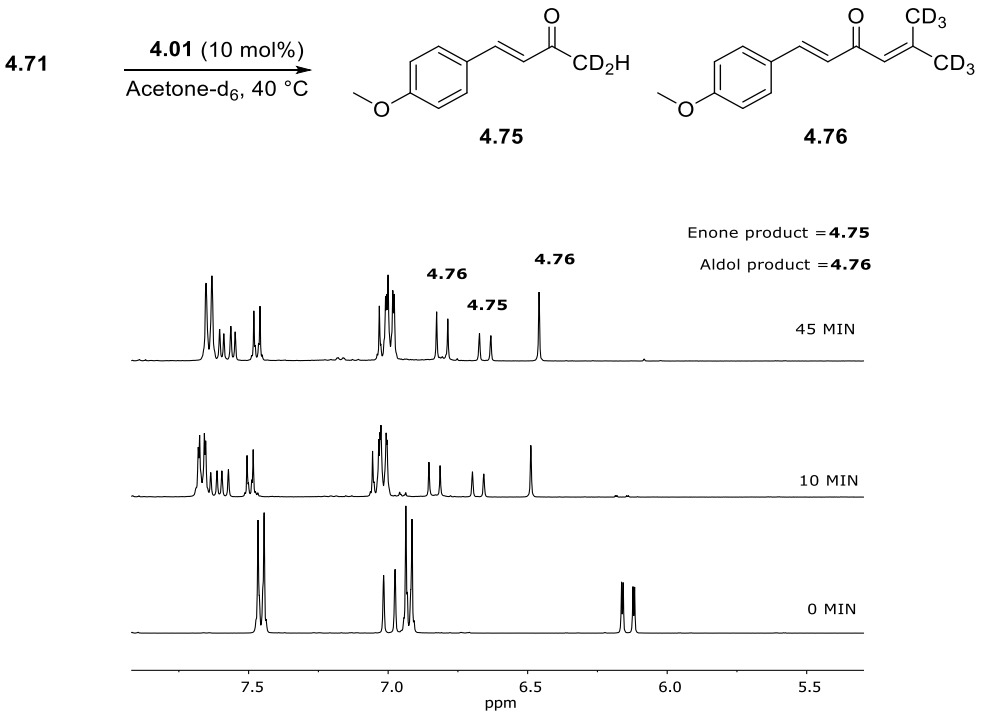
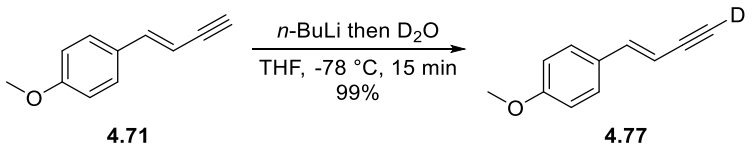


Figure 4.7: *^{1}H NMR spectra studying of hydration of **4.71** in deuterated solvent.*

Interestingly, when compared to the previous experiment (Scheme 4.22), significantly larger quantities of the aldol product **4.76** were observed. The shift in product distribution suggested that deuteration of the solvent altered the rate of the final step of the hydration mechanism: protonation/deuteration to form the enone **4.75**, or nucleophilic attack of acetone to yield dienone **4.76**.

To investigate the hydration of enynes further, the reaction was performed with the deuterated enyne **4.77,** in both standard and deuterated acetone. The deuterated compound **4.77** was prepared through the deprotonation of **4.71** and subsequent quench of the lithiated species with D_2O (Scheme 4.23).



4.71 **4.77**

***Scheme 4.23**: Deuteration of enyne **4.71**.*

The hydration reaction of enynes **4.71** and **4.77** gave similar results in acetone (Table 4.4, entries 1 and 3), however as observed previously, the use of deuterated solvent increased the proportion of the aldol product generated (Table 4.4, entries 2 and 4).

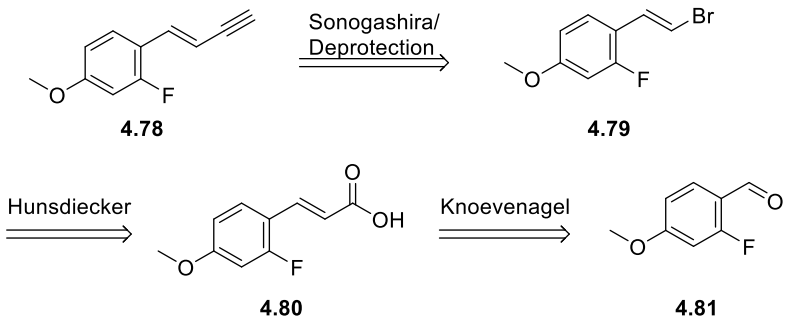
Entry	***Enyne***	***Solvent***	***Enone (%)[a]***	***Aldol (%)[a]***
1	**4.71**	Acetone	69	11
2	**4.71**	Acetone-d_6	19	18
3	**4.77**	Acetone	71	10
4	**4.77**	Acetone-d_6	37	26

[a]-Isolated yields. Conditions: 50°C, 1 h.

***Table 4.4**: Hydration study of enynes **4.71** and **4.77**.*

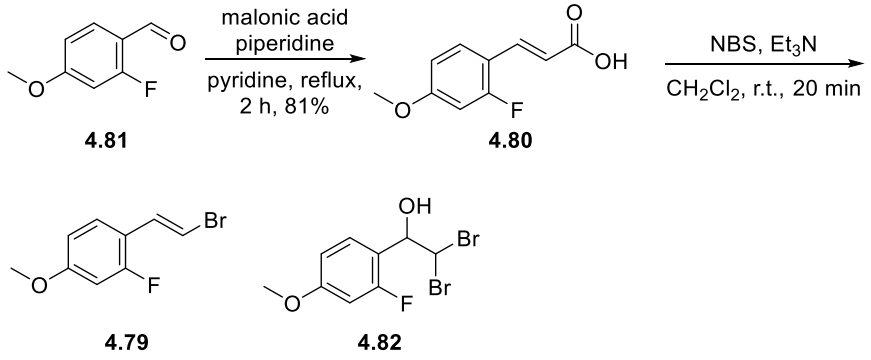
Incomplete consumption of enyne **4.77** was noted in deuterated acetone, in contrast to a previous observation (Figure 4.7), which resulted in a significantly lower isolated yield, however the shift in product distribution was suggested that the rate of protonation or deuteration compared to aldol condensation was solvent dependant (Table 4.4, entry 2).

As switching solvent appeared to alter the observed product distribution, an alternative strategy was pursued to follow reaction progress. It was envisioned that the fluorinated analogue **4.78** would allow the reaction to be monitored by ^{19}F NMR. The retrosynthetic analysis of **4.78** is depicted in Scheme 4.24.



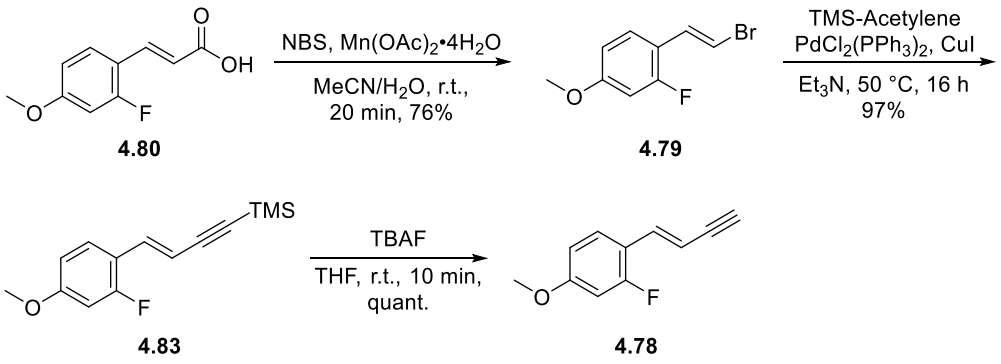
***Scheme 4.24**: Retrosynthetic analysis of fluorinated enyne **4.78**.*

Subjecting 2-fluoro-4-methoxybenzaldehyde (**4.81**) to Doebner's modification of the Knoevenagal reaction yielded the cinnamic acid **4.80**.[221] Upon applying fluorocinnamic acid **4.80** to Roy's modified Hunsdiecker conditions,[219] an unexpected mixture of the target bromostyrene **4.79** and the hydrobrominated product **4.82** was observed (Scheme 4.25).



***Scheme 4.25**: Initial attempt to synthesise bromostyrene **4.79**.*

It was proposed that **4.82** was formed preferentially over **4.79** due to the low solubility of **4.80** in dichloromethane. Therefore, the bromo-styrene **4.79** is initially formed slowly, and then further reacts with *N*-bromosuccinimide to the hydrobrominated **4.82**. To overcome this issue, an alternative methodology described by Roy *et al*. was subsequently adopted, with manganese(II) acetate as catalyst in a mixture of acetonitrile and water.[222] With careful control of reaction stoichiometry and short reaction times, **4.79** was isolated in a good 76% yield. A sequential Sonogashira coupling of **4.79** and TBAF mediated silyl deprotection proceeded in excellent yields to give the enyne **4.78** (Scheme 4.26).

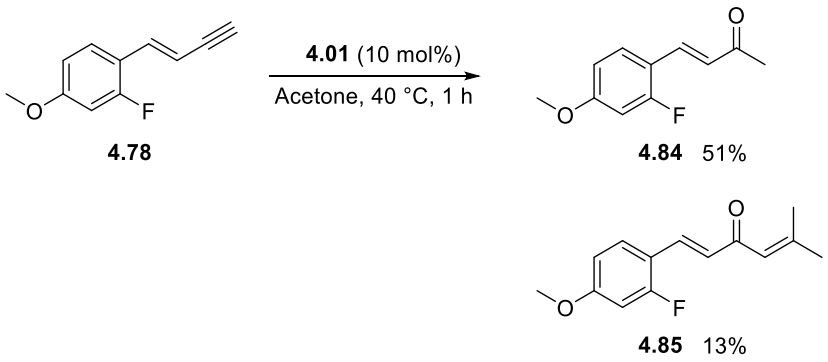


4.80 **4.79**

4.83 **4.78**

Scheme 4.26*: Completion of synthesis of fluorinated enyne* ***4.78****.*

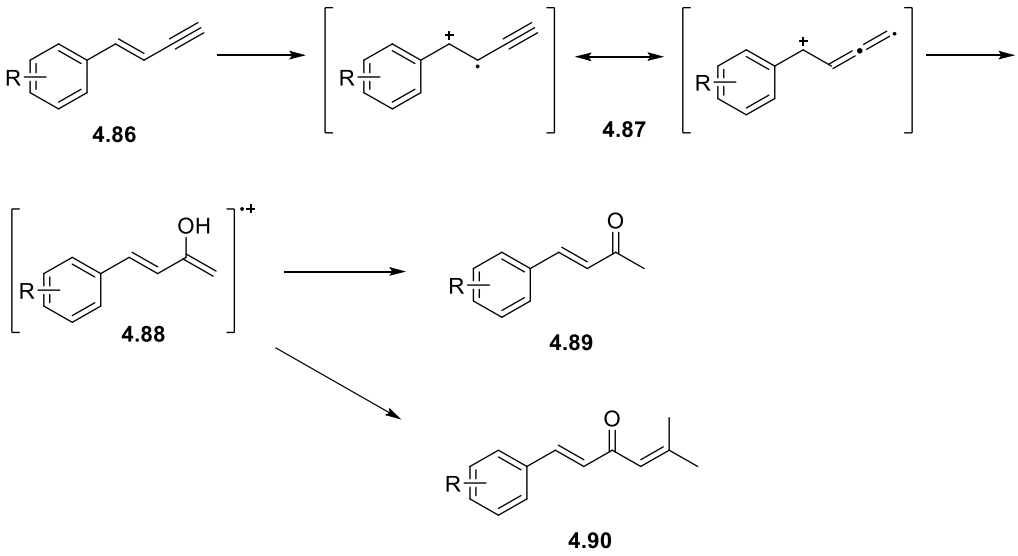
With completion of the synthesis of fluoroenyne **4.78,** the hydration reaction was next performed as normal, with sample aliquots removed at 5 minute intervals to allow the reaction to be monitored by ^{19}F NMR (Scheme 4.27).



Scheme 4.27: *Hydration of fluorinated enyne* ***4.78*** *to generate a mix of hydration* ***4.84*** *and aldol products* ***4.85****.*

Full consumption of the enyne **4.78** was observed by NMR after just 10 minutes at 40 °C, with the ^{1}H and ^{19}F NMR spectra confirming conversion into two new species. Upon work-up and isolation, the enone **4.84** and dienone **4.85** were identified as the products.

The information gleaned from the ^{1}H and ^{19}F NMR experiments allowed a tentative mechanistic proposal to be made (Scheme 4.28). Single electron oxidation of enyne **4.86** forms the radical cation **4.87**. This species is susceptible to nucleophilic attack by water, forming an intermediate enol **4.88**. It is envisioned that this enol can either tautomerise to enone **4.89**, or undergo an aldol condensation to form **4.90**. During this reaction sequence the radical cation of product **4.89** or **4.90** oxidises another molecule of enyne, forming a radical chain reaction.

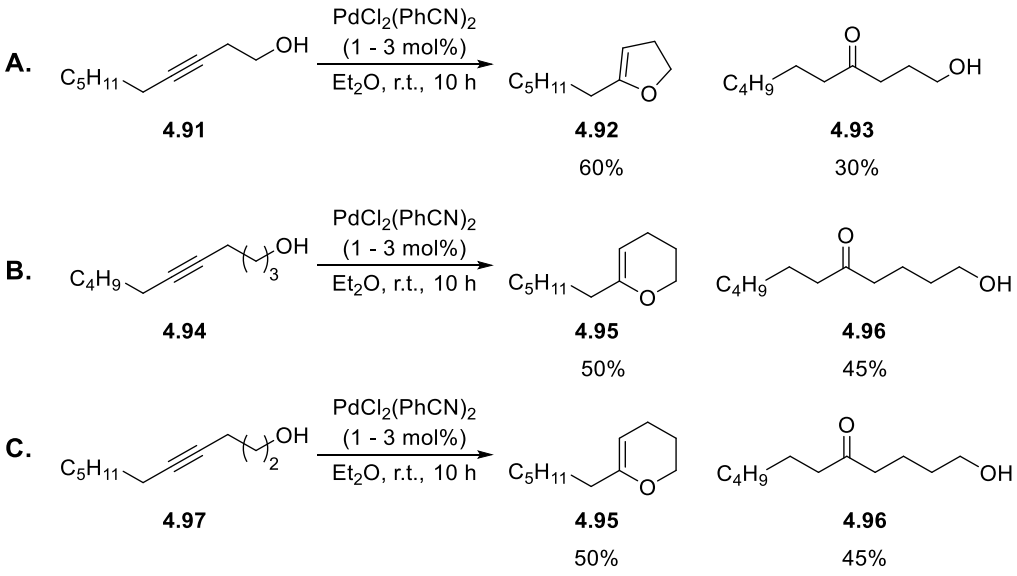


Scheme 4.28: *Mechanistic proposal for the radical cation initiated hydration of enynes.*

INVESTIGATION OF INTRAMOLECULAR CYCLISATION REACTIONS

The proposed mechanism suggested that alternative nucleophiles could be used in place of water, which would allow the synthesis of a diverse range of molecules.

In principle, an intramolecular cyclisation with a pendant nucleophile would proceed faster than intermolecular hydration or polymerisation. During a relevant study, Utimoto observed the a mixture of hydration and cyclisation products whilst studying the palladium mediated reactions of alkyn-1-ols **4.91**, **4.94** and **4.97** (Scheme 4.29).[223]



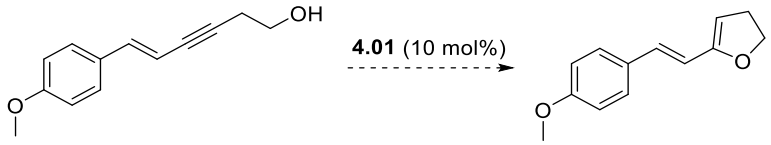
Scheme 4.29: *Utimoto's palladium catalysed synthesis of dihydrofurans and dihydropyrans.*[223]

Variation of the chain length resulted in different modes of cyclisation. Palladium mediated cyclisation of 3-decyn-1-ol (**4.91**) proceeded in a 5-*endo-dig* manner to furnish dihydropyran **4.92** (Scheme 4.29.A).[223] Both alkynols **4.94** and **4.97** gave a mixture of dihydropyran **4.95** and the

hydrolysed hydroxyketone **4.96**, however the cyclisation mechanism was different in each case, with 6-*exo*-*dig* (Scheme 4.29.B) and 6-*endo*-*dig* (Scheme 4.29.C) pathways followed respectively.

The products formed through these cyclisation pathways are of synthetic interest, with the oxygen containing heterocycles commonly found in natural product synthesis.[224] Therefore, the development of novel methodologies to form these valuable targets is an attractive prospect.

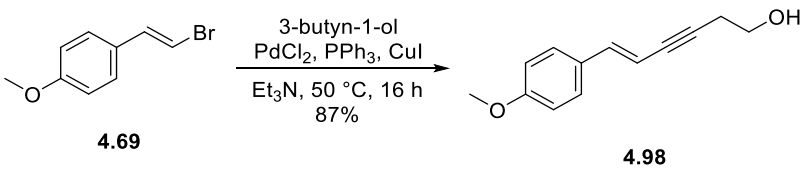
Encouraged by these reports, an analogous reaction utilising aromatic enynols in place of alkyl alkyn-1-ols was proposed (Scheme 4.30). The cyclisation of an internal enyne with a pendant alcohol would generate the activated diene **4.99**, however due to the highly reactive nature of this species, further reactions were expected.



4.98 **4.99**

Scheme 4.30: *Proposed radical cation initiated intramolecular cyclisation.*

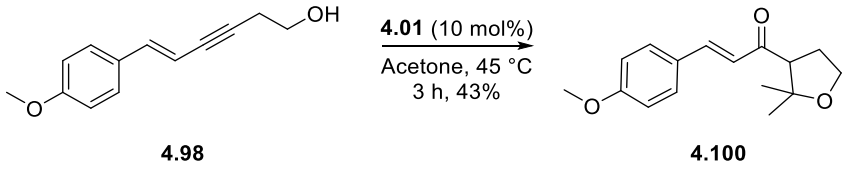
To investigate the proposed cyclisation, the enynol **4.98** was synthesised from the previously prepared bromo-styrene **4.69**, in a Sonogashira reaction with 3-butyn-1-ol, which proceeded in good overall yield (Scheme 4.31).



4.69 **4.98**

***Scheme 4.31**: Synthesis of proposed cyclisation precursor **4.98**.*

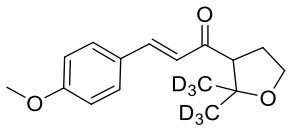
As water was no longer required for the proposed transformation, dichloromethane was selected as the initial solvent. However, only starting material was recovered, suggesting an increased stability of this species compared to the previously studied terminal enynes. The reaction was repeated in acetone at 45 °C, resulting in the isolation of a new product in 43% yield (Scheme 4.32). However, the proposed dihydrofuran **4.99** was not obtained, with the isolated product tentatively assigned as **4.100**, containing a 2,2-dimethyltetrahydrofuran-3-yl moiety.



4.98 **4.100**

***Scheme 4.32**: Intramolecular radical cation initiated reaction of **4.98**.*

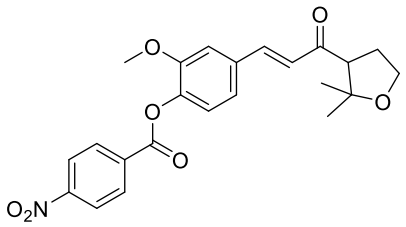
Analysis of the ^{1}H, ^{13}C and 2D NMR spectra revealed the presence of two inequivalent methyl peaks. Coupled with the mass of the molecular ion, this data implied the incorporation a molecule of acetone in the product, and this was confirmed by running the reaction in deuterated solvent. Analysis of the ^{1}H NMR spectrum showed the disappearance of the inequivalent methyl singlets and an increase in mass by HRMS suggested formation of the deuterated product **4.101** (Figure 4.8).



4.101

***Figure 4.8**: Proposed structure of deuterated cyclisation product **4.101**.*

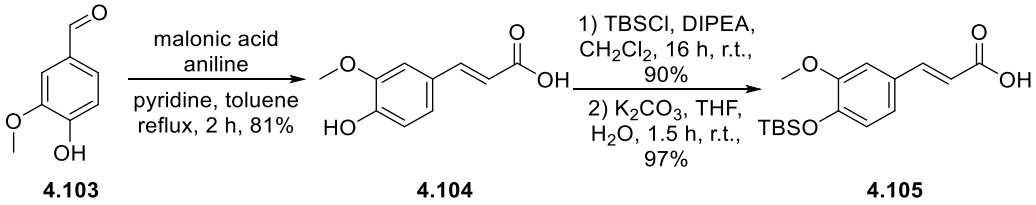
To corroborate the proposed structure, attempts were made to produce a crystalline derivative for X-ray analysis. The incorporation of nitro groups is often used to generate crystalline samples and as such, it was proposed that the enone **4.102** would allow structural confirmation. A vanillin core was selected, which provided both an electron-donating methoxy moiety to facilitate initial oxidation, as well as a phenolic handle to allow for functionalisation. Esterification with 4-nitrobenzoic acid would result in the formation of the target analogue **4.102** (Figure 4.9).



4.102

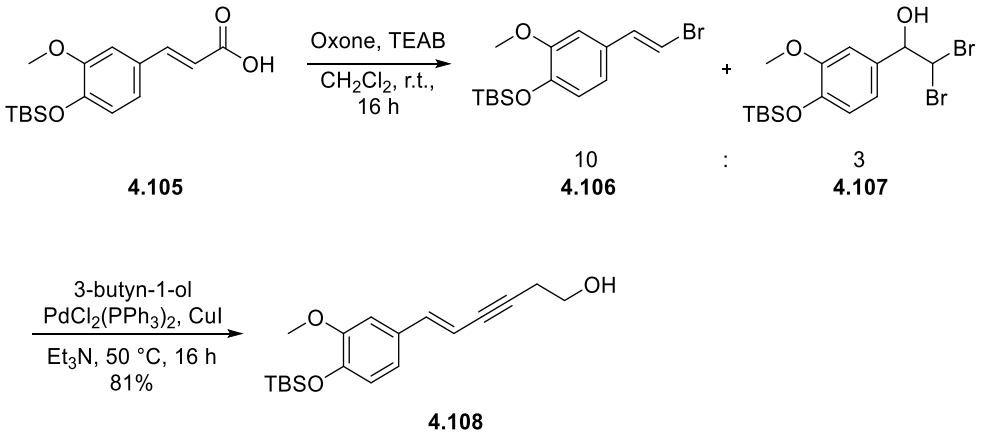
***Figure 4.9**: Proposed vanillin based analogue **4.102** for structural confirmation.*

A synthetic route was designed to synthesise enone **4.102**, culminating in a late-stage esterification to introduce the nitrobenzoate functionality. The route began with the formation of the silyl-protected phenol **4.105** in a two-step procedure from ferulic acid (**4.104**), itself accessed from the Knoevenagel reaction between vanillin (**4.103**) and malonic acid (Scheme 4.33).[225,226]



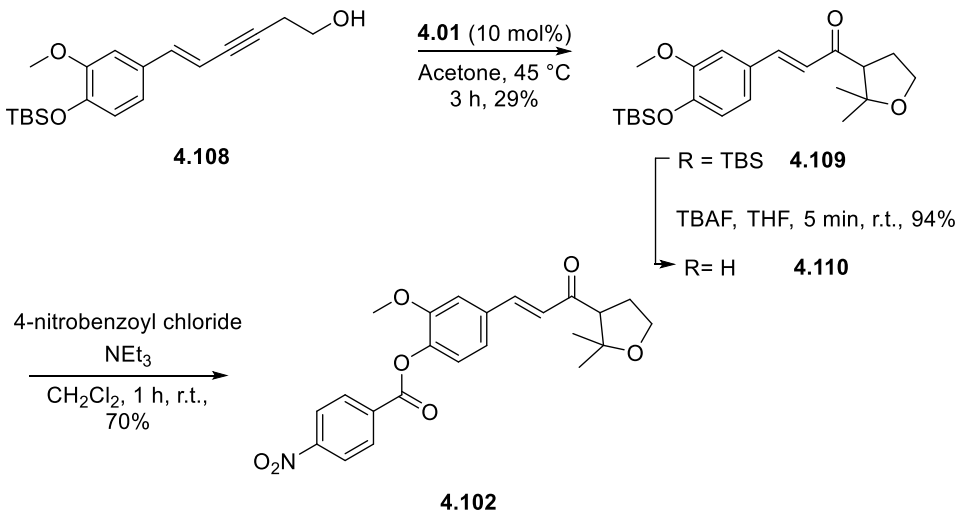
Scheme 4.33: *Synthesis of TBS protected cinnamic acid derivative* ***4.105****.*[225,226]

Conversion of the cinnamic acid derivative **4.105** to the bromo-styrene **4.106** with an Oxone/TEAB reagent combination gave a 10:3 mixture of **4.106** and the hydro-bromination side product **4.107**.[227] The mixture of compounds was then subjected to a Sonogashira coupling with 3-butyn-1-ol, which yielded the target alcohol **4.108** (Scheme 4.34).



Scheme 4.34: *Hunsdiecker and Sonogashira coupling reaction sequence to provide* ***4.108****.*

The radical-cation initiated cyclisation generated the enone **4.109** in a modest yield of 29% (Scheme 4.35). TBAF-mediated silyl deprotection followed by esterification with 4-nitrobenzoyl chloride yielded the ester **4.102** in good yield, and as a crystalline solid.



Scheme 4.35: *Completion of the synthesis of crystalline* ***4.102****, through a cyclisation/ deprotection/esterification sequence.*

The X-ray structure of crystalline **4.102**, depicted in Figure 4.10, confirmed the connectivity of the compound as containing the 2,2-dimethyltetrahydrofuran-3-yl moiety.

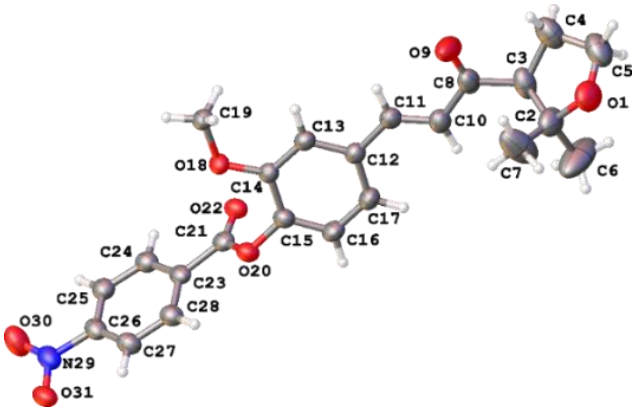
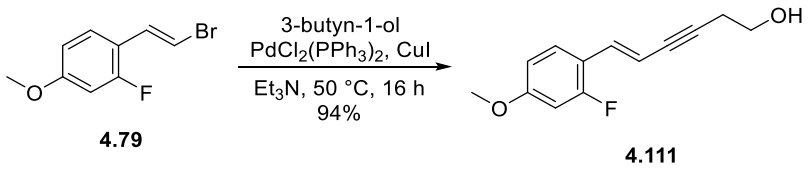


Figure 4.10*: X-Ray structure of cyclisation product* ***4.102****.*

MECHANISTIC STUDIES OF THE CYCLISATION REACTION

In an attempt to understand the reaction mechanism of the conversion of the linear enynol to the cyclised product, the transformation was monitored by NMR spectroscopy. The fluorinated alcohol **4.111** was prepared through the Sonogashira coupling of bromo-styrene **4.79**, allowing for the progression of the reaction to be monitored by ^{19}F NMR (Scheme 4.36).



***Scheme 4.36**: Synthesis of fluorinated alcohol **4.111**.*

Enynol **4.111** was exposed to 5 mol% of the radical cation salt **4.01**, and product formation was observed over the first 45 minutes (Figure 4.11).

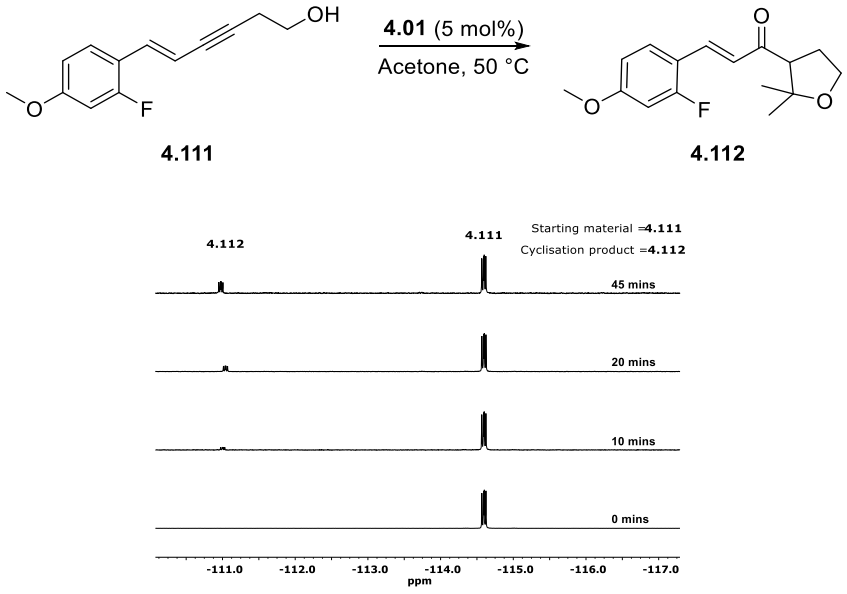


***Figure 4.11:** Progression of the radical cation initiated cyclisation of **4.111**. Peak of **4.111** referenced to -114.59 ppm.*

Increasing the reaction time from 45 to 270 minutes showed a corresponding increase in conversion, however significant amounts of starting material was still present (Figure 4.12). No substantial increase in conversion was noted between 270 minutes to 16 hours, suggesting that the radical cation salt **4.01** had degraded. As mentioned earlier, this is likely due to the quenching of the salt through reaction with water in the solvent.[220]

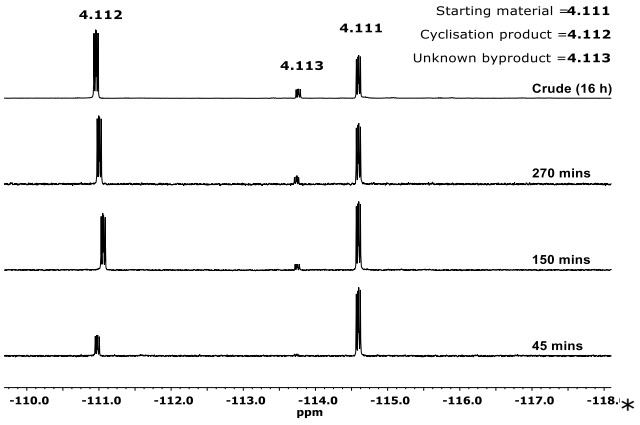
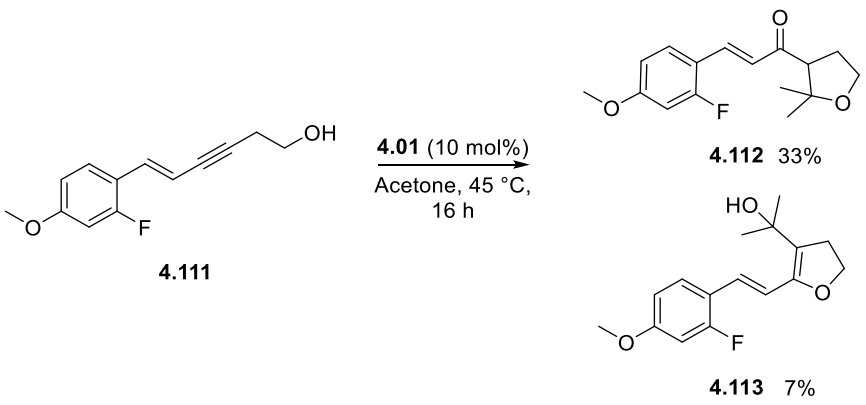


***Figure 4.12**: Progression of formation of **4.112**. Peak of **4.111** referenced to -114.59 ppm.*

Progression of the reaction also resulted in the formation of an additional product, albeit in significantly smaller quantities. Upon isolation, this product was tentatively assigned as the dihydrofuran **4.113** (Scheme 4.37).



Scheme 4.37: *Formation of cyclisation products **4.112** and **4.113**, through a radical cation initiated reaction of **4.111**.*

Formation of this byproduct indicated that there is competition between the intermolecular hydration and intramolecular cyclisation. To explain the formation of both products, the following mechanistic proposal was made (Figure 4.13).

Single electron oxidation of the substrate **4.114** results in the formation of reactive radical cation **4.115**. Hydration of this species gives the enol **4.116**, which cyclises onto a pendant oxonium moiety, itself likely formed through the condensation of the alcohol and acetone. Single electron reduction of this species results in the formation of enone **4.118**, through a formal 5-*endo*-*trig* cyclisation.

Alternatively, the enone product **4.118** could be formed through the condensation of the radical cation **4.115** with a molecule of acetone, followed by a ring closing oxa-Michael reaction and subsequent reduction.

Dihydrofuran **4.120** is likely formed through the intramolecular nucleophilic cyclisation of the pendant hydroxyl moiety onto the oxidised enyne **4.119**, followed by a radical attack onto acetone and single electron reduction by a molecule of enyne **4.114**, allowing propagation of the reaction cycle.

It is therefore possible that the ratio of **4.120** can be improved by the utilisation of dry solvent, and that a range of products could be formed through the presence of radical traps.

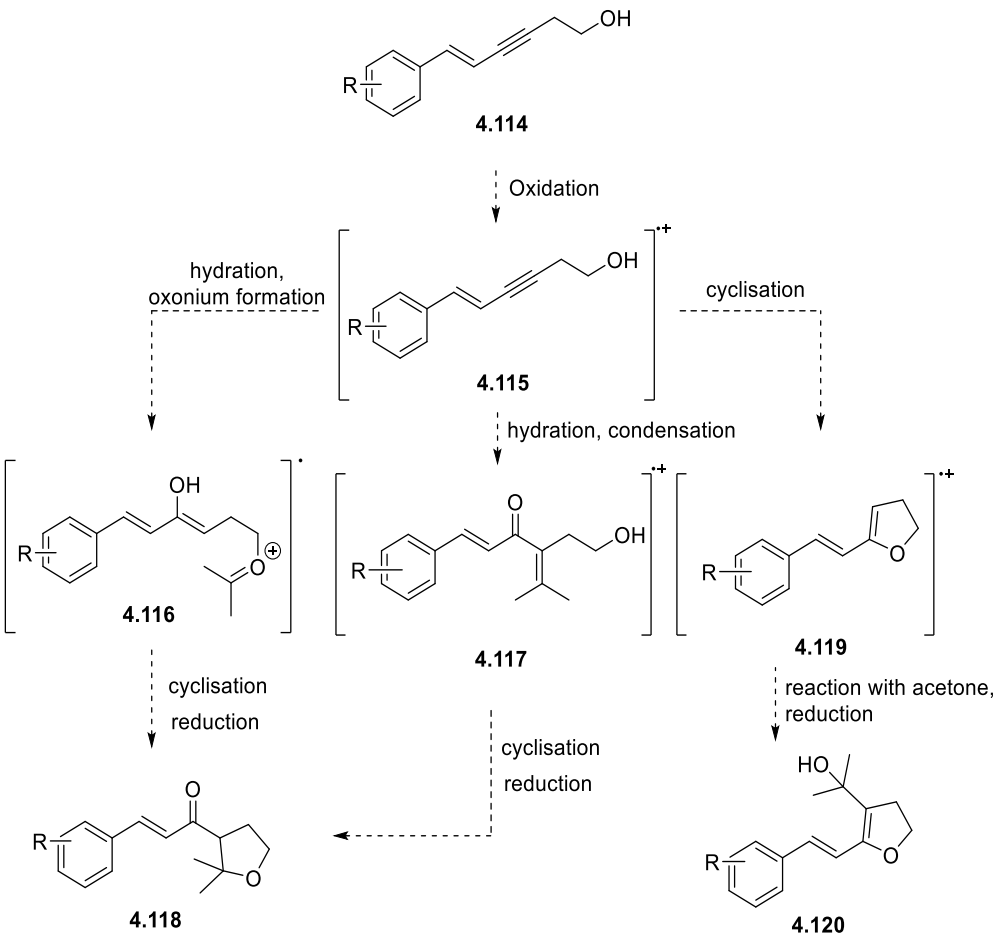
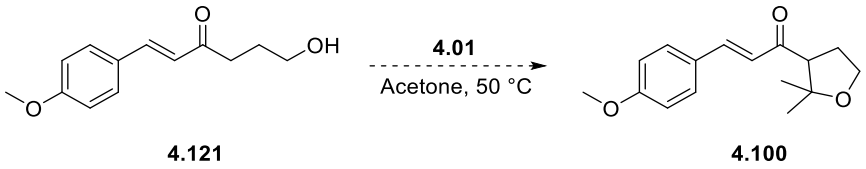


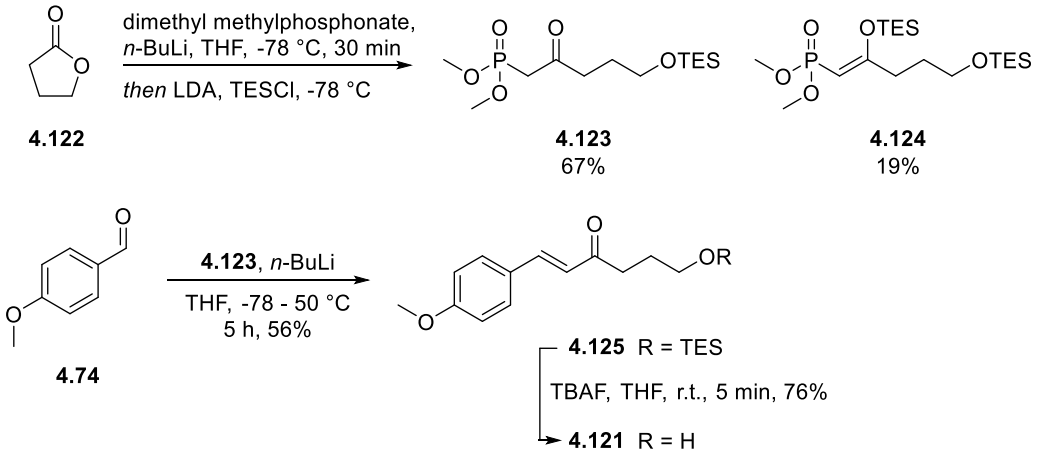
***Figure 4.13**: Proposed mechanism for radical cation initiated formation of **4.118** and **4.120**.*

In order to further understand the formation of cyclisation product **4.118**, through the putative species **4.116**, it was decided to synthesise a potential intermediate, the hydroxy-enone **4.121**. If the hydration to form **4.116** is the initial step of the cyclisation reaction, then treatment of the pre-formed enone **4.121** with the radical cation salt **4.01** should result in conversion to the cyclisation product **4.100** (Scheme 4.38).



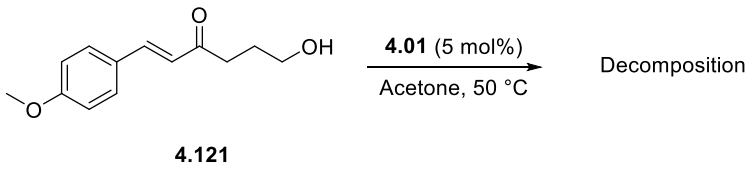
***Scheme 4.38**: Proposed cyclisation of **4.121** to gain mechanistic insight.*

The protected enone **4.125** was synthesised *via* a Horner-Wadsworth-Emmons reaction. HWE reagent **4.123** was synthesised through the reaction of dimethyl methylphosphonate and γ-butyrolactone **4.122**, followed by quenching the dianion with TESCl.[228,229]. Acidic workup resulted in the incomplete hydrolysis of **4.124** to **4.123**. Deprotonation of the phosphonate **4.123** was effected by *n*-BuLi, and heated at 50 °C with anisaldehyde to yield the protected enone **4.125** in a modest yield of 56%. A fluoride mediated deprotection proved facile, giving the target enone **4.121** (Scheme 4.39).



***Scheme 4.39:** Synthesis of putative cyclisation intermediate **4.121** through a HWE/deprotection synthetic sequence.*

The alcohol **4.121** was subjected to the usual reaction conditions, using 5 mol% of initiator **4.01**. However, instead of the formation of the cyclisation product **4.100**, a complex mixture of degradation products was observed. Analysis of the crude material by ^{1}H NMR revealed no sign of enone peaks, suggesting that oxidation of the alkene moiety had occurred (Scheme 4.40).



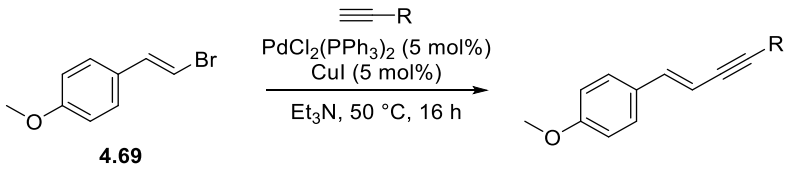
4.121

Scheme 4.40: *Radical cation induced degradation of proposed cyclisation intermediate* ***4.121****.*

The experiment implied that the initial step in the reaction mechanism to generate the cyclisation product **4.100** is not hydration of **4.114** to the corresponding enone **4.121**, and therefore an alternative, as of yet undetermined, pathway must be followed.

REACTION SCOPE

Following the synthesis of the two cyclisation products **4.112** and **4.113**, the scope of the reaction was investigated. A small library of alkynes was synthesised, varying both the length of the alkyl chain and the terminal functionality, through a Sonogashira coupling of the bromo-styrene **4.69** and appropriate alkynes (Table 4.5).



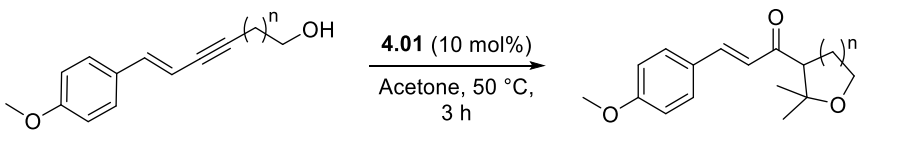
4.69

Entry		*R =*	*Yield (%)[a]*
1	**4.126**	$(CH_2)_3OH$	quant.
2	**4.127**	$(CH_2)_4OH$	90
3	**4.128**	$(CH_2)_4Cl$	90
4	**4.129**	CH_2OCOCH_3	96

[a]Isolated yields reported. 2 eq. of alkyne used.

Table 4.5: *Sonogashira coupling to synthesise a range of internal aryl enynes.*

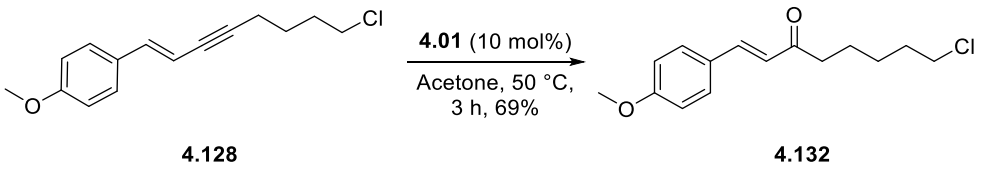
Initially, the length of the alkyl chain was varied, to determine whether larger saturated ring systems could be synthesised through our methodology (Scheme 4.41), however, analysis of the crude product mixtures showed minimal enone formation, and no products were isolated.



4.130 n = 2 trace
4.131 3 trace

Scheme 4.41*: Unsuccessful radical cation initiated reaction of enynes* ***4.126*** *and* ***4.127****.*

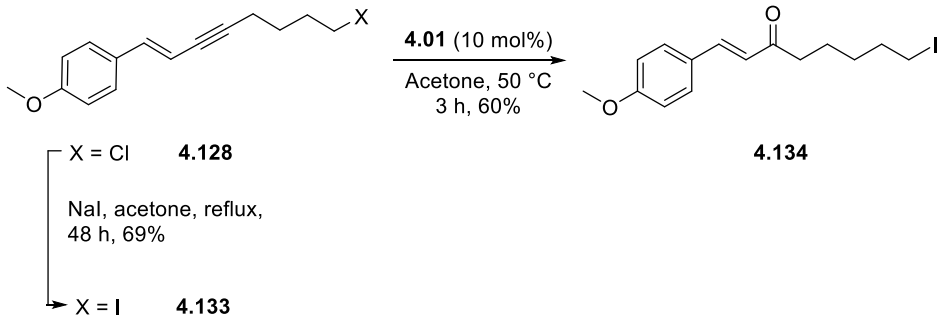
As the proposed mechanism involves a nucleophilic ring closing step, an investigation incorporating terminal electrophilic moieties was undertaken. It was hypothesised that alkyl chloride **4.128** maybe sufficiently electrophilic to cyclise into the substituted cyclopentane. However, upon exposure to the reaction conditions, no cyclised product was detected, although the linear enone **4.132** was isolated in good yield (Scheme 4.42).



4.128 **4.132**

Scheme 4.42*: Radical cation induced hydration of enyne* ***4.128***.

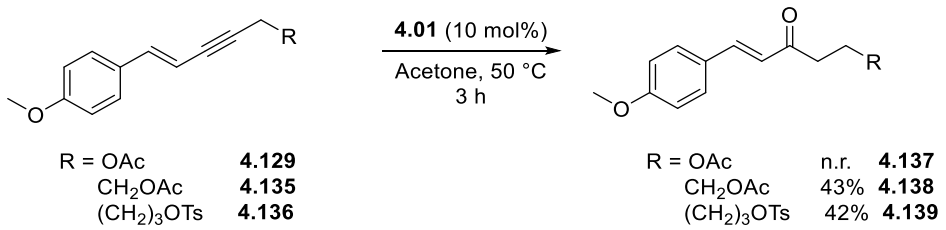
Extending this reaction further, the corresponding iodo species **4.133** was synthesised and subjected to the radical cation salt **4.01** to produce a similar result (Scheme 4.43).



Scheme 4.43*: Reaction of iodoalkane* ***4.133*** *under radical cation conditions.*

The stability of the alkyl iodide moiety under the reaction conditions highlighted the functional group tolerance of this reaction, and this led to

the synthesis of additional substrates to study the stability of other electrophiles under these conditions. Tosylate **4.136** and acetate **4.135** were prepared from alcohols **4.98** and **4.127** respectively and along with acetate **4.129** were subjected to the reaction conditions (Scheme 4.44).



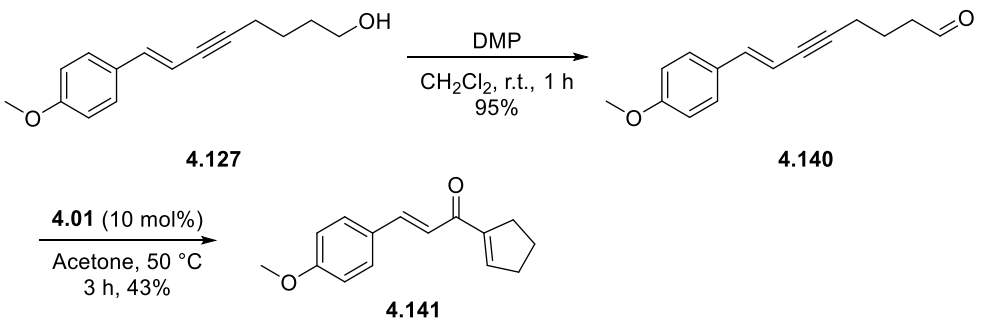
R = OAc	**4.129**	R = OAc	n.r. **4.137**
CH_2OAc	**4.135**	CH_2OAc	43% **4.138**
$(CH_2)_3OTs$	**4.136**	$(CH_2)_3OTs$	42% **4.139**

Scheme 4.44: *Presence of electrophilic moieties under radical cation conditions.*

Over a set period of 3 hours, varying results were obtained. Intriguingly, the length of the alkyl chain had a significant effect on the reactivity of acetates **4.129** and **4.135**. Acetate **4.135** generated the linear enone **4.138** in a modest 43% yield, however the absence of a methylene unit rendered **4.129** inert to the reaction conditions.

Conversely, the presence of a remote tosylate did not hinder conversion, with 42% of enone **4.139** isolated. The yields of this set of reactions were disappointing, however, it is important to note that the reaction conditions were not optimised.

Next, alkyl alcohol **4.127** was converted to the corresponding aldehyde **4.140** utilising Dess-Martin periodinane (DMP).[230] It was proposed that the higher electrophilic nature of the newly formed aldehyde would promote cyclisation. Upon treatment with the radical cation salt **4.01**, the aldehyde **4.139** converted in the cyclopentene product **4.141**, albeit in modest yield (Scheme 4.45).



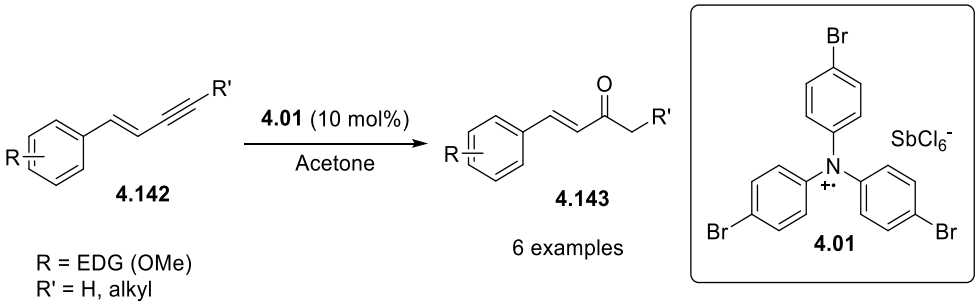
Scheme 4.45: *Radical cation initiated hydration/aldol condensation cascade of* ***4.140****.*

Formation of the dienone **4.141** is consistent with both of the proposed mechanisms for the formation of the 2,2-dimethyltetrahydrofuran-3-yl based product **4.100** (*vide supra*), with both structures formed through a nucleophilic attack onto an electrophilic species.

Although the yields of both the cyclised products and the linear enones are modest and further optimisation is evidently required, this methodology potentially demonstrates a previously unexplored mode of reactivity which could be developed to be of significant synthetic utility.

CONCLUSIONS AND FUTURE WORK

In summary, a novel methodology for the hydration of conjugated aromatic enynes has been developed, utilising radical cation salt **4.01** as the reaction initiator (Scheme 4.46).

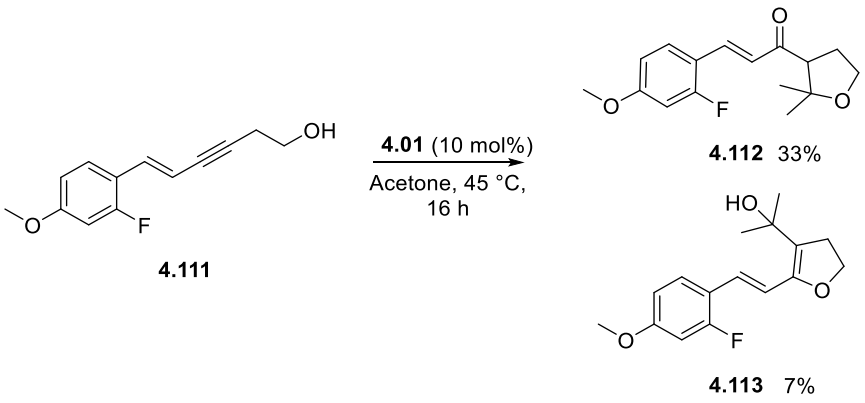


***Scheme 4.46**: Summary of hydration of enynes to enones.*

This reaction was shown to convert both terminal and internal conjugated enynes **4.142** into the corresponding enones **4.143**, with varying yields. It was shown to tolerate alkyl halides, tosylate and acetate functionality, which highlights the mildness of this protocol.

The generated enone products are valued synthetic intermediates, undergoing a host of useful chemistry, and so the ability to convert the relatively inert enyne moiety into enones is a potentially valuable transformation. The most common literature procedures for this reaction requires the use of either forcing conditions, or expensive transition metal catalysts.[184] Therefore, the development of a mild, radical cation initiated methodology maybe a welcome addition to this field of research.

The methodology has been extended further to generate cyclised products. For example, a substrate containing a pendant alcohol was converted into both an enone substituted with a 2,2-dimethyltetrahydrofuran-3-yl moiety **4.112** and a dihydrofuran **4.113**, both resulting from divergent cyclisation pathways (Scheme 4.47).



***Scheme 4.47**: Summary of the two cyclisation products from enynol **4.111**.*

Future work on this project would include additional optimisation studies to improve reaction yields for internal enynes, particularly in the case of cyclisation products.

The use of alternative, more highly oxidising, radical cation salts would also be investigated to improve the scope of the developed transformations from just electron-rich substrates.

To further expand the scope of the developed methodologies, different nucleophiles would be employed. For instance, pendant amines may lead to useful dihydropyrroles, and the analogous sulfur species to dihydrothiophenes.

EXPERIMENTAL SECTION

Unless stated, reactions were carried out in flame-dried glassware, under an atmosphere of argon with magnetic stirring. THF was freshly distilled over sodium and benzophenone; CH_2Cl_2 was freshly distilled over CaH_2 under a nitrogen atmosphere. NEt_3 was distilled from CaH_2 and stored over 4 Å molecular sieves. *N*-Bromosuccinimide was recrystallised from water. All other reagents were obtained from commercial sources and used without further purification. Reactions were monitored using Thin Layer Chromatography (TLC), and visualised using UV light and stained using a basic $KMnO_4$ (potassium permanganate) solution. Flash column chromatography was performed using Merck silica gel 60 as the stationary phase. Petrol refers to petroleum spirit (b.p. 40-60 °C).

NMR spectra (^1H, ^{13}C and ^{19}F) were recorded on Bruker DPX300 (300 MHz), AV400 (400 MHz), DPX400 (400 MHz), AV3400 (400 MHz), AV3400HD (400 MHz) and AV3500 (500 MHz) spectrometers, in $CDCl_3$, D_2O, CD_3OD, DMSO-d^6 and Acetone-d^6. Infra-red spectra were obtained using a Bruker Alpha FTIR spectrometer with a platinum ATR adaptor, with the peaks recorded as υ_{max} (cm^{-1}). HRMS were obtained using a Bruker MicroTOF mass spectrometer operating in electrospray ionisation (ESI) or electron ionisation (EI) mode. Melting point data was collected using a Stuart SMP3. Where referenced, spectral data showed agreement with the literature.

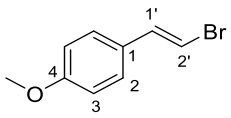
General Procedure 4.1: Sonogashira Reaction

A solution of bromo-styrene (1 mol eq.) in triethylamine was degassed by purging with argon for 5 min. $PdCl_2(PPh_3)_2$ (0.05 mol eq.) and CuI (0.05 mol eq.) were added successively, and the solution degassed with argon for a further 5 min. To this suspension was added alkyne (2 mol eq.) and the resultant mixture stirred at 50 °C until TLC indicated completion, before being filtered through Celite® and washed with Et_2O (100 mL). Volatiles were removed under reduced pressure and purification by flash column chromatography yielded the desired compound.

General Procedure 4.2: **Enyne Hydration**

A solution of enyne (1 mol eq.) in acetone was degassed by purging with argon for 5 min. Radical cation salt **4.01** (0.1 eq.) was added, and the resultant solution stirred for 3 h at 50 °C. The reaction was quenched by the addition of sat. K_2CO_3 in methanol (1 mL) and extracted between Et_2O (2 x 50 mL) and washed with water (50 mL). The organic phases were combined, dried over $MgSO_4$, filtered and concentrated under reduced pressure. Purification by flash column chromatography yielded the desired product.

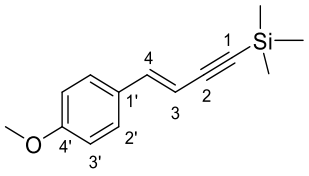
(*E*)-1-(2-Bromovinyl)-4-methoxybenzene[231] **(4.69)**



To a solution of 4-methoxycinnamic acid (**4.68**) (1.78 g, 10.0 mmol) in anhydrous CH_2Cl_2 (30 mL) was added triethylamine (70 µL, 0.50 mmol). The reaction mixture was stirred for 5 min and *N*-bromosuccinimide (2.14 g, 12.0 mmol) added. After 10 min, the reaction mixture was concentrated under reduced pressure and purified by flash column chromatography (1% EtOAc/Petrol) to yield the title compound as a white solid (1.93 g, 90%). m.p. 54-55 °C (lit: 51 °C).[231]

υ_{max} (cm^{-1}): 3009, 1607 (C=C), 1511, 1253 (C-O); δ_H($CDCl_3$, 400 MHz): 7.26 - 7.22 (m, 2H, 2-H), 7.05 (d, *J* = 14.0 Hz, 1H, 1'-H), 6.89 - 6.84 (m, 2H, 3-H), 6.62 (d, *J* = 14.0 Hz, 1H, 2'-H), 3.82 (s, 3H, OCH_3); δ_C($CDCl_3$, 101 MHz): 159.6 (C-4), 136.6 (C-1'), 128.8 (C-1), 127.3 (C-2), 114.2 (C-3), 104.0 (C-2'), 55.3 (CH_3); **HRMS** (EI) calculated for C_9H_9OBr $[M]^+$ 211.9831, found 211.9838.

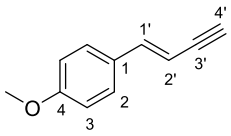
(*E*)-(4-(4-Methoxyphenyl)but-3-en-1-yn-1-yl)trimethylsilane[232] **(4.70)**



Synthesised from (*E*)-1-(2-bromovinyl)-4-methoxybenzene (**4.69**) (500 mg, 2.13 mmol) and trimethylsilyl acetylene (813 µL, 5.88 mmol) following **General Procedure 4.1** at room temperature for 16 h. Purification by flash column chromatography (2% Et_2O/Petrol) yielded the title compound as a yellow oil (507 mg, 94%).

υ_{max} (cm^{-1}): 2962, 2117 (C≡C), 1604 (C=C), 1512, 1250 (C-O). δ_H($CDCl_3$, 400 MHz): 7.34 - 7.30 (m, 2H, 2'-H), 6.97 (d, *J* = 16.2 Hz, 1H, 4-H), 6.88 – 6.84 (m, 2H, 3-H), 6.05 (d, *J* = 16.2 Hz, 1H, 3-H), 3.82 (s, 3H, OCH_3), 0.23 (s, 9H, $Si(CH_3)_3$); δ_C($CDCl_3$, 101 MHz): 160.2 (C-4'), 142.0 (C-4), 129.0 (C-1'), 127.7 (C-2'), 114.1 (C-3'), 105.6 (C-3), 104.8 (C-2), 95.9 (C-1), 55.3 (OCH_3), 0.0 ($Si(CH_3)_3$); **HRMS** (EI) calculated for $C_{14}H_{18}OSi$ $[M]^+$ 230.1121, found 230.1110.

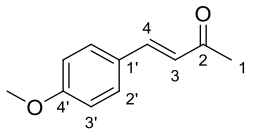
(*E*)-1-(But-1-en-3-yn-1-yl)-4-methoxybenzene[232] **(4.71)**



To a solution of (*E*)-(4-(4-methoxyphenyl)but-3-en-1-yn-1-yl)trimethylsilane (**4.70**) (300 mg, 1.30 mmol) in methanol (5 mL) was added potassium carbonate (359 mg, 2.60 mmol), and the reaction stirred for 3 h. The suspension was diluted with Et_2O (50 mL) and washed with sat. $NH_4Cl_{(aq)}$ (50 mL). The aqueous phase was washed with Et_2O (50 mL), the organic phases combined, dried over $MgSO_4$, filtered and concentrated under reduced pressure to yield the title compound as a pale yellow solid (192 mg, 93%). m.p. 45-46 °C (lit: 46-47 °C).[233]

υ_{max} (cm^{-1}): 3307, 1605 (C=C), 1512, 1249 (C-O), 1175, 1034; δ_H($CDCl_3$, 400 MHz): 7.35 - 7.32 (m, 2H, 2-H), 7.00 (d, *J* = 16.3 Hz, 1H, 1'-H), 6.89 - 6.85 (m, 2H, 3-H), 6.00 (dd, *J* = 16.3, 2.4 Hz, 1H, 2'-H), 3.83 (s, 3H, OCH_3), 3.02 (dd, *J* = 2.4, 0.6 Hz, 1H, 4'-H); δ_C($CDCl_3$, 101 MHz): 160.3 (C-4), 142.7 (C-1'), 128.7 (C-1), 127.7 (C-2), 114.2 (C-3), 104.5 (C-2'), 83.3 and 78.4 (C-3' and C-4'), 55.3 (OCH_3); **HRMS** (EI) calculated for $C_{10}H_{11}O$ $[M]^+$ 158.0726, found 158.0720.

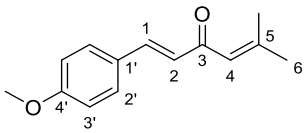
(*E*)-4-(4-Methoxyphenyl)but-3-en-2-one[234] **(4.72)**



Synthesised from (*E*)-1-(but-1-en-3-yn-1-yl)-4-methoxybenzene (**4.71**) (200 mg, 1.26 mmol) in acetone (5 mL) following **General Procedure 4.2** at 40 °C for 1 h. Purification by flash column chromatography (10-20% EtOAc/Petrol) yielded the title compound as a pale yellow solid (153 mg, 69%) and **4.73** as a pale yellow solid (30 mg, 11%).

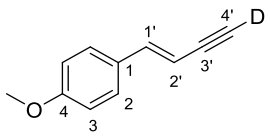
m.p. 73 °C (lit: 74-76 °C).[234] υ_{max} (cm^{-1}): 1682 (C=O), 1603, 1514, 1265 (C-O); δ_H($CDCl_3$, 400 MHz): 7.55 – 7.45 (m, 3H, 4-H and 2'-H), 6.95 – 6.90 (m, 2H, 3'-H), 6.62 (d, *J* = 16.2 Hz, 1H, 3-H), 3.85 (s, 3H, OCH_3), 2.37 (s, 3H, 1-H_3); δ_C($CDCl_3$, 101 MHz): 198.4 (C-2), 161.6 (C-4'), 143.2 (C-4'), 129.9 (C-2'), 127.0 (C-1'), 125.0 (C-3), 114.4 (C-3'), 55.4 (OCH_3), 27.4 (C-1); **HRMS** (ESI) calculated for $C_{11}H_{13}O_2$ $[M+H]^+$ 177.0910, found 177.0913.

(*E*)-1-(4-Methoxyphenyl)-5-methylhexa-1,4-dien-3-one[235] **(4.73)**



m.p. 48 °C (lit: 56 °C).[236] υ_{max} (cm^{-1}): 1623 (C=O), 1604, 1511, 1251 (C-O); δ_H($CDCl_3$, 400 MHz): 7.58 – 7.49 (m, 3H, 1-H and 2'-H), 6.95 – 6.89 (m, 2H, 3-H), 6.68 (d, *J* = 16.1 Hz, 1H, 3'-H), 6.33 (hept, *J* = 1.2 Hz, 1H, 4-H), 3.85 (s, 3H, OCH_3), 2.22 (d, *J* = 1.2 Hz, 3H, 6-H_3), 1.97 (d, *J* = 1.2 Hz, 3H, 5-CH_3); δ_C($CDCl_3$, 101 MHz): 190.3 (C-3), 161.3 (C-4'), 155.5 (C-5), 141.8 (C-1), 129.8 (C-2'), 127.7 (C-1'), 126.1 (C-2), 123.7 (C-4), 114.3 (C-3'), 55.4 (OCH_3), 27.8 (5-CH_3), 21.0 (C-6); **HRMS** (ESI) calculated for $C_{14}H_{17}O_2$ $[M+H]^+$ 217.1223, found 217.1229.

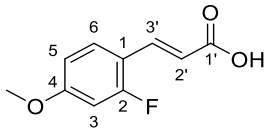
(*E*)-1-(But-1-en-3-yn-1-yl-4-*d*)-4-methoxybenzene (4.77)



To a solution of (*E*)-1-(but-1-en-3-yn-1-yl-4-)-4-methoxybenzene (4.71) (200 mg, 1.26 mmol) in anhydrous THF (10 mL) at −78 °C was added *n*-BuLi (0.70 mL, 1.52 mmol of a 2.17 M solution in hexanes), and the reaction stirred for 15 min. D_2O (1.00 mL) was added, the reaction warmed to room temperature, diluted with Et_2O (50 mL) and washed with sat. $NH_4Cl_{(aq)}$ (50 mL). The organic phase was dried over $MgSO_4$, filtered and concentrated under reduced pressure to yield the title compound as a yellow solid (199 mg, 99%). m.p. 45 °C.

υ_{max} (cm^{-1}): 3264, 2562 (C-D), 1601 (C=C), 1509, 1247 (C-O), 1176, 1029; δ_H($CDCl_3$, 400 MHz): 7.36 - 7.32 (m, 2H, 2-H), 7.00 (d, *J* = 16.3 Hz, 1H, 1'-H), 6.90 - 6.85 (m, 2H, 3-H), 6.00 (d, *J* = 16.3, 1H, 2'-H), 3.83 (s, 3H, OCH_3); δ_C($CDCl_3$, 101 MHz): 160.3 (C-4), 142.7 (C-1'), 128.7 (C-1), 127.7 (C-2), 114.2 (C-3), 104.5 (C-2'), 83.3 (t, *J* = 7 Hz, C-3'), 78.4 (t, *J* = 38 Hz, C-4'), 55.3 (OCH_3); Does not ionise by ESI.

(*E*)-3-(2-Fluoro-4-methoxyphenyl)acrylic acid (4.80)

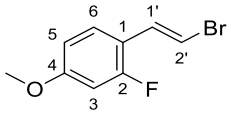


2-Fluoro-4-methoxybenzaldehyde (**4.81**) (1.54 g, 10.0 mmol) and malonic acid (2.29 g, 22.0 mmol) were suspended in pyridine (3.6 mL) and piperidine (148 µL, 1.50 mmol) and refluxed for 2 h. The resultant solution was cooled, poured into 2M $HCl_{(aq)}$ and the precipitate collected and dried in

a vacuum oven to yield the title compound as a white solid (1.59 g, 81%). m.p. 195 °C.

υ_{max} (cm^{-1}): 2845 (OH), 1681 (C=O), 1608, 1267 (C-O); δ_H(DMSO-d_6, 400 MHz): 7.75 (dd, *J* = 8.9, 8.8 Hz, 1H, 6-H), 7.59 (d, *J* = 16.2 Hz, 1H, 3'-H), 6.91 (dd, *J* = 13.0, 2.5 Hz, 1H, 3-H), 6.84 (dd, *J* = 8.9, 2.5 Hz, 1H, 5-H), 6.44 (d, *J* = 16.2 Hz, 1H, 2'-H), 3.81 (s, 3H, OCH_3); δ_C(DMSO-d_6, 101 MHz): 167.6 (C-1'), 162.3 (d, *J* = 12 Hz, C-4), 161.6 (d, *J* = 251 Hz, C-2), 135.8 (d, *J* = 3 Hz, C-3'), 130.1 (d, *J* = 5 Hz, C-6), 118.9 (d, *J* = 6 Hz, C-2'), 114.2 (d, *J* = 12 Hz, C-1), 111.4 (d, *J* = 3 Hz, C-5), 101.7 (d, *J* = 26 Hz, C-3), 55.9 (OCH_3); δ_F(DMSO-d_6, 282 MHz): −113.6 (dd, *J* = 13.0, 8.9 Hz); **HRMS** (ESI) calculated for $C_{10}H_8FO_3$ $[M-H]^-$ 195.0463, found 195.0460.

(*E*)-1-(2-Bromovinyl)-2-fluoro-4-methoxybenzene (4.79)

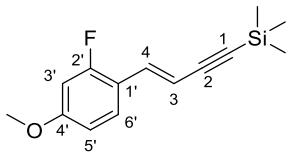


To a suspension of (*E*)-3-(2-fluoro-4-methoxyphenyl)acrylic acid (**4.80**) (1.00 g, 5.10 mmol) in MeCN (10 mL) and water (10 mL) was added *N*-bromosuccinimide (953 mg, 5.35 mmol) followed by $Mn(OAc)_2.4H_2O$ (250 mg, 1.02 mmol). The resultant suspension was stirred for 15 min, when complete dissolution had occurred. Volatiles were removed under reduced pressure, and the residue extracted between Et_2O (2 x 50 mL) and brine (50 mL). The organic phases were combined, dried over $MgSO_4$, filtered and concentrated under reduced pressure. Purification by flash column chromatography (10% Et_2O/Petrol) yielded the title compound as a pale yellow oil (896 mg, 76%).

υ_{max} (cm^{-1}): 2837, 1620 (C=C), 1503, 1153 (C-O); δ_H($CDCl_3$, 400 MHz): 7.22 (dd, *J* = 8.6, 8.6 Hz, 1H, 6-H), 7.11 (d, *J* = 14.1 Hz, 1H, 1'-H), 6.78

(d, *J* = 14.1 Hz, 1H, 2'-H), 6.67 (ddd, *J* = 8.6, 2.6, 0.7 Hz, 1H, 5-H), 6.61 (dd, *J* = 12.5, 2.6 Hz, 1H, 3-H), 3.81 (s, 3H, OCH_3); δ_C($CDCl_3$, 101 MHz): 160.7 (d, *J* = 11 Hz, C-4), 160.5 (d, *J* = 251 Hz, C-2), 130.1, 128.5 (d, *J* = 6 Hz), 116.3 (d, *J* = 13 Hz), 110.4 (d, *J* = 3 Hz), 106.9 (d, *J* = 8 Hz), 101.9 (d, *J* = 26 Hz), 55.6 (OCH_3); δ_F($CDCl_3$, 376 MHz): −113.9 (dd, *J* = 12.5, 8.6 Hz); **HRMS** (EI) calculated for C_9H_8FOBr $[M]^+$ 229.97371, found 229.97277.

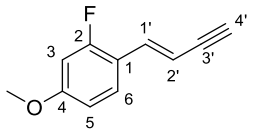
(*E*)-(4-(2-Fluoro-4-methoxyphenyl)but-3-en-1-yn-1-yl)trimethylsilane (4.83)



Synthesised from (*E*)-1-(2-bromovinyl)-2-fluoro-4-methoxybenzene (**4.79**) (461 mg, 2.00 mmol) and trimethylsilyl acetylene (568 µL, 3.99 mmol) following **General Procedure 4.1** at 50 °C for 3 h. Purification by flash column chromatography (5% EtOAc/Petrol) yielded the title compound as a yellow oil (481 mg, 97%).

υ_{max} (cm^{-1}): 2958, 1619 (C=C), 1504, 1249 (C-O); δ_H($CDCl_3$, 400 MHz): 7.33 (dd, *J* = 8.7, 8.7 Hz, 1H, 6'-H), 7.06 (d, *J* = 16.5 Hz, 1H, 4-H), 6.70 – 6.64 (m, 1H, 5'-H), 6.60 (dd, *J* = 12.5, 2.5 Hz, 1H, 3'-H), 6.14 (d, *J* = 16.5 Hz, 1H, 3-H), 3.81 (s, 3H, OCH_3), 0.23 (s, 9H, $Si(CH_3)_3$); δ_C($CDCl_3$, 101 MHz): 161.1 (d, *J* = 11 Hz, C-4'), 161.0 (d, *J* = 252 Hz, C-2'), 134.8 (d, *J* = 2 Hz, C-4), 127.8 (d, *J* = 6 Hz, C-6'), 116.7 (d, *J* = 13 Hz), 110.5 (d, *J* = 3 Hz), 107.9 (d, *J* = 7 Hz), 104.7 (C-2), 101.7 (d, *J* = 26 Hz), 96.5 (C-1), 55.6 (OCH_3), -0.1 ($Si(CH_3)_3$); δ_F($CDCl_3$, 376 MHz): −114.2 (dd, *J* = 12.5, 8.7 Hz); **HRMS** (EI) calculated for $C_{14}H_{17}OFSi$ $[M]^+$ 248.1027, found 248.1017.

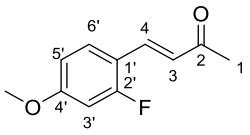
(*E*)-1-(But-1-en-3-yn-1-yl)-2-fluoro-4-methoxybenzene (4.78)



To a solution of (*E*)-(4-(2-fluoro-4-methoxyphenyl)but-3-en-1-yn-1-yl)trimethylsilane (**4.83**) (450 mg, 1.81 mmol) in THF (10 mL) was added TBAF (1M in THF, 2.17 mL, 2.17 mmol) at room temperature. The resultant solution was stirred for 15 min and volatiles removed under reduced pressure. The residue was diluted with Et_2O (100 mL) and washed with water (100 mL). The organic phase was dried over $MgSO_4$, filtered and concentrated under reduced pressure. Purification through a short silica pad (Et_2O) yielded the title compound as an orange oil (320 mg, quant.)

υ_{max} (cm^{-1}): 3290, 1617 (C=C), 1503, 1273 (C-O); δ_H($CDCl_3$, 400 MHz): 7.34 (ddd, *J* = 8.7, 8.7, 0.6 Hz, 1H, 6-H), 7.10 (dd, *J* = 16.5, 0.7 Hz, 1H, 1'-H), 6.68 (dddd, *J* = 8.7, 2.6, 0.6, 0.6 Hz, 1H, 5-H), 6.61 (dd, *J* = 12.5, 2.6 Hz, 1H, 3-H), 6.10 (dd, *J* = 16.5, 2.4 Hz, 1H, 2'-H), 3.82 (s, 3H, 4-OCH_3), 3.05 (dd, *J* = 2.4, 0.7 Hz, 1H, 4'-H); δ_C($CDCl_3$, 101 MHz): 161.2 (d, *J* = 12 Hz, C-4), 161.1 (d, *J* = 252 Hz, C-2), 135.6 (d, *J* = 2 Hz, C-1'), 127.9 (d, *J* = 6 Hz), 116.5 (d, *J* = 13 Hz), 110.5 (d, *J* = 3 Hz), 106.9 (d, *J* = 7 Hz), 101.7 (d, *J* = 26 Hz), 83.2 (C-1'), 78.9 (C-2'), 55.6 (OCH_3); δ_F($CDCl_3$, 376 MHz): −114.2 (dd, *J* = 12.5, 8.7 Hz); **HRMS** (EI) calculated for $C_{11}H_9OF$ $[M]^+$ 176.0632, found 176.0630.

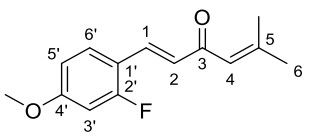
(*E*)-4-(2-Fluoro-4-methoxyphenyl)but-3-en-2-one (4.84)



Synthesised from (*E*)-1-(but-1-en-3-yn-1-yl)-2-fluoro-4-methoxybenzene (**4.78**) (125 mg, 0.710 mmol) in acetone (5 mL) following **General Procedure 4.2** at 40 °C for 1 h. Purification by flash column chromatography (10-20% EtOAc/Petrol) yielded the title compound as a pale yellow solid (70 mg, 51%) and **4.85** as a pale yellow oil (22 mg, 13%).

υ_{max} (cm^{-1}): 1668 (C=O), 1614 (C=C), 1505, 1251 (C-O); δ_H($CDCl_3$, 400 MHz): 7.62 (d, *J* = 16.4 Hz, 1H, 4-H), 7.50 (dd, *J* = 8.7, 8.6 Hz, 1H, 6'-H), 6.74 (ddd, *J* = 8.7, 2.5, 0.7 Hz, 1H, 5'-H), 6.71 – 6.63 (m, 2H, 3'-H and 3-H), 3.85 (s, 3H, OCH_3), 2.38 (s, 3H, 1-H); δ_C($CDCl_3$, 101 MHz): 198.5 (C-2), 162.8 (d, *J* = 11 Hz, C-4'), 162.4 (d, *J* = 254 Hz, C-2'), 135.8 (d, *J* = 3 Hz, C-4), 129.6 (d, *J* = 5 Hz, C-6'), 126.9 (d, *J* = 5 Hz, C-3), 115.0 (d, *J* = 12 Hz, C-1'), 111.0 (d, *J* = 3 Hz, C-5'), 101.8 (d, *J* = 26 Hz, C-3'), 55.7 (OCH_3), 27.4 (C-1); δ_F($CDCl_3$, 376 MHz): −112.1 (dd, *J* = 12.4, 8.6 Hz); **HRMS** (ESI) calculated for $C_{11}H_{12}FO_2$ $[M+H]^+$ 195.0816, found 195.0809.

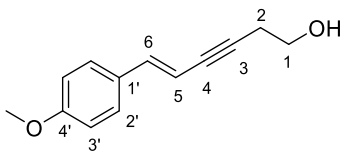
(*E*)-1-(2-Fluoro-4-methoxyphenyl)-5-methylhexa-1,4-dien-3-one (4.85)



υ_{max} (cm^{-1}): 2917, 1670 (C=O), 1615 (C=C), 1504; δ_H($CDCl_3$, 400 MHz): 7.65 (d, *J* = 16.2 Hz, 1H, 1-H), 7.49 (dd, *J* = 8.7, 8.6 Hz, 1H, 6'-H), 6.76 (d, *J* = 16.2 Hz, 1H, 2-H), 6.72 (dd, *J* = 8.7, 2.6 Hz, 1H, 5'-H), 6.64 (dd, *J* = 12.5, 2.6 Hz, 1H, 3'-H), 6.34 (qq, *J* = 1.3, 1.3 Hz, 1H, 4-H), 3.83 (s, 3H,

OCH_3), 2.22 (d, *J* = 1.3 Hz, 3H, 6-H), 1.97 (d, *J* = 1.3 Hz, 3H, 5-CH_3); δ_C($CDCl_3$, 101 MHz): 190.2 (C-3), 162.5 (d, *J* = 253.8 Hz, C-2′), 162.4 (d, *J* = 11.6 Hz, C-4′), 156.0 (C-5), 134.5 (d, *J* = 2.3 Hz, C-1), 129.9 (d, *J* = 5.1 Hz, C-6′), 128.2 (d, *J* = 5.9 Hz, C-2), 123.6 (C-4), 115.6 (d, *J* = 11.9 Hz, C-1′), 110.8 (d, *J* = 2.9 Hz, C-5′), 101.8 (d, *J* = 25.6 Hz, C-3′), 55.7 (OCH_3), 27.8 (5-CH_3), 21.0 (C-6); δ_F($CDCl_3$, 376 MHz): −111.7 (dd, *J* = 12.5, 8.6 Hz); **HRMS** (ESI) calculated for $C_{14}H_{16}FO_2$ $[M+H]^+$ 235.1129, found 235.1130.

(*E*)-6-(4-Methoxyphenyl)hex-5-en-3-yn-1-ol (4.98)

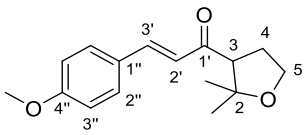


A solution of (*E*)-1-(2-bromovinyl)-4-methoxybenzene (**4.69**) (760 mg, 3.57 mmol) in triethylamine (20 mL) was degassed by purging with argon for 5 min. $PdCl_2$ (32 mg, 0.18 mmol), PPh_3 (47 mg, 0.18 mmol) and CuI (34 mg, 0.18 mmol) were added successively, and the solution degassed with argon for a further 5 min. To this suspension was added 3-butyn-1-ol (500 mg, 7.13 mmol) and the resultant mixture stirred for 16 h at 50 °C, before being filtered through Celite® and washed with Et_2O (100 mL). Volatiles were removed under reduced pressure and purification by flash column chromatography (30% EtOAc/Petrol) yielded the title compound as a white solid (625 mg, 87%). m.p. 85 °C.

υ_{max} (cm^{-1}): 3011 (OH), 1606 (C=C), 1511; δ_H($CDCl_3$, 400 MHz): 7.33 – 7.29 (m, 2H, 2′-H), 6.90 – 6.83 (m, 3H, 3′-H and 6-H), 6.01 (dt, *J* = 16.3, 2.2 Hz, 1H, 5-H), 3.82 (s, 3H, OCH_3), 3.78 (dt, *J* = 6.3, 6.3 Hz, 2H, 1-H_2), 2.65 (td, *J* = 6.3, 2.2 Hz, 2H, 2-H_2), 1.93 (t, *J* = 6.3 Hz, 1H, OH); δ_C($CDCl_3$, 101 MHz): 159.9 (C-4′), 140.5 (C-6), 129.1 (C-1′), 127.4 (C-2′), 114.1 (C-3′),

105.7 (C-5), 87.8 (C-3), 81.9 (C-4), 61.2 (C-1), 55.3 (OCH_3), 24.0 (C-2); **HRMS** (ESI) calculated for $C_{13}H_{15}O_2$ $[M+H]^+$ 203.1067, found 203.1075.

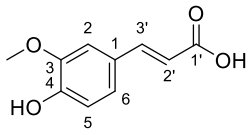
(*E*)-1-(2,2-Dimethyltetrahydrofuran-3-yl)-3-(4-methoxyphenyl)prop-2-en-1-one (4.100)



Synthesised from (*E*)-6-(4-methoxyphenyl)hex-5-en-3-yn-1-ol (**4.98**) (126 mg, 0.62 mmol mmol) in acetone (5 mL) following **General Procedure 4.2** at 45 °C for 3 h. Purification by flash column chromatography (20-30% EtOAc/Petrol) yielded the title compound as a pale yellow oil (69 mg, 43%).

υ_{max} (cm^{-1}): 2973, 1593 (C=O), 1510, 1171; δ_H($CDCl_3$, 400 MHz): 7.58 (d, *J* = 15.9 Hz, 1H, 3'-H), 7.56 – 7.51 (m, 2H, 2''-H), 6.96 – 6.90 (m, 2H, 3''-H), 6.71 (d, *J* = 15.9 Hz, 1H, 2'-H), 4.02 (ddd, *J* = 8.6, 8.6, 4.5 Hz, 1H, 5-H), 3.90 (ddd, *J* = 8.6, 7.9, 7.6 Hz, 1H, 5-H), 3.85 (s, 3H, 4''-OCH_3), 3.24 (dd, *J* = 8.5, 8.2 Hz, 1H, 3-H), 2.55 (dddd, *J* = 12.7, 8.6, 8.5, 7.6 Hz, 1H, 4-H), 2.10 (dddd, *J* = 12.7, 8.2, 7.9, 4.5 Hz, 1H, 4-H), 1.48 (s, 3H, 2-CH_3), 1.09 (s, 3H, 2-CH_3); δ_C($CDCl_3$, 101 MHz): 198.4 (C-1'), 161.7 (C-4''), 142.9 (C-3'), 130.2 (C-2''), 127.0 (C-1''), 123.5 (C-2'), 114.4 (C-3''), 81.9 (C-2), 65.5 (C-5), 58.8 (C-3), 55.4 (4''-OCH_3), 28.9 (2-CH_3), 28.8 (C-4), 23.5 (2-CH_3); **HRMS** (ESI) calculated for $C_{16}H_{20}NaO_3$ $[M+Na]^+$ 283.1305, found 283.1302.

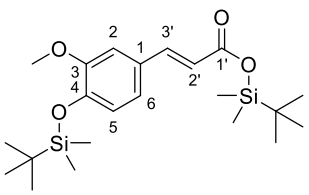
(*E*)-3-(4-Hydroxy-3-methoxyphenyl)acrylic acid[217] **(ferulic acid) (4.104)**



Vanillin (**4.103**) (989 mg, 6.50 mmol) and malonic acid (1.49 g, 14.3 mmol) were suspended in pyridine (1.05 mL, 13.0 mmol), toluene (1.5 mL) and aniline (70 μL) and refluxed for 3 h. The resultant solution was cooled, poured into 2M $HCl_{(aq)}$, the precipitate collected and dried in a vacuum oven to yield the title compound as an off-white solid (1.12 g, 88%). m.p. 170 °C.

υ_{max} (cm^{-1}): 3433 (OH), 1662 (C=O), 1598 (C=C), 1513, 1267 (C-O); δ_H(DMSO-d_6, 400 MHz): 9.53 (br. s, 1H), 7.48 (d, *J* = 15.9 Hz, 1H, 3'-H), 7.27 (d, *J* = 2.0 Hz, 1H, 2-H), 7.08 (dd, *J* = 8.2, 2.0 Hz, 1H, 6-H), 6.78 (d, *J* = 8.2 Hz, 1H, 5-H), 6.36 (d, *J* = 15.9 Hz, 1H, 2'-H), 3.81 (s, 3H, OCH_3); δ_C(DMSO-d_6, 101 MHz): 168.0 (C-1'), 149.1 (C-3), 147.9 (C-4), 144.5 (C-3'), 125.7 (C-1'), 122.8 (C-6), 115.6 (C-2'), 115.5 (C-5), 111.1 (C-2), 55.7 (OCH_3); **HRMS** (ESI) calculated for $C_{10}H_9O_4$ $[M-H]^-$ 193.0506, found 193.0503.

***tert*-Butyldimethylsilyl (*E*)-3-(4-((tert-butyldimethylsilyl)oxy)-3-methoxyphenyl)acrylate**[225]

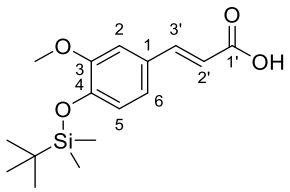


To a suspension of (*E*)-3-(4-hydroxy-3-methoxyphenyl)acrylic acid (**4.104**) (800 mg, 4.12 mmol) in anhydrous CH_2Cl_2 (12 mL) was added TBSCl (1.55

g, 10.3 mmol) and diisopropylethylamine (2.15 mL, 12.4 mmol) and the resultant solution stirred for 16 h at room temperature. The solution was diluted with CH_2Cl_2 (50 mL) and washed with sat. $NaHCO_{3(aq)}$ (50 mL) and 2M $HCl_{(aq)}$ (50 mL) successively. The organic phase was dried over $MgSO_4$, filtered and concentrated under reduced pressure. Purification by flash column chromatography (20% EtOAc/Petrol) yield the title compound as a white solid (1.57 g, 90%). m.p. 53 °C.

υ_{max} (cm^{-1}): 2929, 1688 (C=O), 1509, 1253 (C-O); δ_H($CDCl_3$, 400 MHz): 7.55 (d, *J* = 15.9 Hz, 1H, 3'-H), 7.06 – 7.00 (m, 2H, 2-H and 6-H), 6.88 – 6.83 (m, 1H, 5-H), 6.27 (d, *J* = 15.9 Hz, 1H, 2'-H), 3.85 (s, 3H, OCH_3), 1.00 (s, 18H, $SiC(CH_3)_3$), 0.34 (s, 6H, $Si(CH_3)_2$), 0.18 (s, 6H, $Si(CH_3)_2$); δ_C($CDCl_3$, 101 MHz): 167.2 (C-1'), 151.2 (C-3), 147.5 (C-4), 145.2 (C-3'), 128.3 (C-1), 122.3 (C-6), 121.1 (C-5), 117.8 (C-2'), 110.8 (C-2), 55.5 (OCH_3), 25.7 ($SiC(\underline{C}H_3)_3$), 25.7 ($SiC(\underline{C}H_3)_3$), 18.5 ($Si\underline{C}(CH_3)_3$), 17.8 ($Si\underline{C}(CH_3)_3$), −4.6 ($Si(CH_3)_2$), −4.7 ($Si(CH_3)_2$); **HRMS** (ESI) calculated for $C_{22}H_{39}O_4Si_2$ $[M+H]^+$ 423.2381, found 423.2379.

(*E*)-3-(4-((*tert*-Butyldimethylsilyl)oxy)-3-methoxyphenyl)acrylic acid[225] **(4.105)**

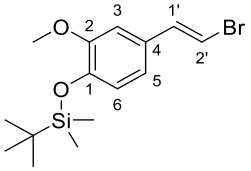


To a solution of tert-butyldimethylsilyl (*E*)-3-(4-((tert-butyldimethylsilyl)oxy)-3-methoxyphenyl)acrylate (1.40 g, 3.31 mmol) in THF (15 mL) and water (3 mL) was added K_2CO_3 (1.14 g, 8.28 mmol) and the resultant solution stirred for 1.5 h at room temperature. Volatiles were removed under reduced pressure and the residue extracted between EtOAc (100 mL) and water (100 mL). The organic phase was dried over $MgSO_4$,

filtered and concentrated under reduced pressure to yield the title compound as a pale yellow solid (988 mg, 97%). m.p. 135 °C (lit: 150-152 °C).[237]

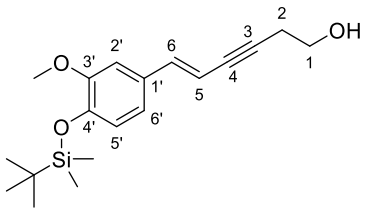
υ_{max} (cm^{-1}): 2928 (OH), 1678 (C=O), 1508, 1285 (C-O); δ_H($CDCl_3$, 400 MHz): 7.75 (d, *J* = 15.9 Hz, 1H, 3'-H), 7.11 – 7.05 (m, 2H, 2-H and 6-H), 6.92 – 6.85 (m, 1H, 5-H), 6.34 (d, *J* = 15.9 Hz, 1H, 2'-H), 3.87 (s, 3H, OCH_3), 1.03 (s, 9H, $SiC(CH_3)_3$), 0.21 (s, 6H, $Si(CH_3)_2$); δ_C($CDCl_3$, 101 MHz): 172.5 (C-1'), 151.2 (C-3), 148.0 (C-4), 147.1 (C-3'), 127.9 (C-1), 122.7 (C-6), 121.1 (C-5), 114.9 (C-2'), 111.0 (C-2), 55.4 (OCH_3), 25.6 ($SiC(\underline{C}H_3)_3$), 18.5 ($Si\underline{C}(CH_3)_3$), −4.6 ($Si(CH_3)_2$); **HRMS** (ESI) calculated for $C_{16}H_{23}O_4Si$ $[M-H]^-$ 307.1371, found 307.1374.

(*E*)-(4-(2-Bromovinyl)-2-methoxyphenoxy)(*tert*-butyl)dimethylsilane (4.106)



To a solution of (*E*)-3-(4-((tert-butyldimethylsilyl)oxy)-3-methoxyphenyl)acrylic acid (**4.105**) (800 mg, 2.59 mmol) in anhydrous CH_2Cl_2 (20 mL) was added oxone (1.91 g, 3.11 mmol) and tetraethylammonium bromide (654 mg, 3.11 mmol). The resultant solution was stirred for 16 h at room temperature, diluted with CH_2Cl_2 (50 mL) and washed with water (50 mL). The organic phase was dried over $MgSO_4$, filtered and concentrated under reduced pressure. Purification by flash column chromatography (5% EtOAc/Petrol) yielded a yellow oil consisting of a mixture of the title compound and a hydrobromination byproduct **4.107** (10:3) which was used without further purification (647 mg).

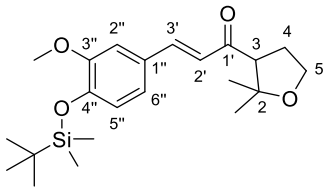
(*E*)-6-(4-((*tert*-Butyldimethylsilyl)oxy)-3-methoxyphenyl)hex-5-en-3-yn-1-ol (4.108)



Synthesised from crude (*E*)-(4-(2-bromovinyl)-2-methoxyphenoxy)(tert-butyl)dimethylsilane (**4.106**) (500 mg, 1.46 mmol) and 3-butyn-1-ol (220 µL, 2.91 mmol) following **General Procedure 4.1** at 50 °C for 2 h. Purification by flash column chromatography (50% EtOAc/Petrol) yielded the title compound as a yellow oil (391 mg, 81%).

υ_{max} (cm^{-1}): 3319 (OH), 2929, 1510, 1280 (C-O); δ_H($CDCl_3$, 400 MHz): 6.88 – 6.78 (m, 4H, 2'-H, 5'-H, 6'-H and 6-H), 6.00 (dt, *J* = 16.2, 2.3 Hz, 1H, 5-H), 3.82 (s, 3H, OCH_3), 3.78 (t, *J* = 6.3 Hz, 2H, 1-H), 2.66 (tdd, *J* = 6.3, 2.3, 0.7 Hz, 2H, 2-H), 1.77 (s, 1H, OH), 1.00 (s, 9H, $SiC(CH_3)_3$), 0.16 (s, 6H, $Si(CH_3)_2$); δ_C($CDCl_3$, 101 MHz): 151.0 (C-3'), 145.8 (C-4'), 140.9 (C-6), 130.3 (C-1'), 121.0 (Ar), 119.6 (Ar), 109.4 (C-2'), 106.0 (C-5), 87.9 (C-3), 81.9 (C-4), 61.2 (C-1), 55.4 (OCH_3), 25.7 ($SiC(\underline{C}H_3)_3$), 24.0 (C-2), 18.4 ($Si\underline{C}(CH_3)_3$), −4.6 ($Si(CH_3)_2$); **HRMS** (ESI) calculated for $C_{19}H_{29}O_3Si$ $[M+H]^+$ 333.1880, found 333.1880.

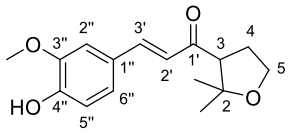
(*E*)-3-(4-((*tert*-Butyldimethylsilyl)oxy)-3-methoxyphenyl)-1-(2,2-dimethyltetrahydrofuran-3-yl)prop-2-en-1-one (4.109)



Synthesised from (*E*)-6-(4-((tert-butyldimethylsilyl)oxy)-3-methoxyphenyl)hex-5-en-3-yn-1-ol (**4.108**) (314 mg, 0.940 mmol) in acetone (5 mL) following **General Procedure 4.2** at 50 °C for 3 h. Purification by flash column chromatography (10-30% EtOAc/Petrol) yielded the title compound as a pale yellow oil (107 mg, 29%).

υ_{max} (cm^{-1}): 2929, 1681 (C=O), 1591 (C=C), 1507, 1283 (C-O); δ_H($CDCl_3$, 400 MHz): 7.55 (d, *J* = 15.9 Hz, 1H, 3'-H), 7.09 (dd, *J* = 8.2, 2.1 Hz, 1H, 6''-H), 7.05 (d, *J* = 2.1 Hz, 1H, 2''-H), 6.87 (d, *J* = 8.2 Hz, 1H, 5''-H), 6.68 (d, *J* = 15.9 Hz, 1H, 2'-H), 4.03 (ddd, *J* = 8.6, 8.6, 4.6 Hz, 1H, 5-H), 3.95 – 3.89 (m, 1H, 5-H), 3.86 (s, 3H, OCH_3), 3.27 (dd, *J* = 8.5, 8.2 Hz, 1H, 3-H), 2.55 (dddd, *J* = 12.7, 8.6, 8.5, 7.7 Hz, 1H, 4-H), 2.10 (dddd, *J* = 12.7, 8.2, 8.0, 4.6 Hz, 1H, 4-H), 1.49 (s, 3H, 2-CH_3), 1.10 (s, 3H, 2-CH_3), 1.01 (s, 9H, $SiC(CH_3)_3$), 0.19 (s, 6H, $Si(CH_3)_2$); δ_C($CDCl_3$, 101 MHz): 198.5 (C-1'), 151.3 (C-3'), 148.0 (C-4'), 143.4 (C-3'), 128.2 (C-1'), 124.0 (C-2'), 122.6 (C-6''), 121.2 (C-5''), 111.3 (C-2''), 81.9 (C-2), 65.5 (C-4), 58.5 (C-3), 55.5 (OCH_3), 28.9 (2-CH_3), 28.9 (C-4), 25.6 ($SiC(\underline{C}H_3)_3$), 23.6 (2-CH_3), 18.5 ($Si\underline{C}(CH_3)_3$), −4.6 ($Si(CH_3)_2$); **HRMS** (ESI) calculated for $C_{22}H_{35}O_4Si$ $[M+H]^+$ 391.2299, found 391.2300.

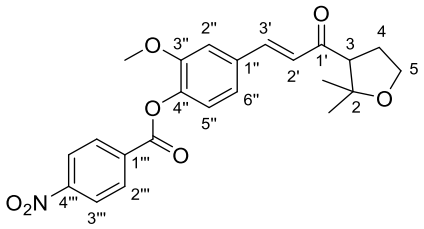
(*E*)-1-(2,2-Dimethyltetrahydrofuran-3-yl)-3-(4-hydroxy-3-methoxyphenyl)prop-2-en-1-one (4.110)



To a solution of (*E*)-tert-butyl(4-(2-(6,6-dimethyl-2,7-dioxabicyclo[3.2.0]heptan-1-yl)vinyl)-2-methoxyphenoxy)dimethylsilane (**4.109**) (27 mg , 0.070 mmol) in THF (1 mL) at room temperature was added TBAF (1M in THF, 104 µL, 0.100 mmol) and the resultant solution stirred for 5 min. The reaction mixture was diluted with EtOAc (25 mL) and washed with water (25 mL). The aqueous phase was washed with EtOAc (25 mL), the organic phases combined, dried over $MgSO_4$, filtered and concentrated under reduced pressure. Purification through a short silica pad (EtOAc) yielded the title compound as a pale yellow oil (18 mg, 94%).

υ_{max} (cm^{-1}): 3328 (OH), 2970, 1582 (C=O), 1512, 1272 (C-O); δ_H($CDCl_3$, 400 MHz): 7.57 (d, *J* = 15.8 Hz, 1H, 3'-H), 7.16 (dd, *J* = 8.2, 1.9 Hz, 1H, 6''-H), 7.08 (d, *J* = 1.9 Hz, 1H, 2''-H), 6.96 (d, *J* = 8.2 Hz, 1H, 5''-H), 6.69 (d, *J* = 15.8 Hz, 1H, 2'-H), 5.98 (s, 1H, OH), 4.05 (ddd, *J* = 8.5, 8.3, 4.6 Hz, 1H, 5-H), 3.97 (s, 3H, OCH_3), 3.92 (ddd, *J* = 8.3, 8.1, 8.0 Hz, 1H, 5-H), 3.28 (dd, *J* = 8.3, 8.2 Hz, 1H, 3-H), 2.57 (dddd, *J* = 12.7, 8.5, 8.3, 8.1 Hz, 1H, 4-H), 2.18 – 2.06 (dddd, *J* = 12.7, 8.2, 8.0, 4.6, 1H, 4-H), 1.50 (s, 3H, 2-CH_3), 1.12 (s, 3H, 2-CH_3); δ_C($CDCl_3$, 101 MHz): 198.5 (C-1'), 148.4 (C-3''), 146.8 (C-4''), 143.4 (C-3'), 126.9 (C-1''), 123.6 (C-2'), 123.4 (C-6''), 114.9 (C-5''), 109.8 (C-2''), 82.0 (C-2), 65.5 (C-5), 58.6 (C-3), 56.0 (OCH_3), 28.9 (2-CH_3), 28.9 (C-4), 23.6 (2-CH_3); **HRMS** (ESI) calculated for $C_{16}H_{21}O_4$ $[M+H]^+$ 277.1434, found 277.1435.

(*E*)-4-(3-(2,2-Dimethyltetrahydrofuran-3-yl)-3-oxoprop-1-en-1-yl)-2-methoxyphenyl 4-nitrobenzoate (4.102)



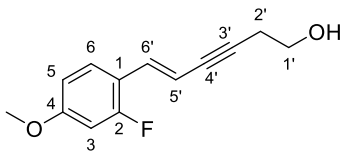
To a solution of (*E*)-4-(2-(6,6-dimethyl-2,7-dioxabicyclo[3.2.0]heptan-1-yl)vinyl)-2-methoxyphenol (**4.110**) (54 mg, 0.19 mmol) in CH_2Cl_2 (2.5 mL) at 0 °C was added triethylamine (54 µL, 0.39 mmol), followed by a solution of 4-nitrobenzoyl chloride (36 mg, 0.19 mmol) in CH_2Cl_2 (2.5 mL). The resultant solution was stirred at 0 °C for 5 min, then 25 min at room temperature. The reaction was then diluted with CH_2Cl_2 (50 mL) and washed with water (50 mL). The organic phase was dried over $MgSO_4$, filtered and concentrated under reduced pressure. Purification by flash column chromatography (50% EtOAc/Petrol) yielded the title compound as a crystalline white solid (58 mg, 70%). m.p. 132 °C.

υ_{max} (cm^{-1}): 2973, 1744 (C=O), 1607, 1254 (C-O); δ_H($CDCl_3$, 400 MHz): 8.42 – 8.35 (m, 4H, 2''-H and 3''-H), 7.61 (d, *J* = 15.9 Hz, 1H, 3'-H), 7.26 – 7.18 (m, 3H, 2''-H_1, 5''-H and 6''-H), 6.80 (d, *J* = 15.9 Hz, 1H, 2'-H), 4.05 (ddd, *J* = 8.7, 8.4, 4.5 Hz, 1H, 5-H), 3.93 (ddd, *J* = 8.7, 7.8, 7.9 Hz, 1H, 5-H), 3.89 (s, 3H, OCH_3), 3.28 (dd, *J* = 8.2, 8.0 Hz, 1H, 3-H), 2.58 (dddd, *J* = 12.6, 8.2, 8.4, 7.9 Hz, 1H, 4-H), 2.14 (dddd, *J* = 12.6, 8.0, 7.8, 4.5 Hz, 1H, 4-H), 1.50 (s, 3H, 2-CH_3), 1.12 (s, 3H, 2-CH_3); δ_C($CDCl_3$, 101 MHz): 198.5 (C-1'), 162.6 (CO_2R), 151.4 (C-3''), 151.0 (C-4'''), 142.2 (C-3'), 141.4 (C-4''), 134.5 (C-1'''), 133.9 (C-1''), 131.5 (C-2'''), 126.3 (C-2'), 123.7 (C-3'''), 123.2 (C-5''), 121.4 (C-6''), 111.9 (C-2''), 82.0 (C-2), 65.5 (C-5), 58.9 (C-3), 56.0 (OCH_3), 28.9 (2-CH_3), 28.8 (C-4), 23.6 (2'-CH_3);

HRMS (ESI) calculated for $C_{23}H_{23}NNaO_7$ $[M+Na]^+$ 448.1367, found 448.1371.

Crystal data and structure refinement for **4.102**	
Identification code	ABJEMC
Empirical formula	$C_{24}H_{25}Cl_2NO_7$ (**4.102** + CH_2Cl_2)
Formula weight	510.35
Temperature/K	120(2)
Crystal system	Triclinic
Space group	P-1
a/Å	6.85821(12)
b/Å	12.4948(3)
c/Å	15.2391(3)
α/°	72.5999(17)
β/°	78.0024(16)
γ/°	89.0863(16)
Volume/Å^3	1217.39(4)
Z	2
ρ_{calc}g/cm^3	1.392
μ/mm^{-1}	2.785
F(000)	532
Crystal size/mm^3	0.318 × 0.164 × 0.098
Radiation	CuKα (λ = 1.54184)
2Θ range for data collection/°	7.424 to 154.776
Index ranges	-8 ≤ h ≤ 8, -15 ≤ k ≤ 15, -19 ≤ l ≤ 18
Reflections collected	24810
Independent reflections	5011 [R_{int} = 0.0212, R_{sigma} = 0.0135]
Data/restraints/parameters	5011/442/394
Goodness-of-fit on F^2	1.053
Final R indexes [I>=2σ (I)]	R_1 = 0.0532, wR_2 = 0.1320
Final R indexes [all data]	R_1 = 0.0560, wR_2 = 0.1339
Largest diff. peak/hole / e Å^{-3}	0.49/-0.45

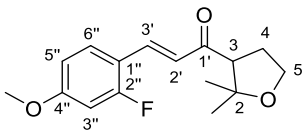
(*E*)-6-(2-Fluoro-4-methoxyphenyl)hex-5-en-3-yn-1-ol (4.111)



Synthesised from (*E*)-1-(2-bromovinyl)-2-fluoro-4-methoxybenzene (**4.79**) (700 g, 3.03 mmol) and 3-butyn-1-ol (459 µL, 6.06 mmol) following **General Procedure 4.1** at 50 °C for 3 h. Purification by flash column chromatography (20-40% EtOAc/Petrol) yielded the title compound as a yellow solid (628 mg, 94%). m.p. 49 °C.

υ_{max} (cm^{-1}): 3349 (OH), 2936, 1618 (C=C), 1504, 1274 (C-O); δ_H($CDCl_3$, 400 MHz): 7.32 (dd, *J* = 8.7, 8.7 Hz, 1H, 6-H), 6.96 (d, *J* = 16.4 Hz, 1H, 6'-H), 6.68 – 6.64 (m, 1H, 5-H), 6.60 (dd, *J* = 12.5, 2.5 Hz, 1H, 3-H), 6.10 (ddd, *J* = 16.4, 2.3, 2.2 Hz, 1H, 5'-H), 3.80 (s, 3H, OCH_3), 3.78 (t, *J* = 6.4 Hz, 2H, 1'-H), 2.66 (tdd, *J* = 6.4, 2.3, 0.6 Hz, 2H, 2'-H_2), 1.90 (s, 1H, OH); δ_C($CDCl_3$, 101 MHz): 160.9 (d, *J* = 251 Hz, C-2), 160.8 (d, *J* = 12 Hz), 133.3 (d, *J* = 2 Hz, C-6'), 127.6 (d, *J* = 5 Hz, C-6), 116.9 (d, *J* = 13 Hz), 110.5 (d, *J* = 3 Hz), 108.1 (d, *J* = 7 Hz, C-5'), 101.6 (d, *J* = 26 Hz, C-3), 88.4 (C-3'), 81.9 (C-4'), 61.1 (C-1'), 55.6 (OCH_3), 24.0 (C-2'); δ_F($CDCl_3$, 376 MHz): −114.6 (dd, *J* = 12.5, 8.7 Hz); **HRMS** (ESI) calculated for $C_{13}H_{14}FO_2$ $[M+H]^+$ 221.0972, found 221.0967.

(*E*)-1-(2,2-Dimethyltetrahydrofuran-3-yl)-3-(2-fluoro-4-methoxyphenyl)prop-2-en-1-one (4.112)

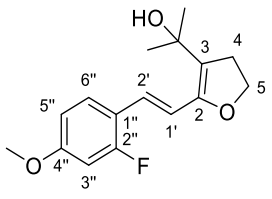


Synthesised from (*E*)-6-(2-fluoro-4-methoxyphenyl)hex-5-en-3-yn-1-ol (**4.111**) (150 mg, 0.68 mmol) in acetone (5 mL) following **General**

Procedure 4.2 at 50 °C for 16 h. Purification by flash column chromatography (10-30% EtOAc/Petrol) yielded the title compound as a pale yellow oil (63 mg, 33%) along with **4.113** as a pale yellow solid (14 mg, 7%).

υ_{max} (cm^{-1}): 2973, 1682 (C=O), 1598 (C=C), 1505, 1270 (C-O); δ_H($CDCl_3$, 400 MHz): 7.68 (d, *J* = 16.1 Hz, 1H, 3′-H), 7.50 (t, *J* = 8.6 Hz, 1H, 6′′-H), 6.80 (d, *J* = 16.1 Hz, 1H, 2′-H), 6.74 (dd, *J* = 8.6, 2.5 Hz, 1H, 5′′-H), 6.66 (dd, *J* = 12.5, 2.5 Hz, 1H, 3′′-H), 4.02 (ddd, *J* = 8.6, 8.6, 4.6 Hz, 1H, 5-H), 3.90 (ddd, *J* = 8.6, 7.9, 7.7 Hz, 1H, 5-H), 3.85 (s, 3H, OCH_3), 3.25 (dd, *J* = 8.5, 8.2 Hz, 1H, 3-H), 2.55 (dddd, *J* = 12.7, 8.6, 8.5, 7.7 Hz, 1H, 4-H), 2.10 (dddd, *J* = 12.7, 8.2, 7.9, 4.6 Hz, 1H, 4-H), 1.48 (s, 3H, 2-CH_3), 1.09 (s, 3H, 2-CH_3); δ_C($CDCl_3$, 101 MHz): 198.6 (C-1′), 162.8 (d, *J* = 12 Hz, C-4′′), 162.8 (d, *J* = 255 Hz, C-2′′), 135.7 (d, *J* = 2 Hz, C-3′), 130.3 (d, *J* = 5 Hz, C-6′′), 125.7 (d, *J* = 7 Hz, C-2′), 115.1 (d, *J* = 12 Hz, C-1′′), 110.9 (d, *J* = 3 Hz, C-5′′), 101.9 (d, *J* = 26 Hz, C-3′′), 81.9 (C-2), 65.5 (C-5), 58.7 (C-3), 55.7 (OCH_3), 28.9 (2-CH_3), 28.8 (C-4), 23.6 (2-CH_3); δ_F($CDCl_3$, 377 MHz): −111.0 (dd, *J* = 12.5, 8.5 Hz); **HRMS** (ESI) calculated for $C_{16}H_{20}FO_3$ $[M+H]^+$ 279.1391, found 279.1385.

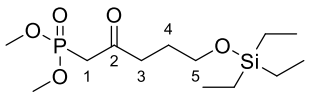
(*E*)-2-(2-(2-Fluoro-4-methoxystyryl)-4,5-dihydrofuran-3-yl)propan-2-ol (4.113)



υ_{max} (cm^{-1}): 2974, 1620 (C=C), 1505, 1274 (C-O); δ_H($CDCl_3$, 400 MHz): 7.32 (dd, *J* = 8.7, 8.7 Hz, 1H, 6′′-H), 7.05 (d, *J* = 15.2 Hz, 1H, 1′-H), 6.93 (d, *J* = 15.2 Hz, 1H, 2′-H), 6.70 (dd, *J* = 8.7, 2.6 Hz, 1H, 5′′-H), 6.64 (dd, *J* = 12.9, 2.6 Hz, 1H, 3′′-H), 3.92 (t, *J* = 6.9 Hz, 2H, 5-H), 3.82 (s, 3H,

OCH_3), 2.94 (t, *J* = 6.9 Hz, 2H, 4-H), 1.54 (s, 6H, CH_3); δ_C($CDCl_3$, 101 MHz): 161.4 (d, *J* = 251 Hz, C-2''), 160.5 (d, *J* = 11 Hz, C-4''), 147.2 (C-2), 129.3 (d, *J* = 5 Hz, C-6''), 124.1 (C-2'), 123.6 (C-3), 122.4 (d, *J* = 8 Hz, C-1'), 117.2 (d, *J* = 12 Hz, C-1''), 110.4 (d, *J* = 3 Hz, C-5''), 102.0 (d, *J* = 26 Hz, C-3''), 81.9 (**C**(CH_3)), 63.7 (C-5), 55.6 (OCH_3), 36.6 (C-4), 26.9 (CH_3); δ_F($CDCl_3$, 377 MHz): −113.8 (dd, *J* = 12.9, 8.7 Hz); **HRMS** (ESI) calculated for $C_{16}H_{18}FO_2$ $[M\text{-}OH]^+$ 261.1285, found 261.1278.

Dimethyl (2-oxo-5-((triethylsilyl)oxy)pentyl)phosphonate (4.123)

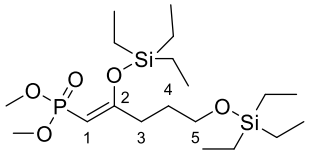


To a solution of dimethyl methylphosphonate (1.07 mL, 10.00 mmol) in anhydrous THF (15 mL) at −78 °C was added *n*-BuLi (4.61 mL, 10.00 mmol, 2.17 M in hexane) dropwise. The resultant suspension was stirred for 15 min and γ-butyrolactone (**4.122**) (860 mg, 10.00 mmol) in anhydrous THF (5 mL) added dropwise. The solution was stirred for 30 min, freshly prepared LDA (10.00 mL, 1M in THF) added and stirred for 30 min then triethylsilyl chloride (3.56 mL, 20.0 mL) added. The reaction was stirred for 16 h, at room temperature, quenched with sat. $NH_4Cl_{(aq)}$ (50 mL) and extracted with Et_2O (2 x 50 mL). The organic phases were combined, dried over $MgSO_4$, filtered and concentrated under reduced pressure. Purification by flash column chromatography (50-100% EtOAc/Petrol) yielded the title compound as a colourless oil (2.16 g, 67%) and the double-silylated byproduct **4.124** as a colourless oil (846 mg, 19%).

υ_{max} (cm^{-1}): 2954, 1714 (C=O), 1253 (C-O), 1025; δ_H($CDCl_3$, 400 MHz): 3.78 (d, *J* = 11.2 Hz, 6H, OCH_3), 3.61 (t, *J* = 6.1 Hz, 2H, 5-H_2), 3.11 (d, *J* = 22.6 Hz, 2H, 1-H_2), 2.69 (t, *J* = 7.2 Hz, 2H, 3-H_2), 1.81 (m, 2H, 4-H_2), 0.94 (t, *J* = 8.0 Hz, 9H, $SiCH_2C\underline{H}_3$), 0.57 (q, *J* = 8.0 Hz, 6H, $SiC\underline{H}_2CH_3$);

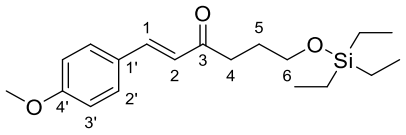
δ_C($CDCl_3$, 101 MHz): 201.8 (d, *J* = 6 Hz, C-2), 61.5 (C-5), 53.0 (d, *J* = 7 Hz, OCH_3), 41.3 (d, *J* = 128 Hz, C-1), 40.6 (d, *J* = 2 Hz, C-3), 26.6 (C-4), 6.7 ($SiCH_2\underline{C}H_3$), 4.3 ($Si\underline{C}H_2CH_3$); **HRMS** (ESI) calculated for $C_{15}H_{30}O_5PSi$ $[M+H]^+$ 325.15950, found 325.1594.

Dimethyl (*Z*)-(2,5-bis((triethylsilyl)oxy)pent-1-en-1-yl)phosphonate (4.124)



υ_{max} (cm^{-1}): 2953, 2876, 1605 (C=C), 1240 (C-O), 1027; δ_H($CDCl_3$, 400 MHz): 4.50 (d, *J* = 9.3 Hz, 1H, 1-H), 3.69 (d, *J* = 11.2 Hz, 6H, OCH_3), 3.64 (t, *J* = 6.9 Hz, 2H, 5-H_2), 2.54 (ddd, *J* = 9.3, 5.6, 1.3 Hz, 2H, 3-H_2), 1.83 – 1.75 (m, 2H, 4-H_2), 1.02 – 0.93 (m, 18H, $SiCH_2C\underline{H}_3$), 0.75 (q, *J* = 7.9 Hz, 6H, $SiC\underline{H}_2CH_3$), 0.60 (m, 6H, $SiC\underline{H}_2CH_3$); δ_C($CDCl_3$, 101 MHz): 173.8 (d, *J* = 23 Hz, C-2), 88.9 (d, *J* = 202 Hz, C-1), 62.5 (C-5), 51.9 (d, *J* = 5 Hz), 31.2 (d, *J* = 2 Hz, C-3), 30.5 (C-4), 6.8 ($SiCH_2\underline{C}H_3$), 6.5 ($SiCH_2\underline{C}H_3$), 4.7 ($Si\underline{C}H_2CH_3$), 4.4 ($Si\underline{C}H_2CH_3$); **HRMS** (ESI) calculated for $C_{19}H_{44}O_5PSi_2$ $[M+H]^+$ 439.2459 , found 439.2466.

(*E*)-1-(4-Methoxyphenyl)-6-((triethylsilyl)oxy)hex-1-en-3-one (4.125)

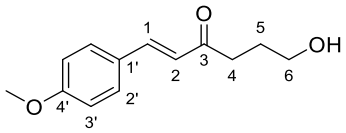


To a solution of dimethyl (2-oxo-5-((triethylsilyl)oxy)pentyl)phosphonate (**4.123**) (487 mg, 1.50 mmol) in anhydrous THF at −78 °C was added *n*-BuLi (0.76 mL, 1.65 mmol, 2.17 M in hexanes) dropwise. The resultant suspension was stirred for 30 min and a solution of anisaldehyde (**4.74**)

(225 mg, 1.65 mmol) in anhydrous THF (5 mL) added. The solution was stirred at 50 °C for 5 h, water (50 mL) added and the mixture extracted with Et_2O (2 x 50 mL). The organic phases were combined, dried over $MgSO_4$, filtered and concentrated under reduced pressure. Purification by flash column chromatography (10% EtOAc/Petrol) yielded the title compound as a colourless oil (283 mg, 56%).

υ_{max} (cm^{-1}): 2952, 2874, 1658 (C=O), 1598 (C=C), 1510, 1249 (C-O), 1171; δ_H($CDCl_3$, 400 MHz): 7.60 – 7.47 (m, 3H, 2'-H and 1-H), 6.96 – 6.89 (m, 2H, 3'-H), 6.64 (d, *J* = 16.1 Hz, 1H, 2-H), 3.85 (s, 3H, 4'-OCH_3), 3.68 (t, *J* = 6.2 Hz, 2H, 6-H_2), 2.75 (t, *J* = 7.3 Hz, 2H, 4-H_2), 1.91 (tt, *J* = 7.3, 6.2 Hz, 2H, 5-H_2), 0.97 (t, *J* = 7.9 Hz, 9H, $SiCH_2C\underline{H}_3$), 0.66 – 0.56 (q, *J* = 7.9 Hz, 6H, $SiC\underline{H}_2CH_3$); δ_C($CDCl_3$, 101 MHz): 200.3 (C-3), 161.5 (C-4'), 142.1 (C-1), 129.9 (C-2'), 127.2 (C-1'), 124.2 (C-2), 114.4 (C-3'), 62.0 (C-6), 55.4 (4'-OCH_3), 37.0 (C-4), 27.5 (C-5), 6.8 ($SiCH_2\underline{C}H_3$), 4.4 ($Si\underline{C}H_2CH_3$); **HRMS** (ESI) calculated for $C_{19}H_{31}O_3Si$ $[M+H]^+$ 335.2037, found 335.2041.

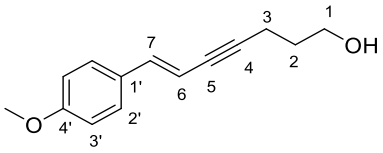
(*E*)-6-Hydroxy-1-(4-methoxyphenyl)hex-1-en-3-one (4.121)



To a solution of (*E*)-1-(4-methoxyphenyl)-6-((triethylsilyl)oxy)hex-1-en-3-one (**4.125**) (200 mg, 0.600 mmol) in THF (10 mL) was added TBAF (0.66 mL, 0.66 mmol, 1M in THF) at room temperature. The reaction was stirred for 5 min, diluted with Et_2O (50 mL) and washed with brine (50 mL). The aqueous phase was washed with Et_2O (50 mL), the organic phases combined, dried over $MgSO_4$, filtered and concentrated under reduced pressure. Purification through a short silica pad (Et_2O) yielded the title compound as a white solid (100 mg, 76%). m.p. 52 °C.

υ_{max} (cm^{-1}): 3396 (OH), 2933, 1645 (C=O), 1595 (C=C), 1510, 1248 (C-O), 1170; δ_H($CDCl_3$, 400 MHz): 7.65 – 7.46 (m, 3H, 2'-H and 1-H), 7.01 – 6.87 (m, 2H, 3'-H), 6.66 (d, *J* = 16.1 Hz, 1H, 2-H), 3.86 (s, 3H, 4'-OCH_3), 3.73 (t, *J* = 6.3 Hz, 2H, 6-H_2), 2.83 (t, *J* = 6.7 Hz, 2H, 4-H_2), 2.17 (s, 1H, OH), 1.96 (tt, *J* = 6.7, 6.3 Hz, 2H, 5-H_2); δ_C($CDCl_3$, 101 MHz): 200.6 (C-3), 161.6 (C-4'), 142.7 (C-1), 130.0 (C-2'), 127.0 (C-1'), 123.9 (C-2), 114.4 (C-3'), 62.4 (C-6), 55.4 (4'-OCH_3), 37.5 (C-4), 27.0 (C-5); **HRMS** (ESI) calculated for $C_{13}H_{17}O_3$ $[M+H]^+$ 221.1172, found 221.1178.

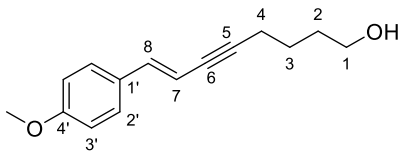
(*E*)-7-(4-Methoxyphenyl)hept-6-en-4-yn-1-ol (4.126)



Synthesised from (*E*)-1-(2-bromovinyl)-4-methoxybenzene (**4.69**) (253 mg, 1.19 mmol) and 4-pentyn-1-ol (221 µL, 2.37 mmol) following **General Procedure 4.1** at 50 °C for 16 h. Purification by flash column chromatography (30% EtOAc/Petrol) yielded the title compound as a white solid (275 mg, quant). m.p. 64 °C.

υ_{max} (cm^{-1}): 3628 (OH), 3008, 2956, 1606 (C=C), 1512, 1249 (C-O); δ_H($CDCl_3$, 400 MHz): 7.33 - 7.28 (m, 2H, 2'-H), 6.88 - 6.81 (m, 3H, 3'-H and 7-H), 6.01 (dt, *J* = 16.2, 2.2 Hz, 1H, 6-H), 3.84 - 3.78 (m, 5H, OCH_3 and 1-H_2), 2.51 (td, *J* = 6.7, 2.2 Hz, 2H, 3-H_2), 1.83 (2H, tt, *J* = 6.7, 6.5 Hz, 2-H_2); δ_C($CDCl_3$, 101 MHz): 159.8 (C-4'), 139.9 (C-7), 129.3, (C-1'), 127.4 (C-2'), 114.0 (C-3'), 106.1 (C-6), 90.9 (C-4), 80.6 (C-5), 61.9 (C-1), 55.3 (OCH_3), 31.4 (C-2), 16.3 (C-3); **HRMS** (ESI) calculated for $C_{14}H_{17}O_2$ $[M+H]^+$ 217.1223, found 217.1221.

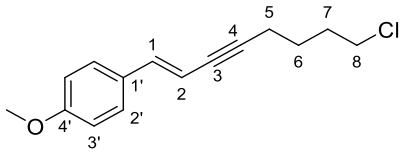
(*E*)-8-(4-Methoxyphenyl)oct-7-en-5-yn-1-ol (4.127)



Synthesised from (*E*)-1-(2-bromovinyl)-4-methoxybenzene (**4.69**) (750 mg, 3.52 mmol) and 5-hexyn-1-ol (760 µL, 7.04 mmol) following **General Procedure 4.1** at 50 °C for 1 h. Purification by flash column chromatography (30-40% EtOAc/Petrol) yielded the title compound as a pale yellow solid (727 mg, 90%). m.p. 74 °C.

υ_{max} (cm^{-1}): 3364 (OH), 2945, 1603 (C=C), 1514, 1248 (C-O); δ_H($CDCl_3$, 400 MHz): 7.33 – 7.28 (m, 2H, 2'-H), 6.88 – 6.79 (m, 3H, 8-H, 3'-H), 6.01 (dt, *J* = 16.2, 2.2 Hz, 1H, 7-H), 3.81 (s, 3H, OCH_3), 3.71 (t, *J* = 6.3 Hz, 2H, 1-H), 2.42 (td, *J* = 6.7, 2.2 Hz, 2H, 4-H), 1.78 – 1.61 (m, 4H, 2-H and 3-H), 1.41 (s, 1H, OH); δ_C($CDCl_3$, 101 MHz): 159.8 (C-4'), 139.7 (C-8), 129.3 (C-1'), 127.3 (C-2'), 114.1 (C-3'), 106.3 (C-7), 91.5 (C-5), 80.3 (C-6), 62.4 (C-1), 55.3 (OCH_3), 31.9 (C-2), 25.1 (C-3), 19.4 (C-4); **HRMS** (ESI) calculated for $C_{15}H_{19}O_2$ $[M+H]^+$ 231.1380, found 231.1377.

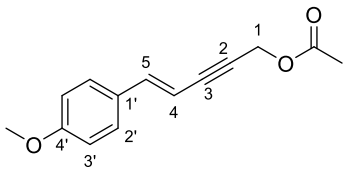
(*E*)-1-(8-Chlorooct-1-en-3-yn-1-yl)-4-methoxybenzene (4.128)



Synthesised from (*E*)-1-(2-bromovinyl)-4-methoxybenzene (**4.69**) (500 mg, 2.35 mmol) and 6-chlorohex-1-yne (569 µL, 4.69 mmol) following **General Procedure 4.1** at 50 °C for 16 h. Purification by flash column chromatography (0-2% Et_2O/Petrol) yielded the title compound as a pale yellow solid (727 mg, 90%). m.p. 40 °C.

υ_{max} (cm^{-1}): 2924, 1604 (C=C), 1510, 1247 (C-O); δ_H($CDCl_3$, 400 MHz): 7.34 – 7.28 (m, 2H, 2'-H), 6.88 – 6.80 (m, 3H, 1-H and 3'-H), 6.01 (dt, *J* = 16.2, 2.3 Hz, 1H, 2-H), 3.82 (s, 3H, 4'-OCH_3), 3.60 (t, *J* = 6.6 Hz, 2H, 8-CH_2), 2.43 (td, *J* = 6.9, 2.2 Hz, 2H, 5-H_2), 1.99 – 1.90 (m, 2H, 7-H_2), 1.77 – 1.68 (m, 2H, 6-H_2); δ_C($CDCl_3$, 101 MHz): 159.8 (C-4'), 139.9 (C-1), 129.3 (C-1'), 127.4 (C-2'), 114.1 (C-3'), 106.2 (C-2), 90.8 (C-4), 80.6 (C-3), 55.3 (4'-OCH_3), 44.6 (C-8), 31.6 (C-7), 26.0 (C-6), 18.9 (C-5); **HRMS** (ESI) calculated for $C_{15}H_{17}ClNaO$ $[M+Na]^+$ 271.0860, found 271.0851.

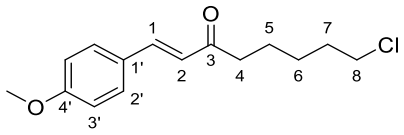
(*E*)-5-(4-Methoxyphenyl)pent-4-en-2-yn-1-yl acetate (4.129)



Synthesised from (*E*)-1-(2-bromovinyl)-4-methoxybenzene (**4.69**) (500 mg, 2.35 mmol) and propargyl acetate (466 µL, 4.69 mmol) following **General Procedure 4.1** at 50 °C for 16 h. Purification by flash column chromatography (10-20% Et_2O/Petrol) yielded the title compound as a pale yellow solid (516 mg, 96%). m.p. 53 °C.

υ_{max} (cm^{-1}): 2935, 1739 (C=O), 1604 (C=C), 1510, 1222 (C-O); δ_H($CDCl_3$, 400 MHz): 7.35 – 7.30 (m, 2H, 3'-H), 6.95 (d, *J* = 16.3 Hz, 1H, 5-H), 6.89 – 6.84 (m, 2H, 2'-H), 6.02 (dt, *J* = 16.3, 2.2 Hz, 1H, 4-H), 4.86 (dd, *J* = 2.2, 0.5 Hz, 2H, 1-H_2), 3.82 (s, 3H, 4'-OCH_3), 2.13 (s, 3H, $COCH_3$); δ_C($CDCl_3$, 101 MHz): 170.3 (C=O), 160.3 (C-4'), 142.3 (C-5), 128.7 (C-1'), 127.7 (C-2'), 114.1 (C-3'), 104.5 (C-4), 86.0 (C-3), 84.1 (C-2), 55.3 (4'-OCH_3), 53.0 (C-1), 20.8 (CH_3); **HRMS** (ESI) calculated for $C_{14}H_{14}NaO_3$ $[M+Na]^+$ 253.0835, found 253.0830.

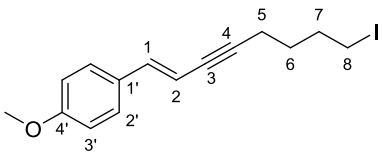
(*E*)-8-Chloro-1-(4-methoxyphenyl)oct-1-en-3-one (4.132)



Synthesised from (*E*)-1-(8-chlorooct-1-en-3-yn-1-yl)-4-methoxybenzene (**4.128**) (100 mg, 0.40 mmol) in acetone (5 mL) following **General Procedure 4.1** at 50 °C for 3 h. Purification by flash column chromatography (20% EtOAc/Petrol) yielded the title compound as a pale yellow oil (64 mg, 69%).

υ_{max} (cm^{-1}): 2935, 1604 (C=C), 1510, 1247 (C-O); δ_H($CDCl_3$, 400 MHz): 7.57 – 7.45 (m, 3H, 1-H and 2'-H), 6.99 – 6.86 (m, 2H, 3'-H), 6.63 (d, *J* = 16.1 Hz, 1H, 2-H), 3.84 (s, 3H, OCH_3), 3.55 (t, *J* = 6.8 Hz, 2H, 8-H_2), 2.67 (t, *J* = 7.3 Hz, 2H, 4-H_2), 1.82 (dq, *J* = 8.1, 6.8 Hz, 2H, 7-H_2), 1.76 – 1.66 (m, 2H, 5-H_2), 1.56 – 1.46 (m, 2H, 6-H_2); δ_C($CDCl_3$, 101 MHz): 200.0 (C-3), 161.5 (C-4'), 142.2 (C-1), 129.9 (C-2'), 127.1 (C-1), 123.9 (C-2), 114.4 (C-3'), 55.4 (OCH_3), 44.8 (C-8), 40.4 (C-4), 32.4 (C-7), 26.6 (C-6), 23.5 (C-5); **HRMS** (ESI) calculated for $C_{15}H_{20}ClO_2$ $[M+H]^+$ 267.1146, found 267.1141.

(*E*)-1-(8-Iodooct-1-en-3-yn-1-yl)-4-methoxybenzene (4.133)

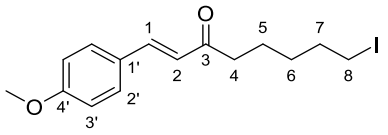


To a solution of (*E*)-1-(8-chlorooct-1-en-3-yn-1-yl)-4-methoxybenzene (**4.128**) (150 mg, 0.600 mmol) in acetone (5 mL) was added sodium iodide (452 mg, 3.02 mmol) and the resultant mixture refluxed for 40 h. The reaction was cooled, volatiles removed under reduced pressure and the residue extracted between Et_2O (2 x 50 mL) and water (50 mL). The organic

phases were combined, dried over $MgSO_4$, filtered and concentrated under reduced pressure to yield the title compound as a yellow solid (142 mg, 69%). m.p. 57 °C.

υ_{max} (cm^{-1}): 2931, 1603 (C=C), 1509, 1247 (C-O); δ_H($CDCl_3$, 400 MHz): 7.33 – 7.29 (m, 2H, 2'-H), 6.88 – 6.80 (m, 3H, 1-H and 3'-H), 6.01 (dt, *J* = 16.2, 2.3 Hz, 1H, 2-H), 3.82 (s, 3H, OCH_3), 3.25 (t, *J* = 6.9 Hz, 2H, 8-H), 2.42 (td, *J* = 6.9, 2.3 Hz, 2H, 5-H), 2.05 – 1.94 (m, 2H, 7-H), 1.74 – 1.64 (m, 2H, 6-H); δ_C($CDCl_3$, 101 MHz): 159.8 (C-4'), 139.9 (C-1), 129.3 (C-1'), 127.3 (C-2'), 114.1 (C-3'), 106.1 (C-2), 90.8 (C-4), 80.6 (C-3), 55.3 (OCH_3), 32.5 (C-7), 29.5 (C-6), 18.6 (C-5), 6.2 (C-8); **HRMS** (ESI) calculated for $C_{15}H_{17}INaO$ $[M+Na]^+$ 363.0216, found 363.0198.

(*E*)-8-Iodo-1-(4-methoxyphenyl)oct-1-en-3-one (4.134)

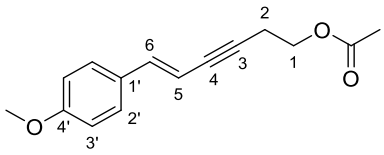


Synthesised from (*E*)-1-(8-iodooct-1-en-3-yn-1-yl)-4-methoxybenzene (**4.133**) (100 mg, 0.29 mmol) in acetone (5 mL) following **General Procedure 4.2** at 50 °C for 3 h. Purification by flash column chromatography (20% EtOAc/Petrol) yielded the title compound as a pale yellow oil (63 mg, 60%).

υ_{max} (cm^{-1}): 2930, 1649 (C=O), 1604 (C=C), 1250 (C-O); δ_H($CDCl_3$, 400 MHz): 7.56 – 7.49 (m, 3H, 1-H and 2'-H), 6.95 – 6.90 (m, 2H, 3'-H), 6.63 (d, *J* = 16.1 Hz, 1H, 2-H), 3.85 (s, 3H, OCH_3), 3.21 (t, *J* = 7.1 Hz, 2H, 8-H), 2.67 (t, *J* = 7.4 Hz, 2H, 4-H), 1.88 (tt, *J* = 7.1, 7.1 Hz, 2H, 7-H), 1.78 – 1.65 (m, 2H, 5-H), 1.54 – 1.43 (m, 2H, 6-H); δ_C($CDCl_3$, 101 MHz): 200.0 (C-3), 161.6 (C-4'), 142.3 (C-1), 130.0 (C-2'), 127.1 (C-1'), 124.0 (C-2), 114.4 (C-3'), 55.4 (OCH_3), 40.4 (C-4), 33.3 (C-7), 30.2 (C-6), 23.2 (C-5),

6.8 (C-8); **HRMS** (ESI) calculated for $C_{15}H_{20}IO_2$ $[M+H]^+$ 359.0503, found 359.0497.

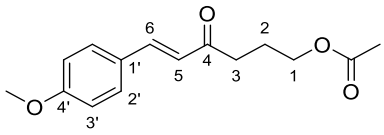
(*E*)-6-(4-Methoxyphenyl)hex-5-en-3-yn-1-yl acetate (4.135)



To a solution of (*E*)-6-(4-methoxyphenyl)hex-5-en-3-yn-1-ol (**4.98**) (200 mg, 0.990 mmol) and acetic anhydride (140 µL, 1.48 mmol) in CH_2Cl_2 at 0 °C was added triethylamine (410 µL, 2.97 mmol) and DMAP (12 mg, 0.10 mmol). The resultant solution was stirred at room temperature for 1 h and diluted with CH_2Cl_2 (50 mL). The solution was washed with sat. $NaHCO_{3\,(aq)}$ (50 mL), the organic phase dried over anhydrous $MgSO_4$, filtered and concentrated under reduced pressure. Purification through a short pad of silica (Et_2O) yielded the title compound as a yellow solid (230 mg, 95%). m.p. 42 °C.

υ_{max} (cm^{-1}): 2957, 1736 (C=O), 1603 (C=C), 1510, 1236 (C-O); δ_H($CDCl_3$, 400 MHz): 7.33 – 7.29 (m, 2H, 2'-H), 6.89 – 6.83 (m, 3H, 6-H and 3'-H), 6.00 (dt, *J* = 16.3, 2.2 Hz, 1H, 5-H), 4.21 (t, *J* = 6.9 Hz, 2H, 1-H), 3.82 (s, 3H, OCH_3), 2.71 (tdd, *J* = 6.9, 2.2, 0.6 Hz, 2H, 2-H), 2.10 (s, 3H, $COCH_3$); δ_C($CDCl_3$, 101 MHz): 170.8 ($COCH_3$), 159.9 (C-4'), 140.5 (C-6), 129.1 (C-1'), 127.4 (C-2'), 114.1 (C-3'), 105.7 (C-5), 86.9 (C-3), 81.3 (C-4), 62.5 (C-1), 55.3 (OCH_3), 20.9 ($COCH_3$), 20.1 (C-2); **HRMS** (ESI) calculated for $C_{15}H_{16}NaO_3$ $[M+Na]^+$ 267.0992, found 267.0991.

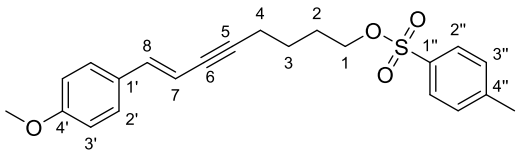
(*E*)-6-(4-Methoxyphenyl)-4-oxohex-5-en-1-yl acetate (4.138)



Synthesised from (*E*)-6-(4-methoxyphenyl)hex-5-en-3-yn-1-yl acetate (**4.135**) (100 mg, 0.410 mmol) in acetone (5 mL) following **General Procedure 4.2** at 50 °C for 3 h. Purification by flash column chromatography (20% EtOAc/Petrol) yielded the title compound as a pale yellow oil (33 mg, 43%).

υ_{max} (cm^{-1}): 2966, 1726 (C=O), 1683 (C=O), 1599 (C=C), 1513, 1253 (C-O); δ_H($CDCl_3$, 400 MHz): 7.58 – 7.47 (m, 3H, 6-H and 2'-H), 6.96 – 6.89 (m, 2H, 3'-H), 6.64 (d, *J* = 16.1 Hz, 1H, 5-H), 4.14 (t, *J* = 6.4 Hz, 2H, 1-H), 3.85 (s, 3H, OCH_3), 2.74 (t, *J* = 7.3 Hz, 2H, 3-H), 2.08 – 1.99 (m, 5H, 2-H and $COCH_3$); δ_C($CDCl_3$, 101 MHz): 199.0 (C-4), 171.0 ($COCH_3$), 161.6 (C-4'), 142.4 (C-6), 130.0 (C-2'), 127.0 (C-1'), 123.8 (C-5), 114.4 (C-3'), 63.8 (C-1), 55.4 (OCH_3), 36.9 (C-3), 23.2 (C-2), 20.9 ($COCH_3$); **HRMS** (ESI) calculated for $C_{15}H_{19}O_4$ $[M+H]^+$ 263.1278, found 263.1280.

(*E*)-8-(4-Methoxyphenyl)oct-7-en-5-yn-1-yl 4-methylbenzenesulfonate (4.136)

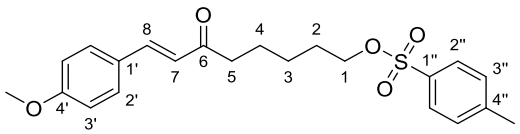


To a solution of (*E*)-8-(4-methoxyphenyl)oct-7-en-5-yn-1-ol (**4.127**) (100 mg, 0.430 mmol) and DMAP (5 mg, 0.04 mmol) in CH_2Cl_2 was added triethylamine (151 µL, 1.09 mmol) followed by tosyl chloride (91 mg, 0.48 mmol). The resultant solution was stirred for 16 h, diluted with CH_2Cl_2 (50 mL) and washed with water (50 mL). The organic phase was dried over

$MgSO_4$, filtered and concentrated under reduced pressure. Purification by flash column chromatography (20% EtOAc/Petrol) yielded the title compound as a colourless oil (113 mg, 68%).

υ_{max} (cm^{-1}): 2937, 1604 (C=C), 1511, 1249 (C-O), 1175; δ_H($CDCl_3$, 400 MHz): 7.84 – 7.78 (m, 2H, 2''-H), 7.38 – 7.32 (m, 2H, 3''-H), 7.32 – 7.28 (m, 2H, 2'-H), 6.88 – 6.83 (m, 2H, 3'-H), 6.81 (d, *J* = 16.2 Hz, 1H, 8-H), 5.97 (dt, *J* = 16.2, 2.3 Hz, 1H, 7-H), 4.09 (t, *J* = 6.2 Hz, 2H, 1-H), 3.82 (s, 3H, OCH_3), 2.45 (s, 3H, 4''-CH_3), 2.35 (td, *J* = 6.8, 2.3 Hz, 2H, 4-H), 1.82 (tt, *J* = 8.1, 6.2 Hz, 2H, 2-H), 1.65 – 1.55 (m, 2H, 3-H); δ_C($CDCl_3$, 101 MHz): 159.8 (C-4'), 144.7 (C-1''), 139.9 (C-8), 133.1 (C-4''), 129.8 (C-3''), 129.3 (C-1'), 127.9 (C-2''), 127.3 (C-2'), 114.1 (C-3'), 106.1 (C-7), 90.5 (C-5), 80.7 (C-6), 70.0 (C-1), 55.3 (OCH_3), 27.9 (C-2), 24.6 (C-3), 21.6 (4''-CH_3), 18.9 (C-4); **HRMS** (ESI) calculated for $C_{22}H_{24}NaO_4S$ $[M+Na]^+$ 407.1288, found 407.1283.

(*E*)-8-(4-Methoxyphenyl)-6-oxooct-7-en-1-yl 4-methylbenzenesulfonate (4.139)

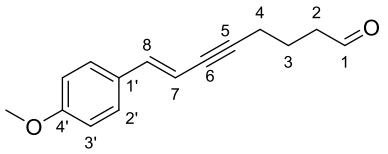


Synthesised from (*E*)-8-(4-methoxyphenyl)oct-7-en-5-yn-1-yl 4-methylbenzenesulfonate (**4.136**) (100 mg, 0.28 mmol) in acetone (5 mL) following **General Procedure 4.2** at 50 °C for 3 h. Purification by flash column chromatography (10-20% EtOAc/Petrol) yielded the title compound as a pale yellow oil (47 mg, 42%).

υ_{max} (cm^{-1}): 2936, 1655 (C=O), 1597 (C=C), 1510, 1171; δ_H($CDCl_3$, 400 MHz): 7.82 – 7.76 (m, 2H, 2''-H), 7.53 – 7.47 (m, 3H, 8-H and 2'-H), 7.37 – 7.31 (m, 2H, 3''-H), 6.95 – 6.89 (m, 2H, 3'-H), 6.60 (d, *J* = 16.2 Hz, 1H,

7-H), 4.03 (t, *J* = 6.4 Hz, 2H, 1-H), 3.85 (s, 3H, OCH_3), 2.61 (t, *J* = 7.3 Hz, 2H, 5-H), 2.44 (s, 3H, 4''-CH_3), 1.73 – 1.57 (m, 4H, 2-H and 4-H), 1.44 – 1.32 (m, 2H, 3-H); δ_C($CDCl_3$, 101 MHz): 199.9 (C-6), 161.5 (C-4'), 144.7 (C-1''), 142.3 (C-8), 133.1 (C-4''), 129.9 (C-2'), 129.8 (C-3''), 127.8 (C-2''), 127.1 (C-1'), 123.9 (C-7), 114.4 (C-3'), 70.3 (C-1), 55.4 (OCH_3), 40.3 (C-5), 28.7 (C-2), 25.1 (C-3), 23.6 (C-4), 21.6 (4''-CH_3); **HRMS** (ESI) calculated for $C_{22}H_{27}O_5S$ $[M+H]^+$ 403.1574, found 403.1573.

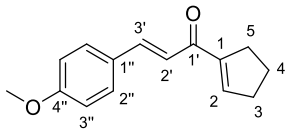
(*E*)-8-(4-Methoxyphenyl)oct-7-en-5-ynal (4.140)



To a solution of (*E*)-8-(4-methoxyphenyl)oct-7-en-5-yn-1-ol (**4.127**) (200 mg, 0.870 mmol) in CH_2Cl_2 (10 mL) at 0 °C was added Dess-Martin periodinane (442 mg, 1.04 mmol) and the resultant solution stirred for 1 h at 0 °C. The reaction was diluted with CH_2Cl_2 (50 mL) and washed with water (50 mL). The organic phase was dried over $MgSO_4$, filtered and concentrated under reduced pressure. Purification through a short silica pad (Et_2O) yielded the title compound as a colourless oil (189 mg, 95%).

υ_{max} (cm^{-1}): 2835, 1719 (C=O), 1603 (C=C), 1509, 1245 (C-O); δ_H($CDCl_3$, 400 MHz): 9.84 (t, *J* = 1.4 Hz, 1H, 1-H), 7.34 – 7.28 (m, 2H, 2'-H), 6.88 – 6.80 (m, 3H, 8-H and 3'-H), 6.00 (dt, *J* = 16.2, 2.2 Hz, 1H, 7-H), 3.82 (s, 3H, OCH_3), 2.63 (td, *J* = 7.2, 1.4 Hz, 2H, 2-H), 2.46 (td, *J* = 6.7, 2.2 Hz, 2H, 4-H), 1.90 (tt, *J* = 7.2, 6.7 Hz, 2H, 3-H); δ_C($CDCl_3$, 101 MHz): 201.9 (C-1), 159.9 (C-4'), 140.0 (C-8), 129.2 (C-1'), 127.4 (C-2'), 114.1 (C-3'), 106.0 (C-7), 90.2 (C-5), 81.1 (C-6), 55.3 (OCH_3), 42.8 (C-2), 21.2 (C-3), 19.0 (C-4); **HRMS** (ESI) calculated for $C_{15}H_{17}O_2$ $[M+H]^+$ 229.1223, found 229.1217.

(*E*)-1-(Cyclopent-1-en-1-yl)-3-(4-methoxyphenyl)prop-2-en-1-one (4.141)



Synthesised from (*E*)-8-(4-methoxyphenyl)oct-7-en-5-ynal (**4.140**) (71 mg, 0.31 mmol) in acetone (4 mL) with radical cation salt **4.01** (25 mg, 0.030 mmol) following **General Procedure 4.2** at 50 °C for 3 h. Purification by flash column chromatography (10% EtOAc/Petrol) yielded the title compound as a pale yellow solid (30 mg, 43%). m.p. 85 °C.

υ_{max} (cm^{-1}): 2954, 1646 (C=O), 1586 (C=C), 1510, 1254 (C-O); δ_H($CDCl_3$, 400 MHz): 7.63 (d, *J* = 15.7 Hz, 1H, 3'-H), 7.58 – 7.52 (m, 2H, 2''-H), 7.16 (d, *J* = 15.7 Hz, 1H, 2'-H), 6.95 – 6.90 (m, 2H, 3''-H), 6.86 (td, *J* = 2.7, 1.3 Hz, 1H, 2-H), 3.86 (s, 3H, 4''-OCH_3), 2.72 – 2.60 (m, 4H, 3-H and 5-H), 2.03 – 1.94 (m, 2H, 4-H); δ_C($CDCl_3$, 101 MHz): 188.0 (C-1'), 161.3 (C-4''), 146.9 (C-1), 143.0 (C-2), 141.9 (C-3'), 129.9 (C-2''), 127.8 (C-1'), 120.4 (C-2), 114.3 (C-3''), 55.4 (4''-OCH_3), 34.1, 31.2, 22.8 (C-4); **HRMS** (ESI) calculated for $C_{15}H_{17}O_2$ $[M+H]^+$ 229.1223, found 229.1221.

Chapter 5 : References

(1) Kolb, H. C.; Finn, M. G.; Sharpless, K. B. *Angew. Chem. Int. Ed.* **2001**, *40* (11), 2004–2021.
(2) Bohacek, R. S.; McMartin, C.; Guida, W. C. *Med. Res. Rev.* **1996**, *16* (1), 3–50.
(3) Moses, J. E.; Moorhouse, A. D. *Chem. Soc. Rev.* **2007**, *36* (8), 1249–1262.
(4) Kolb, H. C.; Sharpless, K. B. *Drug Discov. Today* **2003**, *8* (24), 1128–1137.
(5) Xi, W.; Scott, T. F.; Kloxin, C. J.; Bowman, C. N. *Adv. Funct. Mater.* **2014**, *24* (18), 2572–2590.
(6) Rostovtsev, V. V.; Green, L. G.; Fokin, V. V.; Sharpless, K. B. *Angew. Chem. Int. Ed.* **2002**, *41* (14), 2596–2599.
(7) Tornøe, C. W.; Christensen, C.; Meldal, M. *J. Org. Chem.* **2002**, *67* (9), 3057–3064.
(8) Moorhouse, A. D.; Spiteri, C.; Sharma, P.; Zloh, M.; Moses, J. E. *Chem. Commun.* **2011**, *47* (1), 230–232.
(9) Ritson, D. J.; Moses, J. E. *Tetrahedron* **2012**, *68* (1), 197–203.
(10) McKay, C. S.; Finn, M. G. *Chem. Biol.* **2014**, *21* (9), 1075–1101.
(11) Gierlich, J.; Burley, G. A.; Gramlich, P. M. E.; Hammond, D. M.; Carell, T. *Org. Lett.* **2006**, *8* (17), 3639–3642.
(12) Dong, J.; Krasnova, L.; Finn, M. G.; Sharpless, K. B. *Angew. Chem. Int. Ed.* **2014**, *53*, 9430–9448.
(13) Bellale, E. V.; Chaudhari, M. K.; Akamanchi, K. G. *Synthesis* **2009**, No. 19, 3211–3213.
(14) Lalonde, M. P.; McGowan, M. A.; Rajapaksa, N. S.; Jacobsen, E. N. *J. Am. Chem. Soc.* **2013**, *135* (5), 1891–1894.
(15) Nelson, D. L.; Cox, M. *Principles of Biochemistry*; 2005.
(16) Braun, P.; Gingras, A. C. *Proteomics* **2012**, *12* (10), 1478–1498.
(17) Shi, Y. *Cell* **2014**, *159* (5), 995–1014.
(18) Markwick, P. R. L.; Malliavin, T.; Nilges, M. *PLoS Comput. Biol.* **2008**, *4* (9), doi:10.1371/journal.pcbi.1000168.
(19) Keskin, O.; Tuncbag, N.; Gursoy, A. *Chem. Rev.* **2016**, *116*, 4884–4909.
(20) Sharp, J. S.; Becker, J. M.; Hettich, R. L. *Anal. Biochem.* **2003**, *313* (2), 216–225.
(21) Kendrew, J. C.; Bodo, G.; Dintzis, H. M.; Parrish, R. G.; Wyckoff, H.; Phillips, D. C. *Nature* **1958**, *181*, 662–666.
(22) Berman, H. M.; Westbrook, J.; Feng, Z.; Gilliland, G.; Bhat, T. N.; Weissig, H.; Shindyalov, I. N.; Bourne, P. E. *Nucleic Acids Res.* **2000**, *28* (1), 235–242.
(23) Wüthrich, K. *J. Biol. Chem.* **1990**, *265* (36), 22059–22062.
(24) Wüthrich, K. *Nat. Struct. Biol.* **2001**, *8* (11), 923–925.
(25) Williamson, M. P.; Havel, T. F.; Wüthrich, K. *J. Mol. Biol.* **1985**, *182* (2), 295–315.
(26) Gardner, K. H.; Kay, L. E. *Annu. Rev. Biophys. Biomol. Struct.* **1998**, *27* (1), 357–406.
(27) Kay, L. E. *J. Magn. Reson.* **2005**, *173* (2), 193–207.
(28) Tugarinov, V.; Muhandiram, R.; Ayed, A.; Kay, L. E. *J. Am. Chem. Soc.* **2002**, *124* (34), 10025–10035.
(29) Pan, Y.; Ruan, X.; Valvano, M. A.; Konermann, L. *J. Am. Soc. Mass Spectrom.* **2012**, *23* (5), 889–898.
(30) de Hoffmann, E.; Stroobant, V. *Mass Spectrometry: Principles and*

Applications, Third Edit.; 2007.
(31) Fenn, J. B.; Mann, M.; Meng, C. K. A. I.; Wong, S. F.; Whitehouse, C. M. *Science* **1989**, *246*, 64–71.
(32) Demarque, D. P.; Crotti, A. E. M.; Vessecchi, R.; Lopes, J. L. C.; Lopes, N. P. *Nat. Prod. Rep.* **2016**, *33* (3), 432–455.
(33) Mitchell Wells, J.; McLuckey, S. A. *Methods Enzymol.* **2005**, *402* (1993), 148–185.
(34) Sleno, L.; Volmer, D. A. *J. Mass Spectrom.* **2004**, *39* (10), 1091–1112.
(35) Cravatt, B. F.; Wright, A. T.; Kozarich, J. W. *Annu. Rev. Biochem.* **2008**, *77*, 383–414.
(36) Willems, L. I.; Overkleeft, H. S.; Kasteren, S. I. Van. *Bioconjug. Chem.* **2014**, *25*, 1181–1191.
(37) Greenbaum, D.; Medzihradszky, K. F.; Burlingame, A.; Bogyo, M. *Chem. Biol.* **2000**, *7* (8), 569–581.
(38) Xu, G.; Chance, M. R. *Chem. Rev.* **2007**, *107* (8), 3514–3543.
(39) Wang, L.; Chance, M. R. *Anal. Chem.* **2011**, *83* (19), 7234–7241.
(40) Englander, S. W.; Mayne, L.; Bai, Y.; Sosnick, T. R. *Protein Sci.* **1997**, *6* (5), 1101–1109.
(41) Tsutsui, Y.; Wintrode, P. L. *Curr. Med. Chem.* **2007**, *14* (22), 2344–2358.
(42) Tuma, R.; Coward, L. U.; Kirk, M. C.; Barnes, S.; Prevelige, P. E. *J. Mol. Biol.* **2001**, *306* (3), 389–396.
(43) Eyles, S. J.; Kaltashov, I. A. *Methods* **2004**, *34* (1), 88–99.
(44) Kattat, V.; Chit, B. T. *J. Am. Chem. Soc.* **1993**, *115*, 6317–6321.
(45) Wang, X.; Kim, S. H.; Ablonczy, Z.; Crouch, R. K.; Knapp, D. R. *Biochemistry* **2004**, *43* (35), 11153–11162.
(46) Zhang, H.; Wen, J.; Huang, R. Y. C.; Blankenship, R. E.; Gross, M. L. *Int. J. Mass Spectrom.* **2012**, *312*, 78–86.
(47) Watson, C.; Janik, I.; Zhuang, T.; Woods, R. J.; Sharp, J. S. **2009**, *81* (7), 2496–2505.
(48) Tullius, T. D.; Dombroski, B. A. *Proc. Natl. Acad. Sci. USA* **1986**, *83* (15), 5469–5473.
(49) Guan, J. Q.; Chance, M. R. *Trends Biochem. Sci.* **2005**, *30* (10), 583–592.
(50) Weber, P. J.; Beck-Sickinger, A. G. *J. Pept. Res.* **1997**, *49* (5), 375–383.
(51) Korshunova, G. A.; Sumbatyan, N. V.; Topin, A. N.; Mtchedlidze, M. T. *Mol. Biol.* **2000**, *34* (6), 823–839.
(52) Singh, A.; Thornton, E. R.; Westheimer, F. H. *J. Biol. Chem.* **1962**, *237* (9), 3006–3008.
(53) Gritsan, N. P.; Zhu, Z.; Hadad, C. M.; Platz, M. S. *J. Am. Chem. Soc.* **1999**, *121* (6), 1202–1207.
(54) Gritsan, N. P.; Gudmundsdóttir, A. D.; Tigelaar, D.; Zhu, Z.; Karney, W. L.; Hadad, C. M.; Platz, M. S. *J. Am. Chem. Soc.* **2001**, *123* (9), 1951–1962.
(55) Dubinsky, L.; Krom, B. P.; Meijler, M. M. *Bioorg. Med. Chem.* **2012**, *20* (2), 554–570.
(56) Brunner, J.; Senn, H.; Richards, F. M. *J. Biol. Chem.* **1980**, *255* (8), 3313–3318.
(57) Staros, J. V.; Bayley, H.; Standring, D. N.; Knowles, J. R. *Biochem. Biophys. Res. Commun.* **1978**, *80* (3), 568–572.
(58) Chavan, A. J.; Rychlik, W.; Blaas, D.; Kuechler, E.; Watt, D. S.; Rhoads, R. E. *Biochemistry* **1990**, *29* (23), 5521–5529.
(59) Yang, T.; Liu, Z.; Xiang, D. L. *Chem. Sci.* **2015**, *6*, 1011–1017.
(60) Baldovi, H. G.; Krüger, M.; Reinsch, H.; Alvaro, M.; Stock, N.; Garcia, H. *J. Mater. Chem. C* **2015**, *3* (15), 3607–3613.

(61) Preston, G. W.; Wilson, A. J. *Chem. Soc. Rev.* **2013**, *42* (8), 3289–3301.
(62) Olszewski, J. D.; Dormán, G.; Elliott, J. T.; Hong, Y.; Ahern, D. G.; Prestwich, G. D. *Bioconjug. Chem.* **1995**, *6* (4), 395–400.
(63) Young, T. S.; Young, D. D.; Ahmad, I.; Louis, J. M.; Benkovic, S. J.; Schultz, P. G. *Proc. Natl. Acad. Sci. USA* **2011**, *108* (27), 11052–11056.
(64) Blencowe, A.; Hayes, W. *Soft Matter* **2005**, *1*, 178–205.
(65) Kumar, A. B.; Tipton, J. D.; Manetsch, R. *Chem. Commun.* **2016**, *52* (13), 2729–2732.
(66) Hermanson, G. T. *Bioconjugate Techniques*, 2nd ed.; 2008.
(67) Liu, M. T. H.; Choe, Y.-K.; Kimura, M.; Kobayashi, K.; Nagase, S.; Wakahara, T.; Niino, Y.; Ishitsuka, M. O.; Maeda, Y.; Akasaka, T. *J. Org. Chem.* **2003**, *68* (19), 7471–7478.
(68) Jumper, C. C.; Schriemer, D. C. *Anal. Chem.* **2011**, *83* (8), 2913–2920.
(69) Bayley, H.; Knowles, J. R. *Biochemistry* **1978**, *17* (12), 2420–2423.
(70) Smith, R. A. G.; Knowles, J. R. *J. Chem. Soc. Perkin Trans. 2* **1975**, 686–694.
(71) Hatanaka, Y.; Hashimoto, M. *J. Org. Chem.* **1994**, *59*, 383–387.
(72) Hashimoto, M.; Hatanaka, Y.; Nabeta, K. *Bioorg. Med. Chem. Lett.* **2002**, *12*, 89–91.
(73) Admasu, A.; Gudmundsdóttir, A. D.; Platz, M. S.; Watt, D. S.; Crocker, P. J. **1998**, 1093–1099.
(74) Gómez, G. E.; Cauerhff, A.; Craig, P. O.; Goldbaum, F. a; Delfino, J. M. *Protein Sci.* **2006**, *15* (4), 744–752.
(75) Richards, F. M.; Lamed, R.; Wynn, R.; Patel, D.; Olack, G. *Protein Sci.* **2000**, *9* (12), 2506–2517.
(76) Ureta, D. B.; Craig, P. O.; Gómez, G. E.; Delfino, J. M. *Biochemistry* **2007**, *46* (50), 14567–14577.
(77) McKenna, C. E.; Simeonov, A. M.; Eran, H.; Bravo-Leerabhandh, M. *Biochemistry* **1996**, *35* (14), 4502–4514.
(78) Jumper, C. C.; Bomgarden, R.; Rogers, J.; Etienne, C.; Schriemer, D. C. *Anal. Chem.* **2012**, *84* (10), 4411–4418.
(79) Chen, L. S.; Chen, G. J.; Tamborski, C. *J. Fluor. Chem.* **1981**, *18* (3), 117–129.
(80) Creary, X. *J. Org. Chem.* **1987**, *52* (22), 5026–5030.
(81) Nassal, M. *Liebigs Ann. der Chemie* **1983**, *1983*, 1510–1523.
(82) Goldstein, G.; Scheid, M.; Hammerling, U.; Schlesinger, D. H.; Niall, H. D.; Boyse, E. A. *Proc. Natl. Acad. Sci. USA* **1975**, *72* (1), 11–15.
(83) Shevchenko, A.; Tomas, H.; Havlis, J.; Olsen, J. V; Mann, M. *Nat. Protoc.* **2006**, *1* (6), 2856–2860.
(84) McLafferty, F. W.; Horn, D. M.; Breuker, K.; Ge, Y.; Lewis, M. A.; Cerda, B.; Zubarev, R. A.; Carpenter, B. K. *J. Am. Soc. Mass Spectrom.* **2001**, *12* (3), 245–249.
(85) Reyes-Turcu, F. E.; Horton, J. R.; Mullally, J. E.; Heroux, A.; Cheng, X.; Wilkinson, K. D. *Cell* **2006**, *124* (6), 1197–1208.
(86) Barton, D. H. R.; Jaszberenyi, J. C.; Theodorakis, E. A.; Reibenspiest, J. H. *J. Am. Chem. Soc.* **1993**, *115*, 8050–8059.
(87) Sheppard, W. A. *J. Am. Chem. Soc.* **1965**, *87* (11), 2410–2420.
(88) Cai, D.; Larsen, R. D.; Reider, P. J. *Tetrahedron Lett.* **2002**, *43* (23), 4285–4287.
(89) Gilman, H.; Spatz, S. M. *J. Org. Chem.* **1951**, *16* (9), 1485–1494.
(90) Trécourt, F.; Breton, G.; Bonnet, V.; Mongin, F.; Marsais, F.; Quéguiner, G. *Tetrahedron* **2001**, *56* (10), 1349–1360.
(91) Lai, Y.-H. *Synthesis* **1981**, 585–604.
(92) Pierce, O. R.; McBee, E. T.; Judd, G. F. *J. Am. Chem. Soc.* **1953**, *76*

(3), 474–478.
(93) Haszeldine, R. N. *J. Chem. Soc.* **1953**, 1748–1757.
(94) Prakash, G. K. S.; Mandal, M. *J. Fluor. Chem.* **2001**, *112* (1), 123–131.
(95) Ruppert, I.; Schlich, K.; Volbach, W. *Tetrahedron Lett.* **1984**, *25* (21), 2195–2198.
(96) Prakash, G. K. S.; Krishnamurti, R.; Olah, G. A. *J. Am. Chem. Soc.* **1989**, *111* (9), 393–395.
(97) Prakash, G. K. S.; Yudin, A. K. *Chem. Rev.* **1997**, *97* (3), 757–786.
(98) Bégué, J. P.; Bonnet-Delpon, D. *Tetrahedron* **1991**, *47* (20–21), 3207–3258.
(99) Kelly, C. B.; Mercadante, M. A.; Leadbeater, N. E. *Chem. Commun.* **2013**, *49* (95), 11133.
(100) Linderman, R.; Graves, D. *J. Org. Chem.* **1989**, *54*, 661–668.
(101) Mercadante, M. A.; Kelly, C. B.; Bobbitt, J. M.; Tilley, L. J.; Leadbeater, N. E. *Nat. Protoc.* **2013**, *8* (4), 666–676.
(102) Kelly, C. B.; Mercadante, M. A.; Hamlin, T. A.; Fletcher, M. H.; Leadbeater, N. E. *J. Org. Chem.* **2012**, *77* (18), 8131–8141.
(103) Popov, K.; Somfai, P. *J. Org. Chem.* **2016**, *81* (8), 3470–3472.
(104) Meerwein, H.; Hinz, G.; Hofmann, P.; Kroning, E.; Pfeil, E. *J. für Prakt. Chemie* **1937**, *147* (10–12), 257–285.
(105) Rudzinski, D. M.; Kelly, C. B.; Leadbeater, N. E. *Chem. Commun.* **2012**, *48* (77), 9610–9612.
(106) Roosen, P. C.; Kallepalli, V. A.; Chattopadhyay, B.; Singleton, D. A.; Maleczka, R. E.; Smith, M. R. *J. Am. Chem. Soc.* **2012**, *134* (28), 11350–11353.
(107) Kucher, O. V.; Kolodiazhnaya, A. O.; Smolii, O. B.; Prisuazhnyk, D. V.; Tolmacheva, K. A.; Zaporozhets, O. A.; Moroz, Y. S.; Mykhailiuk, P. K.; Tolmachev, A. A. *Eur. J. Org. Chem.* **2014**, *2014* (34), 7692–7698.
(108) Sauter, F.; Stanetty, P.; Ramer, W.; Sittenthaler, W. *Monatshefte für Chemie / Chem. Mon.* **1991**, *122*, 879–885.
(109) Wang, L.; Yoshida, T.; Muto, Y.; Murai, Y.; Tachrim, Z. P.; Ishida, A.; Nakagawa, S.; Sakihama, Y.; Hashidoko, Y.; Masuda, K.; Hatanaka, Y.; Hashimoto, M. *Eur. J. Org. Chem.* **2015**, *2015* (14), 3129–3134.
(110) Hatanaka, Y.; Nakamura, N.; Wakabayashi, M.; Fujioka, T.; Kikuchi, T. *Heterocycles* **1996**, *43* (3), 519–522.
(111) Kelly, C. B.; Mercadante, M. A.; Carnaghan, E. R.; Doherty, M. J.; Fager, D. C.; Hauck, J. J.; Macinnis, A. E.; Tilley, L. J.; Leadbeater, N. E. *Eur. J. Org. Chem.* **2015**, *2015* (19), 4071–4076.
(112) Tordeux, M.; Francese, C.; Wakselman, C. *J. Chem. Soc. Perkin Trans. 1* **1990**, No. 7, 1951.
(113) Aït-Mohand, S.; Takechi, N.; Médebielle, M.; Dolbier, W. R. *Org. Lett.* **2001**, *3* (26), 4271–4273.
(114) Larson, J. W.; McMahon, T. B. *J. Am. Chem. Soc.* **1982**, *104* (19), 5848–5849.
(115) Narayan, S.; Muldoon, J.; Finn, M. G.; Fokin, V. V.; Kolb, H. C.; Sharpless, K. B. *Angew. Chem. Int. Ed.* **2005**, *44* (21), 3275–3279.
(116) Yeom, C. E.; Kim, H. W.; Lee, S. Y.; Kim, B. M. *Synlett* **2007**, No. 1, 146–150.
(117) Gembus, V.; Marsais, F.; Levacher, V. *Synlett* **2008**, No. 10, 1463–1466.
(118) Poisson, T.; Dalla, V.; Papamicaël, C.; Dupas, G.; Marsais, F.; Levacher, V. *Synlett* **2007**, No. 3, 381–386.
(119) Davies, H. M. L.; Cantrell, W. R.; Romines, K. R.; Baum, J. S. *Org. Synth.* **1992**, *70*, 93–97.
(120) Raushel, J.; Pitram, S. M.; Fokin, V. V. *Org. Lett.* **2008**, *10* (16),

3385–3388.
(121) Goddard-Borger, E. D.; Stick, R. V. *Org. Lett.* **2007**, *9* (19), 3797–3800.
(122) Stevens, M. Y.; Sawant, R. T.; Odell, L. R. *J. Org. Chem.* **2014**, *79* (11), 4826–4831.
(123) Goddard-Borger, E. D.; Stick, R. V. *Org. Lett.* **2011**, *13* (9), 2514–2514.
(124) Fischer, N.; Goddard-Borger, E. D.; Greiner, R.; Klapötke, T. M.; Skelton, B. W.; Stierstorfer, J. *J. Org. Chem.* **2012**, *77* (4), 1760–1764.
(125) Katritzky, A. R.; Widyan, K.; Gyanda, K. *Synthesis* **2008**, *2008* (8), 1201–1204.
(126) Katritzky, A. R.; El Khatib, M.; Bolshakov, O.; Khelashvili, L.; Steel, P. J. *J. Org. Chem.* **2010**, *75* (19), 6532–6539.
(127) Štefane, B.; Koc ̌evar, M.; Polanc, S. *J. Org. Chem.* **1997**, *62* (21), 7165–7169.
(128) Maleki, B.; Hemmati, S.; Tayebee, R.; Salemi, S.; Farokhzad, Y.; Baghayeri, M.; Zonoz, F. M.; Akbarzadeh, E.; Moradi, R.; Entezari, A.; Abdi, M. R.; Ashrafi, S. S.; Taimazi, F.; Hashemi, M. *Helv. Chim. Acta* **2013**, *96*, 2147–2151.
(129) Regitz, M. *Angew. Chem. Int. Ed.* **1967**, *6* (9), 733–749.
(130) Hein, J. E.; Fokin, V. V. *Chem. Soc. Rev.* **2010**, *39* (4), 1302.
(131) Bräse, S.; Gil, C.; Knepper, K.; Zimmermann, V. *Angew. Chem. Int. Ed.* **2005**, *44* (33), 5188–5240.
(132) Wolff, L. *Justus Liebigs Ann. Chem.* **1902**, *325* (2), 129–195.
(133) Ye, T.; Mckervey, M. A. *Chem. Rev.* **1994**, *94*, 1091–1160.
(134) Ford, A.; Miel, H.; Ring, A.; Slattery, C. N.; Maguire, A. R.; McKervey, M. A. *Chem. Rev.* **2015**, *115* (18), 9981–10080.
(135) Cavender, C. J.; Shiner, V. J. *J. Org. Chem.* **1972**, *37* (22), 3567–3569.
(136) Alper, P. B.; Hung, S. C.; Wong, C. H. *Tetrahedron Lett.* **1996**, *37* (34), 6029–6032.
(137) Kitamura, M.; Kato, S.; Yano, M.; Tashiro, N.; Shiratake, Y.; Sando, M.; Okauchi, T. *Org. Biomol. Chem.* **2014**, *12* (25), 4397–4406.
(138) Suárez, J. R.; Trastoy, B.; Pérez-Ojeda, M. E.; Marín-Barrios, R.; Chiara, J. L. *Adv. Synth. Catal.* **2010**, *352* (14–15), 2515–2520.
(139) Horneff, T.; Chuprakov, S.; Chernyak, N.; Gevorgyan, V.; Fokin, V. V. **2008**, 14972–14974.
(140) Miura, T.; Yamauchi, M.; Murakami, M. *Chem. Commun.* **2009**, *7345* (12), 1470–1471.
(141) Spangler, J. E.; Davies, H. M. L. *J. Am. Chem. Soc.* **2013**, *135* (18), 6802–6805.
(142) Bae, I.; Han, H.; Chang, S. *J. Am. Chem. Soc.* **2005**, *127* (7), 2038–2039.
(143) Cassidy, M. P.; Raushel, J.; Fokin, V. V. *Angew. Chem. Int. Ed.* **2006**, *45* (19), 3154–3157.
(144) Cho, S. H.; Yoo, E. J.; Bae, I.; Chang, S. *J. Am. Chem. Soc.* **2005**, *127* (46), 16046–16047.
(145) Dimroth, O. *Justus Liebigs Ann. Chem.* **1909**, *364*, 183–226.
(146) Yoo, E. J.; Ahlquist, M.; Kim, S. H.; Bae, I.; Fokin, V. V.; Sharpless, K. B.; Chang, S. *Angew. Chem. Int. Ed.* **2007**, *46* (10), 1730–1733.
(147) Wang, F.; Fu, H.; Jiang, Y.; Zhao, Y. *Adv. Synth. Catal.* **2008**, *350* (11–12), 1830–1834.
(148) Allred, G. D.; Liebeskind, L. S. *J. Am. Chem. Soc.* **1996**, *118* (11), 2748–2749.
(149) Raushel, J.; Fokin, V. V. *Org. Lett.* **2010**, *12* (21), 4952–4955.
(150) Evans, D. A.; Britton, T. C. *J. Am. Chem. Soc* **1987**, *109* (3), 6881–

6883.
(151) Evans, D. A.; Britton, T. C.; Ellman, J. A.; Dorow, R. L. *J. Am. Chem. Soc.* **1990**, *112* (10), 4011–4030.
(152) Evans, D. A.; Evrad, D. A.; Rychnovsky, S. D.; Früh, T.; Whittingham, W. G.; DeVries, K. M. *Tetrahedron Lett.* **1992**, *33* (9), 1189–1192.
(153) Barral, K.; Moorhouse, A. D.; Moses, J. E. *Org. Lett.* **2007**, *9* (9), 1809–1811.
(154) Jafarzadeh, M. *Synlett* **2007**, No. 13, 2144–2145.
(155) Pound, D. W.; Saunders, B. C. Pest Control Ltd., British Patent. 628796, 1949.
(156) Yeom, C.-E.; Kim, H.; Lee, S.; Kim, B. *Synlett* **2007**, No. 1, 146–150.
(157) Mcmanus, S. P.; Smith, M. R.; Abramovitch, R. A.; Offort, M. N. *J. Org. Chem.* **1984**, *49*, 683–687.
(158) Zhou, B.; Xu, J. *Org. Biomol. Chem.* **2016**, *14* (21), 4918–4926.
(159) Kaljurand, I.; Kütt, A.; Sooväli, L.; Rodima, T.; Mäemets, V.; Leito, I.; Koppel, I. A. *J. Org. Chem.* **2005**, *70* (3), 1019–1028.
(160) Müller, S.; Liepold, B.; Roth, G. J.; Bestmann, H. J. *Synlett* **1996**, No. 6, 521–522.
(161) Vorbrüggen, H. *Synthesis* **2008**, *2008* (8), 1165–1174.
(162) Tang, L.; Yang, Y.; Wen, L.; Yang, X.; Wang, Z. *Green Chem.* **2016**, 1224–1228.
(163) Kirihara, M.; Naito, S.; Nishimura, Y.; Ishizuka, Y.; Iwai, T.; Takeuchi, H.; Ogata, T.; Hanai, H.; Kinoshita, Y.; Kishida, M.; Yamazaki, K.; Noguchi, T.; Yamashoji, S. *Tetrahedron* **2014**, *70* (14), 2464–2471.
(164) Matesic, L.; Wyatt, N. A.; Fraser, B. H.; Roberts, M. P.; Pham, T. Q.; Greguric, I. *J. Org. Chem.* **2013**, *78* (22), 11262–11270.
(165) Barrow, A. S.; Moses, J. E. *Synlett* **2016**, *27* (12), 1840–1843.
(166) Ruppel, J. V; Jones, J. E.; Huff, C. A.; Kamble, R. M.; Chen, Y.; Zhang, X. P. *Org. Lett.* **2008**, *10* (10), 1995–1998.
(167) Ryu, T.; Min, J.; Choi, W.; Jeon, W. H.; Lee, P. H. *Org. Lett.* **2014**, *16* (11), 2810–2813.
(168) Huang, L.; Wulff, W. D. *J. Am. Chem. Soc.* **2011**, *133* (23), 8892–8895.
(169) Moreau, R. J.; Sorensen, E. J. *Tetrahedron* **2007**, *63* (28), 6446–6453.
(170) Cremlyn, R. J. W. *J. Chem. Soc. C* **1968**, 11–16.
(171) Parvizi, P.; Khosravi, A.; Moradian, S.; Gharanjig, K. *J. Chinese Chem. Soc.* **2009**, *56*, 1035–1042.
(172) Muthyala, M. K.; Choudhary, S.; Kumar, A. *J. Org. Chem.* **2012**, *77* (19), 8787–8791.
(173) Nadeau, E.; Ventura, D. L.; Brekan, J. A.; Davies, H. M. L. *J. Org. Chem.* **2010**, *75* (6), 1927–1939.
(174) Chen, X.; Xie, Y.; Xiao, X.; Li, G.; Deng, Y.; Jiang, H.; Zeng, W. *Chem. Commun.* **2015**, *51*, 15328–15331.
(175) Pramanik, S.; Ghorai, P. *Org. Lett.* **2014**, *16* (8), 2104–2107.
(176) Huisgen, R.; Szeimies, G.; Möbius, L. *Chem. Ber.* **1967**, *100*, 2494–2507.
(177) Sletten, E. M.; Bertozzi, C. R. *Acc. Chem. Res.* **2011**, *44* (9), 666–676.
(178) MacKenzie, D. A.; Sherratt, A. R.; Chigrinova, M.; Cheung, L. L. W.; Pezacki, J. P. *Curr. Opin. Chem. Biol.* **2014**, *21*, 81–88.
(179) Van Berkel, S. S.; Dirks, A. J.; Debets, M. F.; Van Delft, F. L.; Cornelissen, J. J. L. M.; Nolte, R. J. M.; Rutjes, F. P. J. T. *ChemBioChem* **2007**, *8* (13), 1504–1508.
(180) Bellvile, D. J.; Wirth, D. D.; Bauld, N. L. *J. Am. Chem. Soc.* **1981**, 718–720.
(181) Harirchian, B.; Bauld, N. *J. Am. Chem. Soc.* **1989**, *111*, 1826–1828.

(182) Haberl, U.; Steckhan, E.; Blechert, S.; Wiest, O. *Chem. -Eur. J.* **1999**, *5* (10), 2859–2865.
(183) Tsuchimoto, T.; Joya, T.; Shirakawa, E.; Kawakami, Y. *Synlett* **2000**, *2000* (12), 1777–1778.
(184) Hintermann, L.; Labonne, A. *Synthesis* **2007**, No. 8, 1121–1150.
(185) Ledwith, A. *Acc. Chem. Res.* **1972**, *5* (4), 133–139.
(186) Ischay, M. A.; Yoon, T. P. *Eur. J. Org. Chem.* **2012**, No. 18, 3359–3372.
(187) Schmittel, M.; Burghart, A. *Angew. Chem. Int. Ed.* **1997**, *36*, 2550–2589.
(188) Moore, J. C.; Davies, E. S.; Walsh, D. A.; Sharma, P.; Moses, J. E. *Chem. Commun.* **2014**, *50*, 12523–12525.
(189) Mihelcic, J.; Moeller, K. D. *J. Am. Chem. Soc.* **2004**, *126* (29), 9106–9111.
(190) Lim, H. N.; Parker, K. A. *Org. Lett.* **2013**, *15* (2), 398–401.
(191) Rosen, B. R.; Werner, E. W.; O'Brien, A. G.; Baran, P. S. *J. Am. Chem. Soc.* **2014**, *136*, 5571–5574.
(192) Beveridge, R. E.; Batey, R. A. *Org. Lett.* **2013**, *15* (12), 3086–3089.
(193) Jang, H. Y.; Hong, J. B.; MacMillan, D. W. C. *J. Am. Chem. Soc.* **2007**, *129* (22), 7004–7005.
(194) Beeson, T. D.; Mastracchio, A.; Hong, J. B.; Ashton, K.; MacMillan, D. W. C. *Science* **2007**, *316*, 582–586.
(195) Seo, E. T.; Nelson, R. F.; Fritsch, J. M.; Marcoux, L. S.; Leedy, D. W.; Adams, R. N. *J. Am. Chem. Soc.* **1966**, *88* (1965), 3498–3503.
(196) Dapperheld, S.; Steckhan, E.; Grosse Brinkhaus, K.; Esch, T. *Chem. Ber.* **1991**, *124*, 2557–2567.
(197) Wu, X.; Davis, A. P.; Lambert, P. C.; Kraig Steffen, L.; Toy, O.; Fry, A. J. *Tetrahedron* **2009**, *65* (12), 2408–2414.
(198) Steckhan, W. S. E.; Schmidt, W. *Chem. Ber.* **1980**, *113*, 577–585.
(199) Platen, M.; Steckhan, E. *Tetrahedron Lett.* **1980**, *21* (6), 511–514.
(200) Schmidt, B. W.; Steckhan, E. *Angew. Chem. Int. Ed.* **1978**, *17* (9), 673–674.
(201) Dapperheld, B. S.; Steckhan, E. *Angew. Chem. Int. Ed.* **1982**, *21* (10), 780–781.
(202) Zhai, L.; Shukla, R.; Wadumethrige, S. H.; Rathore, R. *J. Org. Chem.* **2010**, *75* (14), 4748–4760.
(203) Perkin, W. H. *J. Chem. Soc. Trans.* **1884**, *45*, 170–189.
(204) Fittig, R.; Schrone, A. *Chem. Ber.* **1875**, *8*, 357–369.
(205) Grotjahn, D. B.; Lev, D. A. *J. Am. Chem. Soc.* **2004**, *126* (39), 12232–12233.
(206) Kutscheroff, M. *Berichte der Dtsch. Chem. Gesellschaft* **1881**, *14* (1), 1540–1542.
(207) Kremsner, J. M.; Kappe, C. O. *Eur. J. Org. Chem.* **2005**, *2005* (17), 3672–3679.
(208) Vasudevan, A.; Verzal, M. K. *Synlett* **2004**, *2004* (4), 631–634.
(209) An, J.; Bagnell, L.; Cablewski, T.; Strauss, C. R.; Trainor, R. W. *J. Org. Chem.* **1997**, *62* (8), 2505–2511.
(210) Meseguer, B.; Alonso-Díaz, D.; Griebenow, N.; Herget, T.; Waldmann, H. *Angew. Chem. Int. Ed.* **1999**, *38* (19), 2902–2906.
(211) Liu, W.; Wang, H.; Li, C.-J. *Org. Lett.* **2016**, *18* (9), 2184–2187.
(212) Menashe, N.; Shvo, Y. *J. Org. Chem.* **1993**, *58* (26), 7434–7439.
(213) Norman, R. O. C.; Parr, W. J. E.; Thomas, C. B. *J. Chem. Soc., Perkin Trans. 1* **1976**, 1983–1987.
(214) Mizushima, E.; Sato, K.; Hayashi, T.; Tanaka, M. *Angew. Chem. Int. Ed.* **2002**, *41* (23), 4563–4565.
(215) Ebule, R. E.; Malhotra, D.; Hammond, G. B.; Xu, B. *Adv. Synth. Catal.* **2016**, *358* (9), 1478–1481.

(216) Ohyabu, N.; Nishikawa, T.; Isobe, M. *J. Am. Chem. Soc.* **2003**, *125*, 8796–8805.
(217) Jung, M. E.; Nishimura, N. *Org. Lett.* **2001**, *3* (13), 2113–2115.
(218) Rupe, H.; Glenz, K. *Justus Liebigs Ann. Chem.* **1924**, *436*, 184–204.
(219) Das, J. P.; Roy, S.; Ann, B. L. *J. Org. Chem.* **2002**, No. 7, 7861–7864.
(220) Nishinaga, T. *Organic redox systems : synthesis, properties, and applications*; 2015.
(221) Doebner, O. *Ber. Dtsch. Chem. Ges.* **1902**, *35*, 1136–1147.
(222) Chowdhury, S.; Roy, S. *Tetrahedron Lett.* **1996**, *37* (15), 2623–2624.
(223) Utimoto, K. *Pure Appl. Chem.* **1983**, *55* (11), 1845–1852.
(224) Jacques, R.; Pal, R.; Parker, N. A.; Sear, C. E.; Smith, P. W.; Ribaucourt, A.; Hodgson, D. M. *Org. Biomol. Chem.* **2016**, *14*, 5875–5893.
(225) Albertson, A. K. F.; Lumb, J. P. *Angew. Chem. Int. Ed.* **2015**, *54* (7), 2204–2208.
(226) Xia, C.; Li, H.; Liu, F.; Hu, W. *Bioorg. Med. Chem. Lett.* **2008**, *18* (24), 6553–6557.
(227) Caprioglio, D.; Torretta, S.; Ferrari, M.; Travelli, C.; Grolla, A. A.; Condorelli, F.; Genazzani, A. A.; Minassi, A. *Bioorg. Med. Chem.* **2016**, *24* (2), 140–152.
(228) Ditrich, K.; Hoffmann, R. W. *Tetrahedron Lett.* **1985**, *26*, 6325–6328.
(229) Zhang, Y.; Li, Y.; Wu, Y. *Synlett* **2009**, No. 18, 3037–3039.
(230) Dess, D. B.; Martin, J. C. *J. Org. Chem.* **1983**, *48* (22), 4155–4156.
(231) Patel, N. R.; Kelly, C. B.; Jouffroy, M.; Molander, G. A. *Org. Lett.* **2016**, *18* (4), 764–767.
(232) Schabel, T.; Plietker, B. *Chem. -Eur. J.* **2013**, *19* (22), 6938–6941.
(233) Cai, H.; Nie, J.; Zheng, Y.; Ma, J. A. *J. Org. Chem.* **2014**, *79* (12), 5484–5493.
(234) McConville, M.; Saidi, O.; Blacker, J.; Xiao, J. *J. Org. Chem.* **2009**, *74* (7), 2692–2698.
(235) Harmata, M.; Schreiner, P. R.; Lee, D. R.; Kirchhoefer, P. L. *J. Am. Chem. Soc.* **2004**, 10954–10957.
(236) Evens, E. D.; Gifford, E. C.; Griffiths, W. E. L. *J. Chem. Soc. Trans.* **1915**, *107* (1673–1677).
(237) Brandt, D. R.; Pannone, K. M.; Romano, J. J.; Casillas, E. G. *Tetrahedron* **2013**, *69* (47), 9994–10002.